Characterization and reduction of the release of sulfur and chlorine compounds in pyrolysis and gasification of biomass and waste

Hala Braidy

Ecole Doctorale C2MP

Laboratoire Réacteurs et Procédés LRP
CEA / LITEN - Grenoble

Institut Jean Lamour

Thèse

Présentée et soutenue publiquement pour l'obtention du titre de

DOCTEUR DE l'UNIVERSITE DE LORRAINE

Mention: CHIMIE

par **Hala BRAIDY**

Sous la direction de **Fabrice PATISSON** et **Sylvie VALIN**

Characterization and reduction of the release of sulfur and chlorine compounds in pyrolysis and gasification of biomass and waste

Caractérisation et réduction du relâchement des composés soufrés et chlorés lors de la pyrolyse et de la gazéification de biomasse et de déchets

Le 15 Novembre 2023

Membres du jury:

Directeur de thèse:	**Fabrice PATISSON**	**Professeur, IJL, Université de Lorraine, Nancy**
Co-Directrice de thèse:	**Sylvie VALIN**	**Ingénieure de Recherche, CEA, Grenoble**
Rapporteurs:	**Bechara TAOUK**	**Professeur, INSA Rouen Normandie, Saint Etienne du Rouvray**
	Gwenaëlle TROUVE	**Professeure, Université de Haute-Alsace, Mulhouse**
Examinateur et Président:	**Yann ROGAUME**	**Professeur, Université de Lorraine, Epinal**
Examinatrice:	**Audrey VILLOT**	**Maître-assistante, IMT Atlantique, Nantes**

Acknowledgments

With sincere appreciation, I acknowledge the multitude of individuals who have been part of this challenging yet rewarding academic journey. Their collective support and contributions have nonetheless played an integral role in shaping the outcome of this thesis.

I would like to express my recognition to the members of the thesis jury for their time, expertise, and insightful contributions.

I express my sincere thanks to Fabrice PATISSON, the director of this thesis, for your constant involvement and support, which have added depth and context to this research.

My profound gratitude goes to Sylvie VALIN, my supervisor and co-director, for your guidance and insightful contributions. Your mentorship and expertise have been instrumental in shaping the trajectory of this research, ensuring its quality and coherence.

I would like to acknowledge the contributions of my colleagues in LRP, whose engaging discussions and ideas have enriched my understanding and significantly influenced the development of my research. Special thanks to Sebastien THIERY for his indispensable technical expertise and assistance in conducting the experiments.

To my fellow Ph.D. candidates and interns who shared the journey alongside me, your camaraderie has made the challenges more bearable. Our mutual understanding of the struggles has been a source of solidarity.

Deepest appreciation is reserved for my parents, my sister, my two brothers, and my friends. Your consistent encouragement has been a pillar of strength, providing the resilience needed to persevere.

I recognize the collective efforts that have shaped this thesis. Each contribution, regardless of its magnitude, has left a lasting imprint on this work and has significantly influenced both my personal and academic development.

Contents

List of Figures

List of Tables

List of Abbreviations and Acronyms

EDX	Energy Dispersive X-Ray Spectroscopy
ER	Equivalence Ratio
FPD	Flame Photometric Detector
GC	Gas Chromatography
HDPE	High-Density Polyethylene
ICP	Inductively Coupled Plasma
LDPE	Low- Density Polyethylene
MBMS	Molecular Beam Mass Spectrometry
MS	Mass Spectrometry
OES	Optical Emission Spectroscopy
PET	Polyethylene Terephthalate
PP	Polypropylene
PS	Polystyrene
PTFE	Polytetrafluoroethylene
PVC	Polyvinyl Chloride
RDF	Refuse Derived Fuels
SEM	Scanning Electron Microscopy
SOFC	Solid Oxide Fuel Cell
SRF	Solid Recovered Fuels
TCD	Thermal Conductivity Detector
XPS	X-Ray Photoelectron Spectroscopy
XRD	X-Ray Diffraction

Abstract

Gasification allows producing a synthesis gas that can be used for cogeneration (heat and power) or for the synthesis of liquid or gaseous fuels. However, the presence of inorganic elements, such as sulfur or chlorine in some biomasses and wastes, can lead to the release of inorganic gaseous pollutants that must be cleaned before the final application due to environmental regulations, their corrosive nature (HCl, KCl, NaCl), and their poisoning effect on catalysts (H_2S, COS) in the case of synthesis.

The objectives of this thesis are first to understand and characterize the behavior of sulfur and chlorine during pyrolysis (the first step of gasification) and gasification of biomass and waste, and then to propose and test in-situ methods to limit their release. These methods, which are based on chemical interactions between inorganic elements, include either the use of mineral additives or of mixtures of resources.

Different resources were selected among biomass and waste of biogenic or fossil origin, with varying initial contents of S, Cl, and ash: two agricultural residues (colza straw and corn residues) and three waste components (wool, cardboard, and PVC).

Thermodynamic equilibrium calculations were performed using the Factsage software to predict the behavior of inorganic elements and the stability of sulfur and chlorine compounds as a function of the operating conditions for each resource.

Analytical pyrolysis and gasification experiments were conducted in a laboratory setup at variable temperatures between 365 and 850°C, coupled with gas analysis and characterizations of the solid residues (elemental analysis, XRD, SEM-EDX). The results highlighted the influence of the resource type and composition, as well as temperature on the behavior of S and Cl. S and Cl present in organic forms in wool, cardboard, and PVC are completely released into the gas phase, even at low temperatures, without interaction with other inorganic elements. For agricultural residues, a part of S and Cl present in inorganic form is retained in the char in various crystallized forms (CaS, $CaSO_4$, K_2SO_4, KCl, $MgCl_2$) depending on the pyrolysis temperature and ash composition.

The addition of calcium-based additives showed variable effectiveness in the retention of S and Cl, suggesting that the expected interaction between the additives and S and Cl may not have taken place.

The greatest improvements in sulfur retention were observed during the co-pyrolysis of wool with calcium-rich resources, while chlorine retention was enhanced when mixing agricultural

residues with cardboard. Interactions between the resources then significantly improved sulfur and chlorine retention, exceeding twice the theoretical values calculated with an assumption of no interaction between the resources.

The obtained results contribute to better control the release of inorganic pollutants in syngas and to better size the cleaning stage upstream of the final application.

Résumé

La gazéification permet de produire un gaz de synthèse utilisable en cogénération (chaleur et électricité) ou pour la synthèse de carburants liquides ou gazeux. Cependant, la présence d'éléments inorganiques tels que le soufre (S) ou le chlore (Cl), dans certaines biomasses et déchets peut entraîner un relâchement de polluants inorganiques gazeux qui doivent impérativement être nettoyés avant l'application finale, du fait des normes d'émission dans l'environnement, de leur caractère corrosif (HCl, KCl, NaCl), ou de leur effet d'empoisonnement de catalyseurs dans le cas d'une synthèse (H_2S, COS).

Les objectifs de cette thèse sont d'abord de comprendre et caractériser le comportement du soufre et du chlore lors de la pyrolyse (première étape de la gazéification) et la gazéification de biomasses et de déchets, et ensuite de proposer et tester des méthodes in-situ pour limiter leur relâchement. Ces méthodes sont basées sur des réactions chimiques entre le soufre, le chlore, et des éléments inorganiques, favorisées soit par l'ajout d'additifs minéraux, soit par l'utilisation de mélanges de ressources.

Différentes ressources ont été sélectionnées parmi des biomasses et déchets d'origine biogénique ou fossile, présentant différentes teneurs initiales en S, en Cl et en cendres: deux résidus agricoles (paille de colza et résidus de maïs) et trois composants de déchets (laine, carton et PVC).

Des simulations thermodynamiques ont été effectuées avec le logiciel FactSage pour prévoir le comportement des éléments inorganiques et la stabilité des espèces soufrées et chlorées en fonction des conditions opératoires pour chaque ressource. Des expériences analytiques de pyrolyse et de gazéification ont été menées dans un dispositif expérimental de laboratoire, à température variable entre 365 et 850°C, associées à des analyses de gaz et des caractérisations des résidus solides (analyse élémentaire, DRX, MEB-EDX). Les résultats ont mis en évidence l'influence du type et de la composition de la ressource ainsi que la température sur les comportements du S et du Cl. Le S et le Cl présents sous forme organique dans la laine, le carton et le PVC sont complètement libérés dans la phase gazeuse, même à basse température, sans interaction avec d'autres éléments inorganiques. Pour les résidus agricoles, une partie du S et Cl sous forme inorganique a été retenue dans le char sous différentes formes cristallisées (CaS, $CaSO_4$, K_2SO_4, KCl, $MgCl_2$) dépendant de la température de pyrolyse et de la composition des cendres.

L’ajout d’additifs à base de calcium a montré une efficacité variable sur la rétention de S et Cl, suggérant que l'interaction prévue entre les additifs et le S et Cl n'a peut-être pas eu lieu.
Les plus grandes améliorations de rétention de soufre ont été observées lors de la co-pyrolyse de la laine avec des ressources riches en calcium, tandis que la rétention de chlore a été améliorée lors du mélange de résidus agricoles avec le carton. Les interactions entre les ressources ont alors significativement amélioré la rétention de soufre et de chlore, dépassant deux fois les valeurs théoriques calculées en supposant aucune interaction entre les ressources. Les résultats obtenus pourront servir à mieux contrôler le niveau de polluants inorganiques dans le gaz de synthèse, et à mieux dimensionner l’étape de nettoyage en amont de l’application finale.

Résumé étendu en français

Contexte, état de l'art et objectifs de la thèse

Dans le contexte de transition vers une société climatiquement neutre, la réduction de la dépendance aux ressources fossiles et le basculement vers des sources d'énergie moins polluantes sont essentiels afin de pouvoir réduire les émissions de gaz à effet de serre. Des progrès technologiques significatifs ont été réalisés dans le développement de différents procédés de production (biocarburants, produits chimiques, biomatériaux) en utilisant des ressources durables telles que la biomasse à la place des énergies épuisables (pétrole, gaz naturel, charbon). Ainsi, les technologies de conversion thermochimique basées sur la combustion, la gazéification, la pyrolyse ou la liquéfaction hydrothermale permettent la conversion de biomasse et éventuellement de déchets, en énergie, produits chimiques et différents biocarburants liquides et gazeux.

Parmi ces technologies de conversion, la gazéification se distingue comme un processus thermochimique polyvalent, capable de convertir non seulement la biomasse, mais également divers déchets. Le gaz résultant, connu sous le nom de gaz de synthèse (ou syngaz), se compose d'un mélange de monoxyde de carbone (CO), d'hydrogène (H_2), de dioxyde de carbone (CO_2) et de méthane (CH_4). Il peut être utilisé pour la production de chaleur et d'électricité, ou de différents produits chimiques et carburants, soit par synthèse catalytique, telle que la synthèse Fischer-Tropsch, ou par d'autres méthodes (biologiques, etc.).
Cependant, la présence d'éléments inorganiques comme le soufre ou le chlore dans certaines biomasses et déchets peut entraîner, en fonction de la quantité et de la nature de ces éléments, un relâchement de polluants inorganiques gazeux néfastes pour les procédés avals, en raison de leur nature corrosive (espèces chlorées: HCl, KCl, NaCl) (Bryers, 1996) ou de leur caractère de poisons pour les catalyseurs (espèces soufrées : H_2S, COS) (Hepola and Simell, 1997). Par conséquent, la concentration en polluants inorganiques volatils dans le gaz de synthèse doit être impérativement diminuée avant l'application finale.

Dans la littérature, différentes concentrations et formes chimiques de soufre et de chlore ont été identifiées dans les ressources carbonées et corrélées avec le type de matière d'origine. Le soufre forme une variété de composés en fonction de ses deux natures: le soufre organique incorporé dans la matrice carbonée et le soufre inorganique. Le chlore peut également être présent dans des composés organiques et inorganiques.

Ces dernières années, les études expérimentales (Andrea Jordan and Akay, 2012; Porbatzki et al., 2011; Tchoffor et al., 2016; Valin et al., 2019; Vonk et al., 2019) et thermodynamiques (Defoort et al., 2015; Froment et al., 2013; Kuramochi et al., 2005; Porbatzki et al., 2011; Tchoffor et al., 2016; Zevenhoven-Onderwater et al., 2001) sur la gazéification de la biomasse ou des déchets riches en éléments inorganiques se sont intensifiées, en s'intéressant notamment à la caractérisation des polluants inorganiques gazeux relâchés et aux méthodes pour limiter leur émission. Divers paramètres liés aux ressources et aux conditions opératoires de la gazéification peuvent influencer le relâchement des espèces inorganiques. Il s'agit notamment du type de ressource, de leur teneur en éléments inorganiques (notamment en ce qui concerne Si, Ca, K et Na), de la température, de l'ER (equivalence ratio) et de la composition de l'atmosphère. Malgré tous ces progrès, l'étude du relâchement des espèces soufrées et chlorées lors de la gazéification nécessite encore des investigations expérimentales, en considérant à la fois leur forme chimique initiale dans la ressource, et l'effet des conditions opératoires sur leur rejet. Une attention particulière doit être accordée à la quantification de ces éléments sous les formes condensées et gazeuses pour boucler les bilans élémentaires du soufre et du chlore. Enfin, la caractérisation de leurs formes solides aiderait à identifier leurs mécanismes de rétention.

Une des méthodes in-situ pour limiter le rejet de polluants inorganiques dans le gaz consiste à ajouter des additifs dans le réacteur, afin de capter les composés chlorés et/ou soufrés avant leur rejet. Cette technique présente l'avantage d'éviter ou de limiter l'étape de nettoyage ainsi qu'un éventuel refroidissement du gaz. L'utilisation d'additifs et de minéraux naturels à base de calcium s'est révélée être efficace pour la réduction des concentrations de H_2S dans le gaz de synthèse (Pinto et al., 2014a; Recari et al., 2016a; Schmid et al., 2018; Schweitzer et al., 2018; Cheng et al., 2020), et dans certains cas les concentrations de HCl (Cho et al., 2015). Cependant, il y a encore un manque de compréhension de toutes les réactions impliquées dans le processus lors de l'utilisation de tels additifs.

Par ailleurs, certains chercheurs ont étudié la co-gazéification du charbon et de la biomasse, et ont mis en évidence des effets d'interaction entre les différentes ressources influençant les rejets de soufre et de chlore (Pinto et al., 2014a; Bläsing et al., 2015a, 2017a). En fonction des quantités initiales de soufre et de chlore, du contenu inorganique initial (principalement la teneur en Si, Ca et Al) et des quantités respectives de chacune des ressources, une réduction des polluants gazeux est possible. Toutefois, ces études sont encore rares dans la littérature, en particulier en ce qui concerne des mélanges comprenant de la biomasse et des déchets.

Au vu des limitations et verrous que fait apparaître cet état de l'art, les principaux objectifs de cette thèse sont de :

- comprendre et caractériser le comportement du soufre et du chlore lors de la pyrolyse, représentant la première étape de la gazéification, ainsi que la gazéification de biomasse et de déchets de compositions variées, et évaluer l'influence du type de ressource et de sa composition chimique initiale (notamment la nature et la teneur en éléments inorganiques), ainsi que l'effet des conditions opératoires (température et nature de l'atmosphère – N_2/air) sur ce comportement,
- proposer et tester des méthodes in-situ (basées sur des interactions chimiques entre éléments inorganiques) en utilisant des additifs ou en mélangeant des ressources pour améliorer la rétention du soufre et du chlore dans la phase solide et ainsi limiter leur rejet dans la phase gazeuse.

Matériels et Méthodes

La démarche suivie pour cette étude fait appel à des calculs thermodynamiques, des expériences de pyrolyse et de gazéification et des analyses par diverses techniques.

- **Sélection et caractérisation des ressources**

Différentes ressources ont été sélectionnées et caractérisées parmi des biomasses et des matériaux présents dans les déchets en fonction de leur teneur en soufre et en chlore, ainsi que de leur teneur et composition en cendres :

- la paille de colza et les résidus de maïs (feuilles, rafles, tiges), qui sont des résidus provenant de l'agriculture,
- le carton, le PVC et la laine (textile), qui sont des résidus urbains de post-consommation provenant des industries ou des ménages.

Le **tableau 1** présente l'humidité, la teneur en cendres, ainsi que la teneur en S et en Cl de chaque ressource.

Tableau 1 : Composition des ressources

		Paille de Colza	Résidus de Maïs	Carton	Laine	PVC
Humidité	wt.%	11,3	9,7	7,5	11,7	-
Cendres (550°C)	wt.%	10,1	3,5	12,8	1,2	3,5
S	wt.%	0,33	0,11	0,1	2,66	0,06
Cl	wt.%	0,15	0,36	0,07	0,09	49,37
Ca	wt.%	3,74	0,45	4,17	0,78	0,29
K	wt.%	0,77	0,73	0,11	0,1	<0,04
Si	wt.%	0,54	0,27	2,0	0,6	0,39

Une technique de lixiviation, décrite dans la littérature, a été appliquée aux ressources afin de différencier et de quantifier les fractions de S ou de Cl présentes sous forme organique (liées à la matrice carbonée) ou inorganique (sulfates ou sels alcalins). La **figure 1** ci-dessous présente les résultats de la méthode de lixiviation pour le soufre et le chlore. Les formes inorganiques de S et de Cl sont récupérées dans les lixiviats, tandis que les formes organiques restent dans les résidus solides. Pour les résidus agricoles, le S est réparti entre les 2 formes organiques et inorganiques ($CaSO_4$, K_2SO_4), alors que pour la laine et le carton la forme organique du S est dominante. La majorité du Cl est présente sous forme inorganique dans les résidus agricoles (KCl, $KClO_4$), alors que dans le PVC, le chlore est connu pour être lié organiquement dans la structure du polymère.

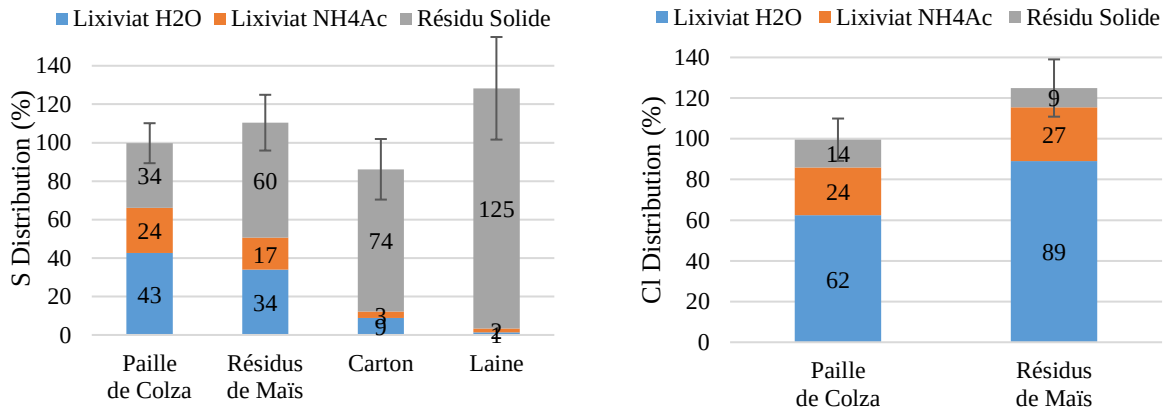

Figure 1 : Distribution de S et Cl dans les lixiviats récupérés et les résidus solides (résultats de la méthode de lixiviation)

- **Simulations thermodynamiques**

Des simulations thermodynamiques été effectuées avec le logiciel FactSage pour explorer la stabilité des espèces soufrées et chlorées pour chaque ressource sélectionnée, et prévoir leur comportement en fonction des conditions de pyrolyse et de gazéification en faisant varier la température (350 - 900°C) ou l'ER (equivalence ratio) (0 – 0.6). Les simulations utilisent

comme données d'entrée la composition élémentaire de la ressource (C, H, N, O, S, Cl, Si, Ca, K, P, Mg, Al, Fe, Na), ainsi que les teneurs en O_2 et N_2 dans le gaz injecté.

- **Description du dispositif expérimental et de la procédure**

Un dispositif de pyrolyse/gazéification traitant des échantillons de quelques grammes en lit fixe (batch) est utilisé pour les expériences analytiques à l'échelle laboratoire (**Figure 2**). Le réacteur est un tube en quartz fixé à un fritté en quartz capable de supporter des températures allant jusqu'à 900°C, suivi d'un système de condensation pour la collecte des produits condensables et d'une section d'analyse des produits gazeux. Le quartz a été choisi comme matériau du réacteur pour éviter toute adsorption ou interaction avec les espèces inorganiques libérées. Des tests de caractérisation thermique ont été effectués à différentes températures de consigne afin de déterminer en particulier la température à l'intérieur du réacteur ainsi que celle de chaque ressource.

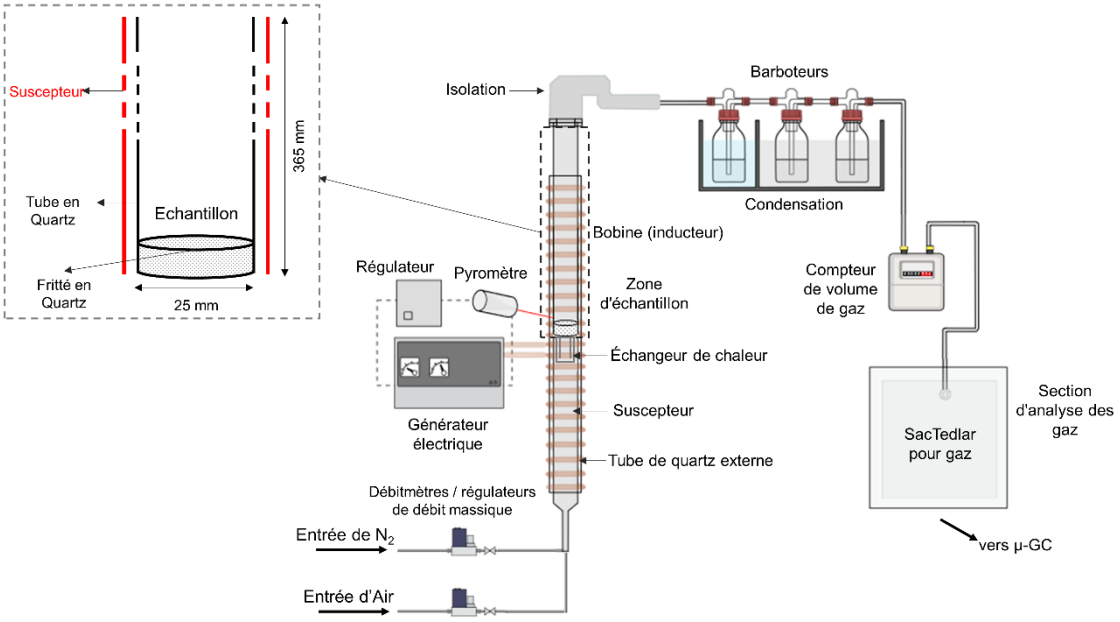

Figure 2 : Représentation schématique du dispositif expérimental et détails de la zone de réaction

Les expériences analytiques ont été conduites afin d'atteindre les deux objectifs de cette étude : caractériser le comportement du soufre et du chlore lors de la pyrolyse et la gazéification, et tester des méthodes visant à améliorer leur rétention dans le résidu carboné (char), en se basant sur l'interaction avec des éléments inorganiques.

Des expériences de pyrolyse ont d'abord été menées sur chaque ressource individuellement à différentes températures entre 365 et 850°C pour mieux comprendre les comportement du S et

du Cl pendant la montée en température, ainsi que des expériences de gazéification en ajoutant de l'air pour une durée de 20 ou 60 minutes à 800°C.

Pour le deuxième objectif, les effets de l'ajout de trois additifs à base de calcium (CaO, $CaCO_3$ et $Ca(OH)_2$) à la ressource ont été évalués expérimentalement en pyrolyse, et dans certains cas également en gazéification. La quantité d'additif a été choisie de manière à obtenir un rapport massique fixe de 10 % entre la quantité de calcium fournie par l'additif et la masse de la ressource. Par la suite, les mélanges de différentes ressources ont été étudiés. Le carton, la paille de colza et l'écorce de chêne, en raison de leur contenu élevé en calcium, ont été sélectionnés pour être mélangés avec les autres ressources (laine, paille de colza, résidus de maïs, PVC). Les fractions massiques des mélanges ont été déterminées pour incorporer des quantités équivalentes de calcium ajouté par rapport aux expériences avec les additifs.

Plusieurs techniques analytiques ont été utilisées pour évaluer qualitativement et quantitativement le comportement du soufre et du chlore. Les expériences de pyrolyse à 800°C et 850°C ont été menées avec une analyse complète de tous les produits obtenus : le char de la phase solide, ainsi que les phases gazeuses et condensées. Les autres expériences se sont limitées à l'analyse du char. La composition élémentaire des chars a été déterminée par analyses chimiques. L'étude de leurs phases cristallines a été réalisée à l'aide d'un diffractomètre à rayons X et leurs morphologies et compositions élémentaires locales ont été analysées à l'aide d'un microscope électronique à balayage couplé à une spectroscopie de rayons X à dispersion d'énergie (MEB-EDX).

Caractérisation du comportement du S et du Cl lors de la pyrolyse et de la gazéification

Les résultats des simulations thermodynamiques mettent en évidence l'influence prépondérante de la température et la composition de la ressource sur le relâchement du soufre et de chlore dans la phase gazeuse, tandis que l'ER (equivalence ratio) a généralement un effet secondaire. La présence de certains éléments, tels que le calcium et le fer, mais aussi de manière indirecte le silicium, exerce une influence sur le comportement du soufre, affectant son relâchement sous forme de H_2S en phase gazeuse ou sa rétention sous forme de composés solides (CaS, FeS). De même, la répartition du chlore est influencée par la composition de la biomasse, en particulier la présence d'éléments alcalins comme le potassium et le sodium. La volatilisation du potassium se révèle particulièrement pertinente pour comprendre le comportement du chlore, car les deux éléments sont généralement associés sous forme de chlorure de potassium, dont la volatilité augmente avec la température. À un ER plus faible, le chlore a tendance à rester en phase condensée. Toutefois, à mesure que l'ER augmente, la volatilité des composés chlorés,

notamment le chlorure de potassium (KCl), devient plus significative, entraînant leur relâchement dans la phase gazeuse.

La **figure 3** ci-dessous présente les rétentions du S et du Cl dans les chars en fonction de la température de pyrolyse, obtenues par les expériences analytiques (points) et par les simulations thermodynamiques (pointillés).

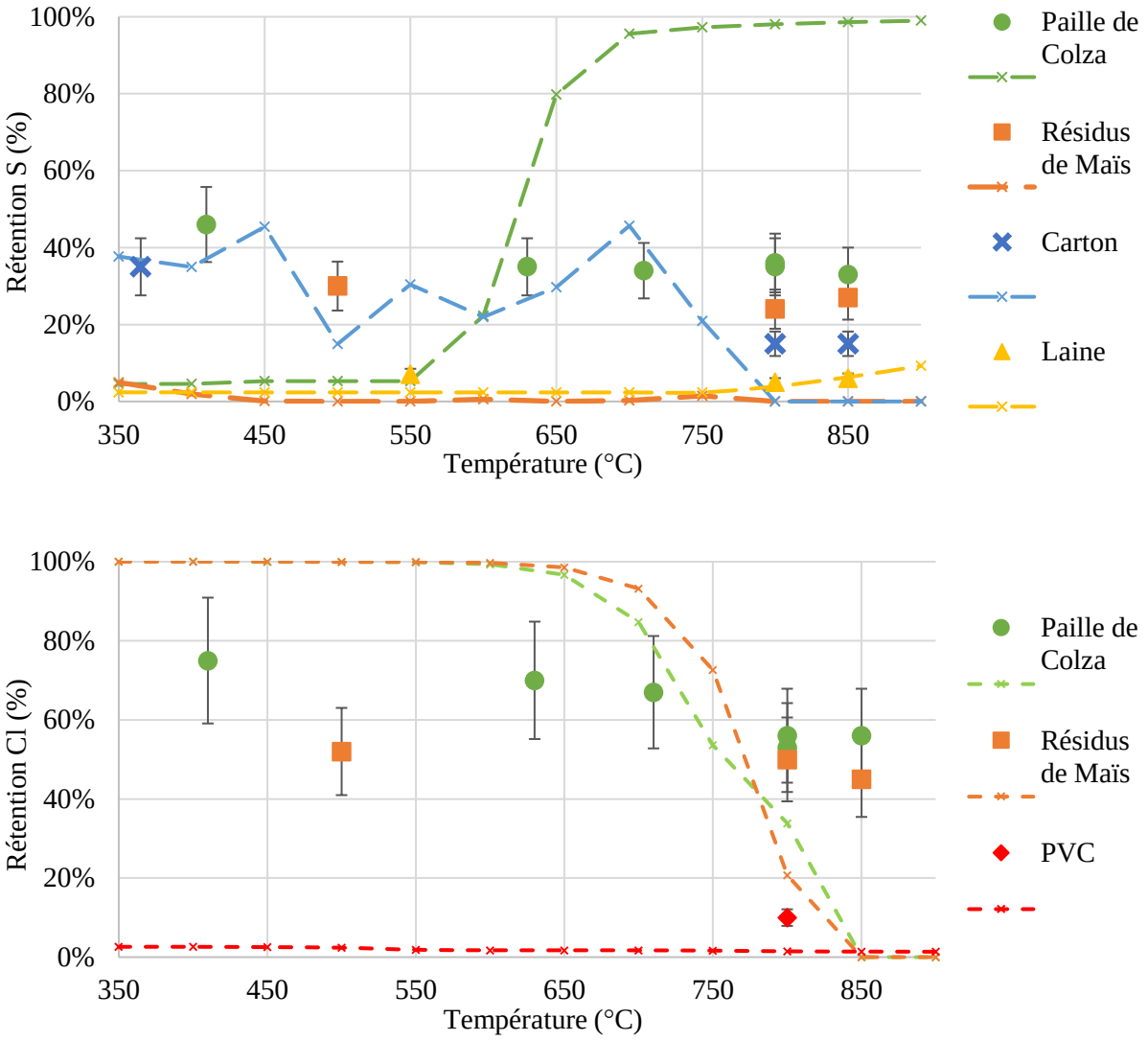

Figure 3 : : Rétention du S et du Cl dans les chars en fonction de la température de pyrolyse: expériences analytiques (points) et simulations thermodynamiques (pointillés)

Les expériences analytiques de pyrolyse effectuées entre 365 et 850°C montrent un comportement de S et de Cl dépendant principalement de la ressource. Pour la laine et le carton, environ 100 % et 65 % du S est libéré dans le gaz respectivement, ce qui correspond à la fraction de S présente initialement sous forme organique. Pour le PVC contenant initialement des

composés chlorés organiques, plus de 90 % du Cl est libéré dans le gaz sous forme d'HCl. Ainsi, il semblerait que le S et le Cl initialement présents sous formes organiques se décomposent et soient facilement relâchés dans la phase gazeuse même à basses températures sans interagir avec d'autres éléments inorganiques. Pour les résidus agricoles, le Cl est principalement sous forme de sels inorganiques (KCl, $KClO_4$), tandis qu'environ la moitié du S est sous forme organique liée à la matrice de carbone et l'autre moitié est sous forme inorganique (sulfates : K_2SO4, $CaSO_4$). En pyrolyse, le relâchement dans le gaz du S et Cl initialement présents sous forme inorganique est partiel. Selon les niveaux de température atteints, différentes phases cristallisées contenant du S et du Cl sont identifiées dans les chars ($CaSO_4$ ou CaS pour la paille de colza, K_2SO_4, KCl, $MgCl_2$ pour les résidus de maïs), ce qui montre la dépendance de la rétention du S et Cl dans le char à la température de pyrolyse et à la composition des cendres de la ressource.

Aucune différence significative dans la rétention de S et de Cl n'a été observée entre les expériences de pyrolyse et de gazéification menées à 800°C pendant une durée de 20 minutes, à l'exception de la paille de colza, qui montre une rétention complète du chlore inattendue après la gazéification. Cependant, après les expériences de gazéification de 60 minutes, la rétention de S et de Cl est nettement inférieure à celle observée après 20 minutes pour les résidus agricoles.

Les résultats obtenus expérimentalement ne sont pas en accord avec les calculs thermodynamiques d'un point de vue quantitatif. Cela peut s'expliquer par les limitations de contact solide-solide et/ou gaz-solide entre le S / Cl et les autres éléments de cendres (Ca, Si, K…) induisant des limitations cinétiques et de transfert de masse en phases gazeuse et/ou condensée. Toutefois, une comparaison qualitative des composés contenant du soufre et du chlore dans les chars tel que le CaS et le KCl montre une cohérence avec les prédictions d'équilibre thermodynamique. Les expériences de gazéification de 60 minutes pour les résidus agricoles se rapprochent davantage des prédictions d'équilibre thermodynamique, en particulier en ce qui concerne la rétention de soufre et de chlore.

Amélioration de la rétention du S et du Cl dans le char par interaction avec les éléments inorganiques

Après avoir mieux compris le comportement du S et du Cl en pyrolyse et gazéification, nous avons exploré l'utilisation d'additifs à base de calcium ainsi que la co-pyrolyse et la co-

gazéification de ressources pour améliorer la rétention de S et de Cl dans le char par leur interaction avec notamment un élément inorganique qui est le calcium.

Les résultats d'ajout d'additifs montrent une légère amélioration de la rétention du soufre dans le char pour certaines ressources, uniquement avec le CaO. Malgré l'ajout d'additifs en quantités suffisantes, l'interaction entre les additifs à base de calcium et le soufre semble n'avoir pas été aussi efficace que prévu. Ces résultats pourraient s'expliquer par le fait que le soufre initialement sous forme organique soit facilement libéré dans le gaz à basse température, tandis que les réactions entre les additifs à base de calcium et le H_2S seraient peu efficaces à ces températures. Nos résultats diffèrent de ceux de la littérature, où sont souvent mis en œuvre des lits fluidisés, dans lesquels le mélange entre les ressources et les additifs est favorisé. Ceci pourrait expliquer des interactions plus favorables entre ressources et additifs dans les lits fluidisés par rapport aux lits fixes, et par conséquent les résultats décevants de nos expérimentations. Cependant, l'ajout de CaO aux résidus agricoles ou au PVC entraîne une augmentation significative de la rétention de chlore. Les analyses par DRX et MEB-EDX révèlent la présence de composés contenant du chlore, tels que le KCl pour les résidus agricoles et le $CaCl_2$ pour le PVC, qui peut expliquer ces résultats.

Le **tableau 2** présente les principaux résultats de la rétention de S et Cl obtenus dans les mélanges de ressources.

Tableau 2 : Principaux résultats de rétention de S et Cl obtenus dans les mélanges de ressources

S			
R1 / **R2**	**Carton**	**Paille de Colza**	**Ecorce de chêne**
Laine	valeurs théorétiques x 2	valeurs théorétiques x 2	valeurs théorétiques x 2
Résidus de Maïs	pas d'effet	-	-
Paille de Colza	pas d'effet	-	pas d'effet

Cl		
R1 / **R2**	**Carton**	**Ecorce de chêne**
Résidus de Maïs	valeurs théorétiques x 1,7	-
Paille de Colza	valeurs théorétiques x 2,5 (rétention totale du Cl dans le char)	Besoin de plus d'investigations avant de tirer une conclusion
PVC	pas d'effet	-

Lorsque la laine est mélangée avec des ressources riches en calcium (carton, paille de colza ou écorce de chêne), les valeurs expérimentales dépassent de plus du double les valeurs calculées théoriquement en supposant qu'il n'y a pas d'interaction entre les ressources. Du sulfure de calcium (CaS) est observé dans les chars par les analyses DRX et MEB-EDX, suggérant une réaction entre S et Ca lors de la co-pyrolyse ou de la co-gazéification. Cependant, dans le cas des résidus agricoles mélangés avec du carton ou de l'écorce de chêne, aucune amélioration substantielle de la rétention du soufre n'est observée. Cette différence pourrait être reliée à la nature du soufre présent dans les ressources : le H_2S et COS relâchés par la laine, qui est riche en soufre organique, réagirait avec le calcium pour former du CaS. Les résidus agricoles, quant à eux, contiennent du soufre organique et inorganique, et montrent une amélioration moins marquée de la rétention du soufre qui pourrait être due aux réactions chimiques moins efficaces avec les ressources riches en calcium. Les ratios molaires Ca/S initiaux dans les ressources varient également, avec un rapport initial inférieur à 1 pour la laine, contrairement à la paille de colza et aux résidus de maïs, ce qui pourrait expliquer les résultats positifs observés pour cette ressource.

D'autre part, les expériences révèlent une augmentation significative de la rétention de chlore pour chaque résidu agricole, les valeurs expérimentales dépassant respectivement 2,5 fois et 1,7 fois les valeurs calculées théoriquement lors du mélange de carton avec de la paille de colza ou des résidus de maïs. En revanche, pour le mélange de carton avec du PVC, aucune amélioration de la rétention de chlore n'est observée. Cela pourrait être attribué aux différences dans le comportement de décomposition thermique entre le PVC et le carton, ainsi qu'à la nature organique du chlore dans le PVC. Le PVC libère rapidement du chlore organique sous forme de composés volatils pendant les premières étapes de la pyrolyse, tandis que le carton nécessite des températures plus élevées pour sa décomposition. Il est possible que ses composés riches en calcium ne puissent initier des interactions réactives avec le chlore qu'à partir de températures supérieures à celle de déchloration du PVC.

Conclusion

Cette étude a révélé que le comportement de S et Cl en pyrolyse ou gazéification dépend principalement de la nature de la ressource, notamment des différentes formes chimiques du S et du Cl et de la composition des cendres (Ca, K). L'ajout d'air lors de la gazéification pendant 20 minutes n'a pas eu d'impact significatif sur la rétention de soufre et de chlore par rapport à la pyrolyse, à l'exception du cas de la paille de colza.

L'amélioration de la rétention du S et du Cl dans le char lors de l'utilisation d'additifs à base de calcium, ainsi que lors de la co-pyrolyse et de la co-gazéification des ressources, a montré des degrés d'efficacité variables, en raison de limites dans l'obtention d'un mélange optimal des additifs au sein des ressources ou des différences de comportement de décomposition thermique entre les ressources. Les meilleurs résultats ont été obtenus, pour S, lors de co-pyrolyse avec ajout d'une ressource riche en Ca (carton, paille de colza ou écorce de chêne) et, pour Cl, en mélangeant la paille de colza ou les résidus de maïs avec du carton. Malgré la mise en évidence d'interactions qui favorisent la rétention de S et Cl, il est essentiel d'approfondir la compréhension des processus chimiques et mécanismes dans ces méthodes afin d'optimiser leur efficacité, dans le but de limiter de manière significative le relâchement du soufre et du chlore dans la phase gazeuse.

Bien que les impacts de ces résultats sur les processus globaux de pyrolyse et de gazéification semblent relativement mineurs, ils peuvent avoir des implications importantes pour le nettoyage du gaz en aval de la gazéification. Cela ouvre des possibilités pour limiter et optimiser le dimensionnement de l'étape de nettoyage.

Introduction

In recent years, the urgent need to address climate change and mitigate its detrimental effects has become increasingly apparent. The improvement of living conditions and the industrial development have led to a significant increase in consumption, resulting in shorter product life cycles and a surge in waste production. This, in turn, has caused a great loss of resources and put immense pressure on the environment, driven by the escalating demand for energy. Furthermore, the subsequent rise in greenhouse gas emissions has resulted in a global temperature increase, extreme weather events, and ecological imbalances. Consequently, there is an undeniable imperative for societies worldwide to transition towards climate neutrality.

In December 2019, the European Commission introduced an ambitious proposal aiming to achieve climate neutrality by 2050, with net-zero greenhouse gas emissions. This objective lies at the core of the European Green Deal, aligning with the EU's commitment to global climate action under the Paris Agreement. Accomplishing such a transition requires a comprehensive and multifaceted approach that encompasses various sectors and industries.

Five sectors emit the bulk of the European Union’s greenhouse gases: 28 percent comes from transportation, 26 percent from industry, 23 percent from power, 13 percent from buildings, and 13 percent from agriculture; across all these sectors, fossil fuel combustion is the biggest source of greenhouse gases, accounting for 80 percent of these emissions (McKinsey & Company, 2020). Consequently, achieving climate neutrality requires a reduction in carbon emissions through the utilization of renewable energy sources and a gradual reduction of reliance on fossil resources.

In the current environmental context, biomass stands out as a remarkable energy source with a near-zero carbon emissions. Unlike exhaustible resources, such as petro-fuels and petrochemicals, biomass presents a sustainable alternative that, when managed responsibly, maintains a relatively short carbon cycle of 1 to 100 years. By using biomass in power utilities, these systems replace exhaustible non-renewable resources with sustainable alternatives that could effectively reduce the overall carbon footprint associated with energy production and consumption.

Moreover, biomass emerges as a particularly attractive renewable power resource due to its versatility. Bioenergy systems, utilizing biomass, can enable the production of various products such as biofuels, biochemicals, and biomaterials.

Considerable technological advances have been made in converting renewable resources, such as biomass and waste feedstocks, into different liquid and gaseous biofuels. Thermochemical

technologies, including combustion, gasification, pyrolysis, hydrothermal liquefaction, and hydro-pyrolysis, show promise in terms of energy (heat and power) production, fuel synthesis, and the generation of fine chemicals. While combustion and pyrolysis primarily focus on energy generation and liquid production respectively, gasification stands out as a versatile thermochemical process capable of handling a wide variety of feedstocks, including agricultural residues, forestry waste, dedicated energy crops, and municipal solid waste.

Gasification has the capability to convert not only biomass but also diverse waste materials, making it a valuable contributor to effective waste management by reducing the burden on landfills and minimizing environmental impacts. The resulting gas, known as syngas, is composed of a mixture of carbon monoxide (CO), hydrogen (H_2), carbon dioxide (CO_2), and methane (CH_4). It can be used for heat and electricity generation or alternatively, it can undergo further processing through catalytic synthesis, such as the Fischer-Tropsch process, or other processes (biological, etc.), to produce chemicals and transportation fuels like methanol, dimethyl ether, and other chemical feedstocks.

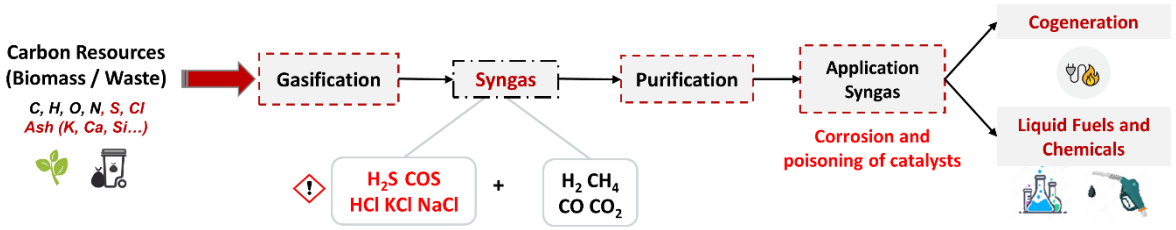

However, as schematized in the figure above, volatile inorganic elements, such as sulfur (S), chlorine (Cl), and potassium (K), commonly found in biomass and waste resources, are often released in the gas phase, in volatile molecules such as H_2S, COS, HCl, KCl or NaCl, during gasification. These molecules present numerous challenges to downstream processes following gasification due to their corrosive nature (e.g., HCl, KCl, NaCl) and their detrimental effects on catalysts employed in subsequent stages of the gasification process (e.g., H_2S, COS). As a result, it is imperative to remove these volatile pollutants to maintain the quality and properties of the product gas.

Moreover, the variability and heterogeneity of waste materials further complicate the situation, making it challenging to establish a clear link between the feedstock composition, operational conditions, and the release of these pollutants.

In this thesis, our primary focus is to improve the understanding and characterization of the behavior of inorganic volatile elements (S, Cl, K...) during biomass and waste pyrolysis and

gasification. Specifically, we aim to explore the impact of different feedstock materials and operating conditions on the release of these pollutants. After gaining a more precise understanding of this release mechanism, the second main objective is to develop and test in-situ cleaning methods that can effectively limit the release of these harmful elements. This approach would not only reduce the need for extensive gas cleaning but also improve the dimensioning of the cleaning process, optimizing the overall gasification system.

We adopted a comprehensive methodology that combines thermodynamic calculations with laboratory experiments and analyses.

Our approach began with a careful selection and characterization of feedstocks from different types of biomass and waste: two agricultural residues with different ash content and composition, as well as three waste components (cardboard, wool, PVC). These feedstocks were chosen as presenting diverse origins and different chemical forms of sulfur and chlorine.

Subsequently, thermodynamic calculations were conducted to explore the stability of sulfur and chlorine species for each selected feedstock, and predict their behavior as a function of pyrolysis and gasification conditions.

The experimental investigations were carried out using a lab-scale induction-heated reactor, with carefully controlled operating conditions. Various analytical techniques were employed to measure the release in the gas and retention in the char of sulfur and chlorine during the conversion, as well as to characterize the solid char produced. We first focused on characterizing the transformation of inorganic volatile elements, studying their distribution between solid and volatile phases, and then, on identifying effective methods for enhancing the retention of sulfur and chlorine in the char.

This methodology enabled us to evaluate the impact of the resource's chemical composition, especially the ash composition, as well as the chemical forms of S and Cl associated with the type of raw material. By combining thermodynamic calculations with experimental data, we could gain a deeper understanding of the transformations.

The present manuscript comprises four distinct chapters completed by the introduction and conclusion.

Chapter 1 provides a comprehensive background on the classification and composition of carbonaceous resources, the gasification process, and downstream cleaning systems. The chapter also discusses the nature and quantity of inorganic species in carbonaceous resources and reviews relevant thermodynamic and experimental studies on their behavior during

pyrolysis and gasification, as well as on the existing solutions implemented to limit their release. It concludes by defining the objectives of the thesis.

Chapter 2 presents the materials and methods used in the study. It covers the selection, procurement, and characterization of the feedstocks, including the chemical fractionation analysis used to characterize the chemical forms of the inorganic elements. The experimental setup, named "PYRATES," is described, along with the thermal characterization of the reactor and the feedstocks during pyrolysis. The chapter also discusses the methods used for the products characterization and presents the experimental conditions of the pyrolysis and gasification tests. Additionally, it details the input of the thermodynamic simulations performed using the FactSage software.

Chapter 3 relates the results obtained through the dual approach, combining both thermodynamic modeling and experiments associated to detailed characterization of the chars. The experimental investigations focus on examining the distribution of S and Cl between the gas and solid phases during pyrolysis. The qualitative characterization of the retention of inorganic elements in the char, X-ray diffraction (XRD) and scanning electron microscopy with energy-dispersive X-ray spectroscopy (SEM-EDX) were used. Additionally, the impact of air addition on the S and Cl behavior was studied, with gasification experiments.

Chapter 4 reports the results obtained from the experimental testing of in-situ cleaning methods aimed at enhancing the retention of sulfur and chlorine in the solid phase through interactions with ash-forming elements. The chapter explores the effectiveness of various additives and investigates co-pyrolysis and co-gasification of resources as potential techniques to achieve this objective.

1.Literature review

1.1 Background of gasification of carbonaceous resources and syngas cleaning systems

1.1.1. Carbonaceous Resources

1.1.1.1 Classification

Carbonaceous resources that are suitable for thermochemical conversion, such as gasification, include different types of biomass and waste feedstocks. However, feedstock having food/feed value and fit for human consumption should not be considered because their use threaten the world's food supply.

The resource can be classified as follow (Gursel et al., 2020):

- Forestry biomass is biomass from forests and other wooded land including tree plantations such as softwoods and hardwoods
- Energy crops are a source of woody biomass for energy, they are fast-growing plants, trees or other herbaceous biomass that are harvested annually specifically for energy production. These include grasses such as switchgrass or wheatgrass, and short rotation woody biomass such as poplar, willow…
- Primary residues include post-harvesting crops and residues deriving from forestry and agriculture:
    - Primary forest residues also called logging residues are the materials resulting from tree collection/harvesting operations and include treetops, twigs, and branches.
    - Crop residues include straw, stem, stalk, leaves… that come from cereals, cotton, vegetables…
- Secondary residues are substances that are not the desired final products of a production process:
    - Processing forestry residues include fine and coarse wood, sawdust, and bark produced during wood processing at pulp and paper industry, sawmills or veneer mills, as well as black liquor produced during the Kraft pulping process (Walsh, 2014).
    - Agro-industrial wastes include peels, seed and shells from fruits and vegetables, rice husks from rice mills, molasses from sugar and bagasse refineries, residues from palm oil mills, wine grape pomace composed of skins, seeds, and the remainder of the pulp.

  - Animal manures are the solid, semisolid, and liquid by-products generated by animals grown to produce meat, milk, eggs, and other agricultural products for human use and consumption.
- Tertiary residues include urban post-consumer residue streams and residues deriving from industries, known as wastes:
  - Paper and cardboard wastes from separate collection by businesses and households, mechanical treatment of waste and pulp, and paper and cardboard production.
  - Wood wastes from wooden packaging, furniture wastes, construction and demolition of buildings.
  - Animal, vegetal and mixed food wastes deriving from municipal waste and coming from food preparation, restaurants and households.
  - Dried wastewater treatment sludge from municipal sewerage water and organic sludge from food preparation and processing.
  - Textile and leather wastes from industries and households.
  - Non-biomass materials such as used tires, plastics and metals from packaging, municipal solid waste, commercial and industrial waste, and electronic waste.

In the context of a circular economy aiming to reduce dependency on primary materials and energy, many factors should be considered when choosing feedstocks for an efficient and sustainable utilization of the resources and an extension of their longevity thorough cascading uses (Sini Eräjää, 2015).

The cascading use principle gives priority to higher value uses that allow the reuse and recycling of products and raw materials and promotes energy use only when other options are starting to run out. For example, products at end of life are first reused or recycled mechanically or chemically, and then, when they cannot be reused or recycled, they are biodegraded or incinerated. Biomass is processed into a material and this product is used at least once more in materials before energy recovery purposes.

Therefore, in the list presented before, feedstock classified as secondary or tertiary residues should be favored for thermochemical conversion for energy applications.

1.1.1.2 Composition

The whole process of thermal conversion of carbonaceous solid fuels is influenced by the type of feedstock used, its physical characteristics (e.g. particle size, bulk density, moisture content, calorific value), and its chemical composition.

Biogenic materials suitable for thermochemical conversion are mainly lignocellulosic materials composed of three different types of natural polymers: 65–85 wt% of sugar polymers (principally cellulose and hemicellulose) with another 10–25 wt% of lignin (De et al., 2018). They may also contain minor amount of extractives (e.g. fats, waxes, alkaloids, proteins, pectins, gum, resins, starches and oils) and ash (inorganic metals and salts). They include forestry and plantation residues, by-products and residues deriving from wood processing industry as well as the pulp and paper industries.

The manufacturing process and the type of added nutrients and additives influence the composition of biomass by-products (e.g. paper, cardboard, textiles). Textiles may be fabricated from natural fibers (wool, cotton, silk, leather), or even from synthetic fibers as (acrylic, nylon, polyester) or even a mixture of both.

Non-biogenic (or partly non-biogenic) tertiary residues as plastics, rubber, and used tires have a more heterogeneous nature depending on the type of product, its manufacturing process and the nature of additives used during the processing. Deriving from fossil-based sources, they contain different types of polymers such as, high density and low- density polyethylene, polyvinyl chloride, polypropylene and additives. Plastics have different chemical structure and contents of carbon, oxygen and hydrogen; their common features include relatively high volatile content and heating value, but very low moisture and ash content (Burra and Gupta, 2018).

Overall, the chemical composition of carbonaceous material can be described by three major parts.

- Moisture, which is the wet content of the feedstock
- An organic part, being the structure of the material, with the main elements C, H and O
- A generally smaller amount of inorganic compounds including the volatile elements S, Cl, N, and F, and ash as the content of non-combustible inorganic matter (mineral) left after the fuel is completely burned (Ca, K, Si, Mg, Na, Al, Fe, P and Zn and other trace elements as Mn, Ti, B, Be, Rb, Cr, Ni, Cu, Se).

Table 1 shows the elemental composition, ash content, and lower heating value for some typical family resources of biomass and waste. In general, biomass and biogenic waste resources exhibit a predominant content of carbon, which is the primary element in organic matter. However, the ash content of biomass and waste resources can vary significantly depending on their nature. While woody biomass typically has a relatively low ash content, other biomass like agricultural residues or fossil resources as waste tires may have higher ash content due to

the presence of minerals. On the other hand, fossil fuel-derived resources, such as rubbers and waste tires, generally have a higher lower heating value compared to biomass and biogenic waste. This is mainly due to their higher carbon content and lower moisture and oxygen content, resulting in a more efficient combustion process.

Table 1: Elemental composition, ash content, and lower heating value of typical biomass and waste family resources

Resource	Elemental Composition (wt %)	Ash Content (wt. %)	Lower Heating Value (MJ/kg)	References
Woody Biomass	C: 43.6 – 50.6 H: 6.4 - 6.8 O: 42 - 43 N: 0.1 - 1.4 S: 0.2	0.3 – 1.23	14 - 20	(Anniwaer et al., 2021; Du et al., 2014; Pinto et al., 2010)
Agricultural residues	C: 36.2 - 40.4 H: 5.4 – 9.3 O: 32.4 - 54.1 N: 0.2 – 0.71 S: 0.2 – 0.5	10.5 – 15	13 – 14.5	(Anniwaer et al., 2021; Du et al., 2014)
Cardboard	C: 40 - 43 H: 5.4 – 5.7 O: 41.7 - 52.7 N: 0.16 – 0.28 S: 0.1 – 0.6	9.4 - 9.6	14	(Cai et al., 2021; Zhou et al., 2013)
Paper	C: 34.9 – 42.7 H: 4.4 O: 31.3 N: 0.14 – 0.2 S: 0.015	29.2		(Zhou et al., 2013)
Waste tires	C: 68.8 - 82.4 H: 0.7 - 8.2 O: 0.8 - 3.3 N: 0 - 0.9 S: 1.9 – 5	5.1 – 18.6	38.7	(Campuzano et al., 2021; Carmo-Calado et al., 2020; Hu et al., 2014)
PVC (Polyvinyl chloride)	C: 47.6 – 69.3 H: 5.2 – 9.8 O: 17.3 - 32.8 N: 0 – 0.1	0.03	20.4	(Bläsing et al., 2015b; Cai et al., 2021)
PS (Polystyrene)	C: 88.5 H: 7.6 O: 5.3 N: 0.5 S: 0.2	1.49	37.7	(Cai et al., 2021)
Rubbers	C: 44.3 - 69.2 H: 4.3 - 7.4 O: 22.8 – 50.6 N: 0 - 0.51 S: 0 – 0.13	0.6 – 3.81	31.6	(Carmo-Calado et al., 2020; Chin et al., 2014)

1.1.2. Gasification

Gasification is a thermochemical transformation in which carbonaceous resources (biomass, waste), subjected to a high temperature, in the presence of an oxidizing gas (air, O_2, H_2O, CO_2), react and are converted into a gaseous fuel.

The obtained products are:

- major gas species: di-hydrogen H_2, carbon monoxide CO, carbon dioxide CO_2, methane CH_4, water vapor H_2O
- other hydrocarbons: C_2H_x, C_3H_y, benzene, toluene and condensable tars
- char particles, ash, and impurity inorganic species.

The product gas known as synthesis gas, or syngas, can be used after purification and cleaning in cogeneration (heat and electricity production) or for the synthesis of liquid or gaseous fuels (**Figure 1**).

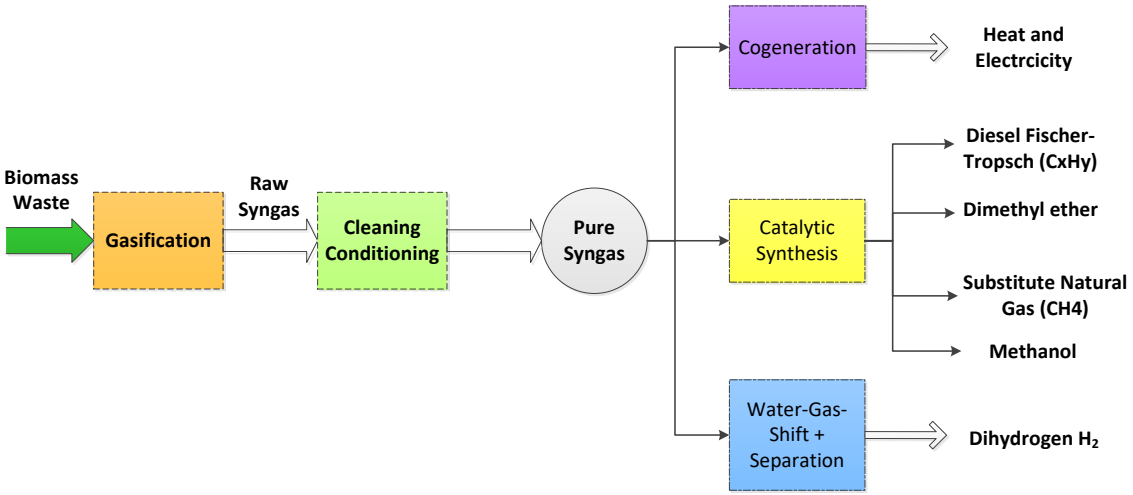

Figure 1: Applications of purified synthesis gas produced from gasification

1.1.2.1 Gasification Phenomenology

In a typical gasification process, the feedstock is initially dried, and then it undergoes a thermal degradation (pyrolysis). The products of pyrolysis (solid, liquid, gas) react among themselves and with the gasifying medium to form the final products. Gasification is a globally endothermic transformation, and therefore requires an input of energy to take place. The gasification process can be either allothermal (external energy input) or autothermal. In the case of allothermal gasification, the gasification agent is composed only of a moderator (steam, carbon dioxide), and the heat needed for the endothermic process has to be supplied from an external source. In the second case, the thermal energy necessary for drying, pyrolysis, and

endothermic reactions comes from exothermic reactions taking place in the gasifier by introducing air or O_2 as the gasifying agent, in a smaller amount than would be required for complete combustion. A scheme of the mechanisms of gasification is presented below (**Figure 2**).

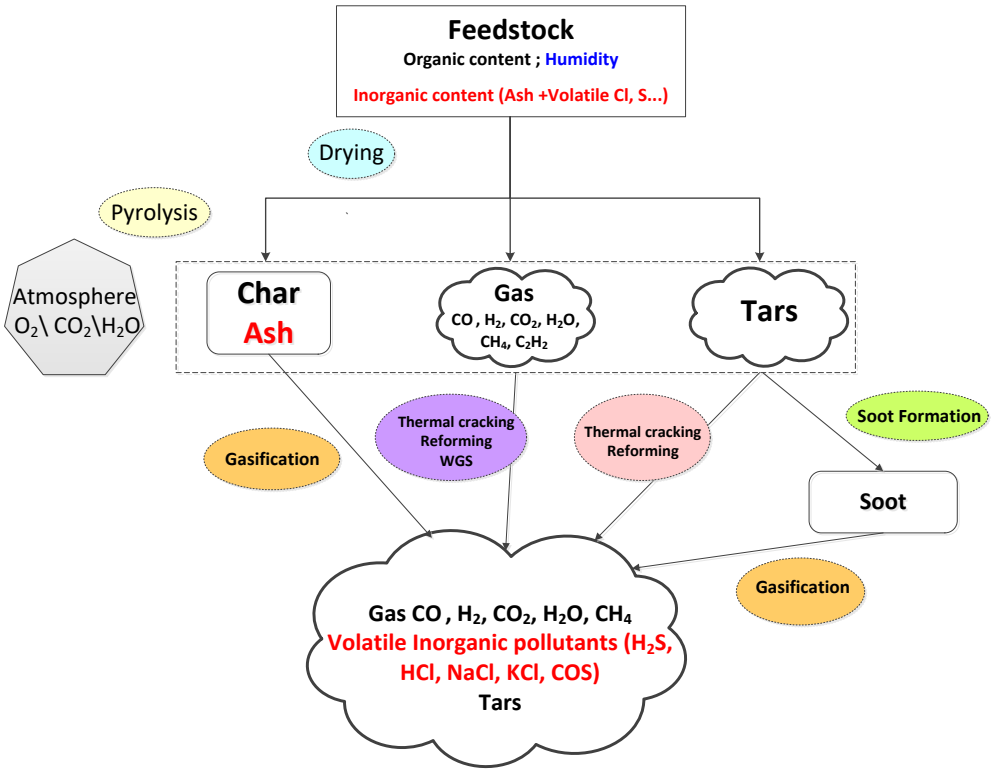

Figure 2: Schematic diagram representing the mechanisms involved in gasification

- Drying

The first step of the gasification process, as soon as the solid fuel is heated, is drying. The drying step is determined by the rate of heat and mass transfer in the feedstock bed and in the particles.

- Pyrolysis

On further heating, as temperature increases, the thermal degradation process of the feedstock, referred to as pyrolysis or devolatilization, takes place from around 250˚C and does not need any external oxidizing agent. Volatile matter present in the solid fuel is liberated, leaving behind a solid residue. This solid phase residue is the char, which is mostly composed of carbon, and can also contain hydrogen, oxygen, and inorganic elements forming the ash. The reaction products are conventionally divided into three main groups: non-condensable gases, condensable species (organic species and water vapor) and char. The gas phase is generally composed of CO, CO_2, H_2, CH_4 and light hydrocarbons C_2 - C_3. Upon cooling, heavy hydrocarbons referred to as tars and water condense into liquids. The yields of these products

and their composition vary according to the feedstock used, the operating temperature and the heating rate.

- Gas Phase Reactions

The main families of reactions likely to take place in the gas phase are presented below (Basu, 2010):

- Thermal cracking reaction:

The hydrocarbons produced during pyrolysis can undergo thermal cracking reactions leading to the production of smaller molecules. Some C-C or C-H bonds are broken under the effect of heat to form smaller molecules of hydrocarbons, unsaturated hydrocarbons and hydrogen.

$$(1)\ C_nH_m \rightarrow C_vC_w + C_xH_y$$

$$(2)\ C_nH_m \rightarrow C_xH_y + H_2$$

- Reforming reaction

In the presence of water vapor or carbon dioxide, tars and light hydrocarbons can react according to the reforming reactions. These reforming reactions are endothermic.

$$C_nH_m + nH_2O \rightarrow nCO + (n + \frac{m}{2})H_2$$

$$(3)\ C_nH_m + nCO_2 \rightarrow 2nCO + \frac{m}{2}H_2$$

- Water-gas shift reaction:

It involves water vapor and carbon monoxide forming dihydrogen and carbon dioxide. This reaction is reversible and slightly exothermic. For temperatures below 800˚C the reaction is favored in the direct direction - production of CO_2 and H_2 – and for temperatures above 800˚C it is favored in the indirect direction - production of CO and H_2O.

$$(4)\ H_2O + CO = CO_2 + H_2 \qquad \Delta H\text{=-41 KJ/mol}$$

- Partial oxidation reaction

In a gasification reactor, it is possible to inject oxygen or air as the gasifying medium in order to provide energy by combustion of part of the fuel (autothermal reactor). In this case, the gases can be partially oxidized following the reaction below. This partial oxidation reaction is exothermic.

$$(5)\ C_nH_mO_l + (\frac{n}{2} + \frac{m}{4} - \frac{l}{2})O_2 \rightarrow nCO + \frac{m}{2}H_2O$$

- Soot Formation

After the pyrolysis process, some of the tars and gases may react and produce soot. Soot consists in solid particles mainly composed of carbon, which can be formed from 1000˚C by polymerization of different precursors in the gas phase. These precursors are poly-aromatic hydrocarbons or other lighter hydrocarbons such as toluene, benzene or acetylene (Higman and Van der Burgt, 2003).

- Gasification of Char

Char is the solid residue from feedstock produced during pyrolysis. It is mostly composed of carbon and can be oxidized. Char gasification is the rate-limiting step in gasification. Devolatilization is completed within a few seconds or tens of seconds, but char gasification requires minutes or hours at current reactor operating conditions. The slowest reactions in gasification, and therefore those that govern the overall conversion rate, are the heterogeneous reactions between carbon and steam or CO_2, namely the water gas and Boudouard reactions (Higman and Van der Burgt, 2003):

$$(6)\ C + H_2O \rightarrow CO + H_2 \qquad \Delta H = +131\ KJ/mol$$

$$(7)\ C + CO_2 \rightarrow 2CO \qquad \Delta H = +172\ KJ/mol$$

Char and soot can also be partially burned by oxygen:

$$(8)\ C + \frac{1}{2}O_2 \rightarrow CO \qquad \Delta H = -111\ KJ/mol$$

1.1.2.2 Characteristic Process Parameters

The important key operational and performance parameters of a gasification process that influence the gasification products are presented below.

- Gasifying Media

The heating value and the composition of the gas produced in a gasifier are strong functions of the nature and amount of the gasifying agent used. The main gasifying agents used for gasification are oxygen, steam, air and carbon dioxide. Oxygen gasification produces gas with the highest heating value followed by steam, carbon dioxide and air gasification (Basu, 2010). When air is used instead of oxygen, the nitrogen dilutes the products; when using steam a higher hydrogen content is expected.

- Equivalence Ratio

The Equivalence Ratio ER is defined in the equation below, as the ratio of the actual oxygen supply to the stoichiometric oxygen required for complete combustion. It must be significantly below 1.0 to ensure a condition far from a complete combustion.

$$\mathrm{ER} = \frac{\text{Actual } O_2 \text{ supply}}{\text{Stoichiometric } O_2 \text{ requirement}} \quad [1.1]$$

The quality of gas obtained from a gasifier strongly depends on the value of ER employed. Higher ER results in lower H_2 and CO yields, with an increase in CO_2, which in turn decreases the heating value of the syngas because of the enhancement in the oxidation reactions (Sikarwar et al., 2017). However, a higher ER induces a higher reactor temperature and therefore enhance the carbon conversion of the feedstock.

- Temperature

The composition of producer gas depends on the operating temperature of the gasifier. Temperature has an effect on the carbon conversion, gas yield, gas heating value, and finally char and tar yields.

- Steam to carbon ratio

When steam is used as a gasifying medium supplied to the gasifier, the steam-to-carbon ratio plays an important role in determining the final gas composition (Jong and Ommen, 2014).

$$\mathrm{S/C} = \frac{\text{Moles of steam}}{\text{Moles of carbon in the feed}} \quad [1.2]$$

1.1.2.3 Types of Gasifiers

In the actual gasification processes, a broad range of reactor types is used with different degrees of development and for various applications. Technologies used for gasification can be classified into four groups: fixed bed or moving bed gasifier, fluidized bed gasifier, entrained flow gasifier, and plasma gasifier. The difference is based on the means supporting the solid fuel in the reactor, the direction of flow of the feed and gasifying agent, and the source of heat supplied to the reactor. The different types of gasifiers with their characteristics are presented in **Table 2.**

Table 2: Characteristics of the different types of gasifiers (Prabir Basu, 2006; Lemmens et al., 2007; Materazzi et al., 2013; Santanu et al., 2018)

	Fixed bed	**Fluidized bed**	**Entrained flow**	**Plasma**
Temperature	500 – 1000°C	700-900°C	1200 – 1500˚C	>1500°C
Pressure	1–100 bar	1–30	20–80	1–30
Particle Size	large particles > 10mm	small particles 2-10mm	very fine particles <1mm	no requirements
Residence time of particles	stay in the bed until their discharge	minutes or hours	very short (1–5 s)	minutes or hours
Residence time of gas	10^3 – 10^4 s	10 – 100 s	a few seconds	a few seconds
Production Capacity	0.01-10 MW_{th}	5 -100 MW_{th}	>50 MW_{th}	
Advantages	- simple and low-cost	- excellent gas–solid mixing - high carbon conversion rate - low tar production	- rapid fuel conversion - low tar production	- no particle size requirements

1.1.2.4 Impurity Species

Besides the desired combustible components (CO, H_2, CH_4 …) obtained from the gasification process, the product gas contains different impurity species, which makes it far from being applicable in downstream conversion processes. Therefore, removal of impurities from the gas is required before the end use of the product gas. The most relevant classes of impurity species are particulate matter, tars, sulfur, chlorine and nitrogen species, alkali and other trace elements. The concentration of such species in the product gas strongly depends on the feedstock composition and on the layout and conditions of the gasification process. Some common impurities include:

- Particulate matter

The particulate matter found in the gas consists of the fine carbon-containing ash particles, soot, dust and unconverted char. These particles are emitted from the gasifier in a diameter range of

0.1 – 100 μm (Jong and Ommen, 2014). The inorganic compounds in these particles are alkaline earth metal compounds (Ca, Mg oxides), silica (SiO_2), alkali species, iron compounds and other minor inorganic species as Zn, Pb, Cu, etc. depending on the biomass source gasified. It is important to know their behavior in the thermal process in order to select an efficient cleaning methodology to avoid their related issues. For example, heavy metals may pose a threat to the environment or to human health by dispersion in the atmosphere or leaching from the solid residues (Järup, 2003).

- Tars

Tars are defined as the entity of all organic hydrocarbons with a molar mass higher than benzene. Tar quantity and species composition depends on the gasifier type, the type of feedstock, and the gasification conditions (temperature, pressure, oxidizer-to-fuel ratio). The condensation of tars and their deposition during the process represents a real hazard, resulting in fouling and clogging of fuel lines. They can also form soot, which in downstream applications leads to higher emissions of particulate matter and CO (Casari et al., 2020).

- Inorganic Pollutants

Inorganic pollutants including sulfur, nitrogen, chlorine and alkali species constitute a major part of the impurity species released in the gasification process.

- Sulfur compounds

Depending on the sulfur content of the feedstock, sulfur species are formed as part of the product gas. These species consist usually of H_2S as a major compound, COS, CS_2, and organic compounds such as thiophenes C_4H_4S, mercaptans R−SH (Jong and Ommen, 2014).

- Alkali salts and other trace elements

The presence of alkali metals salts such as KCl and NaCl in gasification-derived syngas is a serious issue because of their reactive and volatile nature. Apart from the alkali metals, other metallic elements such as mercury, arsenic, cadmium, zinc and selenium can be found depending on the type of the feedstock. Due to their highly toxic nature, their emissions are heavily controlled (Nzihou, 2020).

- Halides

Gaseous hydrochloric acid (HCl) is a common contaminant in syngas, its concentration depends on the initial chlorine content of the feedstock.

- Nitrogen compounds

The main nitrogen compounds in gases produced by biomass gasification are ammonia (NH_3) and to a lesser extent hydrogen cyanide (HCN) and other species like aromatic nitrogen compounds (e.g., pyridine) and HNCO (Sikarwar et al., 2017).

The presence of these inorganic species poses many problems and is one of the major technological barriers to the downstream gasification processes. This problem is present as we seek to use in the process all types of resources including residues and wastes that are particularly rich in inorganics. The compounds formed from the inorganic content, in particular H_2S, COS, HCl, NaCl and KCl, may cause undesirable effects in the gasification reactors as well as in the downstream processes such as corrosion and fouling of heat transfer surfaces (Bryers, 1996), and bed agglomeration (Piispanen et al., 2012) caused by alkali chlorides, sulfates, and silicates. An additional and serious problem caused by the presence of inorganic species, especially S, is the poisoning of catalysts used in downstream gasification processes such as Fischer-Tropsch or methanol syntheses and fuel cell applications (Hepola and Simell, 1997; Richardson et al., 2012). The severity of these effects depends on the inorganic content and properties of the fuels such as ash composition and the nature of the associations of elements in the fuel. In addition, the operating conditions as the reactor temperature, and the atmosphere in the reactor have a major influence on the transformation and release of the inorganic content from the feedstock (Tchoffor et al., 2013). These aspects will be detailed in section 1.2.

1.1.3. Syngas Cleaning Systems

Suitable gas clean-up technologies have to be implemented in order to remove the undesirable compounds. The tolerance of syngas end-use systems for these pollutants is highly variable, and for each plant and application, the acceptable levels may be different. **Table 3** provides examples of syngas specifications of gaseous inorganic impurities required for several applications. There is no hard data on maximum levels for impurities, as a rule-of-thumb the maximum values are assumed.

Table 3: Examples of syngas purification requirements for different applications (Aravind and de Jong, 2012; Arena, 2012; Woolcock and Brown, 2013)

Syngas Application	Sulfur compounds (H_2S, COS)	Halides (mainly HCl)	Alkali compounds (K, Na)	Nitrogen compounds (HCN, NH_3)
Gas engines	<20 ppmv	<1 ppmv	<0.02 ppmv	<55 ppmv
Gas Turbine	<20 ppmv	<1 ppmv	<0.024 ppmv	<50 ppmv
Solid oxide fuel cell (SOFC)	1 ppmv	1 ppmv	Few ppmv	-
Methanol synthesis	<1 mg/m^3	<0.1 mg/m^3	-	<0.1 mg/m^3
Fischer-Tropsch synthesis	<0.01 ppmv	<0.02 ppmv	<0.01 ppmv	<0.01 ppmv

In applications involving the catalytic conversion of syngas into chemicals or fuels, such as methanol and Fischer-Tropsch syntheses, the catalyst poisoning effect is the most known. Its tolerance to impurity is an economic parameter where investing in final gas cleaning versus the catalyst lifetime needs to be considered. Gas quality requirements are highly restrictive in such applications, compared to internal combustion systems as gas engines or gas turbines. The use of steam-cycle power stations for electricity generation is the least demanding application in terms of fuel gas purity.

In order to fit the requirements of the desired application, syngas cleaning aims to remove or convert, apart from tars, particulates (unburnt char as well as ash), sulfur compounds (H_2S, COS), nitrogenous compounds (NH_3, HCN), alkali metals (Na, K), halides, and heavy metals (Pb, Hg). In this section, we delve into post-gasification cleaning systems that are strategically placed downstream and typically involve the use of advanced filtration technologies, scrubbers, and separation units to meet stringent quality standards. However, in section 1.2.3, we explore in-situ cleaning methods implemented within the gasification process itself. Gas cleaning can be carried out at low (ambient) temperature, intermediate temperature, also called warm gas cleaning (up to 350˚C), and high temperature (>350˚C). **Figure 3** represents three different cases of gas cleaning processes at different temperature levels.

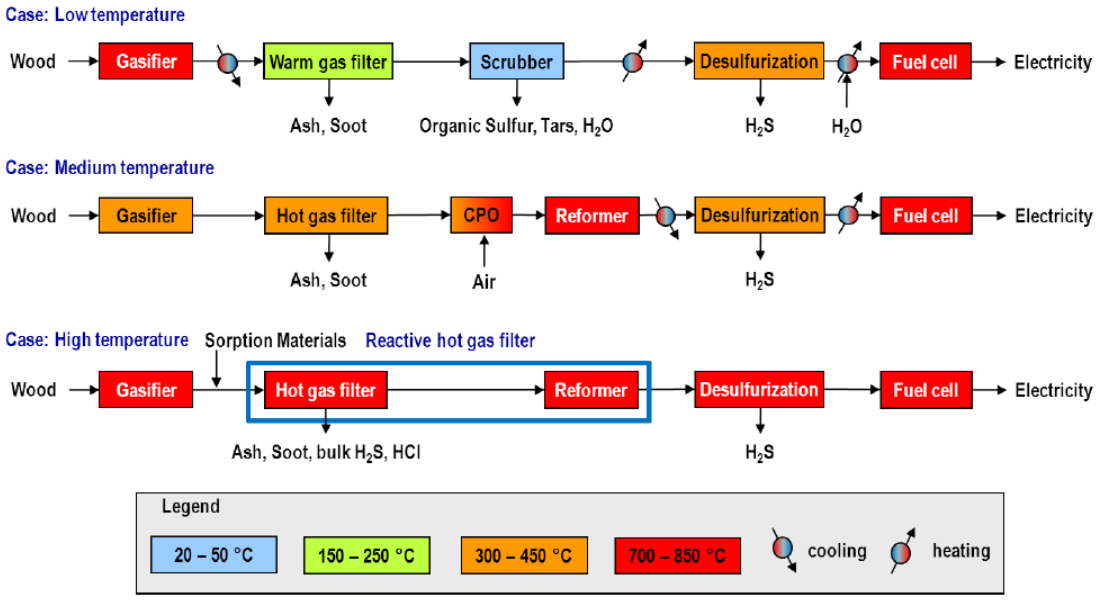

Figure 3 : Representation of gas cleaning processes at low, medium and high temperature (Rhyner, 2013)

Low-temperature cleaning train is mostly separation-based; it employs a combination of physical separation devices to achieve the desired separation. The mostly used devices are scrubbers (both wet and venturi), cyclone separators, filters (metallic, fabric, bed and bag types) used in a sequence to clean raw producer gas. Other cleaning devices have also been developed such as wet electrostatic precipitators, absorber beds, cyclones and rotational particle separators (Santanu et al., 2018). Alkali compounds, mostly in the form of salts of Na and K, remain in vapor phase in raw gas if the temperature is sufficiently high in the gasifier (≥700°C). Gas coolers or spray scrubbers condense these alkali vapors, which then form fine solids (ash) and together with tars, are removed in cyclones and barrier filters. Halides also stay in vaporized form in the hot raw gas, and are then transformed to aqueous acid upon cooling (in cooler or scrubber) to be separated from gas stream. Wet scrubbing can also remove sulfur species and ammonia from the raw gas.

While low temperature gas cleaning requires cooling and reheating of the producer gas in order to fulfill the temperature limits of other units, it is not the case in medium and high temperature cleaning. Medium-temperature clean-up of a producer gas originating from the updraft gasification of wood has been successfully implemented (Nagel et al., 2011). After filtration, the gas passed by catalytic partial oxidation transforming tars and sulfur containing hydrocarbons to lighter S-free hydrocarbons and permanent gas species like CO, CO_2, H_2, H_2O and H_2S. Then, H_2S was removed by passing the gas over an active bed sorption material.

Hot gas cleaning is a combination of separation and conversion and presents many advantages; it improves energy efficiency, reduces costs, avoids heat and thermal losses, and prevents fouling of equipment due to tar condensation (processing above their dew points). A reactive hot gas filter combining the hot gas filtration, sorption of acid gas and catalytic reforming in a single unit operable at higher temperature (850°C) has been proposed by (Rhyner, 2013).

Each cleaning option has its different level of effectiveness depending on the following downstream application. For example, hot gas cleaning presents efficiency benefits and lower operational costs; it is specifically advantageous when applications have high inlet temperatures. However, when low inlet temperature processes are applied directly after the gas cleaning, the syngas has to be cooled, and the potential benefits are expectedly less apparent. Even if medium purity requirements are met with different cleaning systems, significant improvements are necessary to meet the much more severe requirements as those related to catalytic synthesis. New methods and approaches are increasingly being proposed and evaluated in order to upgrade these clean-up technologies, and make them more suitable for implementation with the downstream gasification systems.

1.1.4. Conclusion

Gaseous inorganic pollutants are undesirable by-products of gasification, and one of the major technological barriers to the downstream processes (fuel synthesis or energy transformation) by posing threats to downstream components and energy conversion equipment. Several parameters such as the nature of feedstock, the type of gasifier, and the operating conditions influence their behavior and mechanism of release. Depending on the tolerance levels of the application equipment or final energy conversion process, removal techniques of these gaseous inorganic pollutants and syngas cleaning systems need to be implemented without compromising, as much as possible, the sensible heat of the raw product gas. A complete understanding of the behavior of inorganic species is therefore necessary in order to allow optimizing the design of the cleaning steps for syngas. This thesis will focus particularly on sulfur and chlorine (HCl and alkali compounds) species released during pyrolysis and gasification of biomass and waste. The following section presents a state of the art on the behavior (retention or release) of inorganic pollutants during the gasification of different types of biomass and waste, and the solutions implemented to limit their release found in literature. The following points will be discussed:

- The quantity and chemical forms of sulfur and chlorine present in different resources
- Their transformation (retention or release) in the gasification process based on experimental and thermodynamic approaches
- The abatement methods implemented for reduction of their release.

1.2 State of the art on the behavior of inorganic elements during pyrolysis and gasification

1.2.1 Quantity and chemical form of inorganic species

Biomass and waste can contain a wide variety of inorganic species, including minerals, metals, and metalloids. The quantity and chemical form of these inorganic species can vary depending on the type of biomass or waste, as well as its source and processing history. Some common inorganic species found in biomass and waste include:

- Sulfur, chlorine and nitrogen,
- Minerals such as calcium, potassium, magnesium, sodium and phosphorus,
- Metals: such as aluminum, iron, magnesium, zinc, copper, lead, mercury, and chromium,
- Metalloids: such as arsenic and selenium.

The quantity and chemical form of these inorganic species can have important implications for the handling, processing, and disposal of biomass and waste. On the one hand, some elements, such as metals and rare earth elements, can constitute valuable resources that could be recovered and reused. Some elements can pose environmental and health risks if they are released into the air, water, or soil. An important aspect in understanding the behavior of an element is to investigate first in which chemical form it is present and how it is associated in the fuel structure. Since our focus in this study is the behavior of sulfur and chlorine, a description found in literature on their quantity and chemical forms is detailed below.

1.2.1.1 Sulfur

Sulfur forms a variety of different compounds, both organic and inorganic. In the former case, sulfur is incorporated into the carbon matrix, while it is not in the latter case. **Table 4** presents the sulfur content in different types of biomass and solid wastes.

- Biomass

In biomass, sulfur is a macronutrient for plants that is partly metabolized and partly used in its ionic form. The sulfur is absorbed from the soil through the roots, typically in the form of sulfates. Upon reaching the leaves of the plant, a part of the sulfates undergoes a gradual reduction, resulting in the incorporation of S into the organic structure of the plant (Kopriva, 2017). Organic sulfur is often present in forms involving covalent bonds similar to nitrogen such as in amino acids, cysteine and methionine, from which plant protein is synthesized. These are insoluble or only slightly soluble in water solutions (Maria Zevenhoven et al., 2012). (Struis et al., 2008) reported the presence of organic disulfide, methylthiol and organic sulfonate or organic sulfate in samples of Norway spruce, both in the sap and heartwood, but in different concentrations. Several studies (Knudsen et al., 2004b, 2004a; Werkelin et al., 2010) have shown, that 40-50% of the total sulfur content in woody biomass and annual biomass such as straw, stalks, and other agricultural residues was present as inorganic sulfur, most likely in readily soluble salts such as alkali sulfates (K_2SO_4, …); the rest may be assumed to be organically associated. Virgin or fresh biomass contains little to no sulfur. However, excess sulfate in the soil, such as overconsumption of fertilizer, is absorbed by the plant roots resulting in a greater amount of sulfates (De Kok et al., 1993). This concerns especially agricultural crop residues exposed to large amounts of fertilizer such as wheat straw and rice straw (Davidsson et al., 2002).

Biomass-derived feedstock, such as paper, cardboard, and food waste commonly found in municipal waste, often contains high levels of sulfur. Cardboard and paper production can involve the use of additives and chemicals, with some of them containing sulfur, to improve properties such as strength, brightness, or printability. Sulfur in food waste is derived from some sulfur-containing components, including animal proteins (e.g., fish, pork, and chicken), plant proteins (e.g., tofu) and vegetables (e.g., cabbage and garlic) (Zhang et al., 2023).

Sewage sludge is a by-product from wastewater treatment; it is mainly composed of organic matter and inorganics, and it contains some heavy metals, toxic pollutants, and pathogens. Compared to other biogenic feedstock, sewage sludge contains a high sulfur content. In raw dried sludge, sulfur compounds were found in organic forms mainly as thiol/thioether, thiophene and sulfone and in inorganic forms only as silicon disulfide SiS_2 (Yan et al., 2021).

Leather wastes present sulfur, nitrogen and chromium concentrations that are significantly much higher than those found in other biomass (Godinho et al., 2007, 2011). Several sulfur compounds are used in the hide tanning process. Among those is sodium sulfide, added in the

depilation stage, ammonium sulfate $(NH_4)_2SO_4$ and sodium hydrogen sulfite $NaHSO_3$, applied during deliming, and the tanning agent ($Cr(OH)SO_4$) itself (Godinho et al., 2007; Hu et al., 2011).

Wool fiber have been used as a textile raw material for apparel and home textiles for years. It contains a significant sulfur content that is typical of proteins including amino acids, such as sulfur-containing cystine (Das and Das, 2022).

- Fossil resources

Coal is one of the major fossil feedstocks for power and thermal generation due to its abundance and large accessibility, and it has a high sulfur content that usually varies within the range of 0.5% to 5 wt% (Chou, 2012). Sulfur associations in solid wastes deriving from fossil resources depend on several factors such as the type of product and its manufacturing process.

Rubber, as well as plastic polymers such as, polyethylene terephthalate (PET), high density and low- density polyethylene (HDPE and LDPE), polyvinyl chloride (PVC), polypropylene (PP), polystyrene (PS), have a relatively low sulfur content.

Spent tires constitute another type of waste with a high heating value, that is rich in sulfur. In general, tires are made of rubber, carbon black, plasticizer, vulcanizing agent and other additives (Williams and Besler, 1995). The sulfur content is about 1–3 wt.% (Hu et al., 2014; Lopez et al., 2017; Murena, 2000), originating from sulfur containing additives used to cross-link the polymer chains within the rubber, and to harden and prevent excessive deformation at elevated temperatures (Hu et al., 2014). In addition, the accelerator is typically an organosulfur compound which acts as a catalyst for the vulcanization process (Williams and Besler, 1995). (Hu et al., 2014) investigated the sulfur speciation in scrap tires by X-ray photoelectron spectrometry and found that sulfur was in the form of thiophenic compounds and inorganic sulfides (69.9% and 30.1% respectively).

Table 4: Sulfur content in different types of biomass and solid wastes

Sources	Examples	Sulfur content (wt.%, dry basis)	References
Lignocellulosic biomass	Wood pellets, wood chips, Oak	0.003-0.04	(Cheah et al., 2014; Schmid et al., 2018; Schweitzer et al., 2018)
Crop residues	Rice straw, wheat straw, corn stover	0.07-0.35	(Cheah et al., 2014; Johansen et al., 2011; Schmid et al., 2018)
Paper and cardboard		0.1	(Nasrullah, 2015)
Sewage sludge		0.023-2.4	(Choi et al., 2016a, 2016b; Schmid et al., 2018; Schweitzer et al., 2018)
Animal waste	Pig, poultry, cattle manure	0.3-1.54	(Schweitzer et al., 2018)
Plastics	PE, PVC, PS…	0.08-0.8	(Chin et al., 2014; Nasrullah, 2015)
Waste Tires		1-3	(Hu et al., 2014; Lopez et al., 2017; Murena, 2000)
Rubber		0.5	(Nasrullah, 2015)
Textiles		0.2-0.24	(Nasrullah, 2015)
Leather waste		0.86-3.43	(Godinho et al., 2007, 2011; Pedersen et al., 2010; Kluska et al., 2019)
Car shredder waste		0.34-0.5	(Cheng et al., 2020; Pedersen et al., 2010)

1.2.1.2 Chlorine

Chlorine in biogenic and fossil resources can be differentiated based on its chemical speciation and bonding, which can be grouped as Cl chemically bound in organic or inorganic compounds, which often correlates with the type of material of origin. **Table 5** presents different types of biomass and solid wastes with their respective chlorine content.

- Biomass

In biomass, inorganic chlorine is found in the form of alkali metal chlorides such as NaCl, KCl, and $CaCl_2$. These chlorides are usually present in food waste, forestry and agricultural residues and in biogenic industry products (ex: paper and cardboard).

According to Ma et al. (2010), food waste is an important inorganic chlorine source with more than 95% of chlorine in inorganic chloride salts. It contributes to more than 45% of total Cl in municipal solid waste.

Chlorine concentrations in forestry and agricultural residues are associated with the nutrient cycle and plant growth processes (Tillman et al., 2009). Chlorine and potassium are not metabolized by the plant but remain in ionic form. More than 80% of the K and 90% of the Cl are water-soluble and can be removed by leaching confirming that these elements exist primarily in salt form in the fuel (Knudsen et al., 2004a; Tchoffor et al., 2013). Their main function in plants is to maintain the pH and charge neutrality, regulate the osmotic pressure, and stimulate enzyme activity (Knudsen et al., 2004a). It is important to note that a small amount of organic chlorine (<5% of total Cl), is incorporated in the carbon matrix in forestry and agricultural residues. The chlorine content is highly variable and depends on many factors such as the proximity of biomass to the sea, the use of fertilizers, the leaching of soils by rain, the harvesting techniques, and the treatment and storage methods. Therefore, compared with forestry residue, agricultural residues have a relatively higher Cl content (Du et al., 2014; Tillman et al., 2009).

In leather, most of the chlorine is in an inorganic form, since sodium chloride (NaCl) is utilized as preservative for the hides and added in the pickling step to help with the penetration of certain tanning agents (Godinho et al., 2007).

- Fossil resources

Chlorine is present in several fossil-based resources and wastes: chlorinated plastics such as polyvinyl chloride (PVC), chlorinated polyethylene (CPE), polyvinyl dichloride (PVDC), packaging waste, textile and leather residues, electronic waste, rubbers (Table 2). Chlorine is then mainly organically bound.

PVC is the most representative organic chlorine source in municipal solid waste with a chlorine content as high as 50 wt. % of the total mass.

However, numerous organic Cl-containing compounds, other than PVC, are also used in consumer products. Polyvinylidene chloride (PVdC) is an addition polymer of vinylidene chloride; it is used in flexible packaging as a monolayer film, a coating, or part of a co-extruded product in major applications such as packaging of poultry, cured meats, cheese, snack foods, tea, coffee, and confectionary (Marsh and Bugusu, 2007). It has a higher chlorine content than PVC with nearly 72–73% w/w (Vinas and Dufils, 2012).

Chlorine is also found in polyurethane and polycarbonate plastics because of the use of carbonyl dichloride (phosgene) during their production. Polyurethanes are generally classified into two groups: foams and denominated CASE's (Coatings, Adhesives, Sealants, Elastomers) with highly diverse applications such as in mattresses, automotive seats, buildings isolation, and parts of sport shoes, athletics tracks, and electronic products and ships structures (Kemona and Piotrowska, 2020).

Epichlorohydrin CH_2CHOCH_2Cl (ECH) is another versatile chemical intermediate used in a variety of applications, including, rubbers, textiles, paper products, inks, dyes, automotive and aircraft parts, biocides, personal care products, ion-exchange resins and epoxy resins mainly used in packaging and paper manufacture (Abraham and Höfer, 2012). Therefore, as verified by previous studies, rubber (especially black/grey in colour), synthetic rubber within shoes, cables and textiles (synthetic type) were identified as potential high sources of chlorine (Nasrullah, 2015; Velis et al., 2012; Velis, 2010).

Inorganic chlorine can also be present in form of $TiCl_3$ and $MgCl_2$ compounds in polyolefin plastics resulting from ziegler-natta catalysts used in the polymerization of polyolefin (Shamiri et al., 2014). Also, packaging components, such as plastic bottles of chlorinated detergents, may often contain remnants of chloride compounds such as sodium hypochlorite NaClO, the most common chloride used for bleaching (Gerassimidou et al., 2021; Zoller, 2008).

Table 5: Chlorine content in different types of biomass and solid wastes

Type	Sources	Examples	Chlorine content (wt.%, dry basis)	References
Inorganic Cl sources	Forestry residue	Willow wood, hybrid poplar, sawdust, woody products (paper and cardboard)	0.01-0.3	(Ma et al., 2010; Pedersen et al., 2010; Schmid et al., 2018)
	Crop residues	Rice straw, wheat straw, corn stover	0.28-0.69	(Defoort et al., 2015; Johansen et al., 2011; Schmid et al., 2018)
	Food waste		0.8	(Ma et al., 2010)
	Sewage Sludge	dried, pellets	0.02-0.2	(Schmid et al., 2018; Schweitzer et al., 2018)
	Leather waste		0.45-3.2	(Godinho et al., 2007; Kluska et al., 2019; Pedersen et al., 2010)
Organic Cl sources	PVC		46.6-56.8	(Chen et al., 2019; Ephraim, 2016; Lu et al., 2018)
	PVdC		72-73	(Vinas and Dufils, 2012)
	Rubber		7.6-8	(Nasrullah, 2015)
	Waste Tires		0.2	("Phyllis2," n.d.)
	Textiles		1	(Nasrullah, 2015)
	Plastics from waste from electrical and electronic equipment		3.14-5.64	("Phyllis2," n.d.)

1.2.2 Investigations of S and Cl retention or release in pyrolysis and gasification

The behavior of sulfur and chlorine has been studied using several experimental and thermodynamic approaches. Different types of thermochemical conversion processes were studied (ex: pyrolysis, partial combustion or gasification), for different types of feedstock, of reactor, and variable operating conditions.

1.2.2.1 Experimental Approach

During the conversion processes, inorganic elements present in the feedstock are distributed among the different product streams (gas, liquid, and solid residue). Understanding the behavior of inorganic elements is crucial for process optimization, product quality control, and environmental considerations. However, only a limited number of studies have focused on evaluating the distribution of inorganic elements in thermochemical conversion products, and the available research is relatively scarce. One reason for the limited number of studies is the complexity and challenges associated with the analysis of inorganic species in diverse product streams. Despite these challenges, some studies have made efforts to quantify the inorganic species released in the product gas or retained in the char, but the data provided is not always enough for the assessment of complete elemental balances of the inorganic elements.

1.2.2.1.1 Characterization and quantification methods of chlorine and sulfur species in the pyrolysis and gasification products

The experimental methods for the measurement of the released gaseous inorganic pollutants found in the literature differ from a study to another and depend on the scale of the unit. In some experiments, hot gas analysis was conducted using molecular beam mass spectrometry (MBMS) that allowed semi-quantification of the released inorganic species and has been proven to be a reliable method for high-temperature environment (Bläsing et al., 2015b; Porbatzki et al., 2011). It allowed distinguishing the different chlorine compounds released as KCl, NaCl and HCl.

In other lab-scale studies, HCl and sometimes H_2S were trapped in solvents by passing the syngas through impinger bottles containing specific solutions (chloromethane or deionized water with, in some cases, activated carbon and silica gel). Quantification of chlorine and sulfur were then performed by ionic chromatography (Aljbour and Kawamoto, 2013; Berrueco et al., 2015; Cheng et al., 2020; Cho et al., 2015; Recari et al., 2016a). In some pilot-scale studies, chlorine and sulfur in syngas were also measured by bubbling a slipstream of syngas into a solution of NaOH followed by ion chromatography (Andrea Jordan and Akay, 2012; van Paasen et al., 2006) or into a solution of NaOH with 50% of sulfur anti-oxidant buffer followed by spectrophotometry (Hervy et al., 2021). In other studies, sulfur species (H_2S ,COS) were analysed online using a micro Gas Chromatograph (μGC) coupled with a Thermal Conductivity Detectorn (TCD) (Aljbour and Kawamoto, 2013; Gai et al., 2014; Lopez et al., 2017; Valin et al., 2019).

Moreover, in the study of Vonk et al. (2019), gas bags and isopropanol samples were subjected to analysis using a GC-FPD (Shimatzu 2014 chromatograph, ZB-50 column) equipped with a Flame Photometric Detector (FPD). The purpose of this analysis was to conduct qualitative assessments of sulfur compounds, including gaseous compounds (H_2S, COS, carbon disulfide CS_2) and sulfur-containing tars, also known as "S-tar" such as thiophene and thiophenol. Sulfur compound standards were used to perform identification of unknown compounds by determination of matching retention time.

Several methods are commonly used to quantify the inorganic elements present in the solid residues. In some studies (Knudsen et al., 2004a, 2004b; Hervy et al., 2021), the char residue was digested using acid or fusion techniques to solubilize the inorganic elements, and the resulting solution was then analyzed using Inductively Coupled Plasma-Optical Emission Spectroscopy (ICP-OES) or Inductively Coupled Plasma-Mass Spectrometry (ICP-MS). Other studies (Johansen et al., 2011; Tchoffor et al., 2013, 2014, 2016; Vonk et al., 2019) determined the contents of S and Cl according to the standard EN 15408 and EN ISO 10304-1. The samples were combusted in a closed bomb calorimeter containing a solution of deionized water and NaOH, and the Cl and S content of the receiving solution were then determined by ion chromatography. In Cheah et al. (2014)'s study, the total sulfur content of the biochars was measured with a LECO TruSpec sulfur add-on module. The measurement procedure involved combustion of the material at 1350°C in 99.5% oxygen (to break down all sulfur-bearing material and to oxidize the sulfur to SO_2) followed by infrared measurement of SO_2. In a few other studies, X-ray photoelectron spectroscopy (XPS) was used to determine the sulfur species and concentration in the chars by using a Thermo Escalab 250 with Al-K αX-ray (Zhang et al., 2020), and to determine the ash composition (Godinho et al., 2007).

Below, we present a compilation of qualitative and quantitative information obtained from various experimental studies conducted on different feedstock types, shedding light on the transformation and behavior of sulfur and chlorine during thermal conversion processes.

1.2.2.1.2 Sulfur Behavior

The mechanisms involved in the behavior of sulfur during thermochemical conversion of both biogenic and fossil-based resources were examined. The influence of various factors, such as the operating conditions (temperature, atmosphere), as well as the type and initial composition of the feedstock, on sulfur behavior was investigated. The data obtained included measurements in the gas streams from certain studies, while in other studies, it was derived from difference calculations in the sulfur balance considering chemical analyses of solid residue.

Table 6 presents the fraction of sulfur released in the gas phase mainly as H_2S and COS in studies conducted on different types of feedstock.

Table 6: Quantitative sulfur release in gas phase in different studies

Type of reactor	Feedstock	S content (wt.%)	Thermal treatment	Conditions	S % in gas phase	References
Lab-scale tubular reactor	Wheat straw	0.14-0.2	Pyrolysis	T=400°C	35-50	(Knudsen et al., 2004b)
				T=950-1000°C	45-55	
Lab-scale reactor	Corn stover	0.07	Pyrolysis	T=500-1150°C	60	(Johansen et al., 2011)
Bench scale downdraft fixed bed	Corn straw	0.13	Air / Steam gasification	ER=0.2-0.4 S/B=0.8-1.6	30-60 (10-35 wt.% of S not determined)	(Gai et al., 2014)
Pilot scale bubbling fluidized bed	SRF	0.47-0.51	Pyrolysis	T=820°C	5	(Valin et al., 2019)
			Air gasification	T=800-900°C	43-70	
			Air / Steam gasification	T=870°C S/C=0.22	80	
				T=850°C S/C=0.73	100	
	Woody biomass	0.1	Air gasification	T=850°C	30	
Lab-scale bubbling fluidized bed	Automobile shredder residue	0.34	Air gasification	T=900°C	11.3	(Cheng et al., 2020)
				T=900°C + 10% Oyster shells	6.4	
Bench-scale conical spouted bed reactor	Truck tire rubber	2.4	Flash Pyrolysis	T=425–575°C	5	(Lopez et al., 2017)
Pilot scale fed-batch mode downdraft gasifier	Poplar Wood	0.02	Air gasification ER=0.25	T=710-774°C	10	(Vonk et al., 2019)
	SRF wood	0.05		T=710-810°C	3	
	80% SRF wood + 20% tire	0.3		T=710-760°C	7	
	80% SRF wood +	0.27		T=690-730°C	4	

	20% plastics					
	80% SRF wood + 20% sludge	0.18		T=700-850°C	11	
Bubbling fluidized bed	SRF	0.8	Air gasification	T=800°C ER= 0.22 / 0.27	11-26	(Hervy et al., 2021)

S/B: steam to biomass ratio
S/C: steam to carbon ratio

The release of sulfur during pyrolysis and gasification varies significantly among the different studies. This variability can be attributed to several factors, including the operating conditions and the type and composition of the feedstock.

First, the type of thermal treatment applied to the fuel is a major factor influencing the quantity of gaseous sulfur species released. In pyrolysis, the amount of sulfur released to the gas phase is quite low compared to the amount released in gasification conditions with the presence of an oxidizing agent (Valin et al., 2019).

Another main parameter influencing the conversion of fuel-sulfur to volatile-sulfur gases is temperature. In air gasification of SRF, H_2S has been identified as the main sulfur compound in the syngas and its presence increased with temperature (Berrueco et al., 2015; Valin et al., 2019). The same influence was observed with virgin biomass feedstock (Porbatzki et al., 2011). In waste tires pyrolysis, temperature increase stimulated the cracking of organic polymers in scrap tires and led to more H_2S formation (Hu et al., 2014). In addition, temperature had an effect on increasing the COS released during CO_2 waste tires gasification (Zhang et al., 2020).

The literature review reveals inconsistencies in the influence of equivalence ratio on the evolution of minor contaminants for refuse derived fuels (RDF), solid recovered fuels (SRF), and biomass gasification. Generally, increasing the equivalence ratio leads to higher bed temperatures, which could increase the release of volatile-sulfur gases. In SRF air gasification, the H_2S content increased from 409 to 891 mg/Nm^3 of syngas with increasing ER from 0.22 to 0.27 (Hervy et al., 2021). However, in the air gasification of corn straw (Gai et al., 2014), with increasing the ER from 0.2 to 0.4, the concentration of H_2S decreased.
The addition of steam to air in SRF gasification enhanced the char gasification and induced a higher S fraction in H_2S and COS, as well as a higher H_2S concentrations (Valin et al., 2019).

Moreover, for biomass feedstock, the increase of the steam to carbon (S/C) ratio led to an increase of the conversion of the fuel-sulfur into H_2S and decreased the amount of sulfur present as COS in the product gas (Aljbour and Kawamoto, 2013).
So far, the effects of S/C ratio on the distribution of H_2S and COS are still not entirely clear. Different explanations for this observation were proposed such as:

- the relationship between the H_2S and COS gases based on a hydrolysis reaction:

$$(10)\ COS + H_2O \rightarrow H_2S + CO_2$$

- the increase of hydrogen production resulting the hydrogenation of COS:

$$(11)\ COS + H_2 \rightarrow H_2S + CO$$

The conversion of char with steam, leading to the release of char-bound S, explains how steam facilitates the release of S during char gasification (Tchoffor et al., 2014).

The type of the feedstock and its composition are important parameters influencing the sulfur transformation during thermal treatment.
Several studies focused on the release of sulfur during thermal conversion of biomass feedstock. In particular, they related the release mechanism of S to its chemical form the fuel structure. The S release is expected to begin at the devolatilization step as the organic structure starts to decompose. The temperature for the onset of the S release takes place around 200°C, as this agrees with the decomposition temperature of cystein (178°C) and methionine (183°C), the two main S-containing precursors for plant protein (Dayton et al., 1999). Pyrolysis studies (Johansen et al., 2011; Knudsen et al., 2004b, 2004a; Tchoffor et al., 2016) showed that the majority of the organically bound sulfur present in the feedstock was released into the gas phase during the thermal conversion process. This shows that the gas phase is the primary pathway for the release of organic sulfur during the thermal conversion of biomass fuels.
This release proceeds via the formation of highly reactive SH radicals that either remain in the char or extract H, C, or O from the char, to form later H_2S, COS, or SO_2.

$$(12)\ Fuel - S + heat \rightarrow H_2S + COS + \cdots + Char - S$$

As for inorganic sulfur, at temperatures below 1000°C, the evaporation rates of inorganic sulfates ($CaSO_4$, K_2SO_4) are low. However, some studies (Knudsen et al., 2004b; Tchoffor et al., 2014) showed that a part of these sulfates can be transformed to char-bound S and thus be released to the gas phase.

Moreover, the influence of ash-forming elements on sulfur retention was experimentally observed by Cheah et al. (2014) in pyrolysis and gasification of oak and corn stover; silicon-

poor oak biochar was found to retain a higher fraction of sulfur compared to the biochar of the silicon-rich corn stover. In cane bagasse gasification (Andrea Jordan and Akay, 2012), the release of alkali metals present as water-soluble salts (KCl, K_2SO_4, K_3PO_4, K_2CO_3) and ion exchangeable ions bound to the organic matrix (K^+) was reduced by the presence of aluminosilicates in the feedstock. However, in another study on biomass gasification, the ash composition had a marginal effect on the release of S and Cl, but was relevant for the release of K (Tchoffor et al., 2016).

Other studies have investigated the pyrolysis or gasification of fractions of wastes deriving from diverse resources (from biogenic or fossil origin).

The release of S from four well-characterized waste fractions (copper chromate arsenate impregnated wood, automotive shredder waste, PVC, and shoes - leather) under combustion conditions was investigated by (Pedersen et al., 2010). The release was both temperature dependent and fuel specific. For PVC, the release was almost complete already at 500°C. In the other fuels, the release increased with temperature. The release at low temperature was attributed to the release of organically bound S, whereas the release in the temperature interval [750–1000°C] could be due to decomposition of metal sulfates in the shoes, as well as in CCA impregnated wood, where some S was presumably added as sulfate compounds in connection with the production of the materials. (Kluska et al., 2019) examined the pyrolysis of waste from leather tanneries at 300–500°C and found that about half of the sulfur contained in the leather-tannery waste was released as 2-methyl- 2-Undecanethiol ($C_{12}H_{26}S$).

In waste tire pyrolysis studies (Hu et al., 2014; Lopez et al., 2017), H_2S was the main sulfur-containing gas, whereas other sulfur-containing gases (CH_3SH, COS and SO_2) were found in lower amounts. Only 5% of the total sulfur contained in waste tires was measured in the gaseous products while more than half of it remained in the pyrolysis char (Lopez et al., 2017). Recently, Zhang et al. (2020) investigated the transformation and fate of sulfur during CO_2 gasification of a spent tire pyrolysis char containing initially ZnS (46.1%) and aliphatic sulphur (23.1%). During CO_2 gasification, ZnS reacted with CO_2 to form ZnO and SO_2, or decomposed above 900°C to release elemental sulfur S_x, while aliphatic sulfide was transformed into more thermally stable thiophene.

1.2.2.1.3 Chlorine behavior

Chlorine release during thermal conversion has been studied for different resources. The type of feedstock and its initial composition in terms of quantity and nature of bonding of the different elements, as well as the operating conditions, are important factors influencing the

behavior and amount of chlorine species released during the thermal process. **Table 7** presents the quantities of chlorine released in the gas phase, predominantly as HCl and metal chlorides, as determined by various studies.

Table 7: Quantitative chlorine release in gas phase in different studies

Type of reactor	Feedstock	Cl content (wt.%)	Thermal treatment	Conditions	Cl % in gas phase	References
Spouting-moving bed reactor	RDF (Refuse-derived fuel) rich in PVC	1.52	Pyrolysis	T=660-800°C	30–40	(Wang et al., 2002)
	RDF rich in NaCl	1.52	Pyrolysis	T=660-800°C	60 - 65	
Lab-scale reactor	Corn stover	0.69	Pyrolysis	T=500-1150°C	50 -100	(Johansen et al., 2011)
Lab-scale reactor	Footwear leather wastes	0.62	Pyrolysis	T=500 - 1000°C	75 - 95	(Pedersen et al., 2010)
Air-blown autothermal downdraft gasifier	Cane bagasse	0.05 ± 0.01	Air Gasification	T=910-1170°C ER=0.26	80	(Andrea Jordan and Akay, 2012)
Bench scale gasifier	Cedar wood	0.008	Air Gasification	T=850°C ER= 0 – 0.3	80 – 120 ppmv HCl	(Aljbour and Kawamoto, 2013)
Lab-scale fluidized bed gasifier	SRF	0.7	Air Gasification	T=700 – 850°C ER= 0.3 – 0.35	2268 - 368 Mg/Nm^3 HCl	(Berrueco et al., 2015)
Lab-scale bubbling fluidized bed	Automobile shredder residue	0.34	Air gasification	T=900°C	1.47	(Cheng et al., 2020)
				T=900°C + 10% Oyster shells	2.73	
Bubbling fluidized bed	SRF	0.3	Air gasification	T=800°C ER= 0.22 / 0.27	< 2	(Hervy et al., 2021)
Fixed-bed reactor system	Candlenut wood, Wheat straw, Corn stalk	0.04-0.19	CO_2 gasification	500 – 900°C	20-70	(Deng et al., 2022)

Temperature, atmosphere, and equivalence ratio are key factors influencing the behavior of chlorine in pyrolysis and gasification processes. However, these parameters can have varying influences depending on the characteristics of the resources. The specific behavior of chlorine in pyrolysis and gasification processes firstly depends on the type of feedstock and its composition.

In biomass feedstock (annual biomass and agricultural residues), chlorine exists primarily in inorganic salt forms. Under pyrolysis conditions of biomass, at temperatures ≤700°C, a significant fraction of the Cl (40-60%) in the fuel is released in the form of HCl. It is attributed to an ion-exchange reaction of KCl and oxygen-containing functional groups that are either present in the fuel or formed during the devolatilization step (Johansen et al., 2011; Knudsen et al., 2004a; Tchoffor et al., 2013).

$$(13)\ \text{R-COOH} + \text{KCl (s)} \rightarrow \text{R-COOK} + \text{HCl (g)}$$

At temperatures >700°C, the KCl and NaCl vapor pressure becomes significant resulting in metal chlorides evaporation and therefore in the complete release of chlorine.
Under gasification conditions, Tchoffor et al. (2016) reported that the ash composition appears to exert an influence on the release of Cl. In cane bagasse gasification, alkali release to the syngas was reduced in situ by aluminosilicates contained in the feedstock (Andrea Jordan and Akay, 2012). Porbatzki et al. (2011) reported that HCl was hardly detectable during clean wood gasification due to the high K/Cl ratio and the bonding of chlorine in alkali chlorides. However, for waste wood, miscanthus and straw, HCl was well detectable and the release of alkalis (NaCl and KCl) was not that high due to the reactions of silicates with potassium and sodium. Increasing the amount of oxygen supplied to the gasifier had no significant effect on the concentration of HCl in the gas-phase product in biomass gasification (Aljbour and Kawamoto, 2013).

In plastic materials, chlorine is mainly organically bound. During the devolatilization stage, PVC undergoes three steps, dehydrochlorination at about 150–350°C, condensation at about 350–450°C and fragmentation at about 450–500°C (Bläsing et al., 2015b). Hydrogen chloride HCl was found to be the main product gas component in PVC pyrolysis (50-75 wt.% of the polymer) (Casazza et al., 2019; McNeill et al., 1995) and entrained flow PVC gasification (Bläsing et al., 2015b). In a PVC entrained flow gasification study, the HCl concentration increased with increasing temperature from 1000°C to 1400°C (Bläsing et al., 2015b).

The release of chlorine from gasification of footwear leather wastes was quantified in different studies. Under pyrolysis and combustion conditions, the chlorine release from leather shoes increased from 60 to 95% in the temperature interval 500-1000°C. It was suggested that this increase is caused by the vaporization of metal chlorides at temperatures higher than 700°C (Pedersen et al., 2010). In gasification conditions (Godinho et al., 2007), the sodium chloride being the main source of chlorine in leathers, it was found that NaCl(g) may be converted into HCl according to the reactions below:

$$(14)\ 2NaCl(g) + SO_2 + H_2O + \frac{1}{2}O = Na_2SO_4 + 2HCl$$

$$(15)\ NaCl(g) + \frac{5}{2}SiO_2(s) + \frac{1}{2}Al_2SiO_5(s) + \frac{1}{2}H_2O = NaAlSi_3O_8(s) + HCl$$

In municipal solid waste and solid recovered fuel fractions, chlorine is found in two forms, organic from chlorinated polymers (plastics) and inorganic, for instance salts (NaCl and/or KCl) from food waste. The release of HCl in the producer gas was found to be affected by the materials present in these waste fractions and by the operating conditions during gasification. As in inorganic chlorine sources, the HCl release is related to the equilibrium between Cl and potassium and to the amount of potassium available in the reaction media. At temperatures below 700°C, Cl mainly forms HCl. At higher temperatures, the alkaline metals become available more easily, causing the decrease of the HCl in the gas (Berrueco et al., 2015; Bläsing et al., 2013). This phenomenon was also observed in the SRF gasification (Dunnu et al., 2012; Berrueco et al., 2015).

Moreover, in SRF gasification, HCl level dropped by 85% (from 2268 to 342 mg/Nm^3) upon increasing the equivalence ratio ER from 0.22 to 0.35 (Berrueco et al., 2015). This evolution could be attributed to the release of alkali compounds from the char matrix at higher equivalence ratios and therefore reacting with chlorine and reducing the HCl concentration in the gas. This means that the fraction of Cl released was not affected by ER, but that ER impacted the form under which Cl was released. This is in agreement with the results obtained by Hervy et al. (2021) in which the chlorine was mainly trapped in the fly ash after gasification due to reactions occurring between HCl and the alkali species of SRF removing HCl from the syngas at higher ER.

In PVC entrained flow gasification, the released HCl strongly decreased with increasing oxygen content in the reaction atmosphere (Bläsing et al., 2015b). The addition of steam caused a higher HCl release in SRF gasification (Berrueco et al., 2015), probably due to a larger consumption of the produced char promoting the release of chlorine. However, in cedar wood gasification,

Aljbour and Kawamoto (2013) attributed the decrease of HCl emission with an increasing S/C ratio to the enhanced release of potassium from the solid matrix and thus the increased likelihood of reaction with chlorine to form KCl, leading to a reduced HCl emission.

1.2.2.1.4 Summary and conclusion on the experimental approach

The experimental studies found in the literature show that sulfur and chlorine are mainly released as H_2S, COS, HCl, KCl, and NaCl during pyrolysis and gasification.

This release is in general influenced by several parameters:

- the type of feedstock,
- the chemical form and bonding of inorganic elements (K, Ca, Si, Na, Al…) in the resource,
- the operating conditions : temperature, atmosphere, equivalence ratio, and steam addition.

The fraction of sulfur released in the gas phase varies between 5 and 100% of the initial sulfur content in the feedstock. In typical fluidized bed gasification conditions, between 700 and 1000°C, the sulfur release in the gas phase mainly increases with increasing temperature and steam addition. The sulfur retention in the solid phase is primarily influenced by the presence of silicon, calcium and potassium. Silicon hinders the ability of inorganic elements such as Ca or K to bound sulfur in sulfate solid forms, which would allow decreasing its release in the gas phase.

For chlorine, the released fraction is also significantly variable, from 2 to 80% of the initial chlorine content in the feedstock. Depending on the initial content of K and Na, the gas phase release of Cl varies between HCl and alkali chlorides KCl and NaCl. The inorganic content (mainly Si, K and Na contents), temperature and ER are the main parameters influencing the concentrations and the equilibrium between hydrogen chloride HCl and alkali chlorides KCl/NaCl.

However, not all authors attempted to complete the elemental balance of sulfur and chlorine and to characterize their condensed forms, which makes the distribution of chlorine and sulfur species during gasification and the reactions involved poorly understood and unclear.

To gain further information on the stability of inorganic elements and predict their distribution between the condensed phase and the gas phase, thermodynamic equilibrium studies have also been performed. The following section presents the thermodynamic approach used to investigate the release of inorganic pollutants.

1.2.2.2 Thermodynamic approach

Thermodynamic equilibrium modeling has gained much interest to predict the final products obtained after thermochemical conversion of various feedstock. The thermodynamic databases are developed on the basis of the so-called CALculation of PHAse Diagram (CALPHAD) methodology that consists in optimizing the Gibbs energy functions to reproduce the known phase diagrams and utilize it to make the prediction of unknown phase equilibria (Jung and Van Ende, 2020).

Among the commercial thermodynamic software packages that have been developed, FactSage is the most popular one for high temperature materials processing (Jung and Van Ende, 2020). It was introduced in 2001 as the fusion of the F*A*C*T / FACT Win and ChemSage (SOLGASMIX) thermochemical packages. The Equilib module simulates the equilibrium state, under a large range of possible constraints by minimizing the total Gibbs energy of the system based on the ChemApp algorithm (Bale et al., 2016).

The different studies found in literature and focusing precisely on the sulfur and chlorine species release are listed in **Table 8.**

Table 8: Thermodynamic calculations of sulfur and chlorine species release found in literature

Software/ Database	Thermal treatment	Feedstock	T° (°C)	Atmosphere	References
FactSage 5.1	Pyrolysis and Combustion	Wheat Straw	400-1000	O_2 + N_2	(Knudsen et al., 2004b)
FactSage 5.1	Gasification	Demolition wood, Verge grass, Sewage sludge, Bio-dried wood, Railroad ties, Cacao shells	400-1200	Air	(Kuramochi et al., 2005)
FactSage 5.5 FACT database	Gasification	Clean and waste Wood, Miscanthus Straw	950	O_2	(Porbatzki et al., 2011)
Liquid phases: (Salt-melt, Oxide-melt), Solid solution phases, Pure	Gasification	Forest residue, Miscanthus, Reed canary grass, Eucalyptus, Arundo Donax, Lucerne	600-900	Air	(Zevenhoven-Onderwater et al., 2001)

condensed phases					
FactSage 6.2 FToxid-SLAGA, FT salt-KCO, FT salt-LCSO, FT salt-SALTF	Pyrolysis	Wheat straw pellets	400-1000	$O_2 + N_2$	(Tchoffor et al., 2013)
FactSage 5.4.1 ELEM, FACT 53, FTsteel, FTmisc, FToxid, FTsalt	Gasification	Wood (spruce and pine sawdust including bark)	500-1500	$O_2 + H_2O$	(Froment et al., 2013)
Factsage 6.4 FToxid or GTOX, FTSalt, FactPS	Gasification	Coniferous wood, Eucalyptus, Poplar, Wheat straw, mix of agricultural by-products, Triticale, Tall fescue, Miscanthus	500-1200	H_2O	(Defoort et al., 2015)
FactSage 7.3 FToxid, FTSalt, FactPS	Combustion	Wheat Straw Lignin	600-1000	O_2	(Priscak et al., 2020)

In order to gain further information on the stability of inorganic sulfur forms during gasification, thermodynamic simulations were conducted and compared to experimental results done by the same authors (Knudsen et al., 2004b; Porbatzki et al., 2011; Tchoffor et al., 2013) or found in literature (Kuramochi et al., 2005). In gasification conditions of different biomass fuels, Kuramochi et al. (2005) attributed the lower H_2S release calculated at low temperatures (400-600°C) in some biomasses to their high initial content of metals (Zn and Fe). Calculations showed that metal sulfides (FeS, ZnS, MnS, PbS, Ni_3S_2 and Cu_2S) retaining sulfur in condensed forms were predicted to be formed and allowed for the suppression of H_2S production; however, this was not confirmed experimentally. Porbatzki et al. (2011) found for all the biomass gasification calculations at 950°C, that 95% of the initial sulfur was released as H_2S and 4-5% as COS; no condensed sulfur species were predicted. Similar results were obtained for wheat

straw pyrolysis calculations from 400 to 1000°C (Tchoffor et al., 2013), in agreement with the experimental results obtained by these authors. The effect of silicon on the equilibrium distribution of sulfur was investigated in both Knudsen et al. (2004b) and Tchoffor et al. (2013) studies. It was found that between approximately 600 and 800°C, the presence of silicon (0.85-1.3 wt%) in the feedstock resulted in the formation of potassium and calcium silicates in the condensed phase, which suppressed the presence of sulfur in condensed sulfide forms as CaS and K_2S, and subsequently increased the release of sulfur in the gas phase. This could explain the experimental results obtained by Knudsen et al. (2004b) who showed that the sulfur retention in the bottom ash decreased as temperature increased. It can be concluded from thermodynamic simulations found in literature that the initial composition of feedstock (precisely the contents in sulfur, silicon, potassium, calcium, zinc and iron) and the temperature have a significant influence on the distribution of the sulfur and its forms during thermal process. However, more experimental studies are needed to support these results.

Thermodynamic calculations were also conducted to study the behaviour of chlorine during gasification. Kuramochi et al. (2005) investigated the release of HCl during gasification of different biomass fuels at various temperatures. Zevenhoven-Onderwater et al. (2001) focused on the deposit formation and bed agglomeration caused by alkali components affecting the chlorine release in biomass gasification. According to both of these thermodynamic studies, not all the chlorine present in the feedstock is converted into HCl. The HCl release is strongly affected by the alkaline elements (K and Na) that are capable of forming chlorides, which are volatile. In addition, the Si content also indirectly influences the Cl behaviour. Indeed, a low HCl and a high KCl release was predicted with K/Cl and K/Si ratios higher than 1. The potassium content was then sufficient to form potassium chloride KCl with most of the chlorine present, besides than just forming the more stable compounds which are potassium silicates ($K_2Si_4O_9$ or K_2SiO_3). On the other hand, for K/Cl and K/Si ratios lower than 1, the chlorine release was mainly predicted as HCl. In Defoort et al. (2015)'s study, the different alkali release behaviors during gasification were correlated to the molar ratios Ca/Si and K/Si of biomasses belonging to the silicon-rich or poor corner of the SiO_2-K_2O-CaO ternary diagram (with Ca/Si and K/Si lower or higher than 1 respectively). However, experimental results were not in agreement with the calculations for silicon poor biomasses, as a KCl deposit was observed instead of the K_2CO_3 deposit expected from calculations. This discrepancy was attributed to the experimental procedure (measurement and sampling) and kinetic limitations. Usually, explicit

measurement of gaseous alkali and chloride species is not easy to perform and elemental analysis provides insufficient information.

The effect of operating conditions on the release of inorganic species was also investigated in thermodynamic simulations. No significant effect on H_2S release was observed when varying temperature and total pressure (ranges given in Table 9) in the thermodynamic calculations as well as in experimental results (Kuramochi et al., 2005; Froment et al., 2013). For chlorine species, above 650°C, all condensed KCl was vaporized and above 850°C, K-carbonates were no longer stable and therefore the potassium in carbonates was converted into gas in the form of KOH (Froment et al., 2013). As expected from a thermodynamic point of view, increasing the total pressure favored condensation or delayed volatilization and thus decreased the release fraction of condensable species such as KCl in the exhaust gas, and in consequence increased the potassium fraction remaining in condensed phase as a liquid causing bed agglomeration (Froment et al., 2013). A comparison to experimental results could not be done due to the lack of accurate measurement techniques of these gaseous species KOH/KCl/HCl.

To conclude, thermodynamic equilibrium calculations have been applied in the literature to predict the distribution of inorganic elements between the condensed phase and the gas phase and to enhance the understanding of the chemistry involved. Good qualitative agreements have been found between equilibrium predictions and experimental observations. However, a quantitative comparison to the experimental results is less accurate since the system in real gasifiers is not always close to the chemical equilibrium. The equilibrium assumption implies infinite reaction times and perfect mixing. Thus, possible thermal, kinetic or mass-transfer limitations, which can have an influence on the advancement of reactions among inorganic species, are not taken into account. When these limitations and factors become important, thermodynamic equilibrium becomes far from representing the real case.

1.2.3 Abatement of gaseous inorganic pollutant release

The control and removal of syngas impurities in gasification systems has always been a major challenge. As discussed in the background, among the currently known gas cleaning systems for producer gas, hot gas cleaning system is considered to outperform the condensation technique because it helps with the heat loss problem related to condensation, and therefore avoids heat and thermal losses and improves energy efficiency. Among the contaminants produced in the gasification process, sulfur compounds, which are mainly H_2S with smaller amounts of COS, and chlorine compounds, which are mainly HCl, KCl and NaCl, must be

removed. Different modes and paths were reported for the reduction or removal of sulfur and chlorine released to the gas phase. Generally, they can be captured in two stages: in situ (in bed) and downstream of the gasifier. The implementation of in-situ cleaning in gasification processes is beneficial for apparatus cost and simplicity and it has the potential to reduce the effort of downstream syngas purification and tar removal units significantly. A well-known in-situ sulfur or chlorine capture method consists in the use of additives inside the gasifier, within the bed material or with the feedstock. Another in-situ option for improving gasification and for controlling the release of gaseous inorganic pollutants and tar into syngas is the co-gasification of mixtures of resources. The following sections present these two in-situ cleaning methods reported in literature for inorganic impurities removal during gasification.

1.2.3.1 Use of additives

In-situ sulfur or chlorine capture consists in using additives inside the gasifier, within the bed material or with the feedstock. Most of the in-bed pollutant capture so far has been achieved with calcium-based sorbents that are naturally available, such as limestone or dolomite, or with some commercially available sorbents such as calcium acetate and calcium magnesium acetate. In Campuzano et al. (2021) and Martínez et al. (2022) works, CaO was obtained by the thermal decomposition of $CaCO_3$ (calcination). Dolomite $CaMg(CO_3)_2$ is a mineral composed of calcium magnesium carbonate. Olivine is primarily composed of magnesium iron silicate $(Mg,Fe)_2SiO_4$. These additives present important advantages, mainly in terms of availability, low cost and suitable properties for impurity retention.

Table 9 presents different thermodynamic and experimental studies that have evaluated the effect of additives on the release of gaseous inorganic pollutants during gasification of biomass and waste fractions.

Table 9: Studies using additives to limit the release of inorganic pollutants in the gas phase

Inorganic pollutant	Gasifier Type	Feedstock	Conditions	Additives	References
H_2S NH_3	Bench-scale bubbling fluidized gasifier	SRF	Steam + Air ER =0.2 800°C	Bed material: Lime or Calcined dolomite or Olivine mixed with silica	(Pinto et al., 2014b)
H_2S HCl HCN	Lab-scale fluidized bed reactor	SRF	Air ER=0.31 850˚C	Bed Material: Calcined Dolomite or Silica Sand	(Recari et al., 2016b)
H_2S NH_3	Dual fluidized bed reactor	Sewage sludge	Steam 800°C	Limestone	(Schweitzer et al., 2018)
H_2S NH_3	Bubling fluidized bed gasifer	Sewage sludge	Steam and O_2 850°C	Limestone	(Schmid et al., 2018)
H_2S	Lab-scale bubbling fluidized-bed gasifier	Wood pellets	Steam 760-810°C	CaBa sorbent (10 mol % BaO in CaO)	(Husmann et al., 2016a)
H_2S HCl	Lab-scale bubbling fluidized bed	Automobile shredder residue	Air 900°C	Additives: 10wt.% Oyster shells	(Cheng et al., 2020)
HCl	Two-stage gasifier (fluidized bed reactor and tar-cracking zone)	Waste plastic (LDPE PP and PVC)	Air 800°C	Additives: Quicklime, oyster shells, and dolomite with olivine as bed material	(Cho et al., 2015)
HCl	Two-stage reactor	RDF + PVC	O_2 + Steam 600˚C, 1000˚C	Additives: CaO, $Ca(OH)_2$, Na_2CO_3 mixed with feedstock	(Borgianni et al., 2002)

The use of single metal oxides in high-temperature processes is not feasible due to reduction and evaporation, as in the case of ZnO or CuO, or not efficient as in the case of MnO or iron oxides (reduction to elemental iron unless the oxides are stabilized) (Husmann et al., 2014). Combined sorbent materials such as BaO-based sorbent CaBa (10 mol % BaO in CaO) were tested for in situ utilization as a desulfurization agent in a biomass gasification process and were found to be efficient, resulting in a decrease of H_2S concentration from 85 ppmv down to 35 ppmv with full conversion of BaO to BaS (Husmann et al., 2016a).

The use of CaO, CaO-based sorbents and natural minerals was found possible at temperatures around 800°C, and effective in biomass gasification processes. Pinto et al. (2014) investigated the effect of adding low cost natural minerals to silica used as the initial bed material in fluidized bed SRF (solid recovered fuel) gasification. The addition of dolomite and lime CaO, both containing Ca, induced a pronounced reduction in H_2S concentration and in the fraction of sulfur released to the gas phase, while it was not the case for olivine, which does not contain Ca. These results are in agreement with the results presented by Recari et al. (2016b) and confirm that the presence of Ca in the bed favors the formation of CaS by the following reaction:

$$(16)\ CaO + H_2S \rightarrow CaS + H_2O$$

It is noteworthy to mention that dolomite led to the lowest content of H_2S in the gas; this was attributed to the composition of dolomite that contains, besides CaO, other metal oxides (magnesium oxides) that favored S retention.

The addition of CaO, during sewage sludge gasification, had also a positive effect on reducing the H_2S and NH_3 concentrations in the product gas (Schmid et al., 2018; Schweitzer et al., 2018). The equilibrium H_2S mole fraction was calculated with FactSage in the same conditions as in the experiment and was found close to the experimental result (Schmid et al., 2018). In wood pellets gasification between 700 and 825°C, CaO was found far more active for H_2S capture than $CaCO_3$ (Husmann et al., 2016b). It is important to note that, besides reducing volatile sulfur compounds emission, calcium-based sorbents had a catalytic effect on tar cracking leading to a lower tar content and an increase in the gas yield (Pinto et al., 2014b; Recari et al., 2016b; Schmid et al., 2018; Schweitzer et al., 2018).

Oyster shell is a residue mainly derived from seafood restaurant or fishing harbor and due to its high calcium content it could be a valuable resource for in-situ syngas cleaning. It has also shown a significant influence on enhancing produced gas yield, energy yield, and tar reduction in fluidized bed gasification (Cheng et al., 2020; Cho et al., 2015). Cheng et al. (2020) reported that volatile sulfur compounds emission could be inhibited by adding oyster shell catalyst. The sulfur content in the synthesis gas was significantly decreased from 11.36% to 6.44% during air gasification of automotive shredder residue mixed with 10% oyster shell. Cho et al. (2015) pointed out that oyster shell was also very effective for HCl removal; the HCl content in the producer gas at 800°C decreased significantly from 7.5 ppm to less than1 ppm. Similar effects were obtained when adding quicklime or dolomite. The level of HCl also dropped when using dolomite as bed material during SRF gasification at 850°C (Recari et al., 2016b) probably due

to Ca and Mg available in the dolomite bed. A gas-to-solid reaction described by the equation below can explain the effect of calcium on reducing HCl release during the gasification process:

$$(17)\ CaO + 2HCl = CaCl_2 + H_2O$$

However, the opposite effect was reported in other studies (Cheng et al., 2020), where the HCl removal efficiency was decreased by the calcium-based absorbent at a higher temperature (900°C). Indeed, the melting point of calcium chloride is 772°C. It can then be easily vaporized, or even decomposed above 900°C (Cheng et al., 2020). In gasification of blends consisting of RDF and PVC (Borgianni et al., 2002), sodium carbonate Na_2CO_3 was found to be efficient in eliminating chlorine in the first stage of the reactor at 600°C with a chlorine removal of 99%. On the contrary, the less expensive calcium compounds CaO and $Ca(OH)_2$ showed a less satisfactory chlorine removal (81% and 77% Cl removal respectively) even with twice the quantity needed for a complete reaction with chlorine.

It arises from the different studies found in literature that use of additives to the gasifier is an efficient method for in-situ cleaning and reduction of inorganic pollutants as well as for the reduction of tar content. The temperature of the process and the gasifying agent are parameters affecting the efficiency of the additives. For sulfur removal, calcium-based sorbents and natural minerals were found to be the most effective in decreasing H_2S concentrations in syngas at temperatures between 750 and 900°C. However, for HCl removal it was not always the case. Some studies reported the efficiency of calcium-based sorbents and natural minerals in decreasing HCl concentrations in syngas between 800 and 900°C, while others reported the opposite effect, or a more satisfactory chlorine removal with other additives such as sodium carbonate at 600°C. However, when using additives, the question of reusability and durability of the additives related to cost reduction should be considered. Additives usually leave the reactor with the ash purge; therefore, a recycle of those additives must be considered along with their possible valorization routes.

1.2.3.2 Co-gasification of resources

In-situ cleaning may also be achieved by the co-gasification of resources. Several researchers have studied the co-gasification of coal and biomass, focusing on ash behavior, on syngas quality, and on tar content and pollutants emission. **Table 10** presents different co-gasification studies found in literature that have focused particularly on reducing the pollutants emissions.

Table 10: Co-gasification studies

Gasifier Type	Feedstocks Mixture	Conditions	References
Dual fluidized bed gasifier 100 kW	Lignite + Pine wood	800°C Steam	(Hongrapipat et al., 2015)
Pilot-scale bubbling Fluidized-bed gasifier	Low-grade high-ash coal from Puertollano and Colombian + Pine wood/Olive oil bagasse, RDF/Polyethylene	850-900°C Steam+O_2	(Pinto et al., 2010)
High-T° furnace reactor and MBMS instrument	Straw + Lignite / Hard Coal Miscanthus + Lignite / Hard Coal Wood + Lignite / Hard Coal	1400˚C	(Bläsing et al., 2015a)
High-T° furnace reactor and MBMS instrument	Turkey manure + Hard Coal/Lignite Meat Bone + Hard Coal/Lignite	1400°C	(Bläsing et al., 2017a)
High-T° furnace reactor and MBMS instrument	Sewage Sludge + Hard Coal/Lignite	1400°C	(Bläsing et al., 2017b)
Bench-scale bubbling fluidized gasifier	SRF + Forestry pine/Almond shells/Olive bagasse 50% (w/w)	Steam + Air 800°C	(Pinto et al., 2014b)

The results obtained in these studies show that when coal and biomass are co-gasified, the biomass component, which typically has a lower ash content compared to coal, acts as a diluent for the overall feedstock. As a result, the ash and volatile inorganic content in the mixture is lower than in coal, usually leading to a lower content of inorganic species in the syngas. (Pinto et al., 2010) reported that the H_2S content in syngas depended on the type of co-gasified wastes and coals and on the initial sulfur content in the feed. When blends with overall higher contents of sulfur were used, the release of H_2S was higher, with no observed interaction in blends. However, in co-gasification of coal and pine wood, Hongrapipat et al. (2015) found, by comparing their experimental results with literature data, that the blending method of the fuels by pelletization had a positive effect on the release of H_2S in the producer gas. A non-linear relationship between the initial sulfur content and H_2S concentrations was found, and lower H_2S concentrations were obtained in the producer gas compared to those from co-gasification of non-pelletized fuel found in literature data. This confirms, according to the authors, the existence of an interaction between pelletized coal and wood compared to physically mixed

(non-pelletized) coal and wood. In the co-gasification of biomass feedstocks (wood, straw, and miscanthus) with two lignites and two hard coals under reaction conditions similar to that in entrained-flow gasification (Bläsing et al., 2015a), the release behavior of the blended fuels was quite complex and influenced not only by dilution effect, but also by secondary effects taking place. The reduction in sulfur species (H_2S, COS) release with higher fraction of biomass was explained by the higher calcium content that can effectively trap the sulfur. However, the availability of calcium is dependent on the amount of silicon and alumina (Al/Si ratio) since calcium is well known for its network-modifying characteristics, as it can form calcium aluminosilicates and lose its sulfur capture qualities. For chlorine species, since chlorine is highly volatile, the release of HCl was not influenced by secondary effects or interactions in the blends. However, the release of NaCl and KCl was influenced by the content of chlorine, the ratio Al/Si, and the amount of alkali of the feedstock. With an optimal Al/Si ratio, potassium forms potassium aluminosilicates, which results in decreasing release of volatile KCl. Chlorine is a very strong promotor of the release of sodium, therefore the release of NaCl increased with increasing chlorine content in the feed. Same results and interpretations were obtained in the co-gasification of sewage sludge, turkey manure and meat bone with hard coal and lignite (Bläsing et al., 2017a, 2017b).

Less information can be found on concentrations of gaseous inorganic pollutants in the producer gas from co-gasification of biomass and waste fractions. Kuramochi et al. (2005) suggested mixing a potassium-rich biomass with low chlorine content, with a potassium-rich biomass with high contents of chlorine and silicon to reduce the amount of HCl emission. Their study was based on thermodynamic calculations using FactSage. The calculated HCl emission in the case of gasification of a 1:1 mixture of cacao shells and demolition wood was significantly lower than what would be expected in case of no interaction between the resources, but this effect was not confirmed experimentally. Pinto et al. (2014) investigated the co-gasification of SRF and biomass wastes and found that the release of H_2S in the gas decreased comparing to when only biomass wastes or SRF were gasified alone. It was suggested that the high inorganic content of SRF might have retained some of the sulfur present in the feedstock but not enough experimental evidences confirmed this hypothesis. The co-gasification of mixture of resources of biomass and wastes, to limit the release of inorganic pollutants, has been very little considered and studied so far, and some research is still needed.

1.3 Conclusion and objectives of the thesis

In order to reduce the actual dependence on fossil fuels and to push forward a circular economy, gasification of suitable carbonaceous resources allows producing a synthesis gas that can be used in cogeneration (heat and electricity) or for the synthesis of liquid or gaseous fuel. However, the presence of inorganic elements in the feedstocks causes a high release of inorganic pollutants in the gas phase. This release poses threats to the downstream processes (production of energy or chemicals) because of the corrosive nature of chlorine species (HCl, KCl, NaCl), and the poisoning effect of sulfur species (H_2S, COS) on catalysts used for synthesis.

Different quantities and chemical forms of sulfur and chlorine were identified in carbonaceous resources correlating with the type of material of origin. Sulfur forms a variety of different compounds depending on its two different nature, organic sulfur where it is incorporated into the carbon matrix and inorganic sulfur. Similarly, chlorine can be differentiated based on its chemical speciation and bonding, which can be grouped as Cl chemically bound in organic compounds and inorganic compounds.

In recent years, experimental and thermodynamic studies on the gasification of biomass or waste rich in inorganic elements have increased, focusing in particular on the characterization of the release of gaseous inorganic pollutants and on methods of limiting it. Gaseous sulfur and chlorine pollutants are released mainly under H_2S, COS, HCl, KCl, and NaCl forms. Various parameters related to the feedstock and the operating conditions during the gasification process have been identified to influence their behavior and mechanism of release. These include the type of the feedstock, its inorganic content (especially concerning Si, Ca, K and Na), the temperature, the equivalence ratio and the atmosphere (gasifying media). The influence of varying operating conditions on the pollutant release can be globally explained, and qualitatively well represented by thermodynamic simulations. These simulations bring information on the mechanisms involving the different inorganic elements, leading to trapping or release of S and Cl-based species. However, a quantitative comparison to the experimental results, when it is performed, is less accurate since the system in real gasifiers is not always close to the chemical equilibrium, due to kinetic or mass transfer limitations.

Further investigations are necessary to enhance our understanding of the behavior of inorganic elements, enabling more efficient and sustainable thermochemical conversion processes. Therefore, the study of the behavior of sulfur and chlorine species during gasification still needs

experimental investigation, considering both their initial chemical form in the resource, and the effect of the operating conditions on their release. An attention must also be given on the distribution and the characterization of the species in both condensed and gaseous forms to complete the elemental balance of sulfur and chlorine.

One of the major in-situ method to limit the release of inorganic pollutants in the gas consists in using additives in the reactor, in order to capture the chlorinated and / or sulfur-containing compounds before they are released. This method has the advantage of avoiding or limiting the additional gas-cleaning step as well as a possible cooling of the gas. Calcium-based sorbents and natural minerals were found to be the most effective in reducing H_2S concentrations in the syngas, and in some cases HCl concentrations. However, there is still a lack of understanding of all the reactions involved in the process when using such additives.

Some authors highlighted the interaction between different resources during their co-gasification influencing the releases of sulfur and chlorine in function of the initial inorganic content and the respective quantities of each of the resources. An abatement of these harmful substances may be possible when performing co-gasification of mixtures of resources; however, it is still insufficiently discussed in literature especially in mixtures including biomass and wastes. Moreover, interactions between mineral matters and sulfur and chlorine, the influence of the blending ratio, and of the contact in the blends dependent on the blending method and particles sizes should also be investigated. Attention must also be given to the species remaining in the condensed phase to avoid ash melting, ash slagging and agglomeration problems.

Therefore, in view of this literature review, the objectives of this thesis were:

- to characterize the behavior of sulfur and chlorine during the pyrolysis - pyrolysis representing the first step of gasification – and gasification, of biogenic and non-biogenic carbonaceous resources of various compositions, and to assess the effect of the type of the feedstock and its initial chemical composition (particularly nature and amount of inorganic content) as well as the effect of the operating conditions (variation of temperature and air addition) on this release
- to propose and test in-situ methods (based on chemical interactions between inorganic elements) by using additives and mixing resources to enhance the sulfur and chlorine retention in the solid phase and thus limit their release in the gas phase

2.Materials and Methods

2.1. Feedstock and its Characterization

2.1.1. Feedstock Selection, procurement and preparation

Five feedstocks were selected among agricultural residues and materials present in waste:

- Colza straw and corn residues (leaf, husk, stalk) are post-harvesting crops and residues deriving from agriculture.
- Cardboard, wool (textile), and PVC are urban post-consumer residues deriving from industries or households.

The selection of feedstocks was based on different criteria:

- The quality of the resource that can influence the efficiency of the conversion process into syngas (a calorific value higher than 10 MJ/kg approximately, a moisture content lower than 30%)
- The origin of the resource types: biomass and waste of biogenic or fossil origin
- The initial contents of S and/or Cl: they must be sufficiently high for their accurate measurement in the analytical experimental device; moreover, they are related to the potential quantities of inorganic pollutants released in the syngas, which must exceed the tolerance levels of the downstream gas applications (Appendix A).
- The content and chemical composition of the ash that can have a possible effect on the release of sulfur and chlorine species as shown by the state of the art in the previous chapter
- The chemical forms (organic/inorganic) of the inorganic species and how they are associated in the feedstock (metal salts, oxides, hydroxides, silicates, carbonates, sulfides, phosphates, or other complex compounds) resulting in a diverse range of forms and nature for these inorganic species

The feedstock were procured from different sources: the colza straw was harvested in the east of France (Marne) and the corn residues in the south-west of France (Haute-Garonne); the corrugated cardboard comes from a packaging, the wool from a sweater (textile), and the PVC from a fitting for water drainage.

To obtain the most homogeneous and representative samples possible, starting from agricultural residues batches of a few kg, quartering followed by grinding using a hammer mill was performed to obtain particles between 1 and 1.5 mm (**Figure 4**). The waste components were shredded up to particles between 3 and 10 mm (**Figure 5**).

Colza Straw Corn Residues

Figure 4: Agricultural residues selected for this study

Cardboard Wool PVC

Figure 5: Waste components selected for this study

2.1.2. Feedstock Characterization

The methods used for the characterization of the feedstocks are described below:

- The moisture content is determined according to the standard ISO 21660-3. The sample is dried at a temperature of 105°C under air atmosphere in an oven [Dry-line DL53, VWR] for 24 hours. The moisture content, w_{H_2O}, expressed as mass fraction, is calculated from the loss in mass of the test sample using the following equation:

$$w_{H_2O} = \frac{m_2 - m_3}{m_2 - m_1} \quad [2.1]$$

where m_1 is the mass of the empty weighing dish (g); m_2 is the total mass of the weighing dish and sample before drying (g); m_3 is the total mass of the weighing dish and sample after drying (g).

- The ash content is determined according to the standard ISO 18122 by calculating the mass of the residue remaining after the sample is heated in air in a muffle furnace (LT 15/11/P330, Nabertherm) to a controlled final temperature of 550°C. The ash content on dry basis of the sample expressed as a mass fraction on a dry basis, w_{ash}, is calculated using the following equation:

$$w_{ash} = \frac{m_3 - m_1}{m_2 - m_1} \quad [2.2]$$

where m_1 is the mass of the empty dish (g); m_2 is the total mass of the dish and dried sample (g); m_3 is the total mass of the dish and ash (g).

- The elemental composition of the samples was determined according to the standards:

- EN ISO 21663 for the determination of the total content of C, H, and N using a micro-analyzer (Vario EL Cube, ELEMENTAR).

- EN 15408 and EN ISO 10304-1 for the determination of the total content of S and Cl. This method is carried out in two steps; the sample is first oxidized by combustion with O_2 in a bomb calorimeter (Parr 6200 Isoperibol Calorimeter) where sulfur and chlorine are transformed respectively into chlorides and sulfates, which are dissolved and/or absorbed in a 5M NaOH solution. Then, the bomb is washed out and the recovered solution is analyzed by ion chromatography (chloride ion Cl^- and sulfate ion SO_4^{2-}).

- The oxygen content is calculated by difference using the following equation:

$$w_O = 1 - w_C - w_H - w_N - w_S - w_{Cl} - w_{ash} \quad [2.3]$$

where w_i is the mass content of i (i = C, H, N, S, Cl)

- ASTM D6349 for the determination of major inorganic element contents (Si, Ca, K, Na, Mg, Fe, Al, and P) by Inductively Coupled Plasma (ICP) Spectrometry after microwave mineralization (for the agricultural residues) or alkaline fusion (for the waste components).

Table 11 presents the moisture, ash content, and elemental composition of the feedstock and **Table 12** shows the mass composition of the ashes. Corn residues have an ash content of 3.5 wt. % while colza straw has a higher ash content of 10.1 wt. %. As usually found in agricultural residues (Boström et al., 2012; Vassilev et al., 2012), the main ash-forming elements are silicon, calcium, and potassium. Calcium is largely predominant in colza straw, whereas silicon, calcium, and potassium are closer in content for the corn residues. The presence in soils of fertilizers containing sulfates explains their significant sulfur content (0.11-0.33 wt. %). In the plant, a part of the sulfur remains in sulfate form, and the other part is reduced for its

incorporation as a macronutrient into amino acids, proteins, and coenzymes. Chlorine and potassium are associated with the nutrient cycle and plant growth processes, they remain in ionic form and are not metabolized by the plant. The chlorine content is 0.15 and 0.36 wt. % respectively for colza straw and corn residues. It depends on several factors such as the use of fertilizers, the proximity of biomass to the sea, the leaching of soils by rain, the harvesting techniques, and the treatment and storage methods.

Cardboard is a biomass-derived feedstock, coming from wood or recycled fiber manufactured in the pulp and paper industry. It has a relatively high ash content of 12.8 wt. %. The main ash-forming elements are Ca and Si with 4.2 and 2 wt. % respectively. Besides existing already in wood or recycled fibers, these elements can be found in the additives and mineral fillers that are used in the manufacturing process to change or enhance the cardboard properties. For example, calcium carbonate $CaCO_3$ is a common additive and coating material used to increase the quality of paper and cardboard (Fortuna et al., 2020). Hydrated magnesium silicate $H_2Mg_3(SiO_3)_4$ is added as a filler to increase the smoothness (Boufi et al., 2016). Chemical pulping and bleaching involve the use of chemicals, such as sodium sulfide Na_2S and chlorine, which are responsible for the presence of sulfur and chlorine in the cardboard composition (around 0.1 wt. %).

Wool is a natural fiber of animal origin, and thus presents a high protein content (keratin), which has a polypeptide chain with amino acid side chains (cystine, cysteine, cysteic acid, and methionine) (Pina et al., 2021). Among the selected feedstock, wool has the highest sulfur content (2.7 wt. %) and the lowest ash content (1.2 wt. %).

PVC is a fossil-based resource and one of the most widely used types of plastics, it has a very high chlorine content of 49.4 wt. %. It contains approximately 1 wt. % of lead, which can be attributed to the usage of lead stabilizers during the manufacturing process. These stabilizers are commonly employed to enhance the stability and durability of PVC products**.**

Table 11: Composition of feedstock (all values on a dry basis, except moisture on a raw basis)

	Unit	Colza Straw	Corn Residues	Cardboard	Wool	PVC
Moisture	wt.%	11.3	9.7	7.5	11.7	-
Ash at 550°C	wt.%	10.1	3.5	12.8	1.2	3.5
C	wt.%	43.9	45.8	42.3	49.1	39.5
H	wt.%	5.47	6.02	5.36	6.54	5.23
N	wt.%	0.96	1.24	0.28	14.47	0.09
O by difference	wt.%	38.6	43.5	42.2	25.19	2.25
S	wt.%	**0.33**	**0.11**	**0.1**	**2.66**	0.06
Cl	wt.%	**0.15**	**0.36**	0.07	0.09	**49.37**
K	wt.%	0.77	0.73	0.11	0.1	<0.04
Si	wt.%	0.54	0.27	2.0	0.6	0.39
Ca	wt.%	3.74	0.45	4.17	0.78	0.29
Na	wt.%	0.01	0.003	0.19	0.15	<0.04
Mg	wt.%	0.12	0.21	0.18	0.06	<0.03
Al	wt.%	0.04	0.01	0.77	0.11	0.12
Fe	wt.%	0.03	0.01	0.74	0.11	0.09
P	wt.%	0.13	0.15	0.03	0.04	0.008
Pb	wt.%	na	na	na	na	1.06
Ca/Si	molar ratio	4.85	1.17	1.46	0.91	0.52

na: not analyzed

Table 12: Mass composition of the ashes

	Colza Straw	Corn Residues	Cardboard	Wool
S	6%	5%	1%	57%
Cl	3%	16%	1%	2%
K	13%	32%	1%	2%
Si	9%	12%	24%	13%
Ca	64%	20%	50%	17%
Na	0%	0%	2%	3%
Mg	2%	9%	2%	1%
Al	1%	0%	9%	2%
Fe	1%	0%	9%	2%
P	2%	6%	0%	1%

2.1.3. Characterization of the Chemical Forms of Inorganic Elements

2.1.3.1 Chemical fractionation methodology

In the state of the art (**sections 1.2.1** and **1.2.2**), it was mentioned that various quantities and chemical forms of sulfur and chlorine can be found in the selected resources, depending on the material's origin. Additionally, the behavior and quantity of inorganic species released during the gasification process are influenced by the type of feedstock and its initial composition, including the quantity and bonding nature of different elements. It is crucial to examine the chemical form and association of these inorganic elements within the fuel structure to gain a better understanding of their release behavior. Therefore, a chemical fractionation method was applied to four of the selected feedstock: the two agricultural residues, cardboard, and wool. Lixiviation is not adapted to solid plastic materials. However, it is well known that the organic form of chlorine is dominant in PVC that contains organically chlorinated compounds. This method was developed originally by Benson and Holm (1985) for the characterization of coal and then modified and applied by Baxter et al. (1998) and Zevenhoven-Onderwater (2001) on biomass fuels. It is based on selective leaching by increasingly aggressive solvents, i.e., water, 1 M ammonium acetate and 1 M hydrochloric acid. The different types of ash-forming elements are distinguished according to their solubility in the different solvents. According to Zevenhoven et al. (2012), the ash-forming matter can be divided into four classes: dissolved

salts, organically bound matter, included mineral matter, and excluded mineral matter (coming from "pollutants" such as soil). **Table 13** shows the solvent or fraction of the leaching test in which each of these different types of ash-forming matter is found. Sulfur and chlorine can both be present in the dissolved salts found in water and NH_4Ac leachates, in the form of chlorides Cl^- and sulfates SO_4^{2-}. They can also remain in organically bound matter in the solid residue.

Table 13: Repartition of ash-forming matter in the different stages of the chemical fractionation method

	H_2O leachate	**NH_4Ac leachate**	**Acid leachate (HCl)**	**Remaining solid residue after dissolution**
Dissolved Salts	Metal ions (often inorganic) and anions dissolved in plant fluids or precipitated as soluble salts in dried biomass: - the anions Cl^-, HPO_4^{2-}, $H_2PO_4^-$, SO_4^{2-}, and $Si(OH)_3O^-$ - the cations K^+, Na^+, and Ca^{2+}			
Organically Bound Matter		Metal cations bound to anionic organic groups in the organic molecules: K^+, Na^+, Mn^{2+}, Ca^{2+}, Mg^{2+}, Fe^{2+}, and Al^{3+}		Organic covalent forms of S, Cl and P
Included Minerals			Precipitated Ca-salts (CaC_2O_4 Crystals)	Silica (SiO_2)
Excluded Mineral Matter			Foreign matter originating from the processing of the feedstock as Fe and Al from cutting equipment	Soil minerals as sand and clay minerals (SiO_2 and aluminosilicates often with some K, Na, or Ca)

Since our main interest in this study is identifying the different chemical forms of S and Cl, we were inspired by the procedure of chemical fractionation analysis described by Pandey et al. (2021), Pettersson et al. (2008), and Zevenhoven et al. (2012). To achieve this, we employed a method that involved consecutive leaching in only two solvents: pure water and a 1M

ammonium acetate (NH_4Ac) solution. First, an excess of Milli-Q water (15 mL/g) was used to leach out 10 g of solid with agitation during 24 hours at ambient temperature. After this period, the solution was filtered and the water leachate was collected. The remaining solid was then leached out in a 1M NH_4Ac solution (pH=7.45) (5 mL/g) with agitation during 24 hours at ambient temperature. After this, the suspension was filtered and the acetate leachate was collected. Water and acetate leachates were analyzed by ICP-OES (Inductively Coupled Plasma Optical Emission spectroscopy) for S and Si and by ion chromatography (ICS 3000) for anions Cl^- and PO_4^{3-} and cations K^+, Na^+, Ca^{2+}, and Mg^{2+}. In addition, the filtered solid residue was dried and its content in S and Cl was determined with the same method as that used for the raw feedstock. To ensure the most accurate elemental balance of sulfur and chlorine in the fractionation method, the unrecovered liquid trapped in the solid residue was quantified by calculating the difference in mass of the solid before and after drying. It was assumed that it had the same concentration of inorganic elements as the NH4Ac leachate in the final step of leaching. The mass fractions of S and Cl found in this unrecovered liquid ranged from 1 to 10% and were added to the mass fractions in the NH_4Ac leachate.

$$m_{i-total} = m_{i-H2O\ leachate} + m_{i-NH4Ac\ leachate} + m_{i-solid\ residue} + m_{i-unrecovered-liquid} \quad [2.4]$$

The mass of each element recovered in each of the leachates was calculated as the measured concentration multiplied by the collected volume of the leachate:

$$m_i\ (mg) = \text{Concentration}\ (mg/L) \times \text{Volume of Leachate}\ (L)$$

The mass fraction of each element in each leachate or solid residue was calculated as the recovered mass divided by the initial mass of element in the feedstock:

$$w_{i-leachate\ or\ residual\ solid} = \frac{m_{i-leachate\ or\ residual\ solid}(mg)}{m_{i-initial}(mg)} \quad [2.5]$$

2.1.3.2 Chemical fractionation results

The distribution of sulfur and chlorine obtained after chemical fractionation analysis is presented in **Figure 6**. Note that only the cases for which the initial S or Cl content is higher than 0.1 wt% were investigated. To ensure the repeatability, the leaching test for each feedstock was performed twice. The results shown are averages of the two replicates. Error bars show the relative uncertainty of the total mass balance calculated by the propagation of uncertainties (Appendix. B). Since the differences obtained in the replicates were smaller than the calculated uncertainties, we considered the calculated uncertainties to be a reasonable estimate of the measurement errors. The mass balances over the fractionation experiment are satisfactory (closing to 100%, considering the uncertainties).

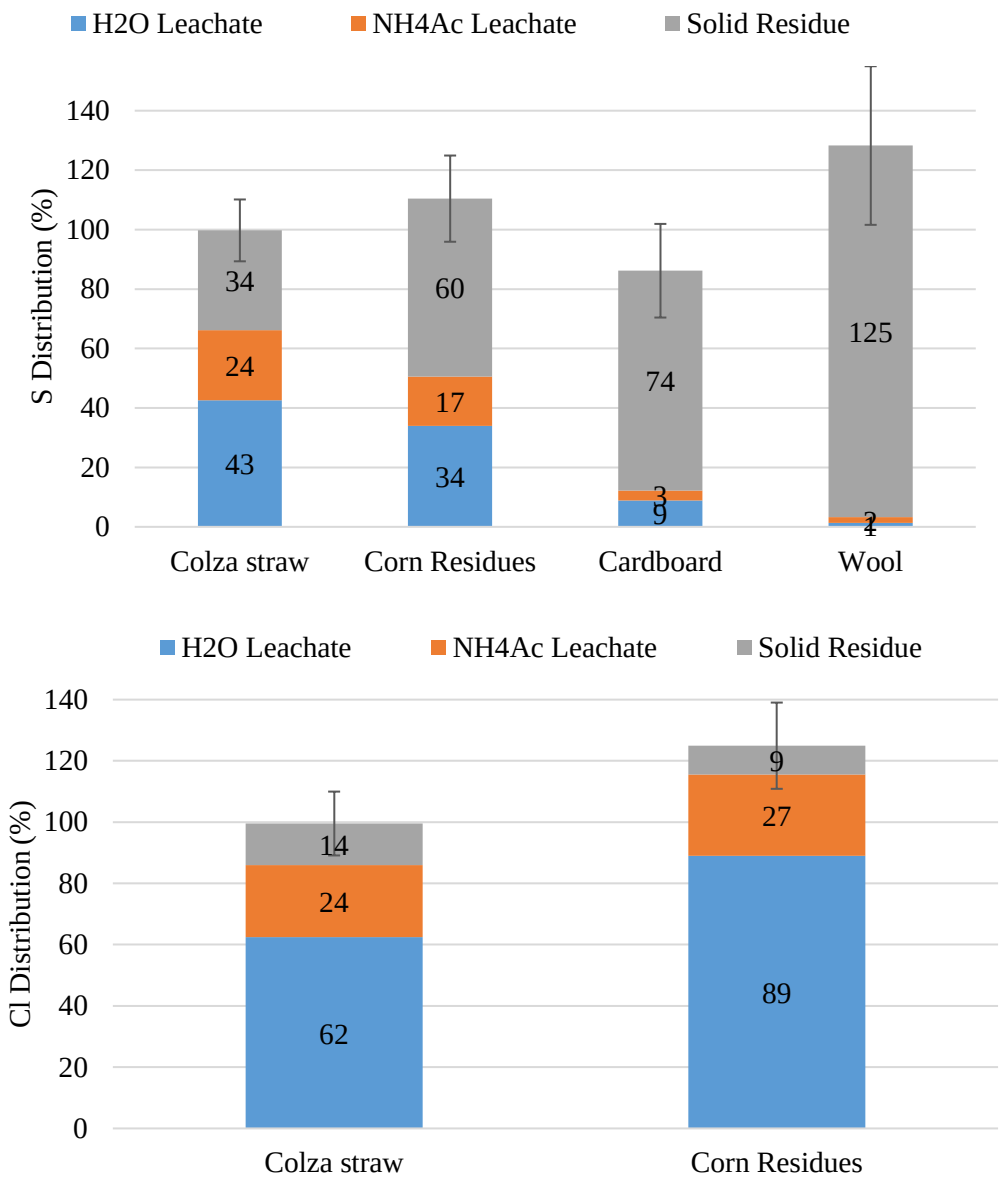

Figure 6: Sulfur and chlorine distribution in recovered leachates and solid residue of the feedstocks

Significant differences can be noted in the distribution of sulfur and chlorine in the leachates and the solid residue between the agricultural residues, cardboard, and wool, which means differences in the relative quantities of their two chemical forms (organic and inorganic).

For the colza straw and corn residues, 67% and 51% of S, respectively, and more than 85% of Cl were found in the water (predominantly) and NH_4Ac leachates. Thus, more than half of the sulfur and almost all the chlorine are present in the inorganic form of soluble salts in the agricultural residues. To get more information on the association of S and Cl with other key inorganic elements, **Table 14** presents the fraction of major ash elements (K, Ca, and Si) measured in the water leachates where they could be associated to S or Cl. A high fraction

(>75%) of the potassium is recovered in water where, similarly to S and Cl, it is present in an inorganic form of soluble salts. The molar ratios K/Cl and K/(S+Cl) in the initial feedstock and in the water leachates are higher than 1. This indicates that the number of moles of potassium is sufficiently high to be able to bond with chlorine and with sulfur. Possible forms of salts made of these elements are potassium chlorides KCl and $KClO_4$ (Deng et al., 2022). The molar ratio K/S is higher than 2 only for the corn residues for which S could thus be present in the form of potassium sulfates K_2SO_4 (Vassilev et al., 2012). Other studies have detected K in other soluble forms such as carbonates (K_2CO_3) (Tchoffor et al., 2016) and phosphates K_2HPO_4 (Piotrowska et al., 2010). For colza straw and corn residues, 20% and 50% of the calcium is recovered in the water, respectively. It can be present in the form of sulfates such as $CaSO_4$ (Suárez-García et al., 2002), or even as calcium oxalates (CaC_2O_4) (Pettersson et al., 2008). The insoluble part of Ca can be organically associated into the biomass (Ca-COO) or in carbonates ($CaCO_3$) (Pettersson et al., 2008). Silicon is only slightly leached in water, which shows that it mainly remains in the solid residue. It can be present as included minerals (silica SiO_2) or excluded minerals coming from soil sand and clay (SiO_2 and aluminosilicates often with some K, Na, or Ca).

Table 14: Fraction of K, Ca, and Si measured in the water leachates of the agricultural residues

	K	Ca	Si
Colza Straw	77 %	20 %	3 %
Corn Residues	77 %	50 %	0.25 %

For cardboard, less than 15% of sulfur is recovered in the leachates as inorganic sulfur, while 74% of sulfur is measured in the solid residue, indicating that S is mainly in an organic form in the cardboard. In the Kraft pulping process, sodium sulfide Na_2S is used to dissolve the lignin that binds the cellulose fibers together in the lignocellulosic biomass. Therefore, at the end of the process, remainder of the sulfur additives may be found as minerals or be included in the lignin structure (organically associated).

For wool, all the sulfur is in the solid residue, which shows that S is mainly in an insoluble organic form. This is in agreement with what was expected, with sulfur mostly present in amino acids in this type of feedstock.

The main objective was to distinguish the different chemical forms of S and Cl in the chosen feedstock to be able to explain later their behavior and their distribution during thermochemical processes. The results confirmed, as previously found in literature, the existence of two different

forms of S and Cl depending on the nature of their bonding with other ash elements. In the two agricultural residues, S was found in its two chemical forms as organically bonded to the carbon matrix and as inorganic soluble sulfates (possibly as $CaSO_4$ in the Ca-rich colza straw and K_2SO_4 in the K-rich corn residues). Cl is mainly in the form of inorganic salts (possibly KCl, $KClO_4$...). However, in wool and cardboard, sulfur was mainly found in an organic form, while in PVC Cl is known to be organically bonded in the polymer structure.

2.2. Experimental Setup and Procedure

2.2.1. Description of the experimental set-up "PYRATES"

The experimental set-up was designed and studied in a previous thesis (Sosa Sabogal, 2022). It consists of an induction-heated reactor, followed by a condensable and gas products collection system, and analysis modules (**Figure 7**).

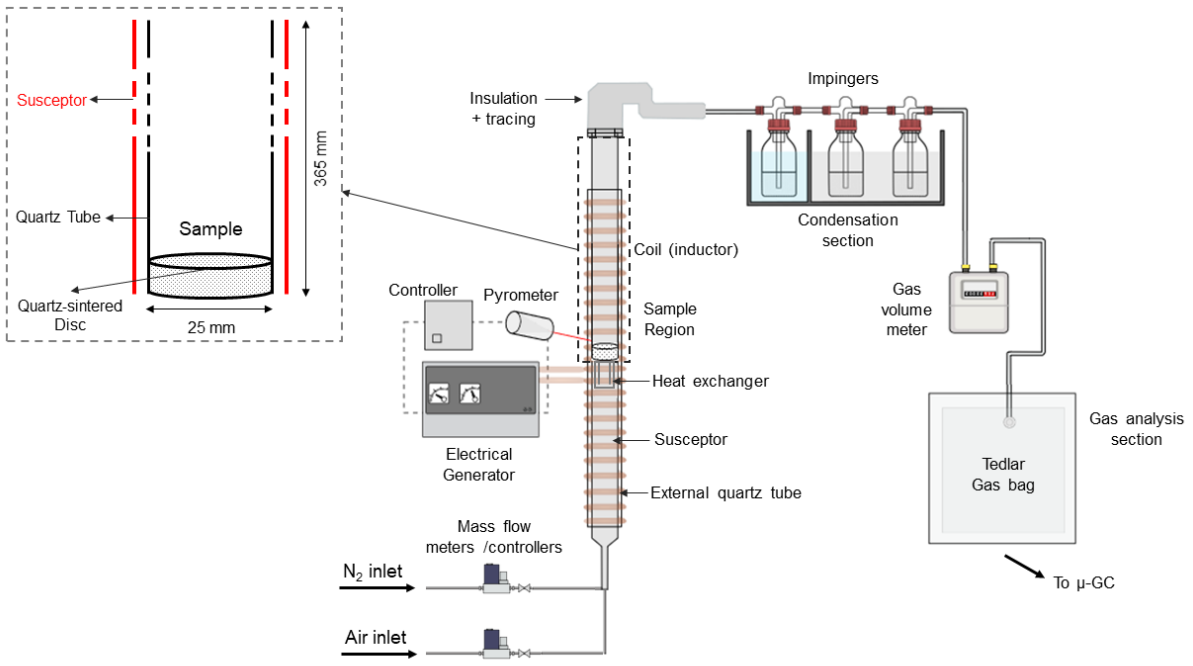

Figure 7: Schematic representation of the lab-scale setup and details of the reaction zone

In our study, the reactor is a quartz tube (365 mm in height, 22 mm in internal diameter, 3 mm in thickness) fixed to a porous quartz-sintered disc (25 mm in diameter, 4 mm in thickness, grade 0 in porosity with maximum pore size from 160 to 250 µm) that can withstand temperatures up to 900°C (**Figure 8**). CERAMABOND glue, having a high thermal and

electrical resistance up to 1800°C, is used to bond the quartz sintered-disc with the quartz tube. This reactor was specifically chosen for the present study, as explained at the end of the present section.

The reactor is placed inside a susceptor that consists in a 316L stainless-steel tube (560 mm in height, 30.15 mm in internal diameter) that is supported by a 5 mm thick ceramic ring.

Under this ring, a metallic heat exchanger made from two concentric tubes of 20 mm and 23 mm of Inconel 600 sheets (50mm height, 0.5 mm thickness) helps to preheat the entering gas.

Two gas inlets, respectively connected to a N_2 and an air bottle, are installed at the bottom of the reactor. The gas flowrates are set using mass flow meters/controllers [Mass flowmeter 5851S, BROOKS Instrument].

The susceptor is surrounded by a water-cooled copper coil inductor (420 mm long), which is connected to a 12 kW electrical generator that supplies energy to the induction circuit.

An external quartz tube is placed between the coil and the susceptor to avoid any contact between them and to center the setup.

Set point temperature is adjusted with a PID controller [GEFRAN 2500 PID], connected to a two-color optical pyrometer [Impac IGAR 6], which aims at the susceptor wall at the sample level.

The upper part of the reactor is connected to an elbow; both are wrapped in insulated heating cable that are kept at 280°C and 170°C, respectively, to avoid early condensation.

The produced gases go through a series of five impingers (500 mL gas washing bottles) followed by a gas volume meter. They are collected in a Tedlar bag and can later be analyzed by micro gas chromatography (Agilent 990).

The first two impingers are filled with deionized water and placed in a bath filled with ice (0°C) to collect the chlorinated species (HCl, KCl, NaCl). They are followed by three impingers filled with 2-propanol placed in a thermostat device (–15°C) to collect condensable species (water and tar) and clean the gas stream before entering the gas analyzers. Before each test, glass wool and glass beads are placed into each gas washing bottle. Isopropanol or deionized water is then added to complete a total volume of 300 mL. The glass wool helps to filter particles and prevents them from being carried away to gas analyzers, while the glass beads help to enhance the liquid-gas contact and therefore the trapping in the solvent. After completing the test, the impingers are removed from the cooling bath. To determine the volume of the recovered solutions, the impingers are weighed and the samples are stored at a controlled temperature of 5°C.

The remaining solid product in the sample holder is collected once the reactor has cooled down. The products characterization procedures are detailed in **section 2.2.3**.

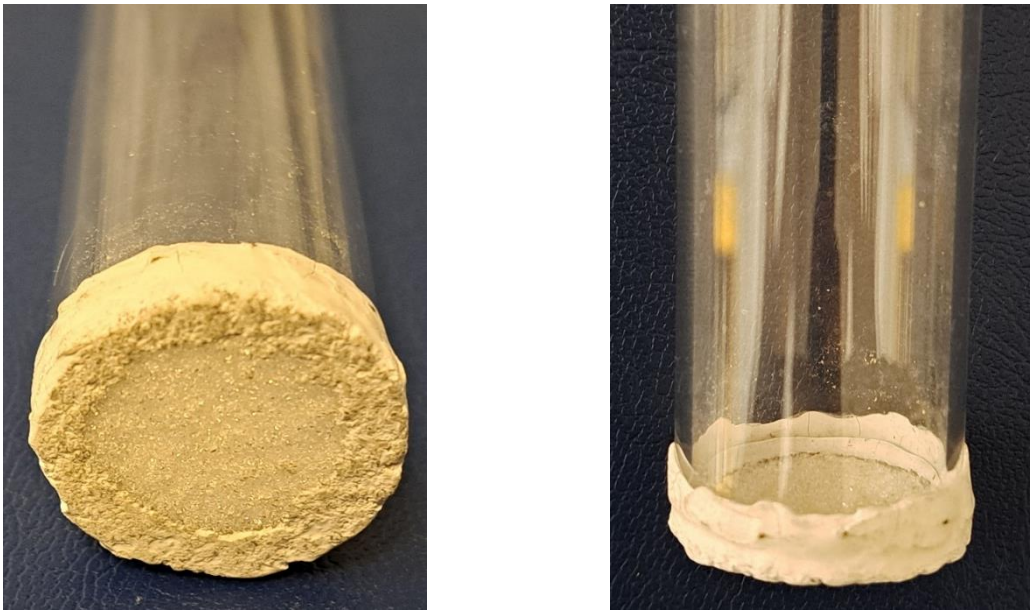

Figure 8: Pictures of the quartz tube fixed to the quartz-sintered disc

It is important to note that in the initial experimental-set-up used in the previous thesis (Sosa Sabogal, 2022), the sample crucible was composed of a steel wire mesh cylinder (550 mm in height and 27 mm in external diameter), in which the sample was placed, with a wire mesh cone of 35 mm high attached at the bottom. It was placed inside the reactor main body made up from the stainless-steel tube (316L).

Contrary to the previous thesis mainly focused on the transformation of the organic part of biomass and waste, our focus in the present study is the distribution of the inorganic species, particularly sulfur and chlorine, between solid and volatile phases. Therefore, before starting the analytical experiments, different tests with gas mixtures and with solid sulfur model molecules were performed to ensure the best possible closure of the elemental balances of S as a first step :

- First, mixtures of different gaseous species including H_2S and COS (concentration of 50 ppmv or 200 ppmv) were injected in the set-up to make sure they are measured correctly by the micro gas chromatography (Agilent 990). Around 90% of the initial gaseous sulfur injected as H_2S and COS was measured by the micro gas chromatography during the tests performed at ambient temperature. However, during the tests performed at 850°C, no sulfur was measured by the micro gas chromatography.

- In addition, tests with solid model molecules representing two forms of sulfur existing in the resources, methionine $C_5H_{11}NO_2S$ (organic) and potassium sulfate K_2SO_4 (inorganic), were performed by heating the reactor at the desired temperature for a duration of 20 minutes and a flow of nitrogen of 0.5 NL/min. The conditions of these tests were chosen based on thermodynamic calculations made with the FactSage software (presented in **section 2.3**), which predicted a complete release in the gas phase. Only 16% of the initial sulfur was measured as H_2S in the gas in the case of methionine at 700°C with no solid residue recovered. This could be due to the incomplete measurement of the released H_2S and COS, or the non-measurement of other sulfur species released in the gas (thiophenes, mercaptans and their derivatives). On the other hand, the potassium sulfate remained intact in the crucible after the two tests performed at 600 and 800°C, which could be due to the kinetic limitation of the reaction.

These tests with gaseous and solid materials have put into evidence some difficulties in detecting or quantifying the released sulfur species. According to de Almeida et al. (2020), the inaccuracies in the contaminants evaluation are especially due to their interaction with the material lining. In the tests performed by these authors, low recovery ratios of H_2S and HCl were found in different tubing alloys at high temperature (above 500°C), suggesting a significant interaction between the reactor and the contaminant and making it challenging to accurately characterize the release of contaminants due to potential corrosion occurring. Even alloys that are considered resistant to corrosion, such as Hastelloy® C-276, Haynes® HR-160 and Kanthal-APM, showed severe limitations for their use at high temperature and corrosive atmospheres. Therefore, interactions of H_2S and COS with the material of our reactor and the heat exchanger (stainless steel and inconel) or their adsorption in the lines (Polytetrafluoroethylene PTFE tubes) of the experimental device were suspected. As it had been highlighted in the work of de Almeida et al. (2020), quartz is inert and is strongly recommended for pyrolysis and gasification tests aiming at measurement of contaminants in syngas.

Therefore, for the present study, the initial steel wire mesh sample holder was replaced by the quartz-sintered disc fixed to the quartz tube, in order to avoid any adsorption or interaction with the released inorganic species.

2.2.2. Thermal Characterization of the reactor and feedstock during pyrolysis

2.2.2.1. Thermal characterization of the empty reactor

A thermal characterization study of the new reactor was performed to precisely measure the temperature of the inner and outer surface of the reactor in function of time.

The empty reactor was heated up at a set point temperature level of 810°C and kept at the desired temperature for 10 minutes to guarantee steady state. The carrier gas used was nitrogen (N_2), and the flowrate was set to 0.5 NL/min. To measure the temperature at the outer surface of the reactor, four K type thermocouples (TO1 to TO4) of 0.5 mm in diameter were positioned on the susceptor's outer surface at z = 10, 207, 268 and 375 mm. z = 0 mm corresponds to the bottom of the susceptor. The temperature profile inside the quartz tube was measured using three thermocouples (TI1 to TI3) of 0.5 mm in diameter at different axial positions (z = 209, 224 and 239 mm, corresponding to 2, 17, 32 mm above the quartz disc) introduced inside the quartz tube. **Figure 9** shows the positions of the thermocouples on the outer surface of the susceptor and inside the reactor quartz tube.

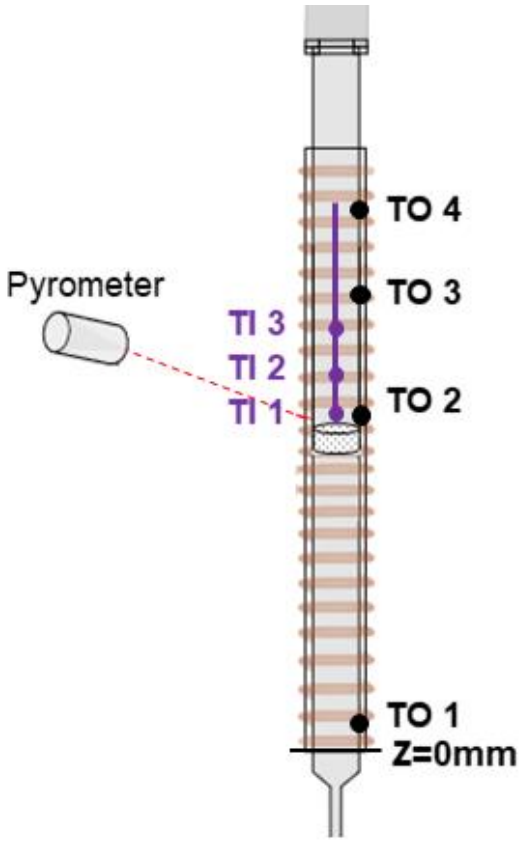

Figure 9: Schematic representation of the positions of pyrometer, the thermocouples on the outer surface of the susceptor and inside the reactor's quartz tube

Figure 10 and **Figure 11** shows the evolution of temperature on the outer surface of the susceptor and inside the quartz tube, respectively, as a function of time at a setpoint of 810°C. The measurements made at the setpoint of 860°C are presented in Appendix C.

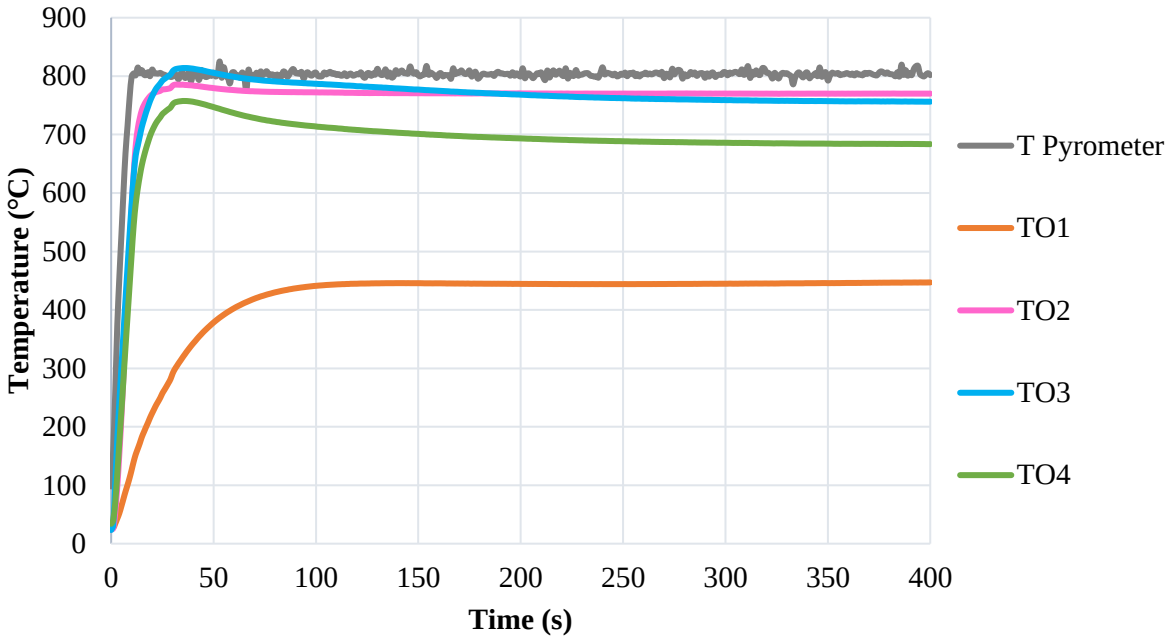

Figure 10: Evolution of temperature at the different positions of the outer surface of the susceptor at a setpoint of 810°C

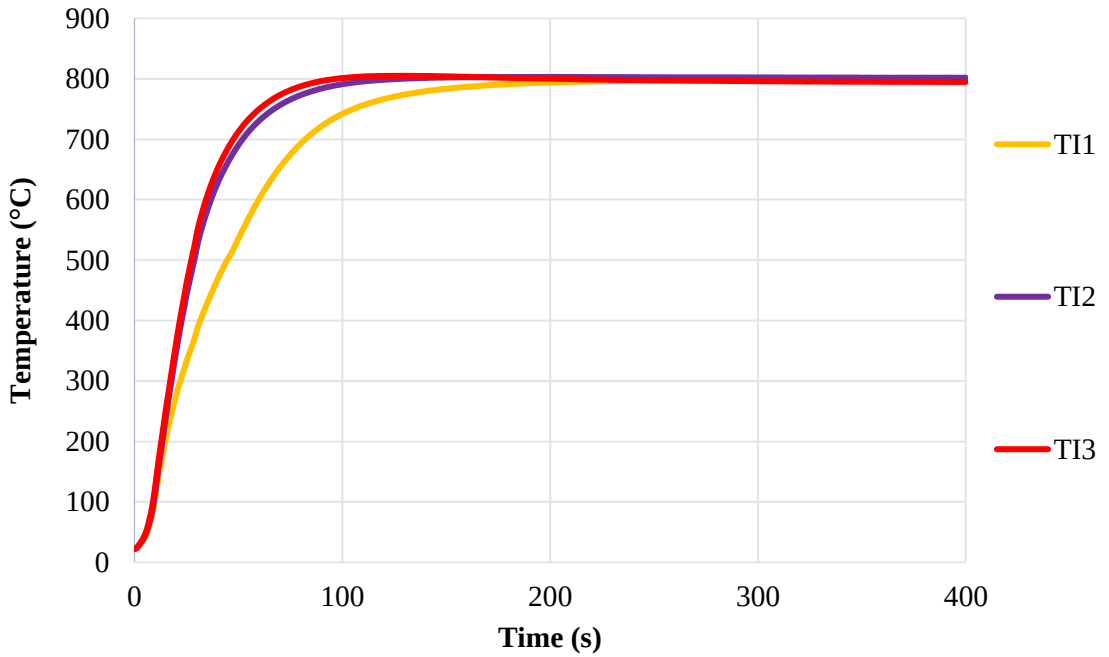

Figure 11: Evolution of temperature at the different positions inside the reactor's quartz tube at a setpoint of 810°C

TO1 measures the lowest temperature, and is far from the set point since it is positioned at the bottom end of the heated zone of the reactor. The temperature of the wall at the sample height (TO2) increases linearly at approximately 80°C per second. It reaches a value close to the setpoint within approximately 30 seconds, specifically reaching 790°C when the setpoint is 810°C and 845°C when the setpoint is 860°C. The temperature of the wall above the sample level (TO3) reaches the setpoint in 30 seconds and then drops to 760°C when the setpoint is 800°C and to 810°C when the setpoint is 850°C. The temperature TO4 along the empty zone above the sample is close to that of the pyrometer at the beginning of the heating, however, it reaches 758°C and then drops to around 680°C.

As expected, the inner space in the quartz reactor takes a longer time to reach the set point than the outer surface of the susceptor, with a heating rate of 10°C/s due to the thermal inertia of the quartz. The thermocouple TI1 placed at the lowest position (z=2 mm) takes more time to reach the set point since it is the closest to the quartz-sintered disc that has a more important thermal inertia. On the other hand, the differences between the temperatures at the three positions after 100 s are not significant which confirms a uniform temperature profile in the axial position between 2 and 32 mm above the quartz-sintered disc. This will be taken into consideration in the analytical experiments by filling the reactor with the feedstocks up to 32 mm maximum above the disc to ensure a homogeneous temperature sample region.

The setpoints 810°C and 860°C were fixed to most importantly reach the desired temperature 800°C and 850°C inside the quartz tube where the feedstock sample is placed. At the sample level, there is a slight difference between the temperature at the outer surface of the reactor (TO2) and the temperature measured inside the quartz tube (TI1-3) (790°C versus 800°C at a setpoint of 810°C) and (845°C versus 850°C at a setpoint of 860°C). In the previous thesis (Sosa Sabogal, 2022), measurements were taken at the preheater zone, revealing that the temperature exceeded the designated set temperature. Therefore, the preheated gas is maintained at a temperature higher than 800°C and when it flows through the reactor, it contributes to the elevation of the temperature inside the quartz tube.

2.2.2.2. Thermal characterization of the feedstock during pyrolysis tests

Before starting the analytical experiments, the thermal characterization of each feedstock was also carried out. The objective was to determine the real temperature of the samples in function of time. To do so, the temperature profile inside the sample was measured by inserting the three thermocouples (TI1 to TI3) previously described inside the sample. N_2 was continuously fed at

a flow rate of 0.5 NL/min. **Figure 12** shows the thermal profiles of each feedstock given by TI1.

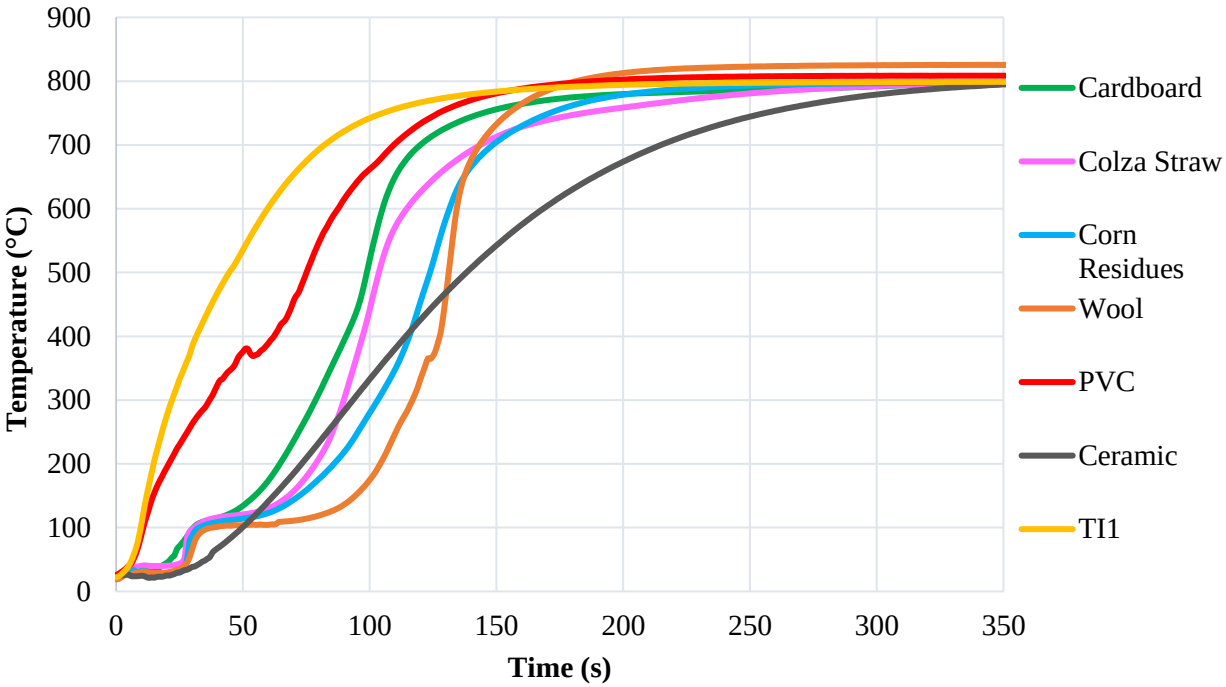

Figure 12: Thermal profiles (TI1) of the feedstock samples, ceramic and the empty reactor

The samples present different heating rates, with PVC being the fastest, followed by cardboard, colza straw, corn residues, and wool. For every feedstock except PVC, the temperature reaches a plateau at 100°C for a short period (30 seconds) before continuing to increase. The observed phenomenon may be attributed to the initial stages of decomposition during pyrolysis, which generate water vapor. However, it is possible that the inadequate removal of this water vapor from the sample is causing the observed effect. It is important to note that PVC is the only material that does not produce water vapor during pyrolysis. In order to further investigate this, we conducted a control experiment using ceramic pieces, an inert material, and no visible effects were observed. This control experiment suggests that the observed phenomenon is specific to the sample feedstocks and is not a result of the experimental setup or external factors. The time taken for each feedstock sample to reach 98.75% of the final temperature, 790°C, is 163 seconds for PVC, 170 seconds for wool, 230 seconds for corn residues and 280 seconds for cardboard and colza straw. The varying times taken for the different feedstock samples to reach 800°C can be attributed to their different thermal conductivities, densities and specific heat capacities.

2.2.3. Products Characterization

2.2.3.1. Char Characterization

The remaining solid product in the sample holder, referred to as the char, was weighed and collected for further analyses once the reactor has cooled down. The mass yield of the char is calculated using the following equation:

$$\text{Char yield} = \frac{m_c}{m_f} \quad [2.6]$$

where m_c and m_f represent the masses of the char and the dried feedstock (g), respectively.

The elemental composition of the char (contents in C, H, N, S, Cl, Si, Ca, K, Na, Mg, Fe, Al, and P) was determined according to the same methods as that used for the feedstocks (**section 2.1.2**).

The retention of an inorganic element *i* in the char is defined as:

$$\text{Retention in the char} = \frac{m_{i-c}}{m_{i-f}} \quad [2.7]$$

where m_{i-c} and m_{i-f} are the masses of each element in the char and the raw material (g), respectively.

The relative uncertainties were calculated by the error propagation method detailed in Appendix B.

The crystalline phase analysis of the char samples was conducted with a powder X-ray diffractometer. XRD patterns were evaluated using the DIFFRAC.EVA software with ICCD RDB databases (PDF-2 and PDF-4). After identifying all the peaks in the diffractograms, a semi-quantitative analysis, which is based on the intensity of the diffraction peaks, was also used to estimate the relative abundance of the different phases in the samples. The powdered samples were prepared by hand grinding using a mortar and pestle. They were placed in the XRD sample holder and pressed using a glass slide to assure a smooth surface of the powder.

The chars' morphology and local surface elemental composition were studied using a scanning electron microscope (Philips XL30 with a 15 kV electron beam) coupled to an energy dispersive X-ray spectroscopy (SEM–EDX). The powdered samples were directly observed after placing them on carbon tapes.

2.2.3.2. Gas and condensable species analysis

The produced gases were collected in a Tedlar bag and analyzed by micro gas chromatography (Agilent 990). The micro gas chromatography was calibrated to detect and quantify the concentration of sulfur-containing gas species H_2S and COS which are our main interest, as well as CO_2, CO, CH_4, H_2, C_2H_2, C_2H_4, C_2H_6, C_3H_x, C_4H_6, C_6H_6, and C_7H_8. Considering the volume of gas released by the sample (measured with the gas volume meter), the mass of S present in H_2S and COS could be determined for each experiment.

The deionized water recovered from the first two impingers was analyzed by ionic chromatography to measure the concentrations of chloride Cl^- anions as well as sodium Na^+ and potassium K^+ cations.

Since the ionic chromatography allows only the measurement of sulfur under its oxidized SO_4^{2-} anion form, the concentration of sulfur present in the water impingers was determined by ICP-OES that measures the total sulfur and therefore ensure the best possible closure of the elemental balance of S.

2.2.4. Experimental conditions

The analytical experiments were carried out in this study to attain two objectives: characterizing the behavior of sulfur and chlorine during pyrolysis and gasification and testing methods to enhance their retention in the char, based on the interaction with non-volatile inorganic elements. Therefore, pyrolysis and gasification experiments of each feedstock alone were carried out in the first place. Then, the effects of adding calcium-based additives to the feedstock and mixing resources were evaluated in pyrolysis, and also sometimes gasification.

It is important to mention that some experiments were carried out with a complete analysis of all the product streams obtained: the char from the solid phase, and the gas and condensed phases. It was the case for the pyrolysis experiments of the individual feedstock conducted at 800 and 850°C. The other experiments were limited to analyzing only the residual char.

For each experiment, the reactor was filled up to 32 mm of its height with 2 to 4 g of dried feedstock to ensure a homogeneous temperature sample region. The procedures of the experiments performed are detailed below.

2.2.4.1 Experimental conditions for stand-alone feedstock

Pyrolysis experiments

Two types of pyrolysis experiments were performed:

- In the first type of experiments, the reactor was heated up and kept at the desired temperature for 20 minutes. Tests were performed at two different set point temperature levels: 800°C and 850°C for all feedstocks. As mentioned above, a complete analysis of the different product streams was carried out in these experiments. Before each test, a pressure drop test was performed to ensure the tightness of the reactor and its connections. A nitrogen flowrate of 0.5 NL/min was used to flush the system and carry the resulting volatiles. The reactor was heated and kept at 800°C or 850°C for 20 minutes. After turning off the heating, nitrogen injection continued for a duration of 40 minutes to ensure complete removal of all produced volatiles. All along the experiment, the condensable species were trapped in the impingers located in the condensation section while the non-condensable gases were collected in a Tedlar sampling bag (Figure 2.4). The gas volume in the bag was measured using a volume gas meter. The gas contained in the bag was analyzed at the end of the experiment using the micro-gas chromatography. The remaining solid was collected, weighed and analyzed after each experiment.

Colza straw was also tested under a different form (pellets) in pyrolysis at 850°C. The objective was to investigate the influence of the feedstock shape and size on the behavior of sulfur and chlorine in pellets. The colza straw pellets (diameter of 13 mm, a height of 4 mm) (**Figure 13**) were obtained using a pellet press with 6-ton hydraulic pump (Nominal Force: 350 N).

Figure 13: Pellet of colza straw

- In the second type of experiments, the heating was interrupted at different times and therefore each sample reached a different temperature. Set point temperature was fixed at 800°C. The temperatures reached by each sample was measured using the same thermocouples (TI1 - TI3) described previously in the thermal characterization section. These tests allowed having a more comprehensive understanding of the behavior of S and Cl during the heating ramp. Each experiment is shown in **Figure 14** as a function

of its heating time, where it is referred to according to the maximum average temperature reached inside the sample. Examples of temperature measurements in this type of experiments are shown in Appendix D. N_2 was continuously fed at a flow rate of 0.5 NL/min.

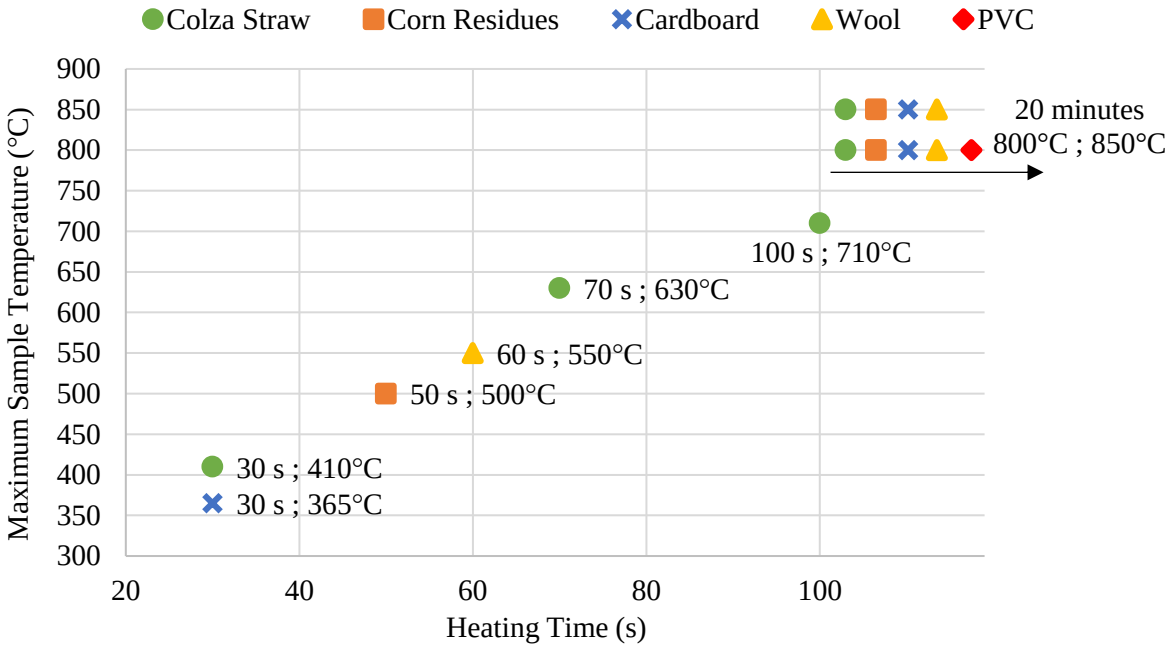

Figure 14: Maximum temperature reached in the sample versus heating time for each pyrolysis experiment

Gasification experiments

The objective was to study the effect of adding an oxidant (air) on the sulfur and chlorine retention in chars. The previous pyrolysis experiments did not show any significant difference in the results obtained at 850°C and 800°C. Therefore, it was decided to investigate the effect of adding an oxidant on sulfur and chlorine retention at 800°C only. The same conditions of air injection were fixed for all of the feedstocks; air was injected at a flowrate of 0.2 NL/min and completed with a nitrogen flow rate of 0.3 NL/min to keep the same gas flowrate of 0.5 NL/min as in the pyrolysis tests. The volume fraction of O_2 was thus of 10%. The reactor was heated up and kept at 800°C for 20 minutes. After 20 minutes, the mixture of air and N_2 was replaced by pure N_2 for cooling. The mass of each sample was adapted to keep the equivalence ratio ER of the feedstock fixed at 0.3 for all the experiments. The equivalence ratio was calculated as the ratio of the real quantity of oxygen introduced in the system to the stoichiometric quantity of oxygen needed for a complete combustion Due to the limited char yield obtained during the pyrolysis experiment of PVC, we opted not to proceed with gasification experiments

specifically targeting PVC. **Table 15** shows the experimental conditions of the gasification tests. In addition, gasification experiments were performed on the agricultural residues with an extended duration of 60 minutes at 800°C, with the objective of further investigating potential changes that might happen with more extended gasification of the samples.

Table 15: Experimental conditions of the gasification tests

Feedstock	Colza Straw	Corn Residues	Cardboard	Wool
Mass (g)	3.2	3.1	3.4	2.1
$\frac{O_2 real}{O_2 stoichiometric}$	0.3			
$\% O_2 (v/v)$	10%			

2.2.4.2 Experimental conditions with use of additives

In an attempt to enhance the retention of sulfur and chlorine in the chars and promote their interaction with immobile species (Ca...) during pyrolysis and gasification, three types of calcium-based additives were used (**Table 16**). The additives are in the form of fine powder. They were mixed with the resources in a flask using a spatula and by manually shaking the flask.

Table 16: Calcium-based additives used in the experiments

	Formula	CAS Number	Molar Mass (g/mol)
Calcium Carbonate	$CaCO_3$	471-34-1	100.09
Calcium Hydroxide	$Ca(OH)_2$	1305-62-0	74.09
Calcium Oxide	CaO	1305-78-8	56.08

For all the experiments, the quantity of additive was chosen to obtain a fixed mass ratio of 10 wt. %. between the calcium provided by the additive and the dried feedstock. Therefore, the resulting mass ratios between the additive and the dried feedstock were 25, 14 and 18.5 wt. % for $CaCO_3$, CaO and $Ca(OH)_2$, respectively. The effect of using these additives was evaluated in pyrolysis and gasification experiments performed at 800°C (**Table 17**).

Table 17: Experiments performed with the use of the Ca-based additives at 800°C (P for pyrolysis and G for gasification)

	Colza Straw	Corn Residues	Cardboard	Wool	PVC
$CaCO_3$		P		P	
CaO	P / G	P / G	P	P / G	P
$Ca(OH)_2$				P	

2.2.4.3 Experimental conditions for mixture of resources

With the same objective of enhancing interactions between inorganic elements, pyrolysis and gasification experiments were carried out on different mixtures of resources. The mixtures were prepared by manually shaking a flask containing the different components, and they were placed in the sample holder in a way to assure the best possible homogeneous mixture. **Table 18** shows the blending ratios (R1/R2) of the mixtures used in the co-pyrolysis and co-gasification experiments. Cardboard and colza straw were chosen to be mixed with others due to their high calcium content (4.17 and 3.74 wt. % respectively). Moreover, oak bark, a feedstock available in the laboratory, grinded to fine powder, was also tested for its high calcium content to be mixed with some resources. Its chemical composition is shown in **Table 19**.

In order to keep a similar Ca mass ratio as in the tests with Ca-based additives, the first blending ratios were determined so that the mass ratio of calcium provided by the resource R1 (cardboard, colza straw or oak bark) to the initial mass of the resource R2 is 10 wt. %. The resulting mass ratios of R1 to R2 were around 70 / 30 wt. %. Additional tests were carried out using blending ratios of 50 / 50 wt. %.

All these experiments were performed at 800°C with a holding time of 20 min.

Table 18: Blending ratios (R1/R2) of the mixtures used in the co-pyrolysis and co-gasification experiments (P for pyrolysis and G for gasification)

R1 / R2	Cardboard	Colza Straw	Bark Oak
Wool	70 / 30 wt.% P/G 50 / 50 wt.% P	72 / 28 wt.% P 50 / 50 wt.% P	76 / 24 wt.% P
Corn Residues	70 / 30 wt.% P		
Colza Straw	70 / 30 wt.% P 50 / 50 wt.% P	-	76 / 24 wt.% P

Table 19: Chemical composition (on dry basis) of the bark oak used in the co-mixtures

Ash 550°C	**C**	**H**	**N**	**O**	**S**	**Cl**	**K**	**Si**	**Ca**	**Na**	**Mg**	**Al**
wt. %	wt. %	wt. %	wt. %	wt. %	wt. %	wt. %	wt. %	wt. %	wt. %	wt. %	wt. %	wt. %
6.3	49.2	4.5	0.5	35.9	0.03	0.13	0.2	0.5	3.1	0.02	0.07	0.1

2.3. Thermodynamic Simulations

To assess the behavior of sulfur and chlorine during pyrolysis and gasification, a series of thermodynamic equilibrium calculations were conducted for the different feedstock. The main objectives were:

- to determine the potential stable sulfur and chlorine compounds in the condensed and gas phases
- to calculate their release in the gas as a function of temperature and Equivalence Ratio (ER).

FactSage is a powerful software package for performing thermodynamic calculations and analyzing phase equilibria in materials science and engineering. It has the ability to simulate complex multi-component systems with various phases and reactions.

The Equilib module in FactSage is used to perform calculations related to phase equilibria. This module allows users to calculate the conditions under which different phases or combinations of phases are in equilibrium, such as the composition of coexisting phases or the temperature

and pressure at which a particular phase transition occurs. It is based on the minimization of the Gibbs free energy and it uses thermodynamic data from the various databases in FactSage to perform these calculations.

Our calculations were performed using the Equilib module of the Factsage 7.3 software, with the compounds database FactPS and two databases including liquid solutions of the FACT package: the oxide and salt solutions databases FToxid and FTsalt (Bale et al., 2016; Jung and Van Ende, 2020). In the case of duplicates, the order of priority of the databases is FTOXID, FTSalt and Fact PS.

FactPS contains thermodynamic data for pure substances, such as elements and compounds. The FToxid databases contain data for pure oxides and oxide solutions of over 20 elements (as well as for dilute solutions of S, SO_4, PO_4, H_2O/OH, CO_3, F, Cl and I in the molten (slag) phase.) The FTsalt databases contain data for pure salts and salt solutions of 27 main cations (Li, Na, K, Rb, Cs, Mg, Ca, Sr, Ba, Mn, Al, Fe(II), Fe(III), Co, Ni, Zn, Pb, La, Ce, Th, U(III), U(IV), Pu(III), Pu(IV), Cr(II), Cr(III), Mo(V)) and 10 main anions (F, Cl, Br, I, NO_3, NO_2, ClO_4, OH, CO_3, SO_4). These databases include stoichiometric solid phases, solid solutions, multicomponent liquid solutions, and a multicomponent gaseous phase. The total number of compounds is 915 (308 gas, 134 pure liquids, 473 pure solids). It is important to note that the calculations comprehensively consider gaseous species, including sulfur-containing compounds (e.g., H_2S, COS, CH_3SH, SO_2 …) and chlorine-containing compounds (e.g., KCl, NaCl, HCl …), in the overall gas phase.

For each feedstock, different calculations (varying temperature or ER) were carried out using as an input the elementary composition of the feedstock (C, H, N, O, S, Cl, Si, Ca, K, P, Mg, Al, Fe, Na) and the contents of O_2 and N_2 in the injected gas:

- The ER was varied between 0 and 0.6 at a fixed pressure of 1 bar and at two different temperatures of 800°C and 850°C.
- The temperature was varied between 350°C and 900°C at a fixed pressure of 1 bar and an ER of 0 and 0.6

The ER equal to 0 corresponds to pyrolysis conditions. The simulation results will be able to be compared to experimental ones.

3.Characterization of S and Cl behavior in pyrolysis and gasification

This chapter includes a multi-faceted approach, starting with thermodynamic calculations to evaluate the behavior of S and Cl at thermodynamic equilibrium. Building upon the thermodynamic analysis, analytical experiments were conducted to investigate the behavior of S and Cl during pyrolysis. The primary focus was to characterize the retention of inorganic compounds within the resulting char, with a particular focus on sulfur and chlorine species. However, first investigations both encompass the quantification of the retention of inorganic elements in the char and of their release in the gas phase. Furthermore, to gain a deeper understanding of the interactions among sulfur and chlorine species, the char matrix, and the ash-forming elements, some characterization of the chars was conducted. This involved the application of specific techniques tailored for such analysis, including XRD (X-ray Diffraction), which is well-suited for examining the crystalline phases of inorganic constituents. Additionally, MEB-EDX (Scanning Electron Microscopy with Energy Dispersive X-ray spectroscopy) was employed to complement the investigation and provide valuable insights into the complex interactions and structures of the inorganic components within the char.

On the other hand, we investigated the influence of the presence of O_2 in the atmosphere (gasification conditions, compared to pyrolysis ones), on the behavior of S and Cl. By combining thermodynamic calculations, experimental measurements, and qualitative characterization, this chapter aims to contribute to the comprehensive understanding of S and Cl behavior during pyrolysis and gasification.

In conjunction with the findings presented in this chapter, the results have been previously published in a scientific article titled “Characterization of sulfur and chlorine behavior during pyrolysis of biomass and waste” in the journal “Sustainable Energy & Fuels”. https://doi.org/10.1039/D3SE00263B

3.1. Behavior of S and Cl at thermodynamic equilibrium

Equilibrium calculations provide a reference state that may be reached under the operating conditions of temperature and pressure. Even if biomass gasification at 1000°C is known to be kinetically limited regarding the formation of the main gaseous species (CO, CO_2, CH_4, H_2), thermodynamic equilibrium calculations were shown to provide valuable indications concerning inorganic species behavior (Defoort et al., 2015). In this section, the focus is placed on assessing the stability of sulfur and chlorine species and predicting their behavior at thermodynamic equilibrium under varying pyrolysis and gasification conditions, for the

different initial resources. These simulations aim to enhance comprehension of how inorganic elements behave and to enable a comparison with the experimental results.

3.1.1. Influence of pyrolysis temperature

In this section, we focus our investigation on the impact of pyrolysis temperature on the distribution of sulfur and chlorine within the resulting products for the different resources.

Figure 15 illustrates the equilibrium distribution of sulfur between gaseous (g) and solid (s) products during pyrolysis of the different resources: corn residues, colza straw, cardboard, and wool, from 350°C to 900°C.

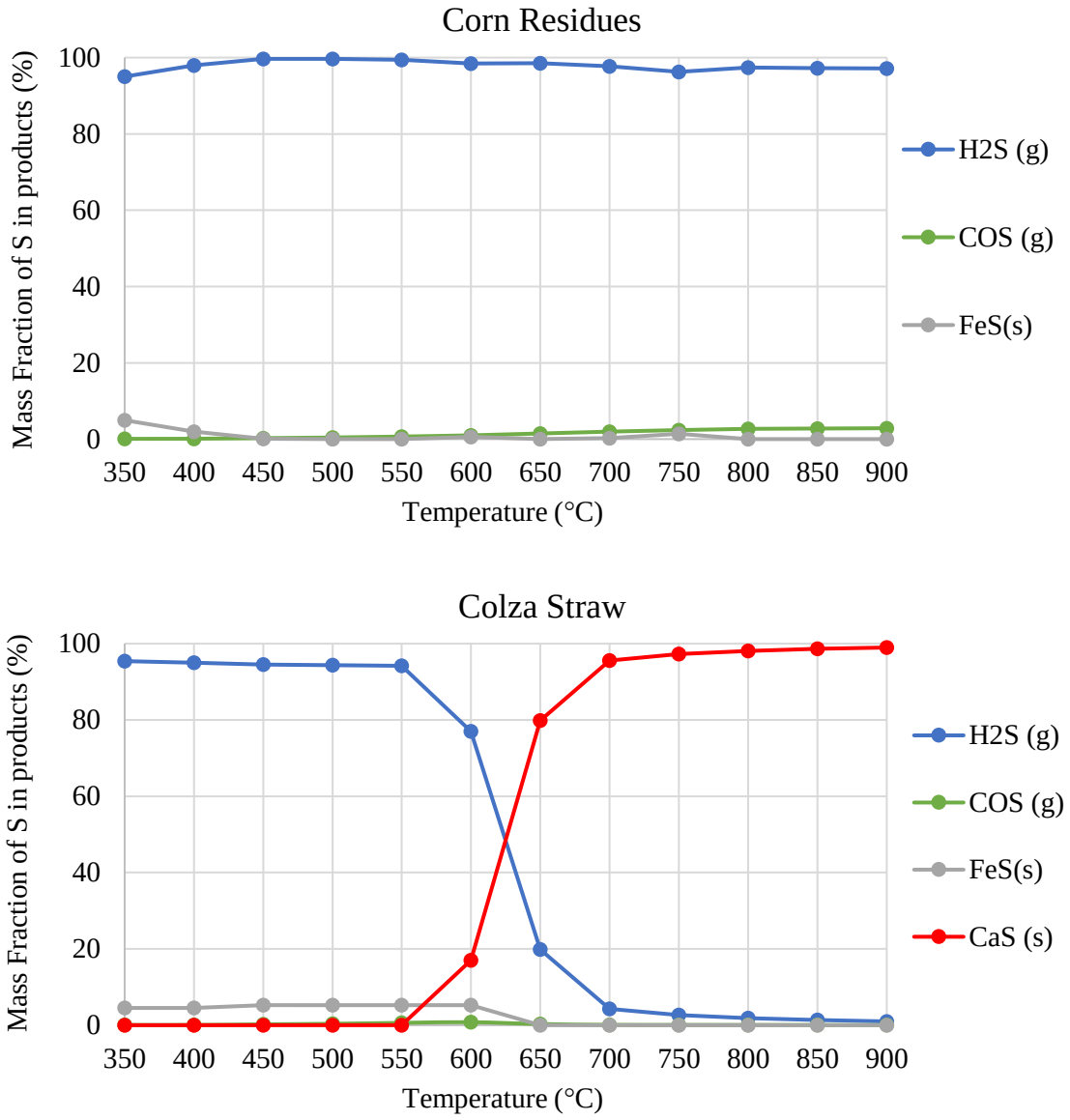

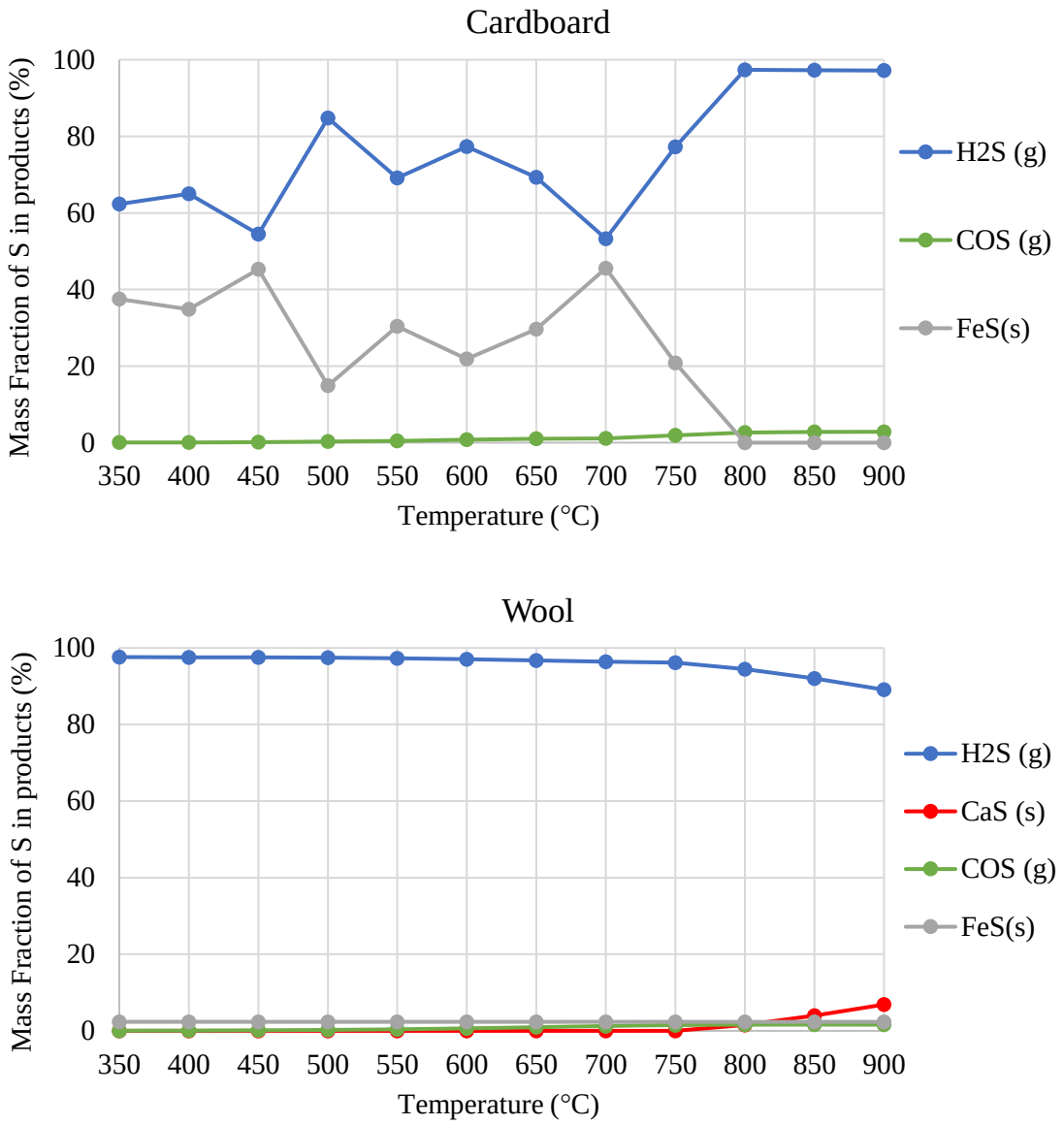

Figure 15: Equilibrium distribution of sulfur in gaseous (g) and solid (s) products as a function of pyrolysis temperature for corn residues, colza straw, cardboard, and wool

For corn residues, sulfur is completely released in the gas phase mainly in the form of hydrogen sulfide H_2S (g). No condensed-phase sulfur species is predicted over the entire temperature interval except at 350°C in the form of iron sulfide FeS (s) (5% of the initial sulfur).

The same case applies for colza straw below 600°C, sulfur being mainly released in the form of hydrogen sulfide H_2S (g) with 5% of S in FeS (s). However, above 650°C, sulfur is predominantly retained in a condensed phase in the form of calcium sulfide CaS (s) which leads to an insignificant release in the gas phase.

For cardboard, between 350 and 750°C, 54 to 84 % of the sulfur is released in the gas phase in the form of hydrogen sulfide H_2S (g) and the rest is retained in the condensed phase in the form

of iron sulfide FeS (s). Above 750°C, sulfur is completely released in the gas phase as H_2S (g) and COS (g).

For wool, H_2S (g) is the main sulfur-containing product over the entire temperature interval, containing 98% of the initial S. Additionally, there is a minor presence of COS (g). The rest of the sulfur is in the condensed phase as iron sulfide FeS (s) and at 850°C and 900°C as calcium sulfide CaS (s).

An important observation in the analysis of the generated gas from the various resources is the consistent presence of hydrogen sulfide (H_2S) as the predominant sulfur-containing compound. H_2S constitutes approximately 98% of the total sulfur released in the gas phase. The remaining sulfur is released as carbonyl sulfide (COS), though in smaller proportions. Based on the results, the COS/H_2S ratio has been calculated to be in average 0.02 indicating a relatively lower concentration of COS compared to hydrogen sulfide H_2S.

The results obtained show that the temperature has no significant effect on the distribution of sulfur in products for the corn residues and wool. However, it is not the case for colza straw and cardboard. The shift in sulfur partitioning with temperature can be attributed to the different reactions and equilibria that occur at varying temperature ranges and depend on the elementary composition of the feedstock. For colza straw, at lower temperatures (below 600°C), the decomposition of organic sulfur compounds and the formation of volatile H_2S gas are favored. However, as temperature increases, the formation of more stable solid compounds, such as CaS, becomes more favorable, leading to the retention of sulfur in the condensed phase. On the other hand, for cardboard, a fraction of S is retained in the solid compound iron sulfide FeS that is thermodynamically stable in the temperature range 350-750°C. Above 700°C, no stable solid compound is found and S is completely released in the gas phase.

The differences in sulfur distribution between the feedstock are linked to their chemical compositions. **Figure 16** shows the evolution of the mass of the major solid ash-components formed at equilibrium for corn residues, colza straw, cardboard, and wool. On the other hand, according to data from Factsage, during pyrolysis, several inorganic elements tend to volatilize, including nitrogen, potassium and sodium. Na is present in very low quantities in the feedstock, which makes K the primary element of interest for our investigation. **Figure 17** presents the volatilization of potassium as a function of pyrolysis temperature at equilibrium. As potassium can be associated both with sulfur (K_2SO_4 for instance) and chlorine (KCl), information on its volatilization can be helpful to analyze the release of S and Cl.

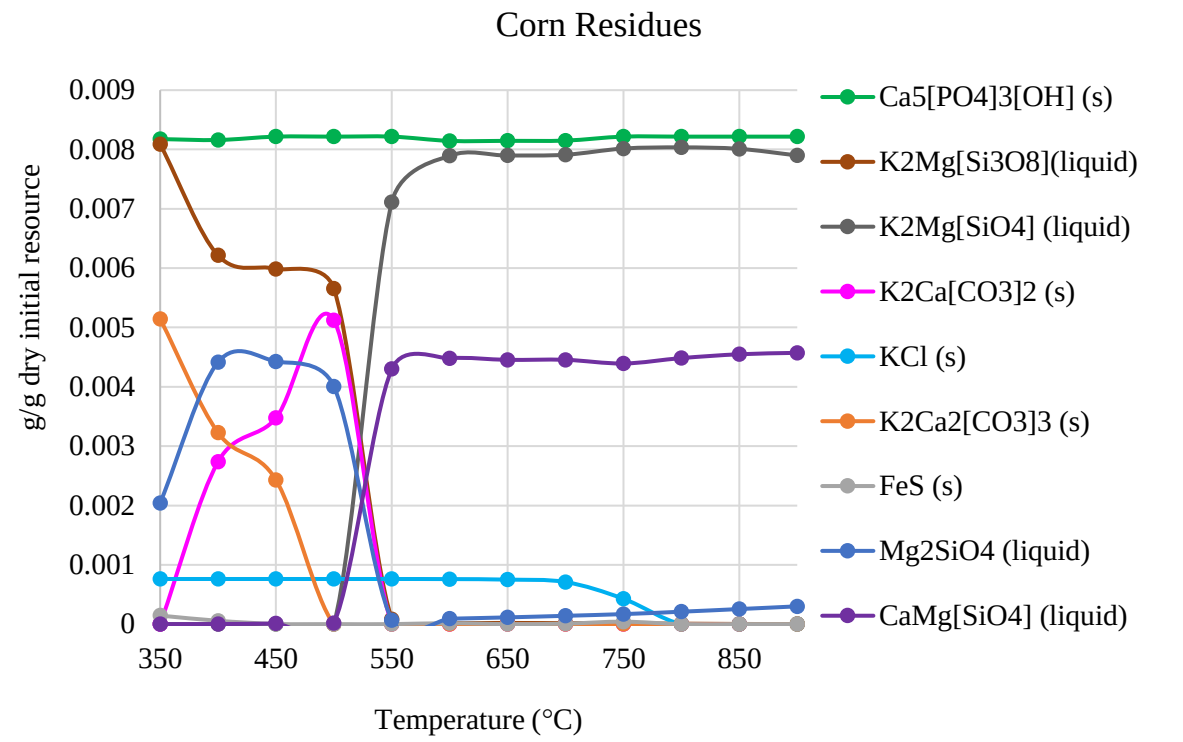
Corn Residues
0.009
0.008
0.007
0.006
0.005
0.004
0.003
0.002
0.001
0
g/g dry initial resource
350
450
550
650
750
850
Temperature (°C)
Ca5[PO4]3[OH] (s)
K2Mg[Si3O8](liquid)
K2Mg[SiO4] (liquid)
K2Ca[CO3]2 (s)
KCl (s)
K2Ca2[CO3]3 (s)
FeS (s)
Mg2SiO4 (liquid)
CaMg[SiO4] (liquid)

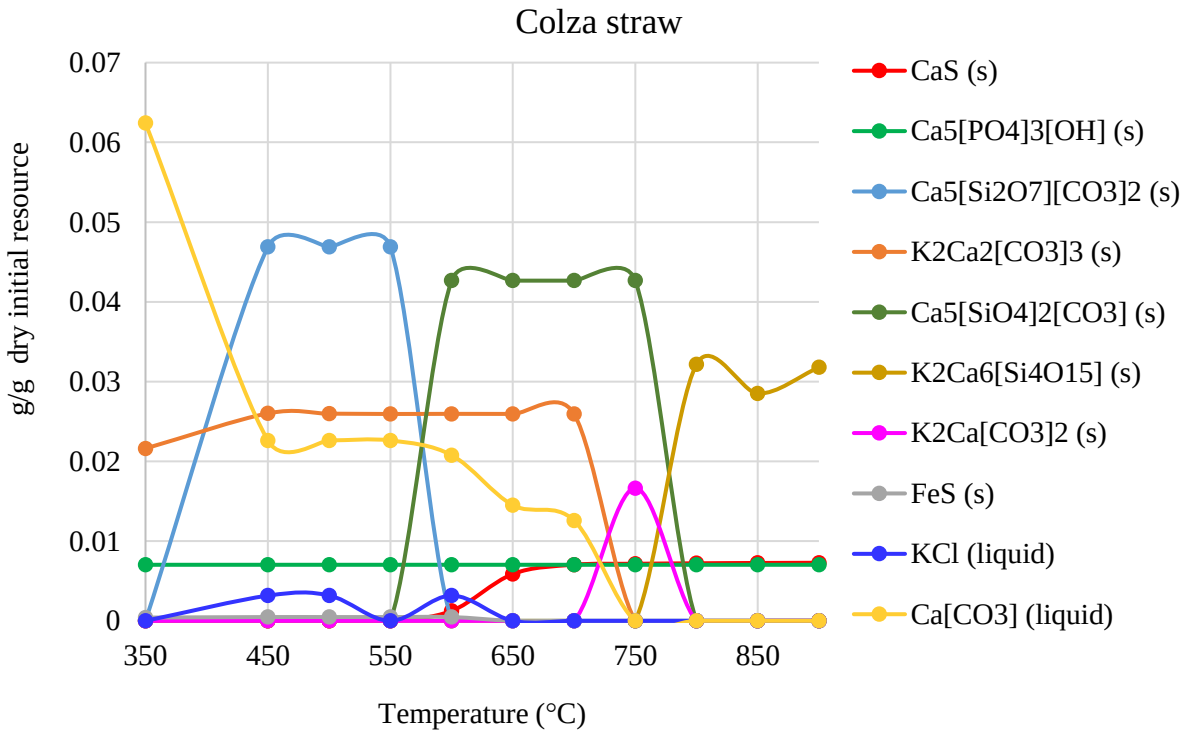
Colza straw
0.07
0.06
0.05
0.04
0.03
0.02
0.01
0
g/g dry initial resource
350
450
550
650
750
850
Temperature (°C)
CaS (s)
Ca5[PO4]3[OH] (s)
Ca5[Si2O7][CO3]2 (s)
K2Ca2[CO3]3 (s)
Ca5[SiO4]2[CO3] (s)
K2Ca6[Si4O15] (s)
K2Ca[CO3]2 (s)
FeS (s)
KCl (liquid)
Ca[CO3] (liquid)

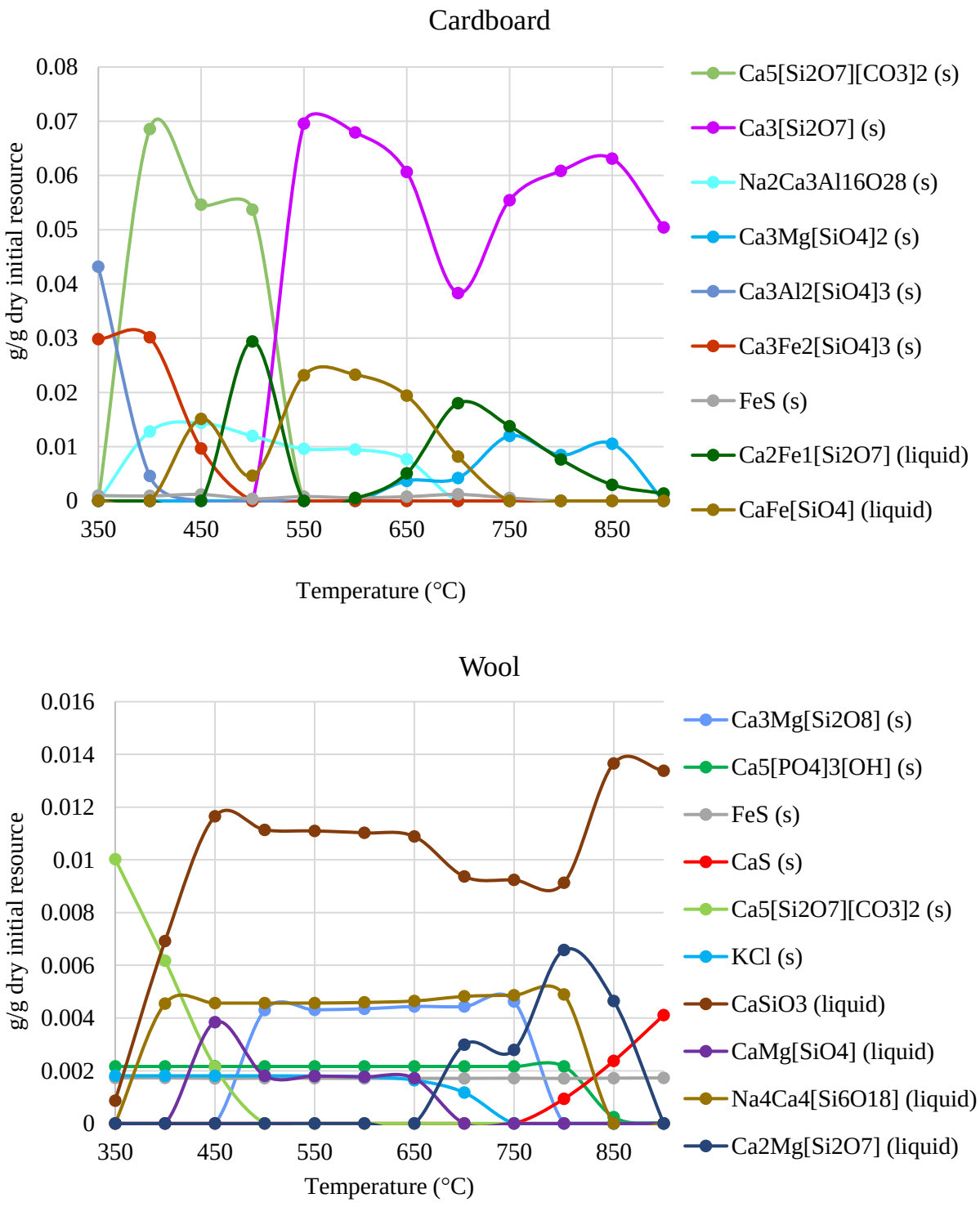

Figure 16: Mass yield of the major solid ash-components formed at equilibrium as a function of pyrolysis temperature for corn residues, colza straw, cardboard, and wool

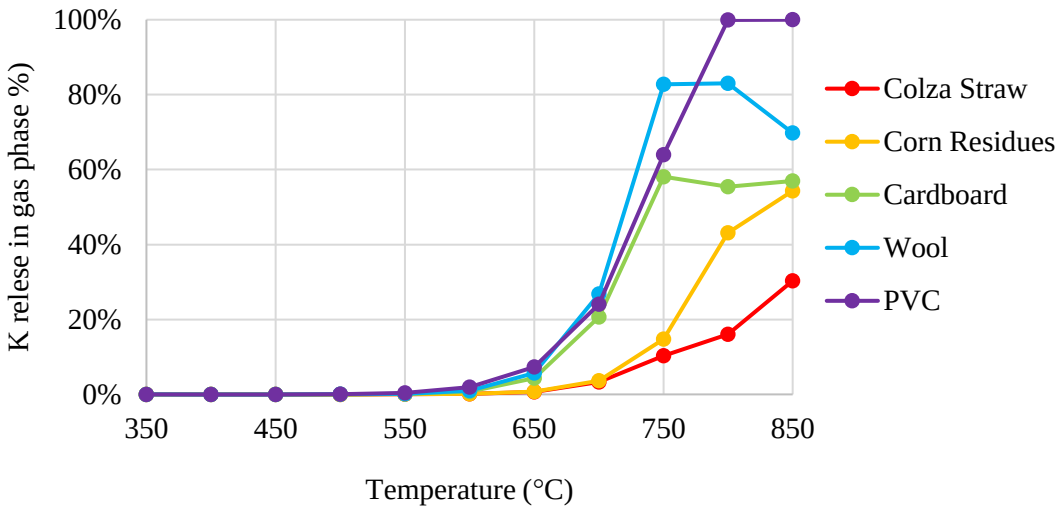

Figure 17: Mass fraction of potassium released in gas phase as a function of pyrolysis temperature at equilibrium

For corn residues, the major condensed defined species in the entire temperature interval is $Ca_5(PO_4)_3(OH)$ (s). Below 550°C, Ca is also associated with K in carbonates: $K_2Ca_2(CO_3)_3$(s) and $K_2Ca(CO_3)_2$(s). Additionally, Ca is observed in silicates in liquid-phase solutions, from 550°C and above. KCl(s) is also present at temperatures below 800°C.

Notably, at temperatures above 650°C, for corn residues as well as all other resources, potassium begins to be released in the gas phase. This can be correlated with a decrease of the mass of potassium-containing condensed species as temperature increases.

In the case of cardboard, it is interesting to note that more calcium than iron is initially present in the raw material. However, only Fe reacts with sulfur to form FeS at temperatures below 750°C. The main species observed are calcium silicates as defined species and solutions, indicating a preferential association of calcium with silicon.

For wool, various compounds are present, including calcium silicates and $Ca_5(PO_4)_3(OH)$ (s), along with FeS(s) and KCl(s), only below 800°C for the latter. Interestingly, the majority of calcium does not react with sulfur; instead, it is involved in the formation of other compounds with silicon, magnesium and phosphorus. At temperatures above 750°C, CaS(s) is observed, yet it accounts for only 5% of the initial sulfur retained in the condensed phase. The S/Ca and S/Fe molar ratios in wool are of 4 and 42, respectively, indicating an excess of sulfur in comparison to calcium and iron. This excess sulfur presence might contribute to the limited retention of sulfur in CaS(s) or FeS(s) compounds. However, the low sulfur retention may not solely be attributed to the quantities available but can also be influenced by the predominant presence of calcium in different compounds.

For colza straw, although the major species are calcium silicates and $K_2Ca_2(CO_3)_3$(s), CaS(s) is formed at 600°C and retains all of the sulfur in the condensed phase. The results indicate that in the case of colza straw only, CaS plays a significant role in retaining sulfur in the char. Solid CaS then stands out as a noteworthy phase, particularly at temperatures above 600°C.

For corn residues, cardboard and wool, calcium presents a higher affinity for other elements, such as phosphorus (in the case of corn residues) or silicon. As a result, calcium preferentially reacts with these elements rather than with sulfur, leading to the formation of other compounds and reducing the availability of calcium for sulfur retention. It is important to note that the Ca/Si molar ratio in colza straw is the highest compared to the other resources studied **(Table 11)**. This ratio may be a contributing factor to its unique sulfur retention capabilities and the formation of stable calcium sulfide rather than being involved with silicon and other elements in other compounds. In the studies conducted by Knudsen (2004b) and Tchoffor (2013), the presence of silicon in the feedstock during pyrolysis significantly impacted sulfur distribution by suppressing the formation of condensed sulfide forms (CaS and K_2S) and increasing sulfur release in the gas phase.

Overall, the varying sulfur retention capabilities among the different agricultural resources can be attributed to the specific chemical compositions of these materials and the availability of reactive compounds (Ca, Fe) that can promote the formation of stable sulfur-containing species.

The distribution of chlorine in the different products, predicted by the thermodynamic equilibrium calculations as a function of the pyrolysis temperature between 350°C and 900°C, is shown in **Figure 18** for each agricultural residue and for PVC.

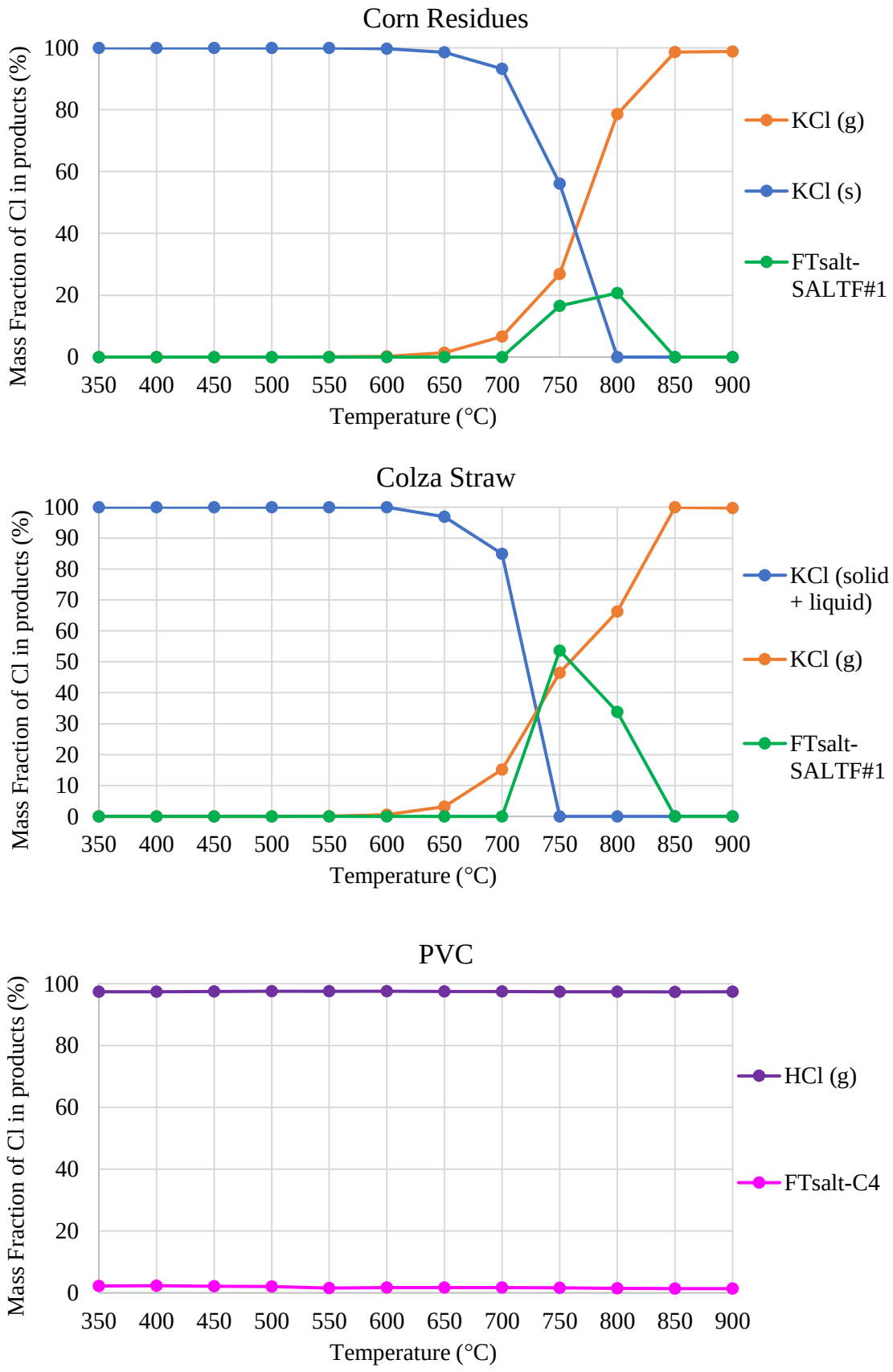

Figure 18: Equilibrium distribution of chlorine in the products as a function of pyrolysis temperature for corn residues, colza straw, and PVC

For corn residues, all the Cl is present in the condensed phase as potassium chloride KCl (s) below 650°C. However, between 700°C and 850°C, a molten alkali salt solution of chlorides FTsalt-SALTF (molten salt solution of all chlorides of Li, Na and K) containing around 20% of the Cl is present. As temperature increases, potassium chloride release increases until being completely released in the gas phase above 850°C.

For colza straw, between 350°C and 700°C, chlorine is present in the condensed phase as KCl(s). Within the temperature range of 700°C to 850°C, the liquid solution of alkali salts FTsalt-SALTF with approximately 20% Cl content emerges. At temperatures exceeding 650°C, potassium chloride release increases with temperature, ultimately being entirely released into the gas phase from 850°C.

For PVC, hydrogen chloride HCl (g) is the main chlorine-containing gaseous product over the entire temperature interval, containing 98 % of the initial Cl. The rest of the chlorine (2%) is present in a solid solution FTsalt-C4 (a molten chloride solution with $AlCl_3$).

The temperature has no effect on the chlorine distribution for PVC, however for the agricultural residues, the shift in chlorine partitioning with temperature is governed by the balance between thermodynamic stability and volatility. At lower temperatures, chlorine compounds tend to remain in the condensed phase. However, as temperature increases, the volatility of chlorine compounds, such as potassium chloride, becomes more significant, leading to their release in the gas phase. This can also be observed with the volatilization of potassium, illustrated in **Figure 17**.

The differences in chlorine distribution between the agricultural residues and PVC can be attributed to the differences in their chemical compositions. Agricultural residues have higher content of potassium that reacts with chlorine. The presence of alkaline elements, especially potassium, affects the release of chlorine as either HCl or KCl. However, contrary to the sulfur distribution, the effect of the chemical composition, in particular the content of calcium, on the chlorine distribution in products is not visible for colza straw and corn residues. Our results are in agreement with thermodynamic studies by Kuramochi (2005) and Zevenhoven-Onderwater (2001) presented in the state of the art.

3.1.2. Influence of the Equivalence Ratio (ER)

The objective of these calculations is to evaluate the effect of addition of air to the system, going from pyrolysis to gasification, on the distribution of sulfur and chlorine within the resulting products for the different resources.

The distribution of sulfur in gaseous (g) and solid (s) products, predicted by the thermodynamic equilibrium calculations as a function of the equivalence ratio at 800°C, is shown in **Figure 19**.

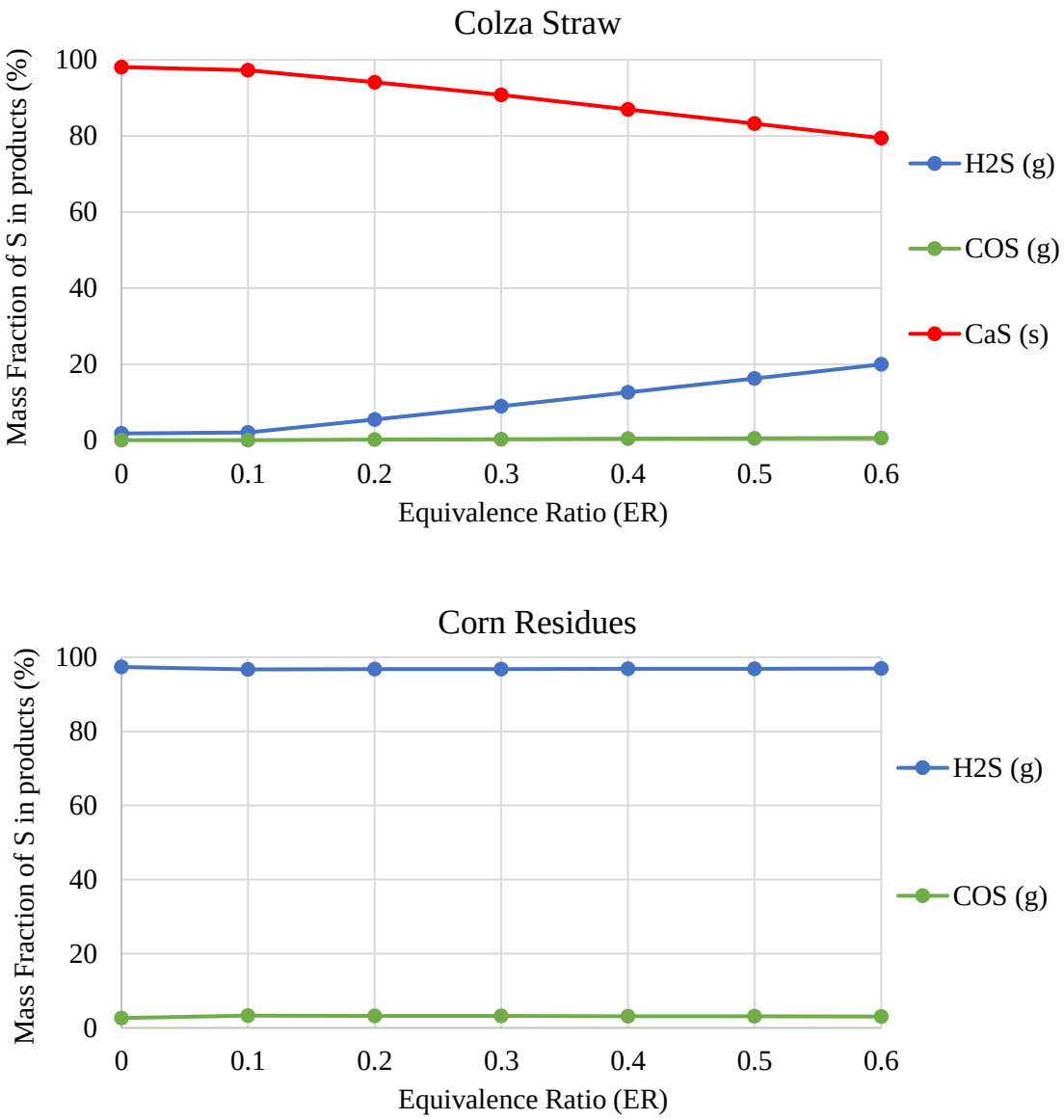

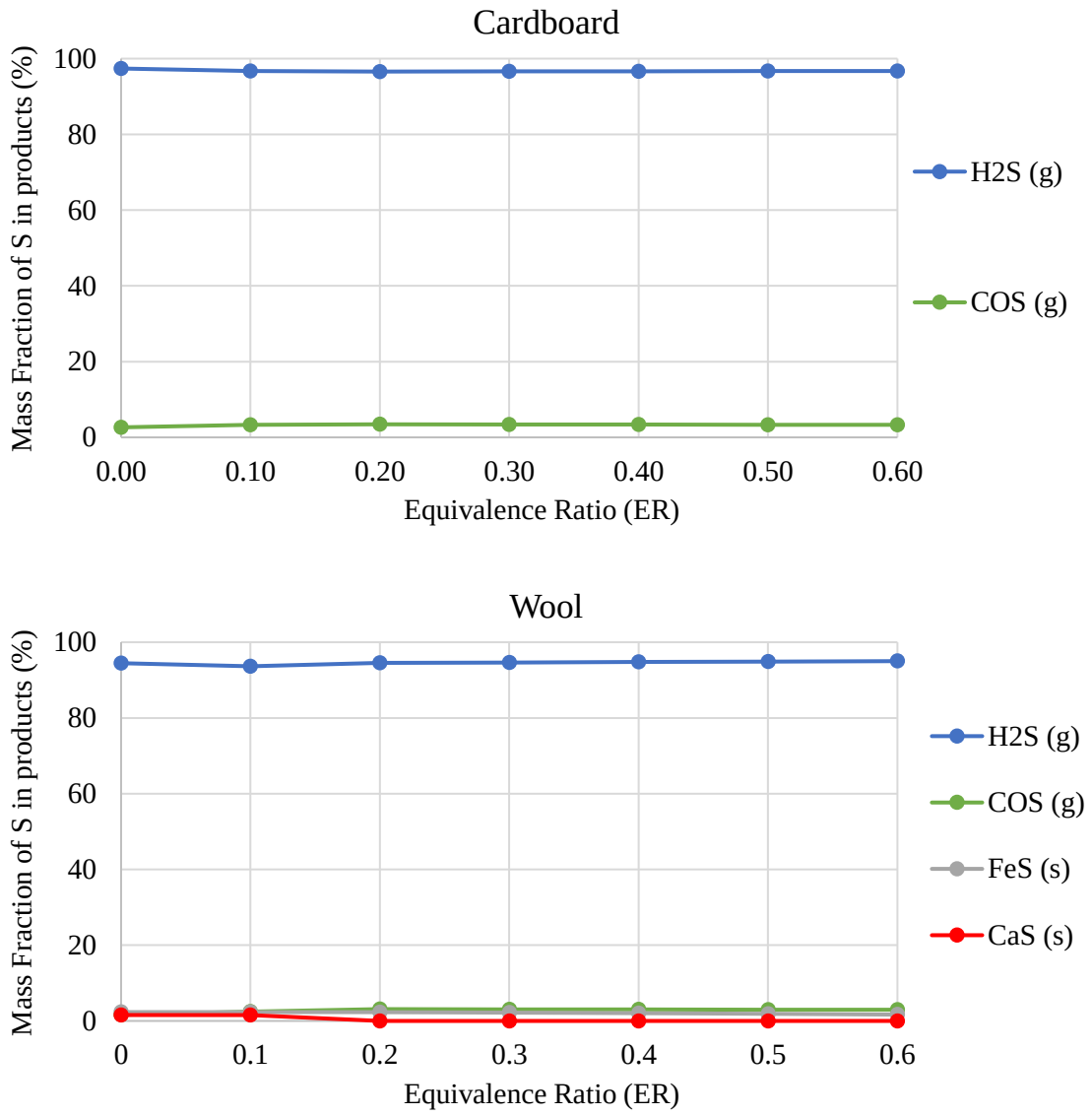

Figure 19: Equilibrium distribution of sulfur in gaseous (g) and solid (s) products as a function of ER for corn residues, colza straw, cardboard, and wool at 800°C

The results of thermodynamic calculations obtained for each feedstock show no significant difference in the distribution of sulfur species between pyrolysis conditions at ER=0 and gasification conditions with 0<ER<0.6. Only in the case of colza straw, the fraction of S retained as CaS(s) decreases from 98% to 80% as ER increases from 0 to 0.6, while the fraction of S released in the gas as H_2S(g) increases from 1 to 20%.

Figure 20 presents the equilibrium distribution of chlorine in the products as a function of the ER, for the agricultural residues and PVC at 800°C. The distribution of chlorine in agricultural residues undergoes significant changes as ER increases. Beyond an ER of 0.1, no chlorine remains in the molten alkali salt solutions. Instead, the entire chlorine content is released into

the gas phase as KCl (g). This transition indicates a clear shift in the distribution of chlorine towards the gaseous phase with increasing ER.

For PVC, the ER has no significant effect on the chlorine distribution. Hydrogen chloride HCl (g) is the main chlorine-containing gaseous product, containing 98 % of the initial Cl. The rest of the chlorine (2%) is present in a solid solution FTsalt-C4 (a molten chloride solution with $AlCl_3$) at pyrolysis condition and as gaseous elemental chlorine Cl_2 (g) and lead chloride $PbCl_2$ (g) for 0.3<ER<0.6.

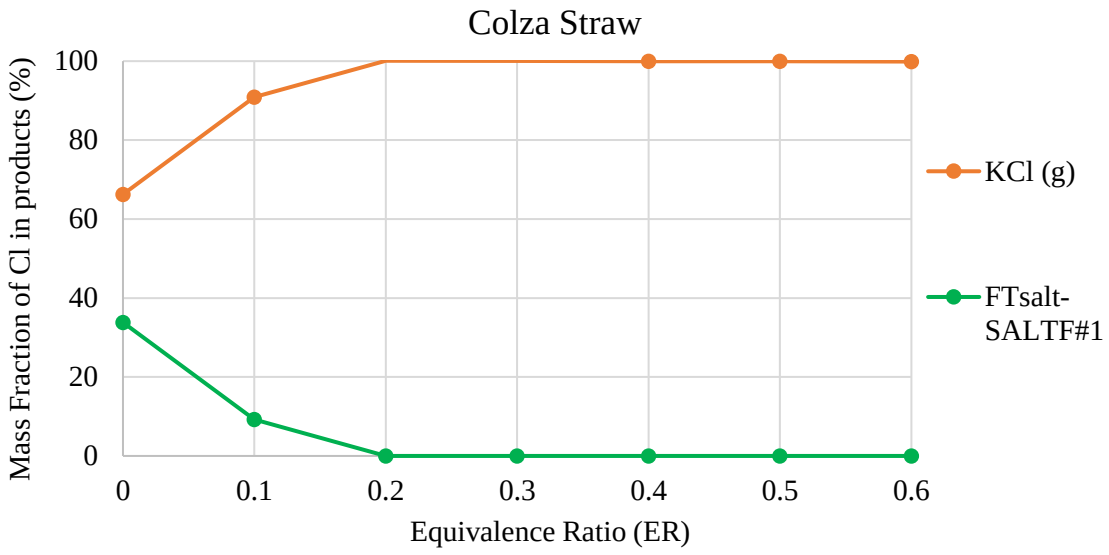

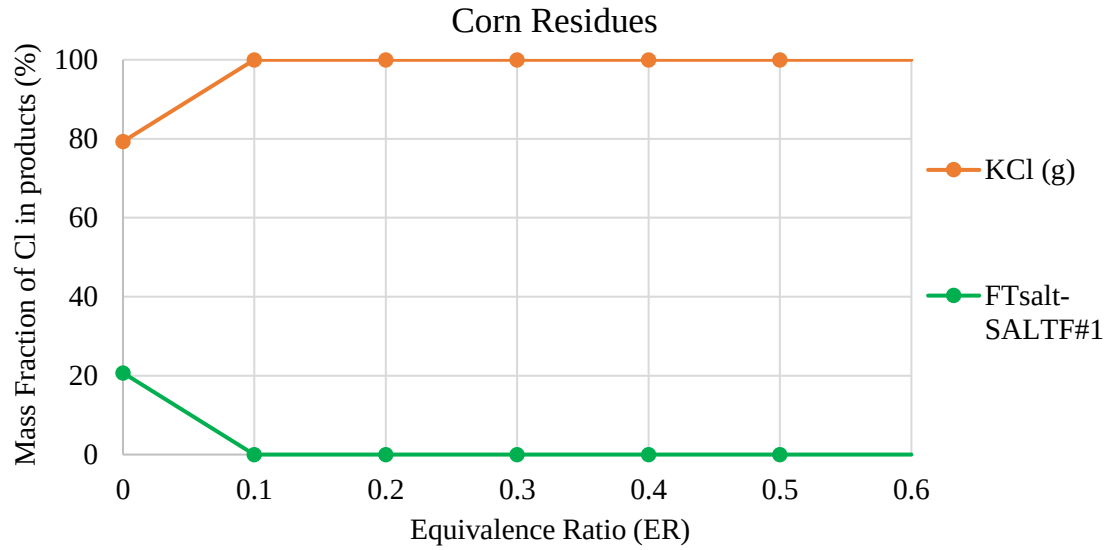

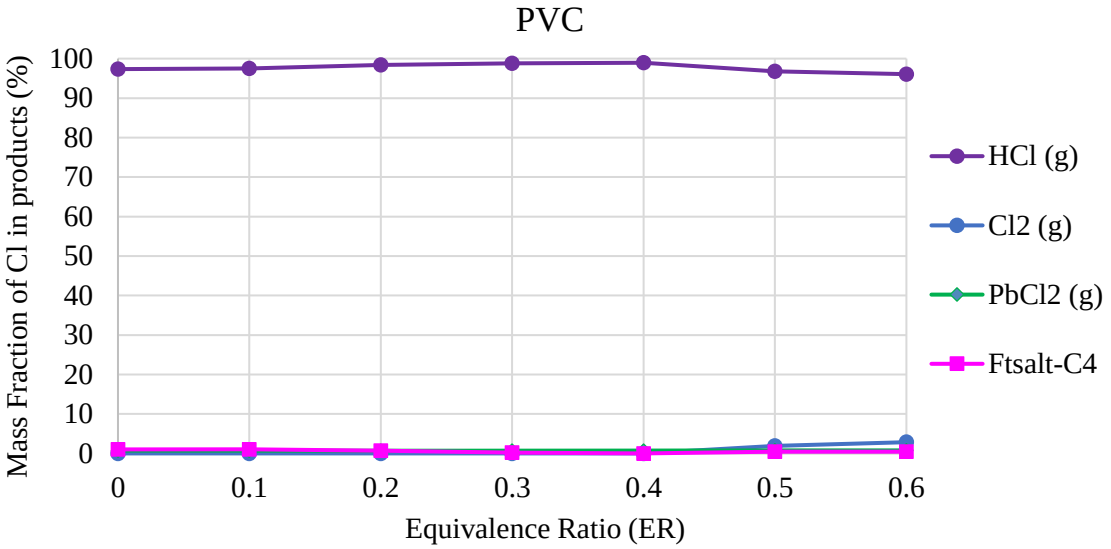

Figure 20: Equilibrium distribution of chlorine in the products as a function of ER for the agricultural residues and PVC at 800°C

3.1.3. Conclusion of the thermodynamic equilibrium study

The results from the thermodynamic calculations provide valuable indications of how sulfur and chlorine behave under varying pyrolysis and gasification conditions, as well as with different initial resource compositions. The composition of the resource plays a crucial role in governing the release of sulfur and chlorine species, while temperature and equivalence ratio have most of the time secondary effects.

The presence of certain elements, such as calcium and iron, but also indirectly silicon, influences the behavior of sulfur compounds, affecting their release as either gas-phase H_2S or their retention in solid-phase compounds. Similarly, the distribution of chlorine is influenced by the biomass composition, particularly the presence of alkaline elements like potassium and sodium. The volatilization of potassium is particularly relevant in understanding the behavior of chlorine, as they are usually associated in potassium chloride, which show increased volatility with temperature rise. At lower equivalence ratios, chlorine tends to remain in the condensed phase. However, as the equivalence ratio increases, the volatility of chlorine compounds, such as potassium chloride (KCl), becomes more significant, leading to their release into the gas phase.

The selected panel of our resources presents an opportunity for diverse behaviors in terms of sulfur and chlorine release, which will be further investigated experimentally to enhance our comprehension of inorganic element behaviors during gasification.

3.2. Sulfur and Chlorine behavior in pyrolysis

This section presents the experimental findings concerning the behavior of sulfur and chlorine during pyrolysis. Initially, we examined their release in the gas phase, which was evaluated in pyrolysis experiments conducted at 800°C and 850°C with the complete analysis of the recovered product streams, including the gas and condensed phases. Subsequently, we focused on the quantitative and qualitative characterization of the retention of inorganic elements in the char, along with their variation as a function of temperature.

3.2.1. S and Cl-species release in gas

We attempted to do a sulfur and chlorine-partitioning analysis to enable a comprehensive understanding of the fate and distribution of sulfur and chlorine compounds during pyrolysis at 800°C and 850°C. Our experimental set-up consists of an induction-heated reactor, followed by a series of five impingers for the condensable and gas products collection system, and a micro gas chromatography **(Figure 7)**.

The contents of sulfur and chlorine retained in the char, and in the condensable products were quantified, as well as the amount of sulfur present in the gas phase using the micro-GC, which detected hydrogen sulfide (H_2S) and carbonyl sulfide (COS).

The first two impingers were filled with deionized water and the three other impingers were filled with 2-propanol. The main objective of placing water impingers downstream of the reactor exit was to trap the chlorinated species released in the gas (HCl, KCl, NaCl…), however, volatile sulfur compounds (H_2S, COS) and possibly organic sulfur compounds were also partly trapped in these water impingers. The S and Cl contents in these two water impingers were measured using inductively coupled plasma (ICP) for S and ion chromatography (IC) for Cl. The three other impingers were filled with 2-propanol to collect tar and clean the gas stream before entering the gas analyzers. These impingers were not analyzed in our study because isopropanol cannot be used in ICP or IC analyzers. Instead, isopropanol is typically analyzed using methods that are suitable for separating and identifying organic compounds. However, in our study, the focus was not on analyzing the organic compounds collected in the isopropanol impingers.

Other experiments were performed with different configurations (impingers filled with glass fibers without any solvent, impingers all filled with 2-propanol). However, the closure of the mass balance for S was not improved.

Only in the experiment performed at 850°C for wool, the two water impingers were replaced by impingers filled with 2-propanol to detect if any sulfur-containing tars are released. The five samples of the isopropanol impingers were then analyzed with a gas chromatograph coupled to a flame photometric detector (GC-FPD) that can detect sulfur compounds.

Figure 21 illustrates the partitioning of sulfur after pyrolysis performed at 800°C and 850°C during 20 minutes, for colza straw, corn residues, cardboard and wool. Error bars show the relative uncertainty of the total fraction quantified calculated by the propagation method (Appendix B).

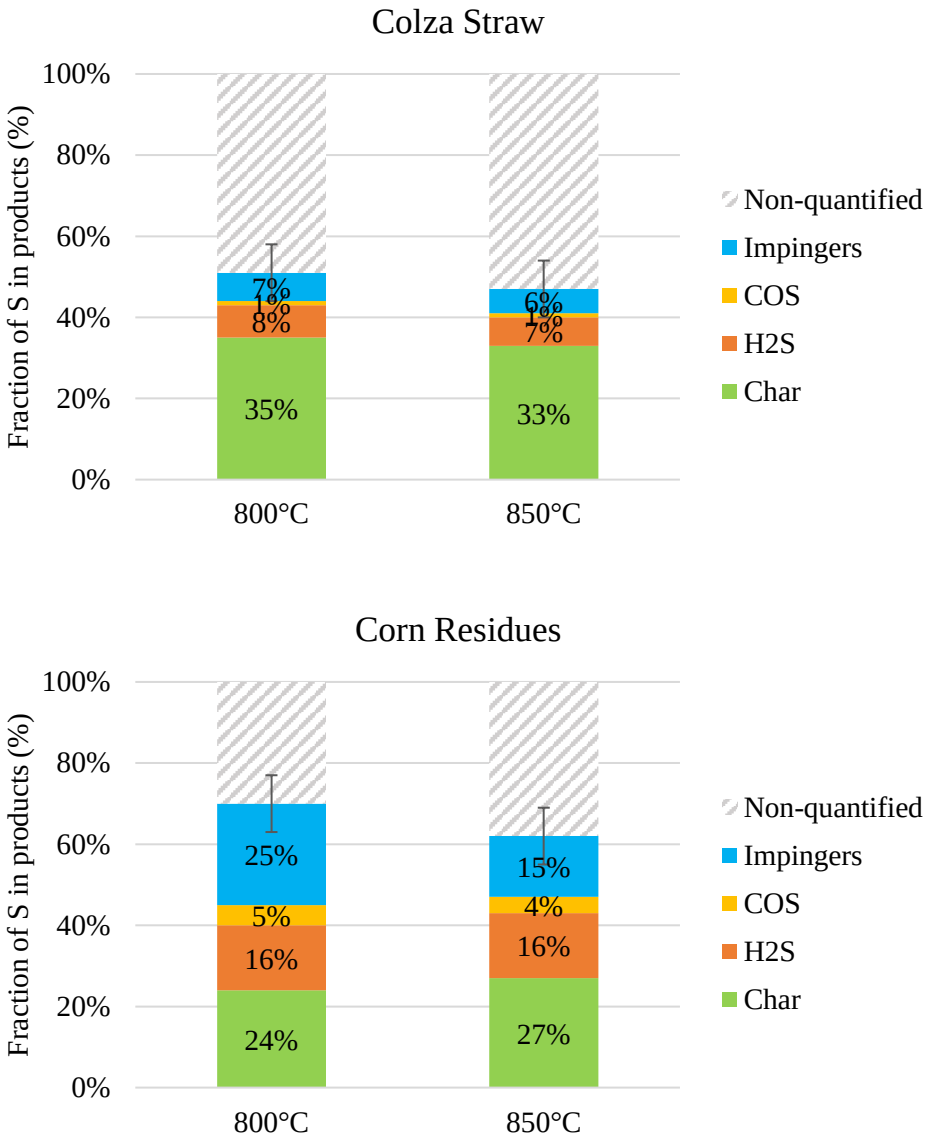

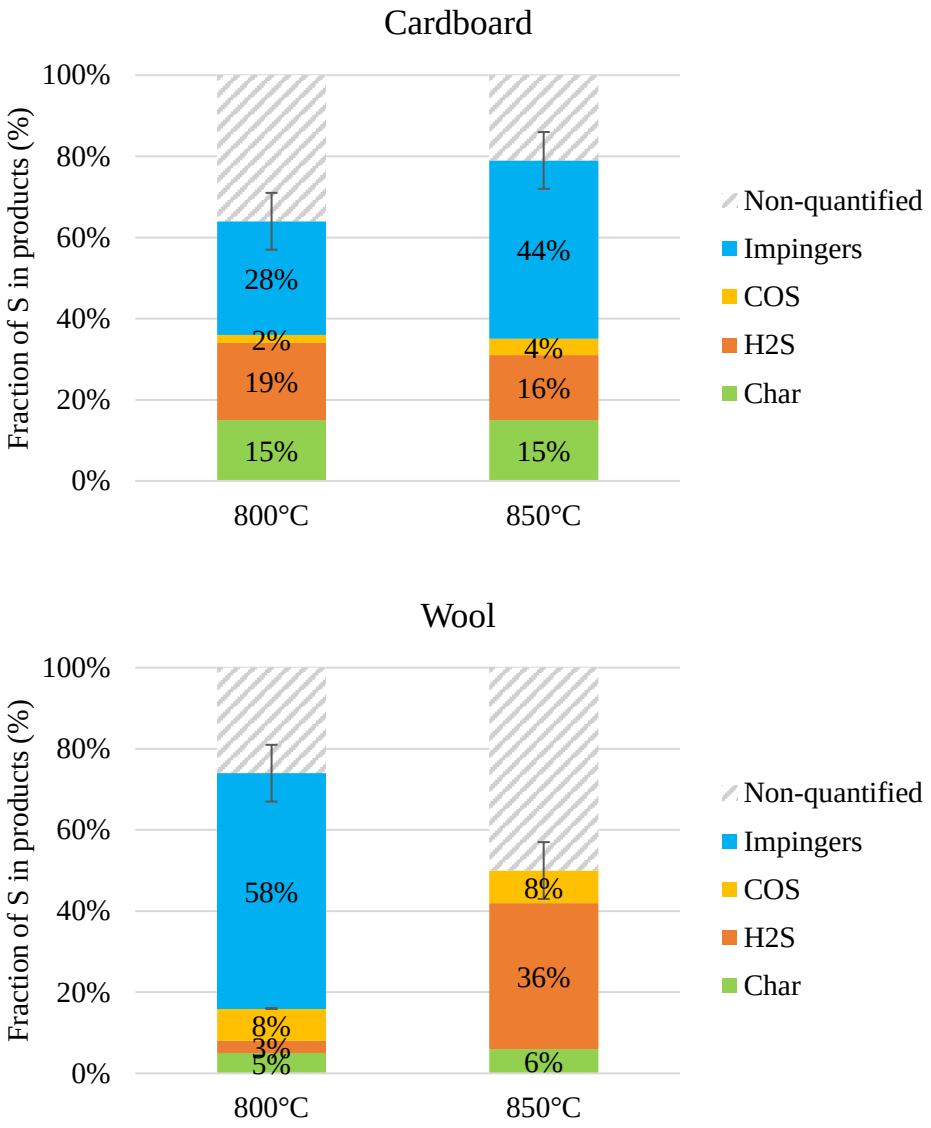

Figure 21: Experimental sulfur distribution in the char, the gas and the impingers for the pyrolysis of colza straw, corn residues, cardboard, and wool at 800°C and 850°C

The obtained results show similar sulfur partitioning patterns at both temperatures of 800°C and 850°C for each feedstock except for wool, which indicates that temperature does not significantly affect the behavior of sulfur during pyrolysis. It is possible that the temperature difference between 800°C and 850°C does not induce significant changes in the chemical reactions and sulfur transformation pathways during pyrolysis.

For colza straw, approximately 35 % of the sulfur is retained in the char. In the gas phase, we were able to measure only 8 % of the sulfur as H_2S and 1 % as COS with the micro-GC, and 6 % trapped in the impingers.

In the case of corn residues, less sulfur is retained in the char (24 %), while more S is measured in the gas (16 % as H_2S and 4 % as COS) and trapped in the impingers (15-25 %).

It is important to emphasize that H_2S and COS measurements are accounted for in both the micro-GC and the impingers.

The mass balance closure is the closest to 100% for cardboard at 850°C. 15 % of the initial S is then found in the char, while around 20 % is measured by the micro-GC mainly as H_2S and some COS, and 28-44 % is trapped in the impingers.

For wool, only 5 % of the initial sulfur is retained in the char and 3 % is released as H_2S and 8 % as COS, while 58 % is found trapped in the impingers at 800°C. This specific partitioning of sulfur in COS and H_2S sets this pyrolysis test on wool apart from the other tests on the other resources. This unique distribution could potentially be linked to the nature of the initial sulfur, which is predominantly organic, in amino acids. At 850°C, in the samples of the five isopropanol impingers analyzed with the GC-FPD, the presence of S-containing tars was detected but no identification or quantification of the compounds was possible. The same fraction of sulfur retained in the char and released as COS is found, however, the measured fraction of S released in the gas as H_2S increases from 3% to 36%. This observation confirms that there is likely a substantial amount of H_2S trapped in the water impingers.

The partitioning of chlorine during pyrolysis of the agricultural residues and PVC is shown in **Figure 22**. For agricultural residues, a large fraction of the initial chlorine remains in the solid char after pyrolysis (45 -56 %). Only 10 to 22% of the initial Cl released in the gas phase is measured in the impingers. The impingers are expected to capture chlorinated species such as HCl, KCl, and NaCl. Low amounts of potassium and sodium, representing less than 5% of their initial contents, are measured in the impingers. The K/Cl and Na/Cl molar ratios were found to be higher than 1, suggesting that the chlorine is present in the form of potassium and sodium chlorides. However, based on the available data, it is difficult to determine the exact chlorinated species present, whether it is HCl, KCl, NaCl, or other compounds. On the other hand, for PVC, 90% of the initial chlorine is measured in the impingers. The analysis of the PVC char was not possible due to its very low mass.

Figure 22: Experimental chlorine distribution in the char and the impingers for the pyrolysis of colza straw, corn residues, and PVC at 800°C and 850°C.

A significant portion of sulfur and chlorine remained unquantified, leading to low mass balance recoveries for S and Cl for all feedstocks. The output sulfur and chlorine were thus incompletely measured, contributing to the observed discrepancies in mass balance recoveries.

The isopropanol of the last three impingers was not analyzed, although it could potentially contain S and Cl compounds. In particular, S-containing tars, which cannot be quantified by the micro-GC, were probably not captured by the water impingers. Consequently, if these S-containing tars, together with some H_2S and COS, were trapped in the isopropanol impingers, they remained unmeasured and contribute to the unquantified portion of sulfur in the analysis.

Furthermore, during the experimental process, some chlorine compounds (KCl, NaCl) released into the gas phase can potentially undergo condensation in the lines of the experimental setup, especially at low temperatures. Although the elbow of the reactor output is rinsed and the rinsed water is analyzed, there is still a possibility that a fraction of chlorine compounds, particularly those that condense at low temperatures (KCl, NaCl), remains unquantified.

According to de Almeida (2020), the recovery of contaminants (HCl, NH3, H_2S…) reported in literature exhibit low values or exceed 100%. These inconsistencies can potentially be attributed to the heterogeneity of the fuel itself, as well as the inherent challenges involved in accurately measuring and sampling certain species, along with potential interaction between the reactor material and some species or uncontrolled condensation in the lines.

These factors, including fuel composition variations and complexities in sampling and analysis procedures, as well as potential interactions with the experimental setup, may contribute to the observed discrepancies. Due to the challenges associated with accurately quantifying the unaccounted sulfur and chlorine, we decided to focus solely on investigating their retention in the char, which will be presented in the next section and chapter. By concentrating our efforts on this aspect, we aim to provide more reliable and consistent data quantitatively and qualitatively regarding the retention of sulfur and chlorine in the char for the various feedstocks.

3.2.2. Inorganic elements retention in char

Our main emphasis in this section is on examining the quantitative aspect of how inorganic elements are retained in the char and how these retention patterns change within the temperature range of 365°C to 850°C. Two types of experiments were conducted: experiments in which the reactor was heated up and kept at the desired temperature (800 or 850°C) for 20 minutes, and experiments in which the heating was interrupted at different times and in which each sample therefore reached a different maximum temperature. The detailed experimental conditions are

described in **section 2.2.4.1**. The elemental compositions of the chars obtained at the different pyrolysis temperatures are shown in **Appendix E**.

The char yields of the different feedstocks are shown in **Figure 23** as a function of maximum pyrolysis temperature. For all feedstocks, the char yield decreases as temperature increases from 365°C to 850°C. The devolatilization occurs during the whole temperature rise until 800°C. However, between 800°C and 850°C, the char yield only slightly changes for most feedstock, which shows a low influence of the temperature on this range. At 800°C, PVC has the lowest char yield (11 wt. %) among the five feedstocks. Subsequently, the characterization of the PVC char was not possible due to its low recovered mass.

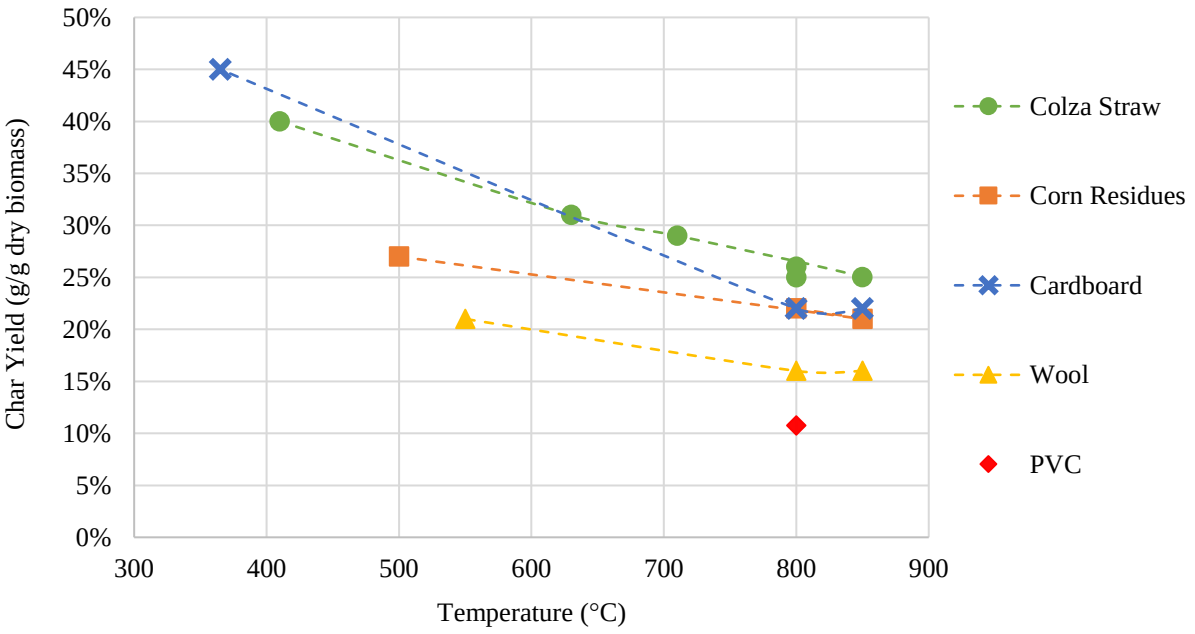

Figure 23: Char yield as a function of maximum pyrolysis temperature

Figure 24 shows the experimental results of the sulfur retention in the chars as a function of maximum pyrolysis temperature. Error bars show the relative uncertainty calculated by the propagation method. The pyrolysis experiment at 800°C was conducted in duplicate for colza straw, and the results obtained were highly reproducible. The thermodynamic equilibrium results, already presented in **section 3.1.1**, are also shown for comparison. For colza straw, 46% of the initial sulfur is retained in the char produced at the pyrolysis temperature of 410°C. The sulfur retention decreases to about 35% in the chars produced at higher temperatures (630°C, 710°C, 800°C and 850°C). For corn residues, the sulfur retention in the char is between 24 and 30% in the pyrolysis experiments performed at 500°C, 800°C and 850°C. For cardboard, 35% of the initial sulfur is found in the char produced at a pyrolysis temperature of 365°C. However,

at 800°C and 850°C, the sulfur retention decreases to 15%. On the other hand, only 5% to 7% of the initial sulfur is retained in the chars of wool produced at 550°C, 800°C and 850°C. These experimental results show a low influence of the final pyrolysis temperature between 500 and 850°C for agricultural residues. This is in agreement with other studies that found a slight decrease of the total sulfur content of the char (Tchoffor et al., 2013) or a constant release of sulfur (Knudsen et al., 2004b) with increasing temperature from 550°C to 900°C during pyrolysis of wheat straw. The temperature increase from 550 to 850°C does not significantly affect the retention of sulfur in the char for wool. However, it is unclear whether the same holds true for cardboard when comparing pyrolysis temperatures of 365°C and 800–850°C, as measurements are not available for intermediate temperature ranges.

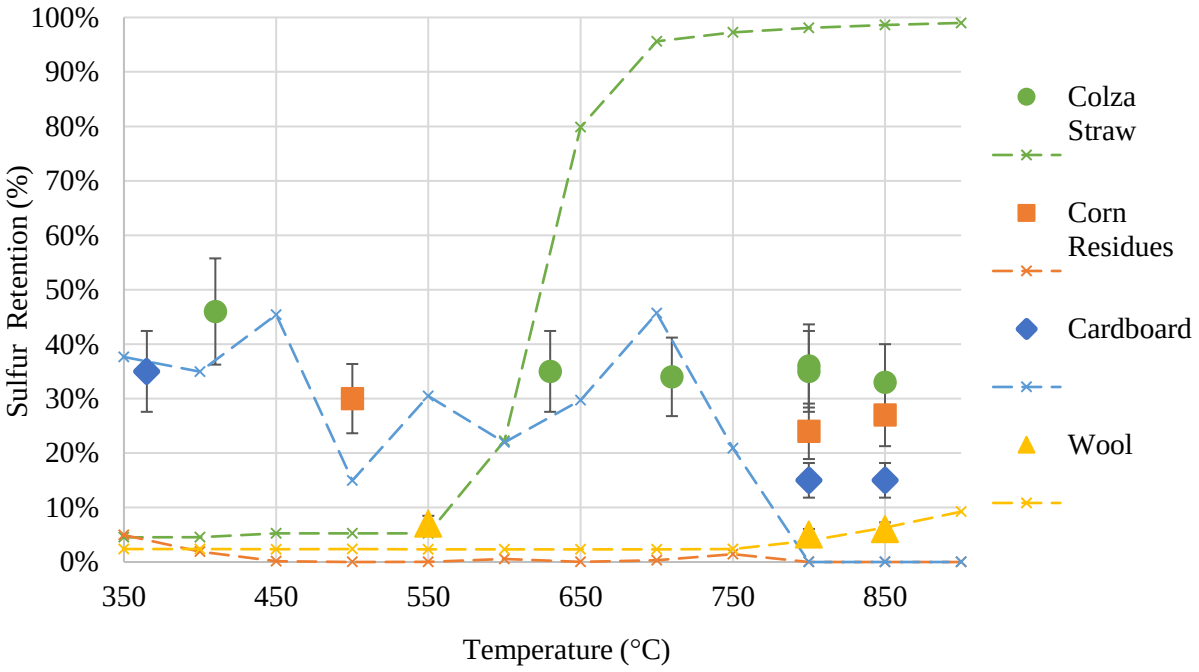

Figure 24: Sulfur retention in the chars as a function of pyrolysis temperature: experimental (dots) and thermodynamic equilibrium reslts (dashed lines)

The thermodynamic equilibrium calculations show some qualitative agreement with the experimental results, particularly concerning the minimal impact of temperature on sulfur retention for all feedstocks except for colza straw. For wool, there is strong agreement between the equilibrium predictions and experimental measurements, with only a small fraction (<5%) of the initial sulfur remaining in the solid residue. Similar behavior is observed for cardboard at 365°C, where sulfur retention also fits well with thermodynamic equilibrium predictions. However, there are notable discrepancies observed when comparing the experimental data with

the thermodynamic predictions for other resources. For colza straw, the thermodynamic simulations initially suggest that above 750°C, over 95% of the initial sulfur should be retained as solid CaS(s). Contrarily, the experimental results reveal that at 800°C and 850°C, only approximately 35% of the initial sulfur remains in the solid residue after pyrolysis. Similarly, for corn residues at all temperatures and for cardboard at 800 and 850°C, the thermodynamic predictions indicate complete sulfur release into the gas. However, the experimental results show that approximately 24% and 15% of the initial sulfur content are detected in the solid residue after pyrolysis of corn residues and cardboard, respectively.

To explain the different results seen among the four feedstocks, the sulfur retention in the char after pyrolysis can be related to the initial chemical form of sulfur in the feedstock. According to studies found in the literature (Johansen et al., 2011; Knudsen et al., 2004b), organic forms of sulfur are more volatile and easily released into the gas phase even below 500°C, compared to inorganic forms. For wool, the fraction (5-7%) of the initial sulfur retained in the solid residue is close to the inorganic fraction (3%) of sulfur measured in the original resource. This shows that the dominating organic form of S in wool is probably completely released in the gas phase before reaching 550°C. Moreover, for cardboard in which S is mainly in organic forms, S retention decreases as temperature increases, until it reaches 15% at 800°C and 850°C, which could correspond to its initial inorganic fraction. If S is considered to be included in the lignin structure in cardboard, the lignin decomposition on a wide temperature range of about 250 to 600°C (de Wild, 2011) could explain why S continues to be released above 365°C. For the agricultural residues, the fraction of S retained in the chars (24-35%) is lower than the fraction of inorganic S (51-67%) quantified by lixiviation. This shows that besides the organic S initially released at low temperatures below 500°C, a part of inorganic S is also released. Indeed, pyrolysis studies (Johansen et al., 2011; Knudsen et al., 2004b, 2004a; Tchoffor et al., 2016) showed that, during the devolatilization process, the organically associated S is released via the formation of highly reactive SH radicals that either remain in the char or extract H, C, or O from the char, to form later H_2S, COS, or SO_2:

$$(17)\ Fuel{-}S + \mathrm{H}eat \rightarrow H_2S + COS + \cdots + Char{-}S$$

As for inorganic sulfur, at temperatures below 1000°C, the evaporation rates of inorganic sulfates are low. However, previous authors (Knudsen et al., 2004b; Tchoffor et al., 2014) showed that a part of these sulfates can be transformed to char-bound S and thus be released to the gas phase. This could explain why the fraction of S retained in the chars is lower than the

fraction of inorganic S in our results and could confirm that both the organically and the inorganically associated S contribute to the amount of S released.

Figure 25 shows the chlorine retention in the chars as a function of maximum pyrolysis temperature, and compares the experimental results and the thermodynamic equilibrium ones. Looking at the experimental results, and considering the uncertainties, the influence of temperature on the retention of chlorine in the chars for agricultural residues is low. However, a slight decrease in chlorine retention as temperature increases may be present, especially for colza straw. About 50% of the initial chlorine is retained in the char between 500°C and 850°C for the corn residues. In the colza straw, 67-75% of the chlorine remains in the char between 410°C and 710°C, while only 55% is retained in the char at 800 and 850°C. In the case of the PVC pyrolysis experiment at 800°C, as presented in the previous section, around 90% of the initial chlorine was measured in the impingers, and therefore, released in the gas phase. This allows us to consider that less than 10% of the initial chlorine is retained in the char in the case of PVC.

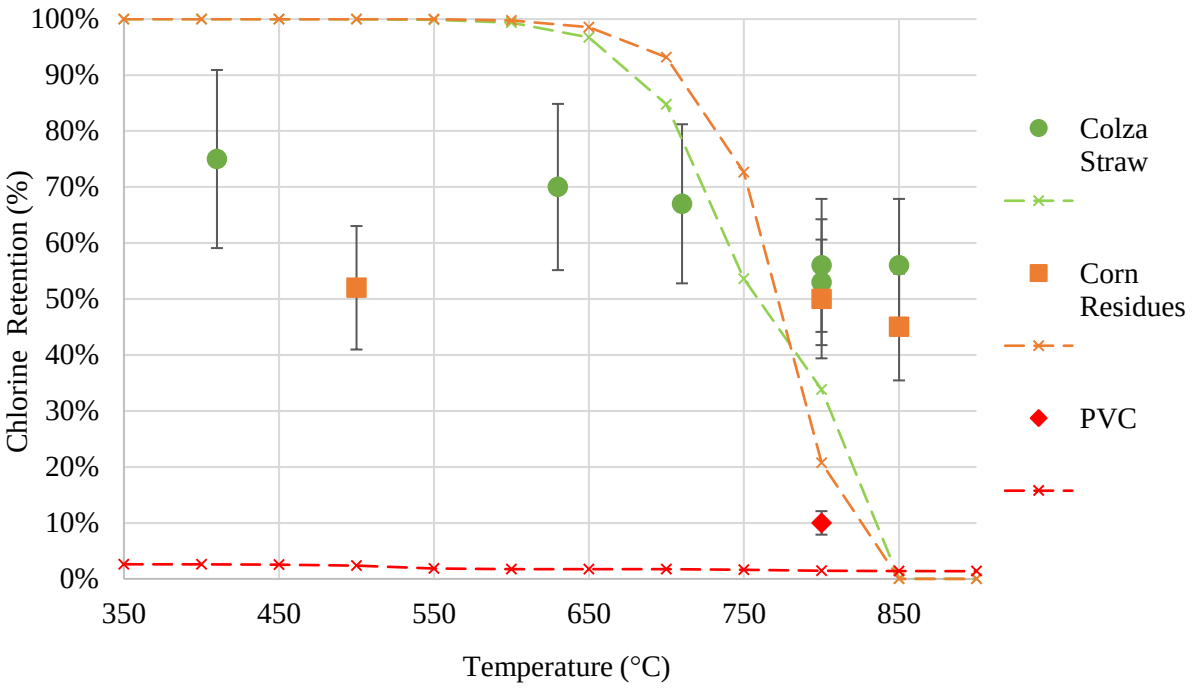

Figure 25: Chlorine retention in the chars as a function of pyrolysis temperature: experimental (dots) and thermodynamic equilibrium reslts (dashed lines)

Similarly to sulfur, the thermodynamic predictions and experimental results are not in good agreement as for the chlorine retention in char for agricultural residues. According to the thermodynamic simulations, chlorine is expected to be present in the condensed phase below

700°C and completely released as a gas at higher temperatures, which is not observed experimentally. On the other hand, for the pyrolysis of PVC, chlorine is found to be completely released in the gas phase as HCl, which is consistent with the equilibrium calculations.

The difference in the retention of chlorine between the agricultural residues and PVC chars can be related to its initial chemical form in the resource. PVC, having the totality of Cl in an organic form, undergoes three steps (dehydrochlorination, condensation and fragmentation) during the devolatilization stage, in the temperature range 150-500°C, which results in the complete release of Cl as HCl (Bläsing et al., 2015a; Casazza et al., 2019).

Furthermore, studies have indicated that hydrogen chloride (HCl) produced during the pyrolysis of PVC can potentially react with lead oxide (PbO) to form lead(II) chloride ($PbCl_2$). This reaction is observed at temperatures exceeding 501°C, as reported by Wang (2014) and Xu (2022). A notable quantity of lead is present in our PVC sample; however, it is challenging to confirm any significant interaction between the two elements Cl and Pb.

On the other hand, more than 85% of chlorine is present in an inorganic form of soluble salts in the agricultural residues. According to previous studies (Johansen et al., 2011; Knudsen et al., 2004a; Tchoffor et al., 2013), under pyrolysis conditions, at temperatures under 700 °C, the release of a significant fraction of the Cl (40-60%) in the fuel as HCl is attributed to an ion-exchange reaction of KCl and oxygen-containing functional groups that are either present in the fuel or formed during the devolatilization step:

$$(18)\ R\text{-}COOH + KCl\,(s) \rightarrow R\text{-}COOK + HCl\,(g)$$

Above 700°C, the evaporation of KCl is considered to be the main pathway for the release of Cl. According to our results, only a part of inorganic chlorine is released in the gas phase in pyrolysis experiments.

A different form of colza straw (pellet) was investigated with pyrolysis at 850°C, to examine the influence of particle shape and size on the behavior of sulfur and chlorine. We obtained similar results compared to the test conducted with the grinded particles of colza straw. This suggests that the particle shape and size did not have a substantial impact on the sulfur and chlorine behavior during pyrolysis at the given temperature.

According to literature (**Chapter 1**), the behavior of inorganic forms of S and Cl can depend on the ash composition of the feedstock. To have a deeper understanding of the influence of the ash-forming elements on the sulfur and chlorine behavior during pyrolysis, the chars were analyzed for their inorganic composition. **Figure 26** presents the retention in the char of the

major inorganic elements (K, Ca, Si) after pyrolysis for the two agricultural residues. Error bars show the relative uncertainty calculated by the propagation method.

Both agricultural residues showed varying levels of these elements. Calcium retention ranged from 67% to 84%, while silicon values were higher, ranging between 84% and 109%. Potassium exhibited a wider range, with values spanning from 82% to 120%.

K totally remains in the char below 700°C for both agricultural residues. In the original feedstock, K is mainly present in soluble inorganic salts (KCl, $KClO_4$, K_2SO_4…). Under 700°C, the evaporation rates of these inorganic salts are low and as said in the preceding paragraph, K can combine with volatile organic compounds and transform into organic K (R-COOK). This could explain its total retention in the char at temperatures below 700°C. At 800°C and 850°C, a low release is observed. By comparing with **Figure 25**, the retentions of K and Cl follow a similar profile, which could suggest that the release of metal chlorides, particularly KCl, can start occurring at temperatures above 800°C. This is in agreement with previous studies that have shown that only a small amount (5-10%) of K is released at temperatures below 700°C (Johansen et al., 2011; Tchoffor et al., 2016, 2013), and that the release of alkali metals and chlorine is closely related to one another (Johansen et al., 2011).

All the silicon is retained in the chars at the different temperatures. As expected, Si is not volatile and remains in the silicate matrix (M. Zevenhoven et al., 2012).

67 to 83% of the Ca is retained in the char between 365 and 850°C for colza straw, while 71% to 84% of Ca remains in the corn residue char between 500 and 850°C. Even considering the uncertainties related to the Ca retention, a fraction of Ca seems to be released on the whole temperature range. The temperature has no significant influence on the Ca retention considering the uncertainties. As mentioned before, 80% and 50% of the total Ca is organically bond or present as carbonates for colza straw and corn residues, respectively. Literature reports that significant fractions of Ca are volatilized during cane bagasse and cane trash pyrolysis at 500°C (Keown et al., 2005) and cane bagasse gasification between 650 and 1170°C (Andrea Jordan and Akay, 2012). The reduction in Ca bound to the organic phase after gasification and the observation of acetate ions in the syngas indicated that during gasification, organically bound Ca (COO—Ca) was volatilized releasing Ca^{2+}, and COO^- ions. The thermal breakdown of carboxylates (COO) in the biomass from large molecular mass structures and the subsequent release of light carboxylates might be an important mechanism for the release of Ca that is organically bound (Ca-COO) from the pyrolysis of biomass at low temperatures. This provides an explanation for the release of Ca in our experiments.

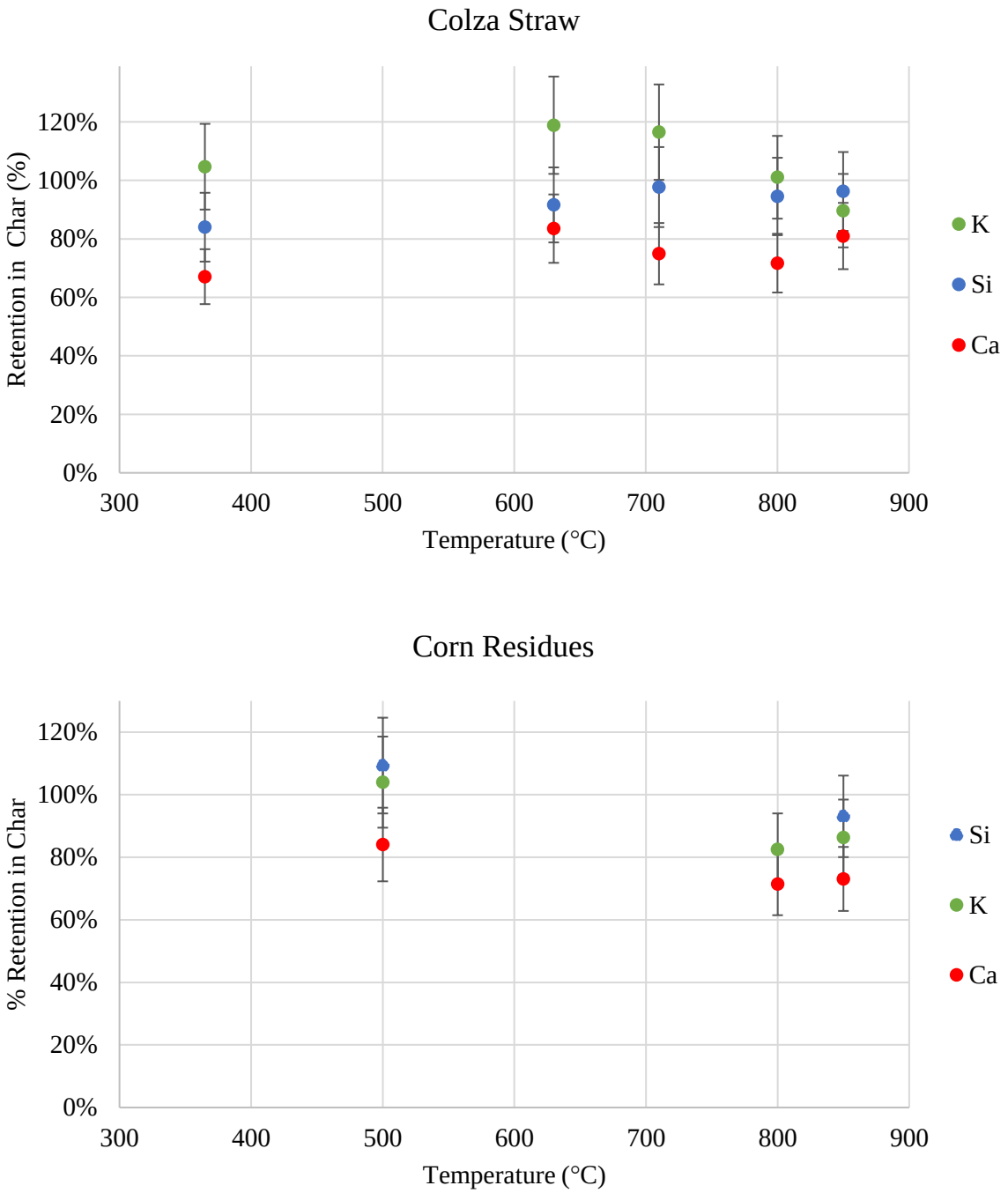

Figure 26: Major ash-forming elements retention in the char as a function of maximum pyrolysis temperature

3.2.3. XRD and SEM-EDX analysis of the chars

Specific experimental investigations are needed to precise the interactions between sulfur, chlorine and the ash-forming elements, and to characterize the forms in which sulfur and chlorine are retained in the char at different pyrolysis temperatures. Therefore, XRD and SEM-

EDX analyses were carried out on the char samples. The experimental procedure is presented in **section 2.2.3.1**. The SEM-EDX analysis was used to study the surface elemental composition, which may give information on the non-crystalline forms present in the chars. The chars obtained at the different temperatures were all analyzed by the SEM-EDX analysis; however, **Figure 27** presents only the SEM observations of the chars obtained at 800°C as examples. The XRD analysis indicates the presence of crystalline minerals in the char samples. The semi-quantitative analysis, which is based on the intensity of the diffraction peaks, was also used to estimate the relative abundance of the different phases in the samples and to compare their evolution at the different temperatures. **Figure 28** reports the XRD patterns and the evolution of the relative weight fraction of the phases estimated by the semi-quantitative analysis for the chars of the agricultural residues and cardboard at the different maximum pyrolysis temperatures.

Moreover, the raw agricultural residues were shredded the best possible to obtain fine powder for their XRD analysis, however, the diffractograms showed no clear mineral phases probably due to their high carbon content and their amorphous nature. No XRD analysis was conducted for the raw samples of cardboard, wool, and PVC.

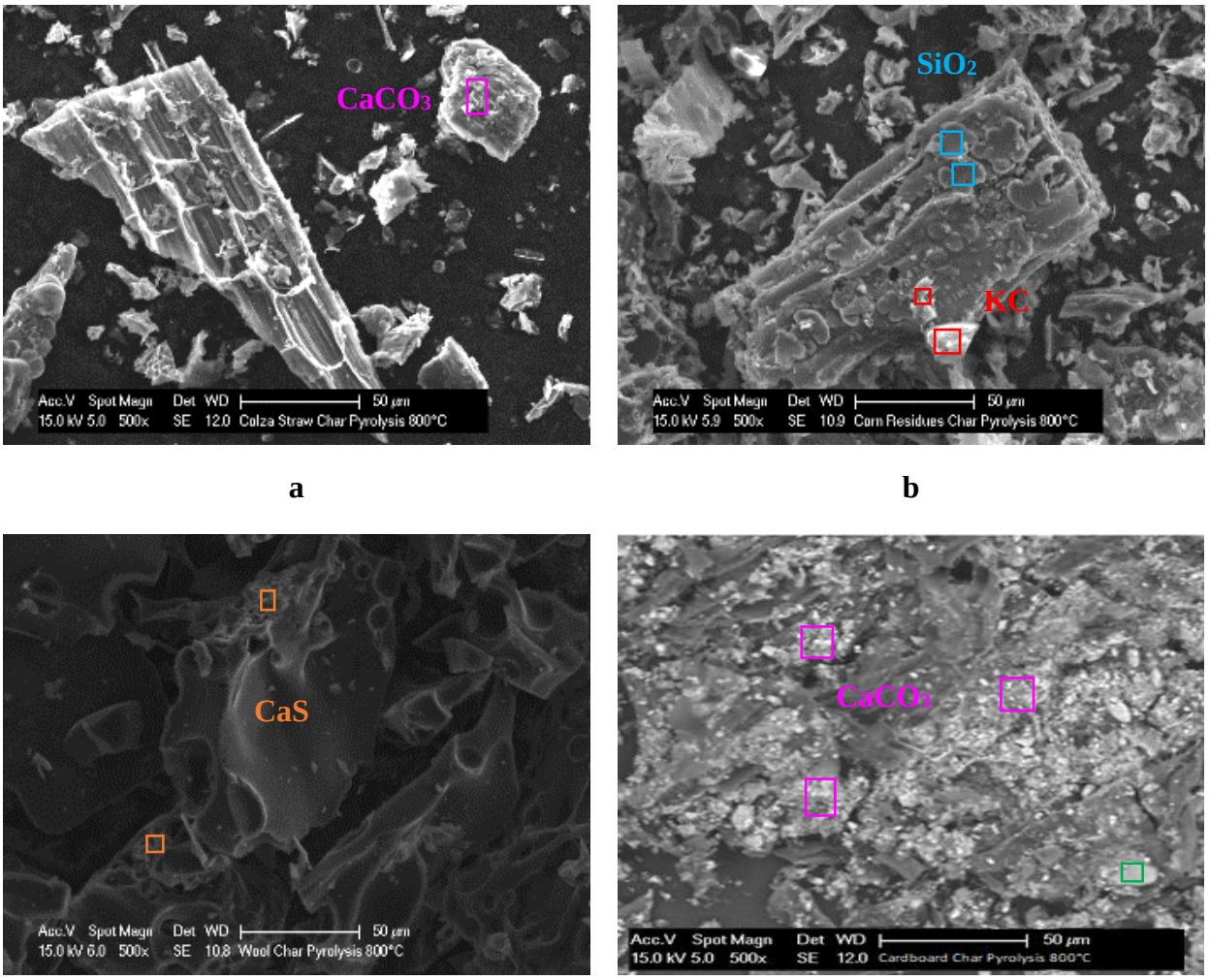

Figure 27: SEM observations of colza straw (a), corn residues (b), wool (c) and cardboard (d) chars at 800°C

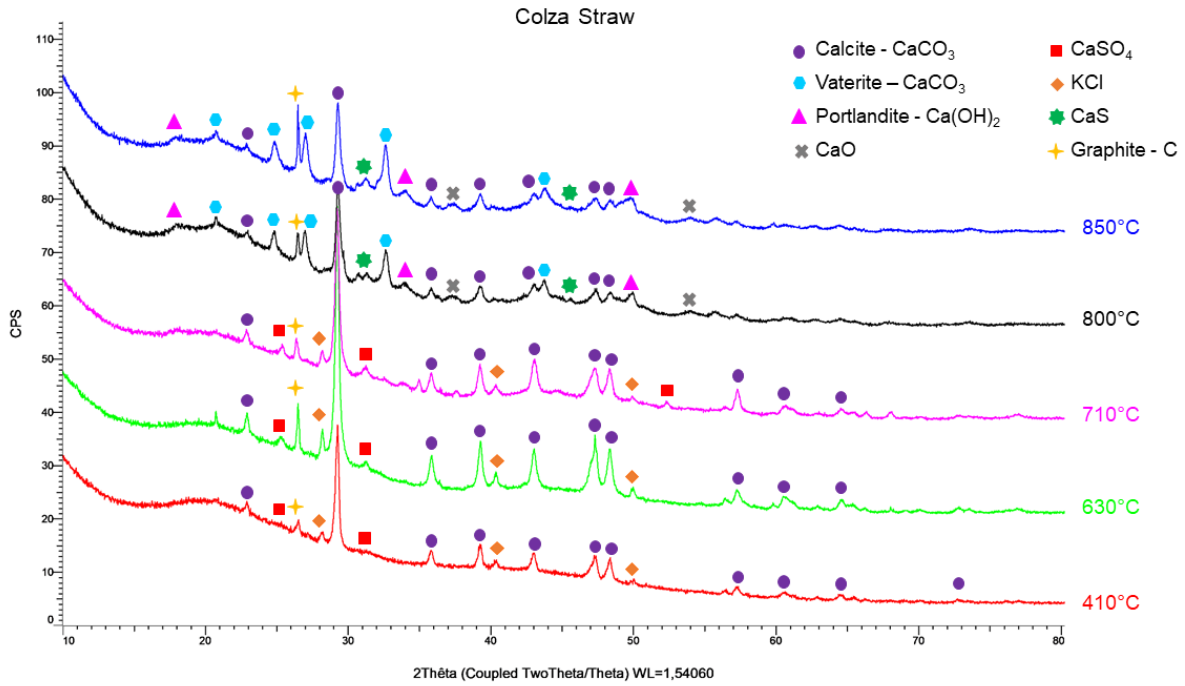
Colza Straw
Calcite - CaCO3
Vaterite – CaCO3
Portlandite - Ca(OH)2
CaO
CaSO4
KCl
CaS
Graphite - C
850°C
800°C
710°C
630°C
410°C
CPS
2Thêta (Coupled TwoTheta/Theta) WL=1,54060

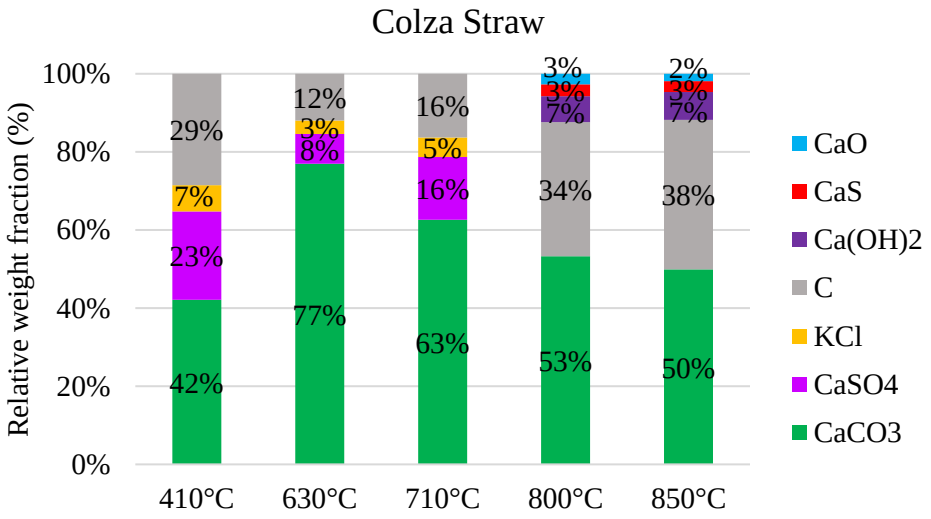
Colza Straw
Relative weight fraction (%)
100%
80%
60%
40%
20%
0%
410°C
630°C
710°C
800°C
850°C
29%
7%
23%
42%
12%
3%
8%
77%
16%
5%
16%
63%
3%
3%
7%
34%
53%
2%
3%
7%
38%
50%
CaO
CaS
Ca(OH)2
C
KCl
CaSO4
CaCO3

(a)

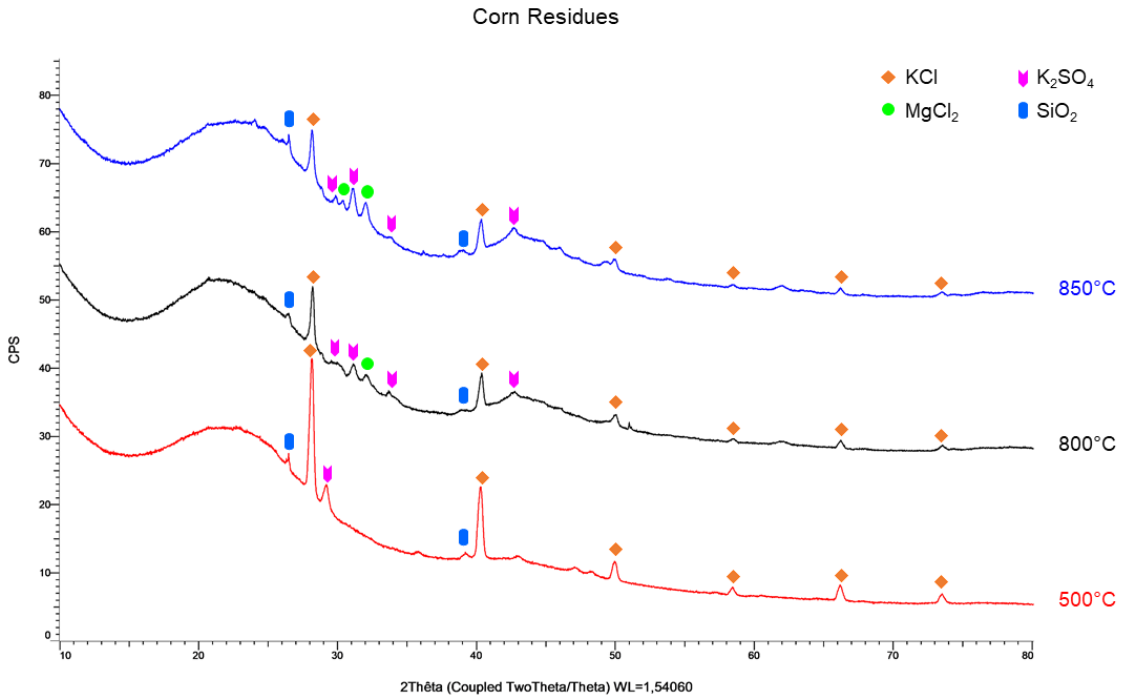
Corn Residues
KCl
K_2SO_4
$MgCl_2$
SiO_2
850°C
800°C
500°C
CPS
2Thêta (Coupled TwoTheta/Theta) WL=1,54060

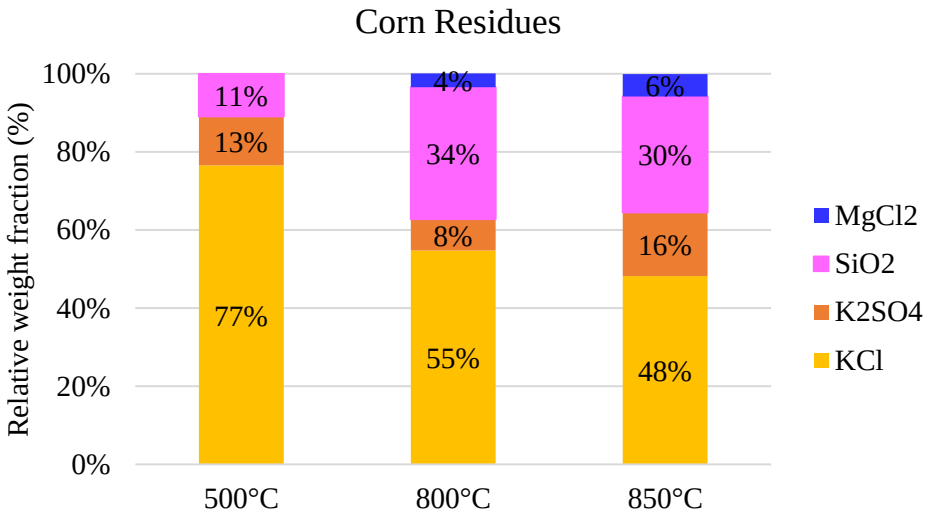
Corn Residues
Relative weight fraction (%)
100%
80%
60%
40%
20%
0%
11%
13%
77%
4%
34%
8%
55%
6%
30%
16%
48%
500°C
800°C
850°C
MgCl2
SiO2
K2SO4
KCl

(b)

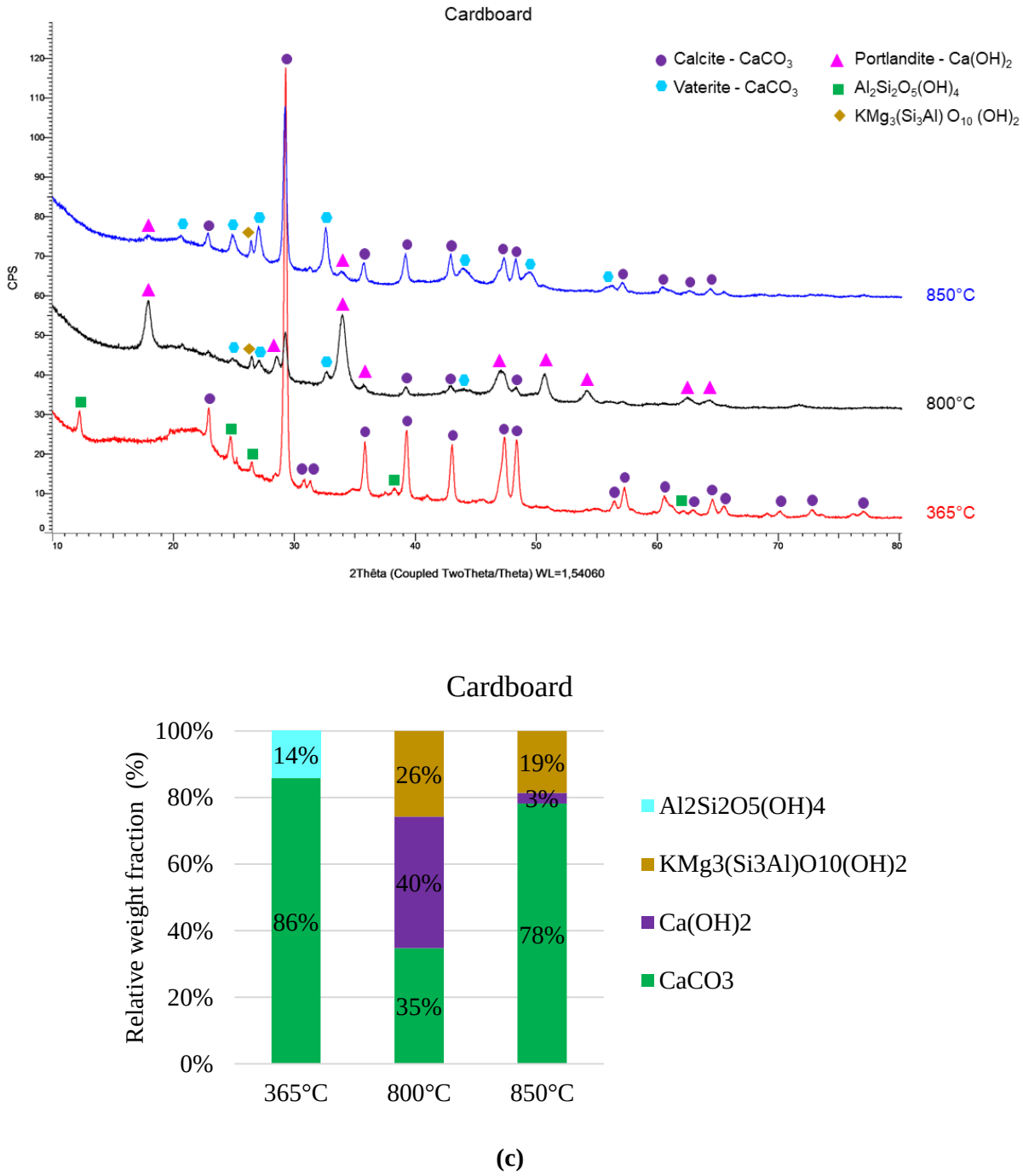

(c)

Figure 28: XRD diffractograms and evolution of the relative composition of the phases estimated by the semi-quantitative analysis of colza straw (a), corn residues (b) and cardboard (c) chars at their different pyrolysis temperatures

The chars from wool showed no clear mineral phases, which can be linked to the low ash content of wool, therefore their XRD results are not presented. The main part of wool chars consists in a carbonaceous matrix containing some inorganic elements, which may explain their amorphous nature seen in the XRD analysis. In the EDX analysis, the measured molar ratios

between calcium and sulfur are higher than 1, which strongly supports the presence of sulfur along with calcium as CaS in the carbonaceous matrix (**Figure 27 (c)**). These findings are in agreement with the thermodynamic calculations, where CaS is identified as one of the sulfur-containing products in the solid phase.

For colza straw (**Figure 28 (a)**), in the samples pyrolyzed between 410 and 710°C, peaks are observed at 2θ=28.2°, 2θ=40.3° and 2θ=50° and are attributed to sylvite (KCl). In the SEM-EDX analysis, Cl is found in a phase at 710°C with a high K content, which could correspond to KCl. However, for the chars produced at higher pyrolysis temperatures, 800°C and 850°C, no presence of sylvite is found in XRD. These observations could confirm that above 800°C there is a release of Cl and K due to the metal chloride volatilization.

The SEM-EDX analysis shows the presence of sulfur in the carbonaceous matrix along with high amount of Ca and some K, P, Mg and Cl at the different pyrolysis temperatures. In the XRD analysis, calcium sulfate $CaSO_4$ (2θ=25.3°and 2θ=31.3°) is identified in the chars produced at 410°C, 630°C, and 710°C. No peaks corresponding to $CaSO_4$ are found for the chars produced at 800°C and 850°C. On the other hand, the presence of calcium sulfide CaS is confirmed by the peaks at 2θ= 31.3° and 2θ=45.5° in these chars. According to the semi-quantitative analysis, CaS represents a smaller fraction within the overall crystalline phases compared to $CaSO_4$. This could show that the inorganic sulfates, besides being partially transformed to organic S bound to the char and released in the gas as discussed previously, can also be reduced to inorganic sulfide at temperatures above 700°C, as seen in previous studies (Knudsen et al., 2004b). The main crystalline phase detected in the chars from colza straw is $CaCO_3$, as indicated by the semi-quantitative results. This observation is further supported by our findings from the SEM-EDX analysis showing corresponding molar ratios of Ca, C and O, which reveals the presence of $CaCO_3$ in the char samples. Moreover, for the chars produced at higher temperatures (800°C and 850°C), additional peaks are observed at 2θ=18°, 28.5°, and 34° and at 2θ=37.5° which are attributed to the presence of portlandite ($Ca(OH)_2$) and lime (CaO) respectively.

When qualitatively comparing the experimental results obtained from XRD and SEM-EDX analysis with thermodynamic equilibrium predictions for colza straw, we observe some agreement regarding the sulfur and chlorine-containing compounds found in the chars, such as CaS and KCl. However, the calcium and potassium silicates or carbonates predisicted at thermodynamic equilibrium are not detected.

For the corn residues char at 500°C, the SEM-EDX analysis show phases containing K and Cl appearing as fine particles attached to the char, which could correspond to KCl. As temperature

rises to 800°C and 850°C, the occurrence of these particles decrease. In addition, we observed grains in the different chars containing Si and O with quantities that well fit with the expected composition of SiO_2, suggesting its presence in the char (**Figure 27 (b)**). These observations are consistent with the XRD results. Indeed, for all temperatures, silica (SiO_2) is detected in the corn residue chars by XRD (**Figure 28 (b)**). Sylvite (KCl) is the major crystalline phase detected with several peaks. Its weight fraction among all crystalline phases decreases with the increase of temperature above 500°C, which can be explained by the partial release of KCl at these temperatures. Contrary to colza straw char, KCl is still detected in the chars produced at 800 and 850°C. On the other hand, magnesium chloride ($MgCl_2$) is then present with a peak at $2\theta=32°$ and two peaks ($2\theta=30.3°$ and $2\theta=32°$) at 850°C. According to (Keown et al., 2005), while Cl may be bonded into the char organic matrix, it may also react with Mg and Ca to form refractory $MgCl_2$ or $CaCl_2$. At all temperatures potassium sulfate K_2SO_4, the only sulfur-containing phase for this feedstock, is detected with peaks present at $2\theta=30°$, $2\theta=31.2°$, $2\theta=34°$ and $2\theta=43°$.

Both the thermodynamic calculations and experimental results for corn residues indicate the presence of KCl in the char. However, the presence of potassium sulfate (K_2SO_4) in the experimental analysis is not in agreement with the thermodynamic calculations, which do not predict any condensed-phase sulfur species.

No crystalline structures containing S are identified in the diffractograms of the cardboard char samples pyrolyzed at the three different temperatures (365°C, 800°C and 850°C (**Figure 28(c)**). Moreover, in the SEM-EDX analysis, S is not observed in the chars at the different temperatures. This could be due to the very low content of S remaining in the char samples (under 0.1 wt.%). This is not in agreement with the thermodynamic calculations that predicted the formation of iron sulfide (FeS) as a condensed-phase sulfur species in cardboard chars. The main crystalline phase detected in the char produced at 365°C is calcite $CaCO_3$, which was neither predicted at thermodynamic equilibrium, Ca rather being included in a silicate phase. In addition, three peaks are identified at $2\theta=12.2°$, $2\theta=24.6°$ and $2\theta=26.5°$ and attributed to kaolin ($Al_2Si_2O_5(OH)_4$). Both calcite and kaolin (clay) are inorganic minerals used in the paper industry as fillers and as surface coatings (Hubbe and Gill, 2016). For the chars produced at 800°C and 850°C, $CaCO_3$ is present in two of its polymorphs: calcite and vaterite. In addition, a silicate of formula $KMg_3(Si_3Al)O_{10}(OH)_2$ is found at 800 and 850°C. Portlandite $Ca(OH)_2$ also appears to be present especially in the char at 800°C.

Upon comparing with the mass composition of the ashes of each resource presented in **Table 12**, the phases identified in the chars in the XRD and SEM-EDX analysis are in agreement with the major ash-forming elements of each resource.

3.2.4. Result synthesis

The release of S and Cl during the pyrolysis of the waste components (S for wool and cardboard, Cl for PVC) can be attributed to the presence of dominating organic forms. As shown by the XRD and SEM-EDX analyses, as well as S and Cl retention measurements, it appears that this release occurs without significant interaction with ash-forming elements. This is remarkable for cardboard which presents a high ash content (12.8 wt%), and especially a high calcium content (4.3 wt%), which could have been expected to react with sulfur. For the agricultural residues, both the organically and the inorganically associated S contribute to the amount of S released. Inorganic sulfates have negligible evaporation rates below 1000°C; however, they may partially transform to organic S and be released in the gas. In the Ca-rich colza straw, the sulfur remaining in the char was found to be associated with calcium, especially in sulfates $CaSO_4$, that were reduced to calcium sulfide CaS above 800°C. On the other hand, for the K-rich corn residues, the sulfur remaining in the char is associated with potassium in sulfates K_2SO_4, which could be detected up to 850°C.

For colza straw and corn residues, the dominating inorganic Cl is partially released, probably as HCl at temperatures below 700°C (no K release detected), and by partial evaporation of metal chlorides above 700°C. In corn residue chars, the presence of Cl is clearly visible, existing in crystallized phases (KCl and $MgCl_2$) even above 800°C, while in colza straw, such Cl salts were not observed. These findings suggest that the composition of the biomass can exert an influence on the retention behavior of Cl.

Regarding the thermodynamic calculations, the characterization results reveal the presence of inorganic forms originating from the feedstock, such as sulfates and sulfides in the agricultural residues, as well as potential cardboard additives. However, the predicted phases at thermodynamic equilibrium differ significantly from the observed ones. These discrepancies in phase distribution suggest that the experimental conditions, even during the 20-minute pyrolysis experiment, may not be sufficient for the system to reach thermodynamic equilibrium.

3.3. Effect of air addition: switching to gasification

In this section, we investigated the influence of air addition on the behavior of sulfur and chlorine. The experiments were conducted at a temperature of 800°C for a duration of 20 minutes. The detailed experimental conditions are outlined in **section 2.2.4.1**. The objective was to investigate the influence of the atmosphere (N_2 + O_2 for gasification versus N_2 for pyrolysis) on the S and Cl retention in the char. In addition, we also performed gasification experiments on the agricultural residues with an extended duration of 60 minutes at 800°C, with the objective of further investigating potential changes that might happen with more extended gasification of the samples. The gasification experiment of 20 minutes for colza straw was performed in duplicate.

Figure 29 shows the char yield comparison between the pyrolysis and gasification experiments at 800°C. As expected, the graph shows a decrease in the char yields when switching from pyrolysis to gasification of 20 minutes for the four feedstocks During gasification, in the presence of air, the char undergoes oxidation, leading to its partial conversion into gaseous products and therefore a decrease in its yield.
Notably, the char yield reduction for colza straw is lower compared to the other resources. However, in the case of gasification experiments conducted for 60 minutes, there was a significant further decrease in char yield for both agricultural residues. This observation indicates that longer gasification time contributed to a more pronounced conversion of char into gaseous products, thereby confirming the impact of extended gasification on reducing char yield.

The measurement of carbon retention in the char after gasification provides further valuable insights into the findings. **Figure 30** presents the carbon retention comparison between the pyrolysis and gasification experiments. Similar to the char yield observations, the carbon retention for agricultural residues, particularly colza straw, exhibits a minor decrease when transitioning from pyrolysis to gasification with a duration of 20 minutes. The characteristics of the agricultural residues, such as the chemical composition (inorganics in particular) and structure, could be the factors contributing to this finding.
Nevertheless, it becomes evident that a gasification duration of 20 minutes is not sufficient, in our conditions, to complete the carbon conversion in the case of agricultural residues. This hypothesis gains further support from the results obtained from the gasification experiment

conducted for 60 minutes. Here, the longer duration allows for a more extensive gasification of carbon, leading to a significant decrease in carbon retention down to 1%.

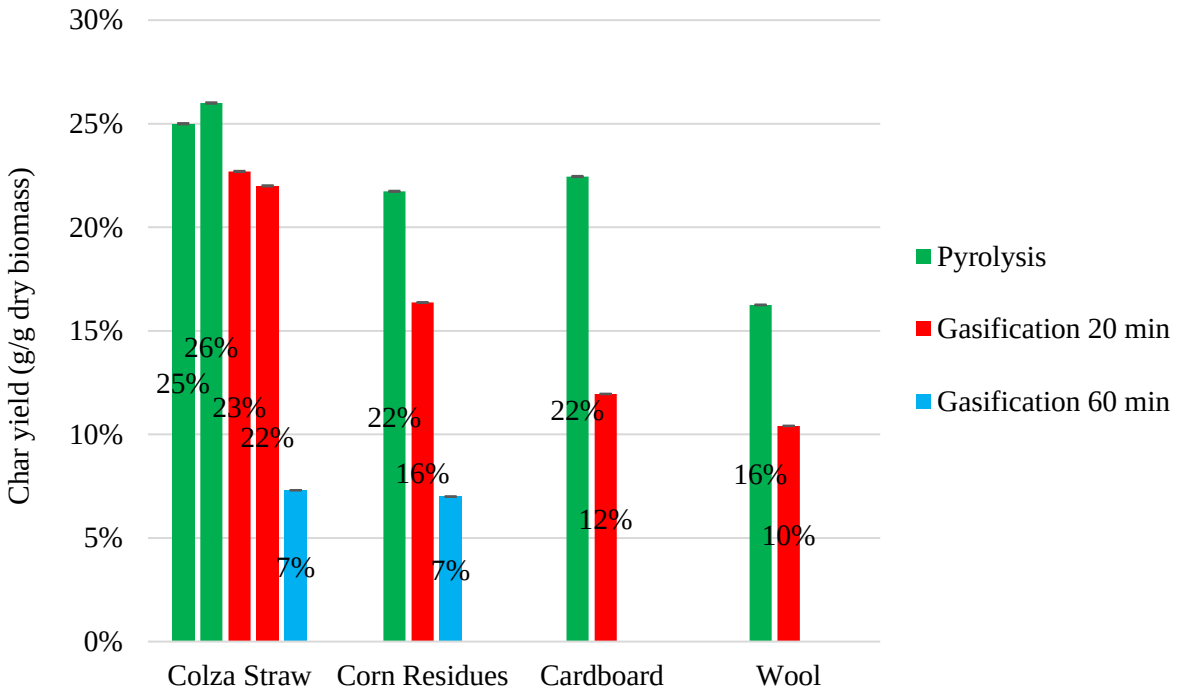

Figure 29: Comparison of the char yield between pyrolysis and gasification

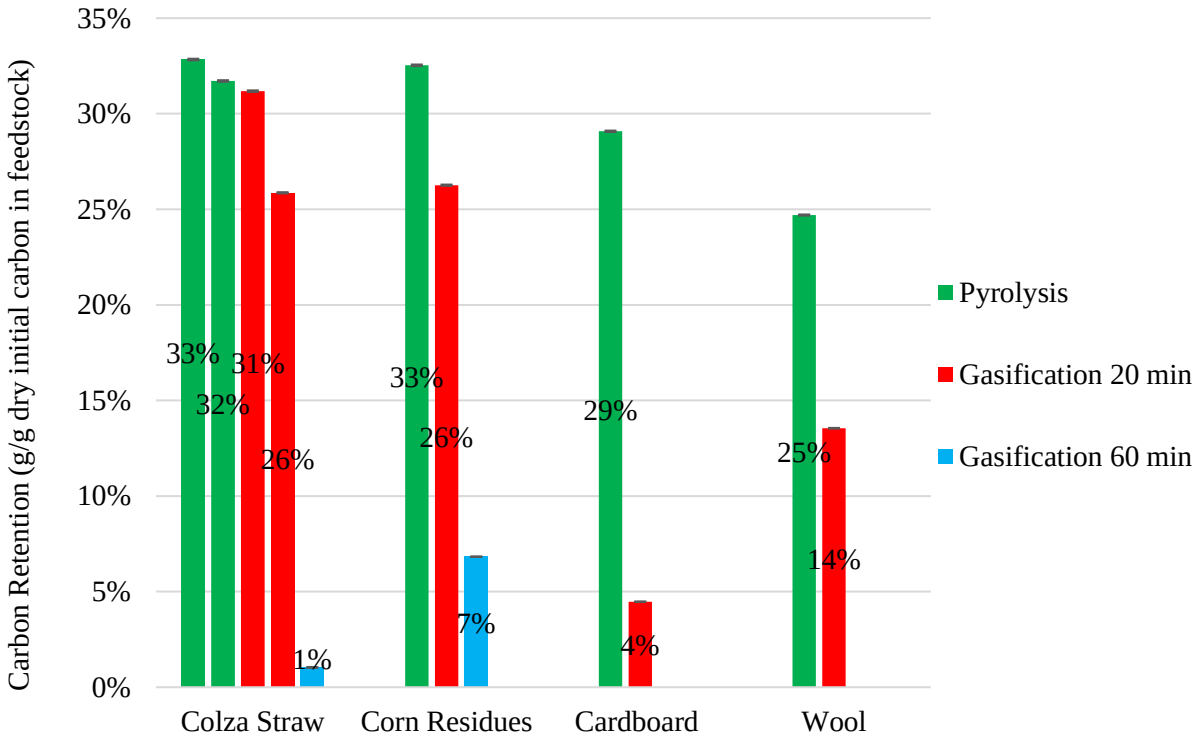

Figure 30: Comparison of carbon retention in char: pyrolysis vs. gasification

Figure 31 shows the sulfur and chlorine retention in the char in pyrolysis and gasification at 800°C. Error bars show the relative uncertainty calculated by the propagation method (Appendix A).

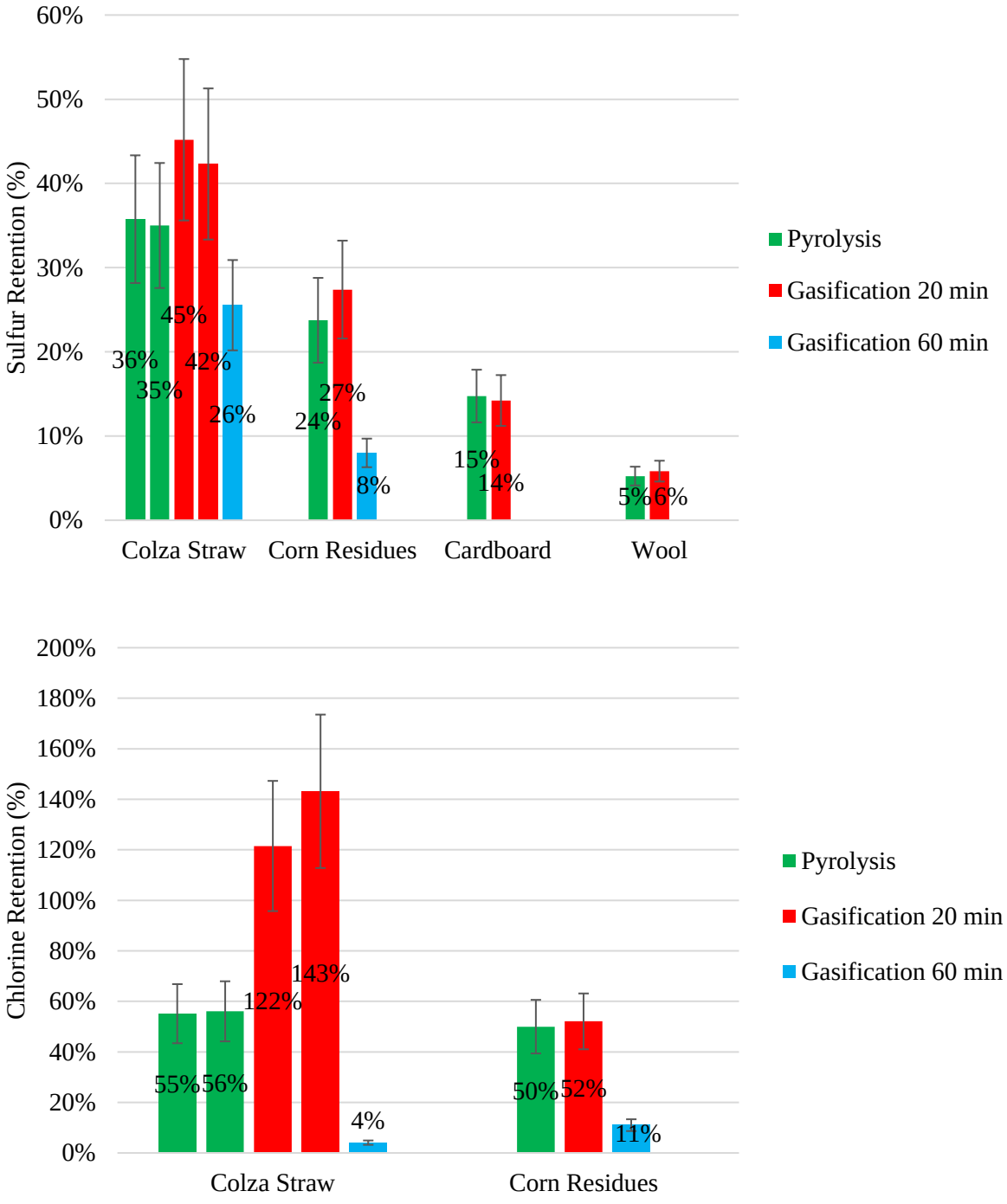

Figure 31: Comparison of sulfur and chlorine retention in char: pyrolysis vs. gasification

The addition of air in the gasification experiments for 20 minutes do not have a significant impact on the sulfur retention in the chars for cardboard, wool and corn residues. However, for

colza straw, the sulfur retention seems to slightly increase, which is supported by the duplicate experiments. For the gasification experiment conducted over a duration of 60 minutes, the sulfur retention in the agricultural residues decreases. The decrease is more significant for corn residues, reaching a sulfur retention of 8%.

For corn residues, there is no significant change in the fraction of chlorine retained in the char when switching to a 20-minute gasification experiment. However, intriguingly, for colza straw, there is a remarkable difference, with complete retention of chlorine in the char under 20-minute gasification conditions. As for sulfur, for the gasification experiment conducted over a duration of 60 minutes, notable changes in chlorine retention can be observed for both agricultural residues. In the case of colza straw, the chlorine retention drastically decreases to 4%, while for corn residues, it decreases to 11%.

To better understand the interactions among sulfur, chlorine, and the ash-forming elements, during gasification, the char samples were subjected to XRD analysis. **(d)**

Figure 32 shows the XRD patterns of the chars obtained from colza straw, corn residues, cardboard and wool in pyrolysis and gasification conditions at 800°C as well as the semi-quantitative analysis results.

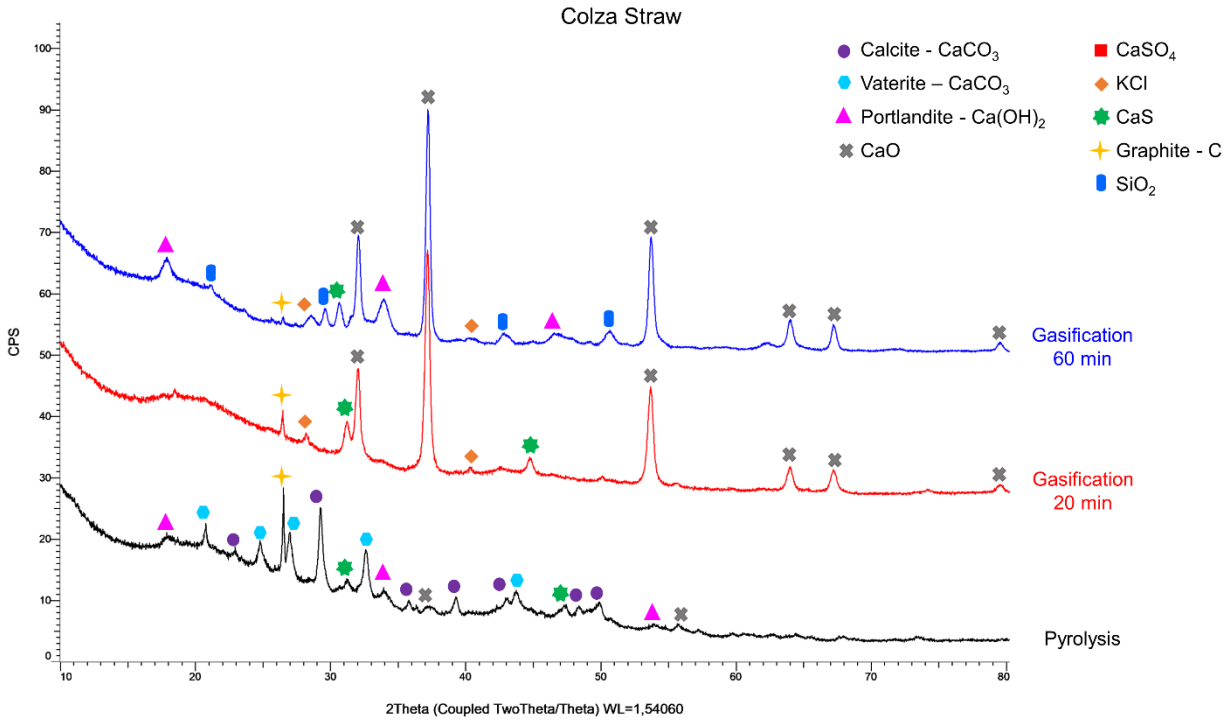
Colza Straw
Calcite - CaCO3
Vaterite – CaCO3
Portlandite - Ca(OH)2
CaO
CaSO4
KCl
CaS
Graphite - C
SiO2
Gasification 60 min
Gasification 20 min
Pyrolysis
CPS
2Theta (Coupled TwoTheta/Theta) WL=1,54060

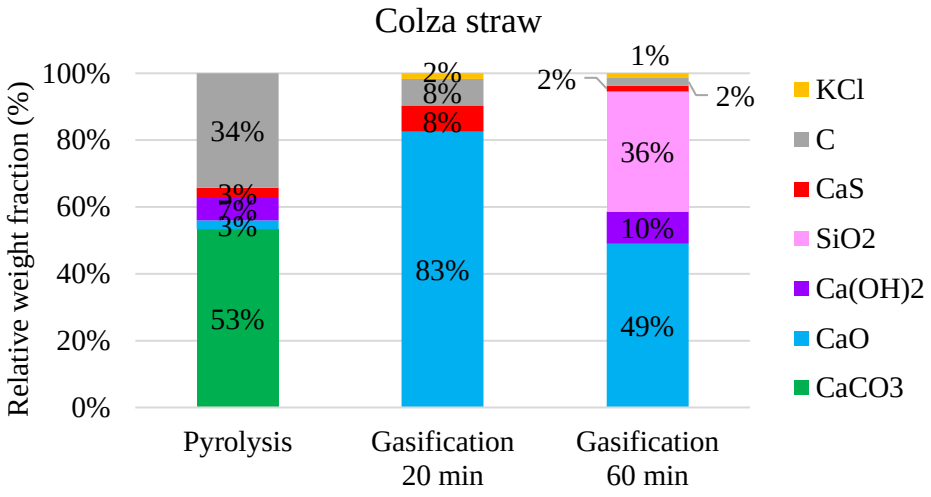
Colza straw
Relative weight fraction (%)
100%
80%
60%
40%
20%
0%
34%
3%
7%
3%
53%
2%
8%
8%
83%
2%
1%
2%
36%
10%
49%
Pyrolysis
Gasification 20 min
Gasification 60 min
KCl
C
CaS
SiO2
Ca(OH)2
CaO
CaCO3

(a)

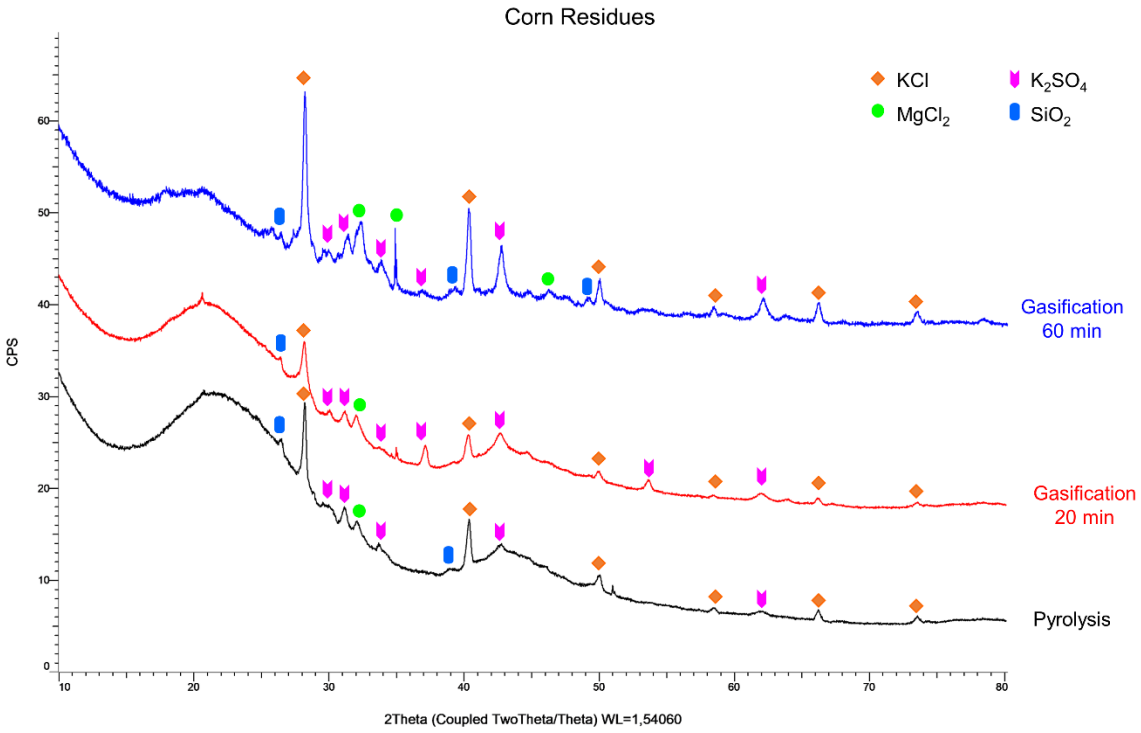
Corn Residues
KCl
K_2SO_4
$MgCl_2$
SiO_2
Gasification 60 min
Gasification 20 min
Pyrolysis
CPS
2Theta (Coupled TwoTheta/Theta) WL=1,54060

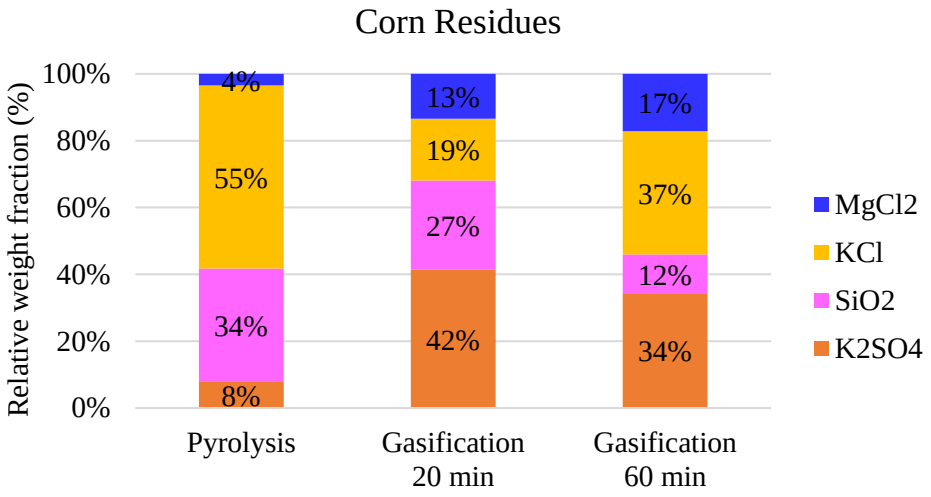
Corn Residues
Relative weight fraction (%)
100%
80%
60%
40%
20%
0%
4%
55%
34%
8%
13%
19%
27%
42%
17%
37%
12%
34%
Pyrolysis
Gasification 20 min
Gasification 60 min
MgCl2
KCl
SiO2
K2SO4

(b)

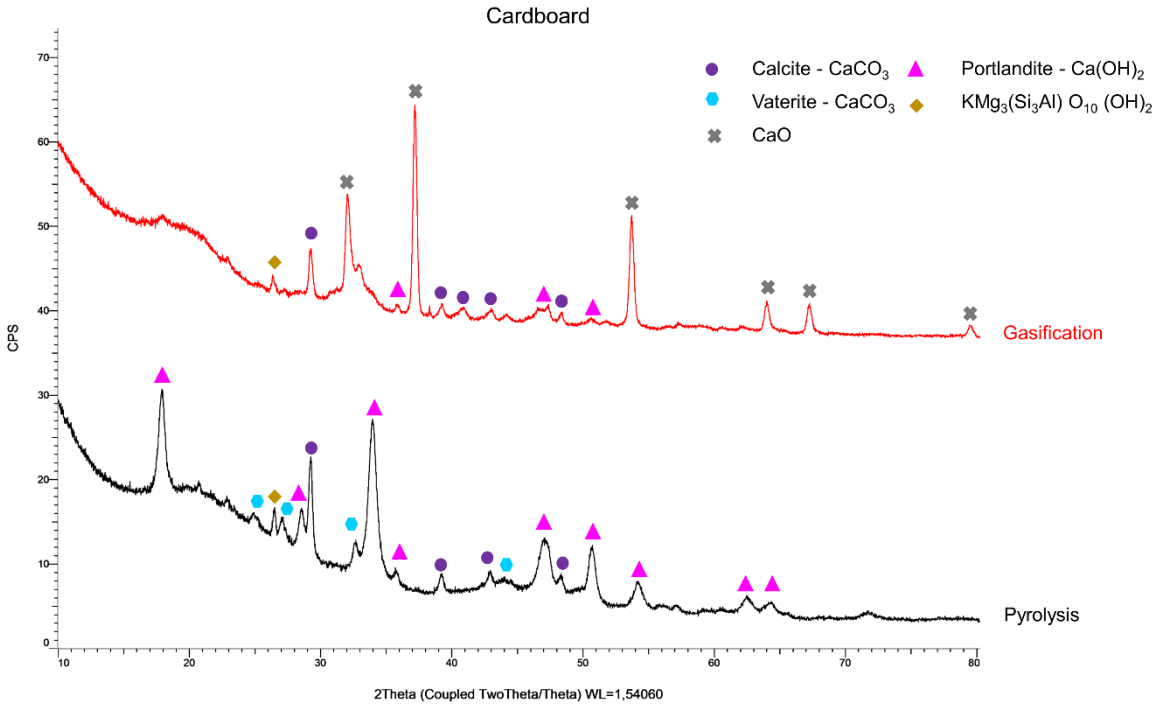
Cardboard
Calcite - CaCO3
Portlandite - Ca(OH)2
Vaterite - CaCO3
KMg3(Si3Al) O10 (OH)2
CaO
Gasification
Pyrolysis
CPS
2Theta (Coupled TwoTheta/Theta) WL=1,54060

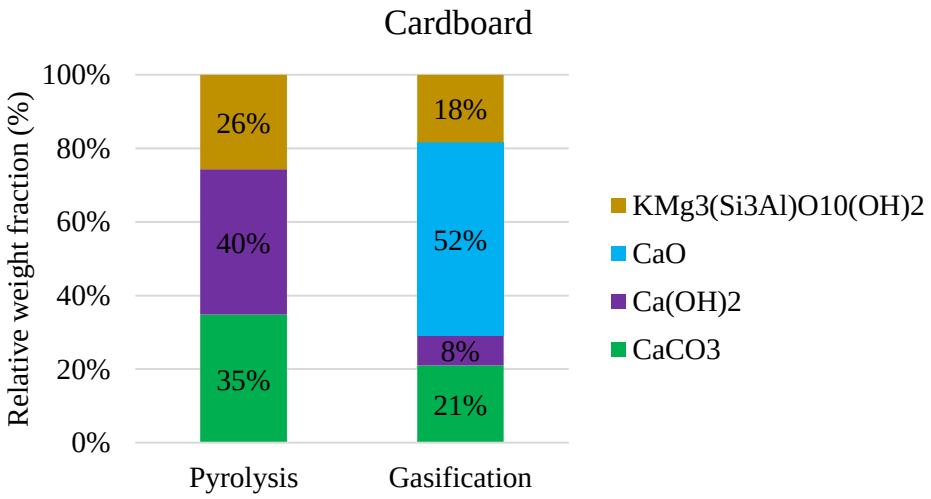
Cardboard
Relative weight fraction (%)
100%
80%
60%
40%
20%
0%
26%
40%
35%
18%
52%
8%
21%
Pyrolysis
Gasification
KMg3(Si3Al)O10(OH)2
CaO
Ca(OH)2
CaCO3

(c)

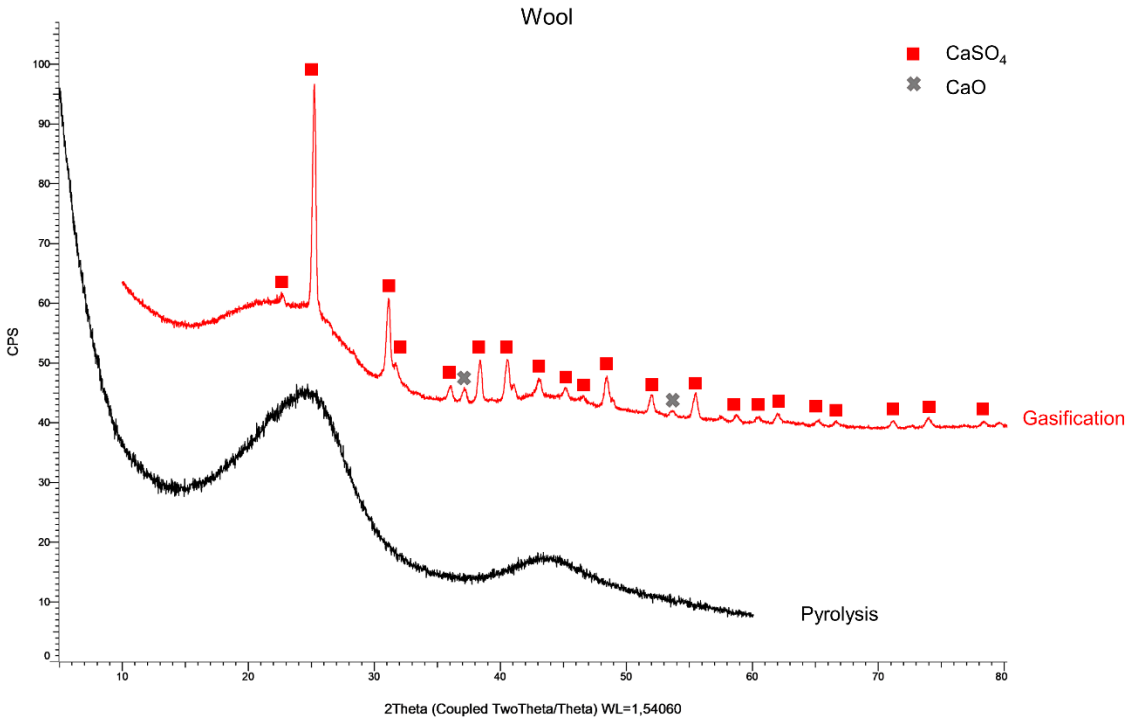

(d)

Figure 32: XRD diffractograms and semi-quantitative analysis of chars obtained from pyrolysis and gasification at 800°C: colza straw (a), corn residues (b), cardboard (c) and wool (d)

For colza straw, both in the 20 minutes and 60 minutes gasification diffractograms, peaks corresponding to calcium sulfide (CaS) indicate its presence in the gasification char. The proportion of CaS remains relatively stable compared to pyrolysis. However, some changes are observed in the semi-quantitative results. The fraction of calcium oxide (CaO) significantly increases with the addition of air, while that of calcium carbonate ($CaCO_3$) decreases sharply. Moreover, in the gasification diffractogram of 60 minutes, peaks corresponding to SiO_2 are detected, which do not appear in the 20 minutes gasification diffractogram, probably due to less amorphous carbon in the char. New peaks corresponding to potassium chloride (KCl) appear in the gasification diffractograms, which could explain the increase in chlorine retention in the char after the 20 minutes gasification. However, this contradicts the drastic decrease in chlorine retention in the char after the 60 minutes gasification

In the 20 and 60 minutes gasification diffractograms of corn residues, we observe the same peaks as those present in the pyrolysis diffractogram. These peaks are attributed to potassium chloride (KCl), silicon dioxide (SiO_2), potassium sulfate (K_2SO_4), and magnesium chloride ($MgCl_2$). The semi-quantitative results show a decrease in the weight fraction of potassium

chloride (KCl) from pyrolysis to gasification, and an increase in the weight fraction of potassium sulfate (K_2SO_4).

For cardboard, fewer peaks corresponding to $CaCO_3$ and $Ca(OH)_2$ are present in the gasification diffractogram and new peaks of CaO appear. The semi-quantitative analysis shows a decrease in the fractions of $CaCO_3$ and $Ca(OH)_2$ in gasification compared to pyrolysis.

As shown in the previous section, the XRD diffractogram of the wool char obtained after pyrolysis does not exhibit any peaks or clear mineral phases, indicating its amorphous nature. In addition, the SEM-EDX analysis shows the presence of sulfur along with calcium in the carbonaceous matrix. However, the XRD diffractogram of the wool sample obtained after gasification shows prominent peaks corresponding to calcium sulfate $CaSO_4$ and other peaks corresponding to CaO. The semi-quantitative analysis reveals a weight percentage of 98% for $CaSO_4$ and 2% for CaO, which confirms that the major crystalline phase in the wool char is calcium sulfate. It is possible for calcium sulfide (CaS) to be oxidised and to form calcium sulfate ($CaSO_4$). The switch from pyrolysis to gasification results in a reduction of approximately 14% in retained carbon in the char (**Figure 30).** This decrease may be linked to a decrease in the presence of the amorphous carbon phase, which could potentially account for the emergence of crystalline peaks.

The XRD analysis reveals that the characteristic peaks of sulfur and chlorine compounds remain relatively unchanged between the pyrolysis and gasification experiments except for colza straw, for which the peaks of KCl could explain the increased retention of chlorine in the char from the 20 minutes gasification but contradicts the decrease of chlorine retention at the 60 minutes gasification. On the other hand, the significant increase in the relative weight fraction of CaO can be attributed to the enhanced decomposition of calcium-containing compounds, $CaCO_3$ and $Ca(OH)_2$, during the gasification process (Ingraham and Marier, 1963).

For corn residues, cardboard and wool, the lack of significant differences in the qualitative XRD analysis and quantitative measurements of sulfur and chlorine retention, between pyrolysis and the 20-minute gasification experiments, may suggest that S and Cl-containing compounds are retained in the char without undergoing substantial transformation or decomposition during gasification. As demonstrated in the previous section, organic forms of sulfur and chlorine are typically converted into volatile species during pyrolysis. The addition of air can enhance oxidation reactions; however, the retention of sulfur and chlorine in the char seems not to be affected if they are present in stable compounds, such as sulfates (K_2SO_4, $CaSO_4$), sulfides-

CaS) or chlorides, whose volatility or stability is not impacted by the type of atmosphere (N_2, N2+O2).

For wool and cardboard, the experimental results are in agreement with thermodynamic equilibrium calculations, showing a negligible effect of the variation in the equivalence ratio (ER) on the distribution of sulfur.

In contrast, colza straw stands out with unexpected results, showing an increase in the S and especially Cl retention in the 20 minutes gasification and the emergence of new phases compared to pyrolysis (CaO, KCl), suggesting possible modifications in S and Cl retention mechanisms. However, these changes with an oxygen-containing atmosphere remain hardly explainable.

The decrease in S and Cl retentions after 60 min gasification could be linked to oxidation reactions in the carbonaceous matrix, which would allow releasing sulfur and chlorine linked to the carbon. This shows that the relatively short duration of the 20-minute gasification experiment might not have been sufficient to fully convert the S and Cl compounds into volatile species. Another possible reason for this change could be the association of potassium with chlorine and sulfur in the feedstock. Agricultural residues contain sulfur in the form of potassium sulfates (K_2SO_4) and chlorine in the form of potassium chlorides (KCl). As the gasification time is extended, a higher amount of these compounds may be volatilized. Consequently, the sulfur and chlorine that were initially present in stable compounds as potassium sulfates or chlorides could undergo transformations, leading to the formation of more volatile species.

The 60-minute gasification experiment results show a good agreement with the thermodynamic equilibrium calculations concerning the Cl and S retentions in char. This indicates that, at longer holding times, the system tends to approach thermodynamic equilibrium, potentially reflecting the influence of kinetic factors and non-equilibrium effects during earlier stages of gasification.

3.4. Conclusions

The thermodynamic equilibrium predictions showed that the composition of the resource, in particular the ash-forming elements as Ca, K and Si, is the main factor influencing the distribution of S and Cl in gaseous and solid products, whereas temperature and equivalence ratio have a lower impact.

The experimental tests showed a resource-dependent retention of S and Cl in the char. The table below presents the main findings. Organic forms of S and Cl are volatile and easily released in the gas phase even below 550°C without interacting with other ash-forming elements. On the other hand, inorganic forms are partially released in the gas phase. Their retention in the char under different chemical forms (CaS, K_2SO_4, KCl, $MgCl_2$) depends on the pyrolysis temperature and the ash composition of the resource.

No significant difference in S and Cl retention was observed between the pyrolysis and gasification experiments conducted for a duration of 20 minutes, except for colza straw, which shows an unexpected full retention of Cl after gasification. However, after the 60-minute gasification experiments, the S and Cl retention are quite lower than after 20 minutes for the agricultural residues.

Table 20: Main findings of S and Cl behavior in pyrolysis and gasification

		Initial form in the resource	During pyrolysis	During gasification at 800°C
S	**Wool**	Organic Amino acids	93 – 95% released (>550°C)	94% released Retention in char as $CaSO_4$
	Cardboard	75% Organic bonded to the C matrix	65% released à 365°C ↗ T° >800°C => ↗ S released	86% released
	Colza Straw	35% Organic bonded to the C matrix 65% Inorganic (sulfates)	65–75% released (>420°C) Retention in char as $CaSO_4$ or CaS	20 min: 48-55 % released Retention in char as CaS
				60 min: 74% released
	Corn Residues	50 % Organic bonded to the C matrix 50 % Inorganic (sulfates)	65–75% released (>420°C) Retention in char as K_2SO_4	20 min: 73% released Retention in char as K_2SO_4
				60 min: 92% released Retention in char as K_2SO_4
Cl	**PVC**	Organo-chlorinated (100%)	>90% of Cl released in the gas as HCl	-
	Colza Straw	>85% Cl Inorganic (KCl, $KClO_4$…)	25 – 45% released Retention in char (<800°C) as KCl	20 min: 100% retained in char as KCl
				60 min: 4% retained in char as KCl
	Corn Residues	>85% Cl Inorganic (KCl, $KClO_4$…)	48 – 55% released Retention in char (>500°C) as KCl - $MgCl_2$	20 min: 48% released Retention in char as KCl - $MgCl_2$
				60 min: 89 % released Retention in char as KCl - $MgCl_2$

Comparing thermodynamic predictions with experimental results, the retention of sulfur and chlorine in the solid phase lacks quantitative accuracy. This discrepancy may be due to limitations in solid-solid and/or gas-solid contact between S and Cl and the other ash-forming elements (Ca, Si, K…), leading to kinetic and mass-transfer limitations in gas and/or condensed phases.

On the other hand, a qualitative comparison for S and Cl-containing compounds in chars shows notable agreement with equilibrium predictions, especially for certain feedstocks like cardboard, wool, and PVC pyrolysis.

Additionally, the 60-minute gasification experiments for agricultural residues aligned more closely with thermodynamic equilibrium predictions, particularly regarding sulfur and chlorine retention. This suggests that longer gasification durations may approach thermodynamic equilibrium.

However, it is important to acknowledge that thermodynamic equilibrium assumptions assume perfect mixing and complete reaction, disregarding thermal, kinetic, and mass-transfer limitations. When these factors become significant, thermodynamic equilibrium may not represent the real experimental case.

These results constitute a basis for the completion of our study in the next chapter on in-situ cleaning methods based on interactions between inorganic elements to limit the release of inorganic volatile pollutants.

4.Enhancement of S and Cl retention in char by interaction with ash-forming elements

In the previous chapter focusing on characterizing the behavior of S and Cl during pyrolysis and gasification, results have shown that S and Cl are mostly released in the gas phase as H_2S, COS, HCl and KCl. With the objective to limit the release of these inorganic pollutants, we have chosen to test methods aiming at enhancing the sulfur and chlorine retention in the char through interactions with ash-forming elements. These methods include the use of additives mixed with our resources, and the co-pyrolysis and co-gasification of our resources.

4.1. Use of Additives

As shown in the literature review in **Chapter 1**, using calcium-based additives within the bed material or with the feedstock is a common method to enhance sulfur and chlorine retention in the char during pyrolysis and gasification. Calcium-based materials possess advantageous properties that facilitate the formation of stable compounds. Consequently, they can effectively react with sulfur and chlorine compounds, resulting in the formation of stable condensed compounds, thereby reducing S and Cl release in the gas phase. However, the chemical association of Ca in these additives might have an influence on the reactions occurring during pyrolysis or gasification. So, three calcium-based additives were tested in our study: $CaCO_3$, CaO and $Ca(OH)_2$. The detailed experimental conditions are described in **section 2.2.4.2**.

Figure 33 shows the sulfur retention in the chars of the feedstock alone and feedstock-additive mixtures, after pyrolysis and gasification experiments at 800°C for 20 min. Error bars show the relative uncertainty calculated by the propagation method. The gasification experiments for colza straw mixed with CaO were performed in duplicate.

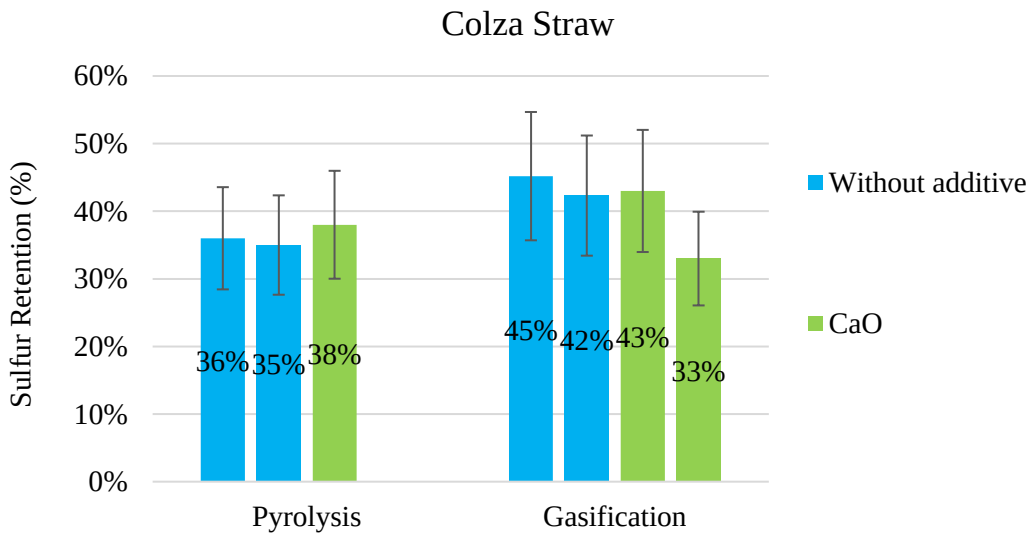

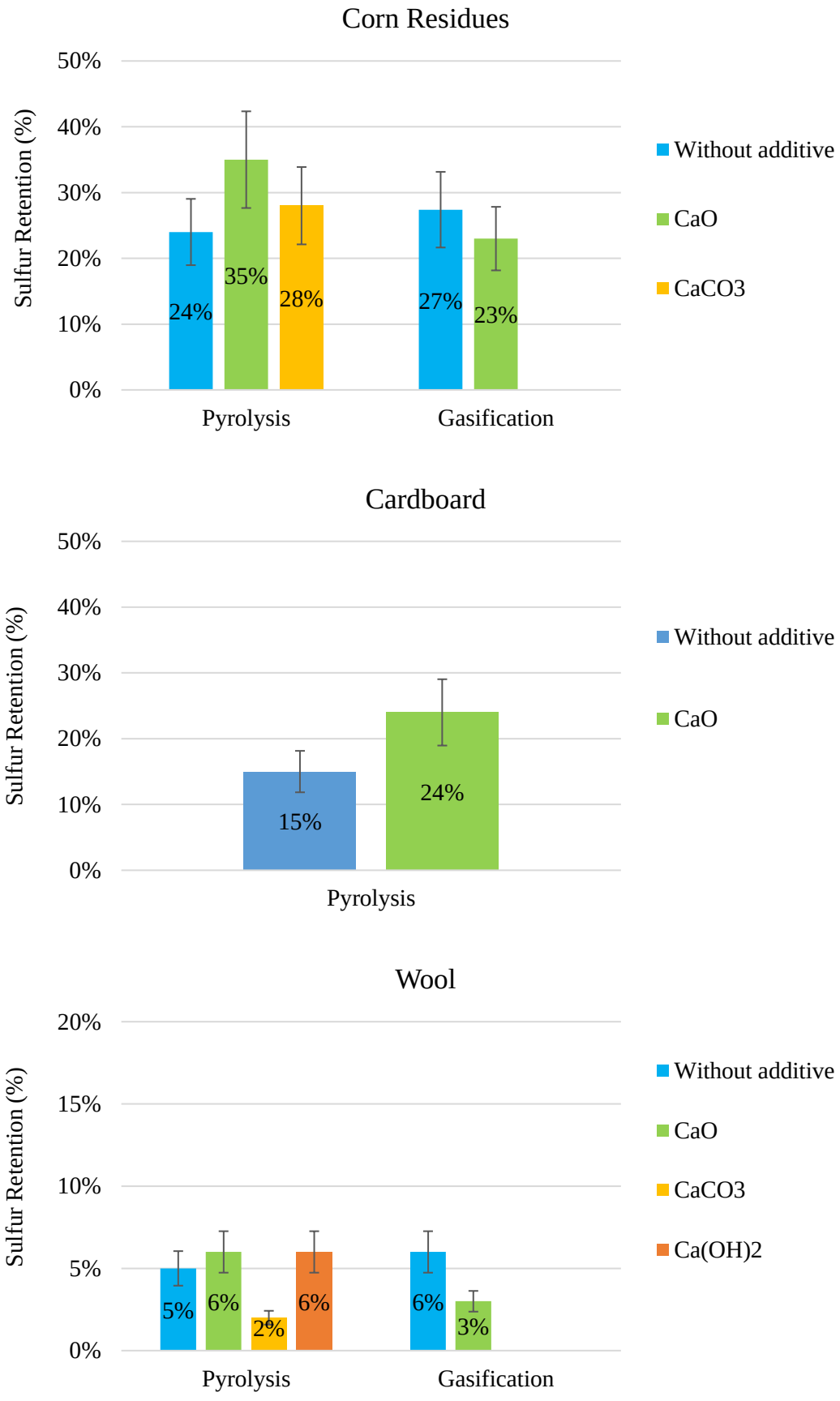

Figure 33: Effect of calcium-based additives on sulfur retention in char in pyrolysis and gasification experiments at 800°C

As shown in **Figure 33**, the addition of CaO seems to induce an increase of about 10 points in sulfur retention during pyrolysis for corn residues and cardboard. The addition of $CaCO_3$ in pyrolysis has no or a negative influence on sulfur retention (wool, corn residues).

The chlorine retention in the chars of the feedstocks without and with additive is shown in **Figure 34.** Error bars show the relative uncertainty calculated by the propagation method.

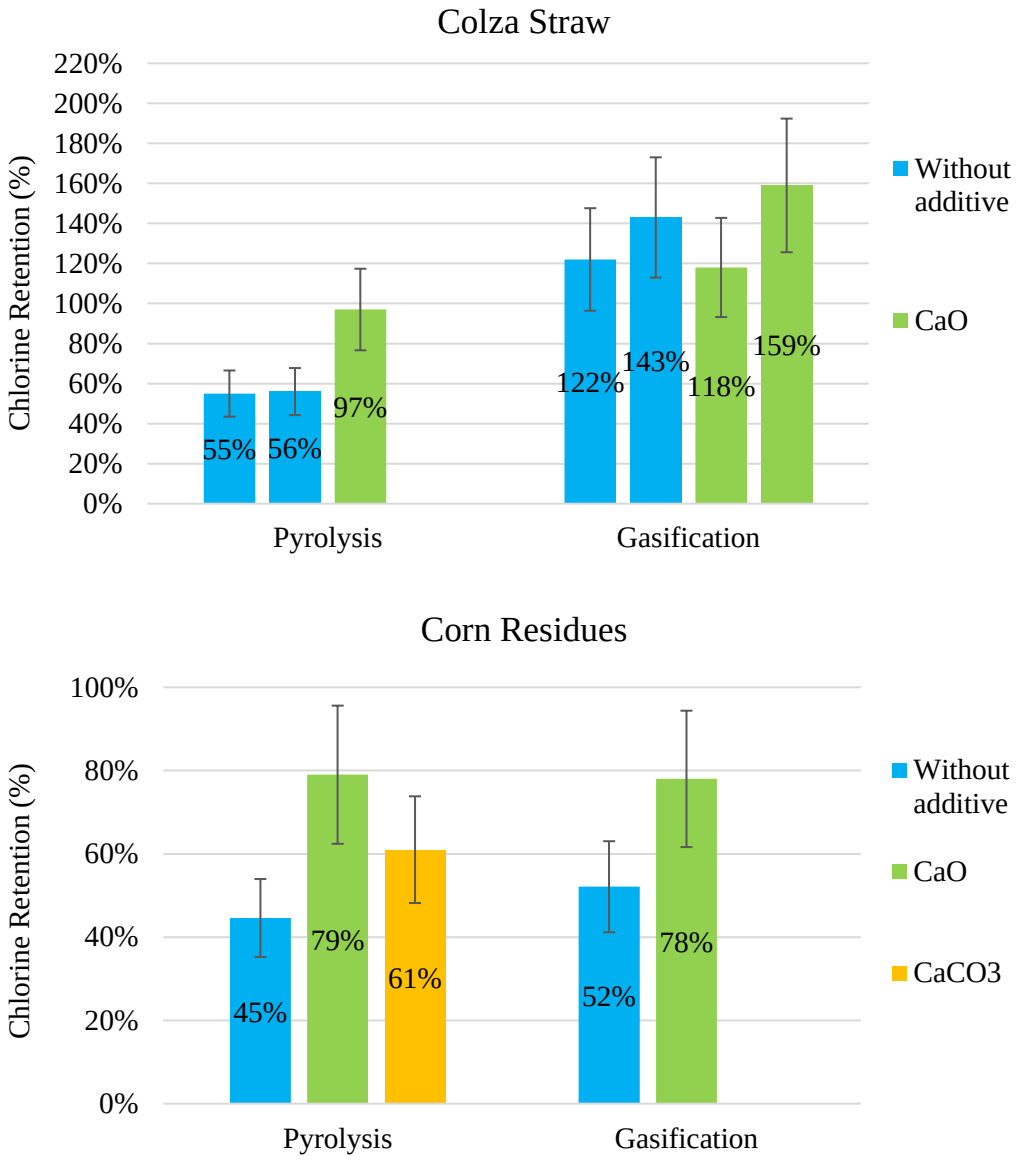

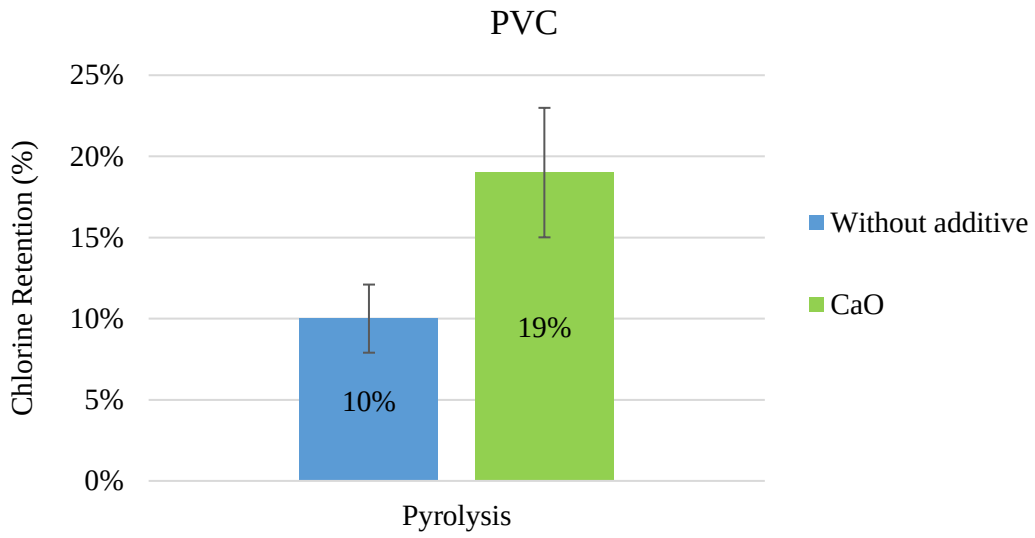

Figure 34: Effect of calcium-based additives on chlorine retention in char in pyrolysis and gasification experiments at 800°C

By mixing CaO with colza straw, corn residues, and PVC, the chlorine retention in the chars is significantly increased after pyrolysis at 800°C. Specifically, the chlorine retention increases from 55% to 97% when CaO is mixed with colza straw, from 45% to 79% when mixed with corn residues, and from 10% to 19% when mixed with PVC.

On the other hand, the addition of $CaCO_3$ to corn residues has a lower impact than CaO on chlorine retention after pyrolysis at 800°C.

For the gasification experiments, the addition of CaO to colza straw does not have a significant impact on chlorine retention, which is already at 100% without CaO. However, with corn residues, similarly to pyrolysis, the addition of CaO results in an increase, from 52 % to 78 %, in chlorine retention.

Figure 35 shows the XRD diffractograms and evolution of the relative composition of the phases estimated by the semi-quantitative analysis of the chars of the feedstocks without additive and feedstock-additive mixtures. In the case of PVC with CaO, some peaks remain unidentified, thus, the semi-quantitative analysis of the char is not presented. **Figure 36** shows the SEM observations of the chars obtained after pyrolysis at 800°C of the mixtures colza straw/CaO and corn–residues/CaO

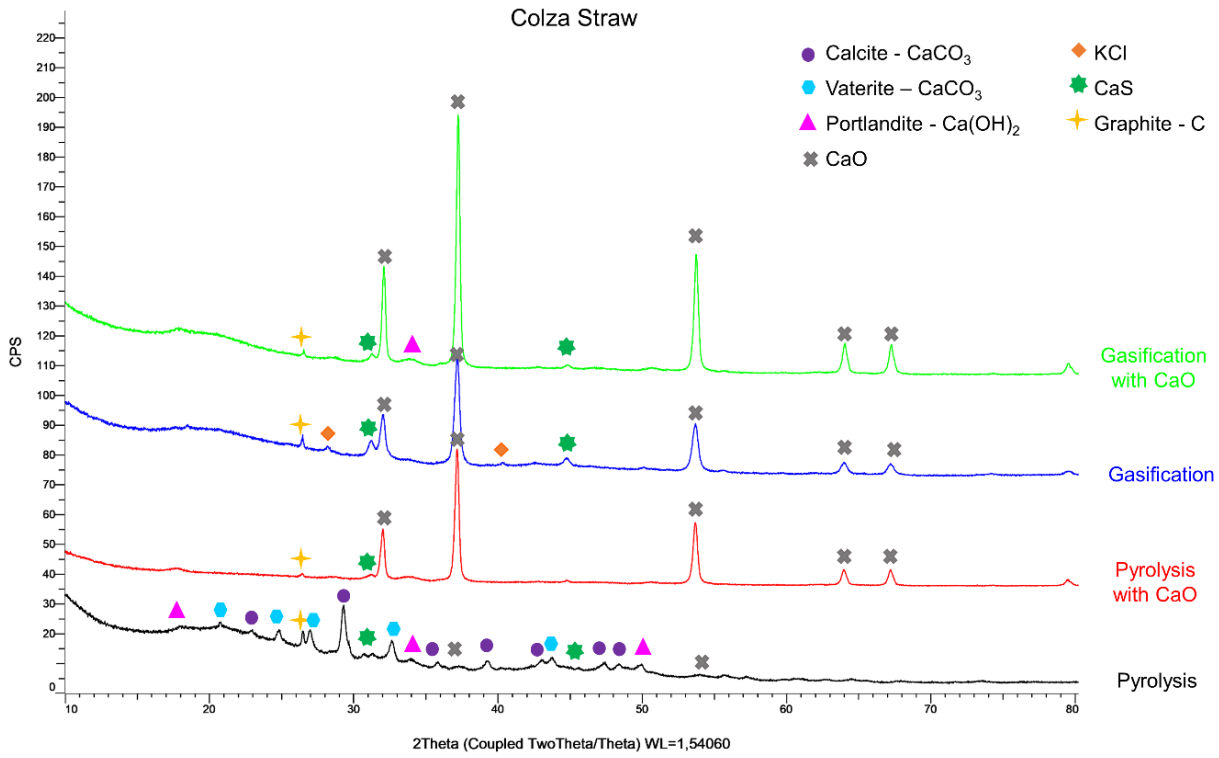
Colza Straw
Calcite - CaCO3
Vaterite – CaCO3
Portlandite - Ca(OH)2
CaO
KCl
CaS
Graphite - C
Gasification with CaO
Gasification
Pyrolysis with CaO
Pyrolysis
CPS
2Theta (Coupled TwoTheta/Theta) WL=1,54060

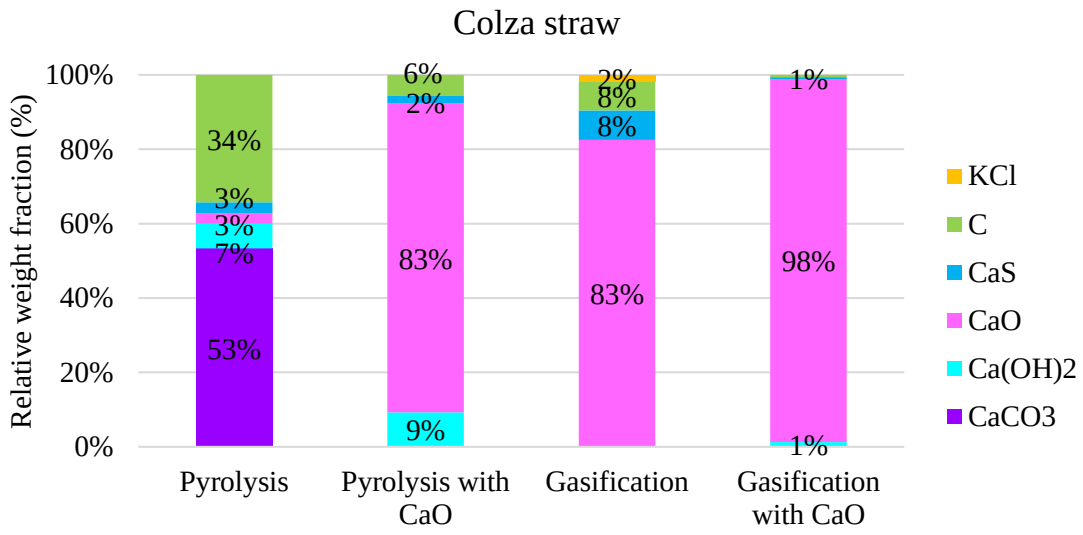
Colza straw
Relative weight fraction (%)
100%
80%
60%
40%
20%
0%
34%
3%
3%
7%
53%
6%
2%
83%
9%
2%
8%
8%
83%
1%
98%
1%
Pyrolysis
Pyrolysis with CaO
Gasification
Gasification with CaO
KCl
C
CaS
CaO
Ca(OH)2
CaCO3

(a)

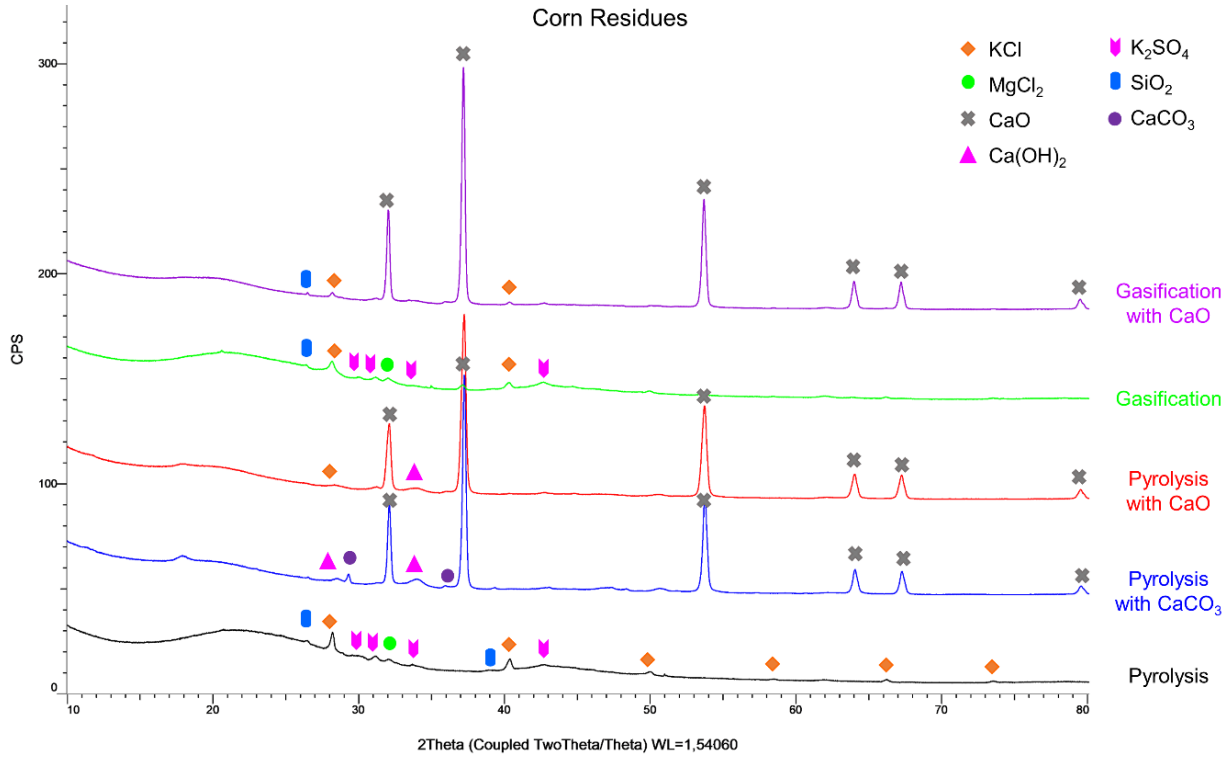
Corn Residues
KCl
K_2SO_4
$MgCl_2$
SiO_2
CaO
$CaCO_3$
$Ca(OH)_2$
Gasification with CaO
Gasification
Pyrolysis with CaO
Pyrolysis with $CaCO_3$
Pyrolysis
CPS
2Theta (Coupled TwoTheta/Theta) WL=1,54060

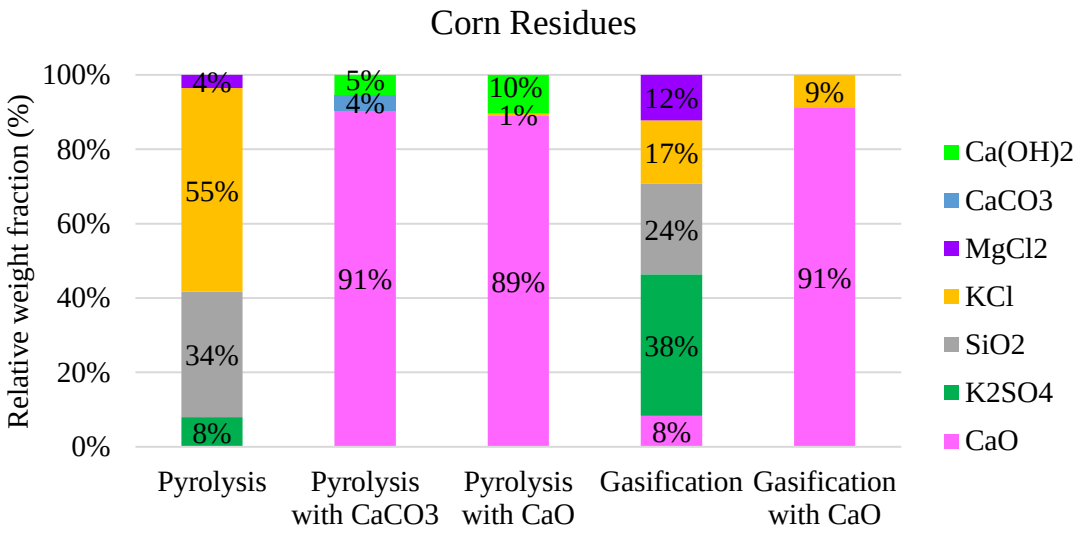
Corn Residues
Relative weight fraction (%)
100%
80%
60%
40%
20%
0%
4%
55%
34%
8%
5%
4%
91%
10%
1%
89%
12%
17%
24%
38%
8%
9%
91%
Pyrolysis
Pyrolysis with CaCO3
Pyrolysis with CaO
Gasification
Gasification with CaO
Ca(OH)2
CaCO3
MgCl2
KCl
SiO2
K2SO4
CaO

(b)

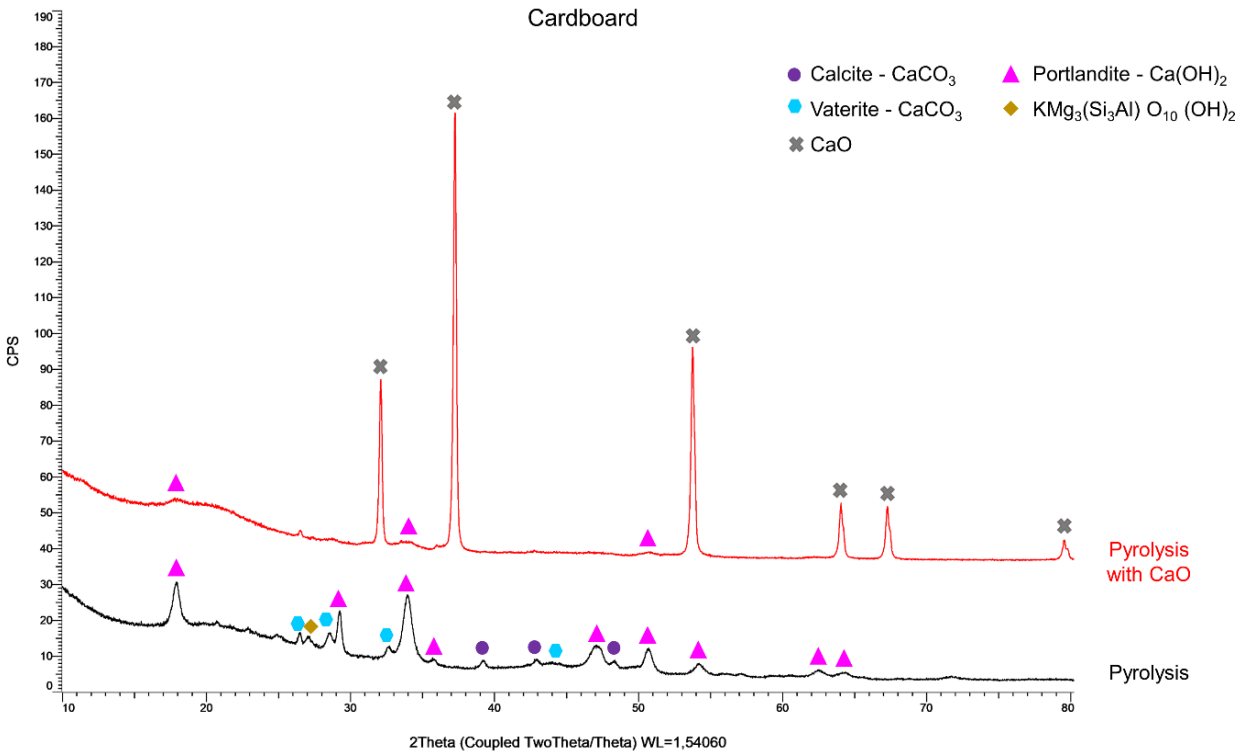
Cardboard
Calcite - CaCO3
Portlandite - Ca(OH)2
Vaterite - CaCO3
KMg3(Si3Al) O10 (OH)2
CaO
CPS
Pyrolysis with CaO
Pyrolysis
2Theta (Coupled TwoTheta/Theta) WL=1,54060

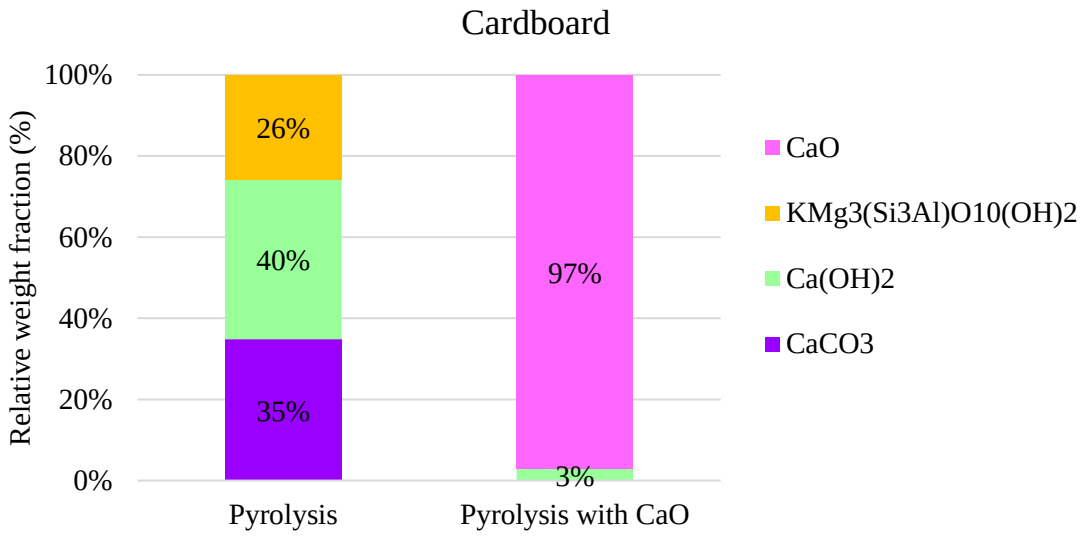
Cardboard
Relative weight fraction (%)
100%
80%
60%
40%
20%
0%
26%
40%
35%
97%
3%
Pyrolysis
Pyrolysis with CaO
CaO
KMg3(Si3Al)O10(OH)2
Ca(OH)2
CaCO3

(c)

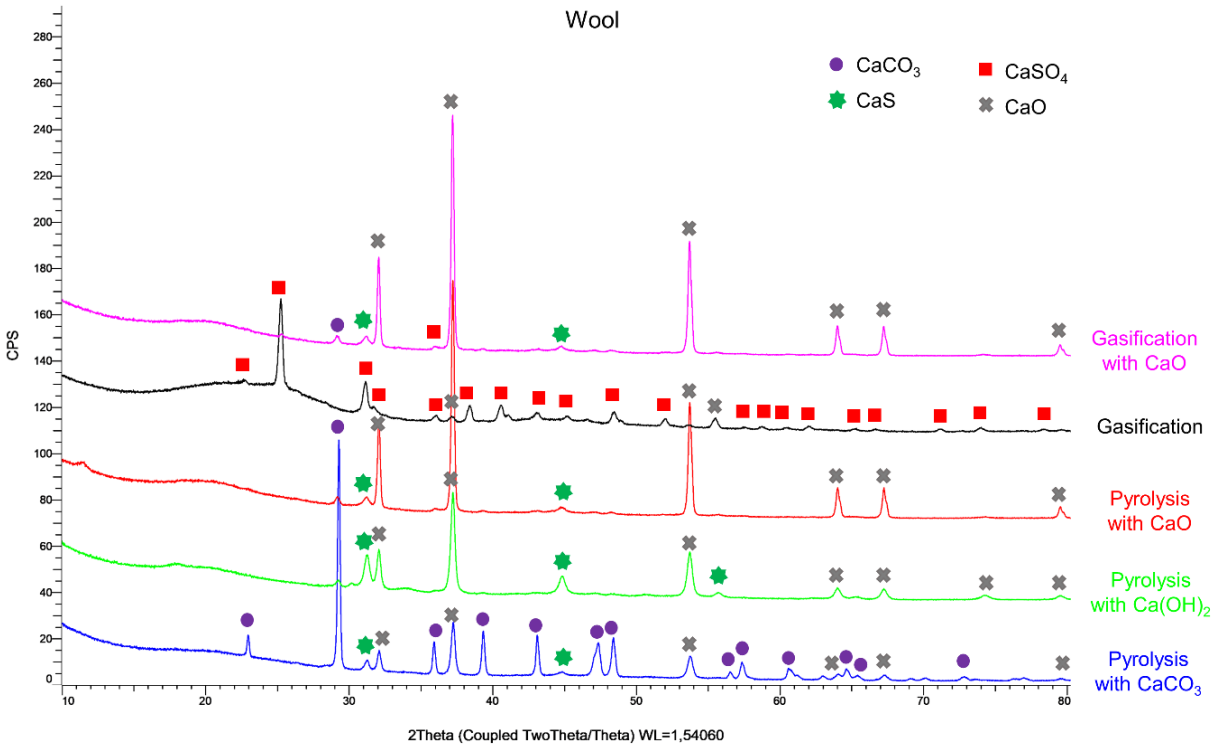
Wool
CaCO3
CaS
CaSO4
CaO
CPS
Gasification with CaO
Gasification
Pyrolysis with CaO
Pyrolysis with Ca(OH)2
Pyrolysis with CaCO3
2Theta (Coupled TwoTheta/Theta) WL=1,54060

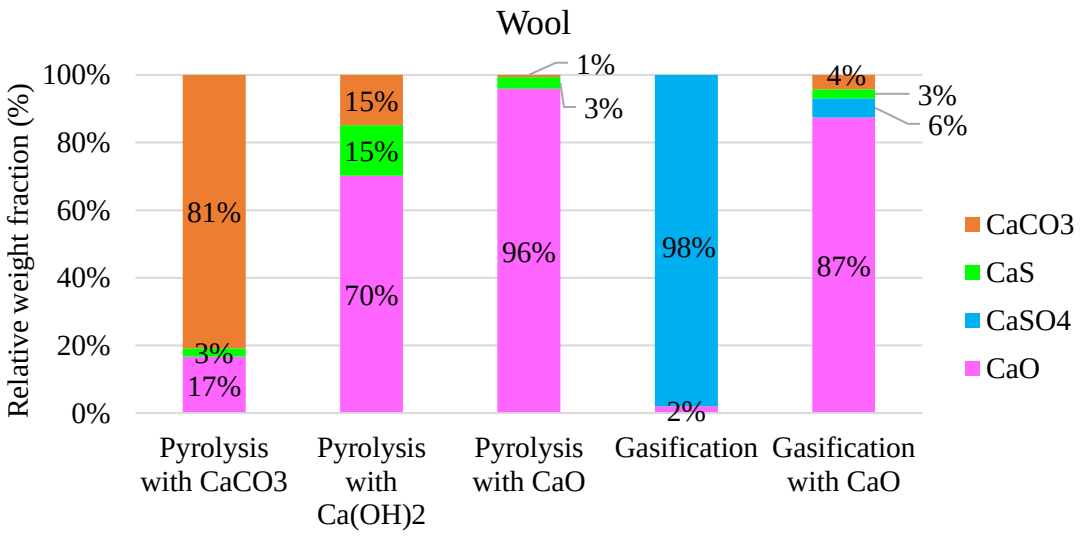
Wool
Relative weight fraction (%)
100%
80%
60%
40%
20%
0%
81%
3%
17%
15%
15%
70%
1%
3%
96%
98%
2%
4%
3%
6%
87%
CaCO3
CaS
CaSO4
CaO
Pyrolysis with CaCO3
Pyrolysis with Ca(OH)2
Pyrolysis with CaO
Gasification
Gasification with CaO

(d)

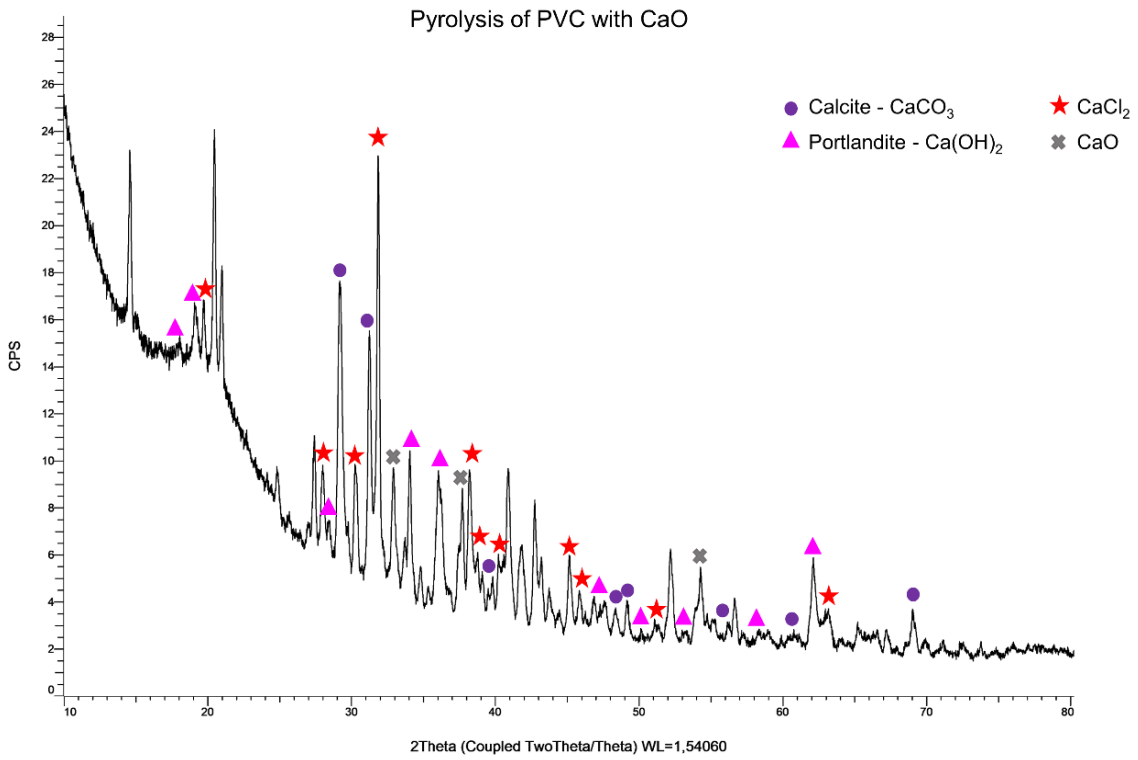

(e)

Figure 35: XRD diffractograms and evolution of the relative composition of the phases estimated by the semi-quantitative analysis of the chars of the feedstocks alone and feedstock-additive mixtures

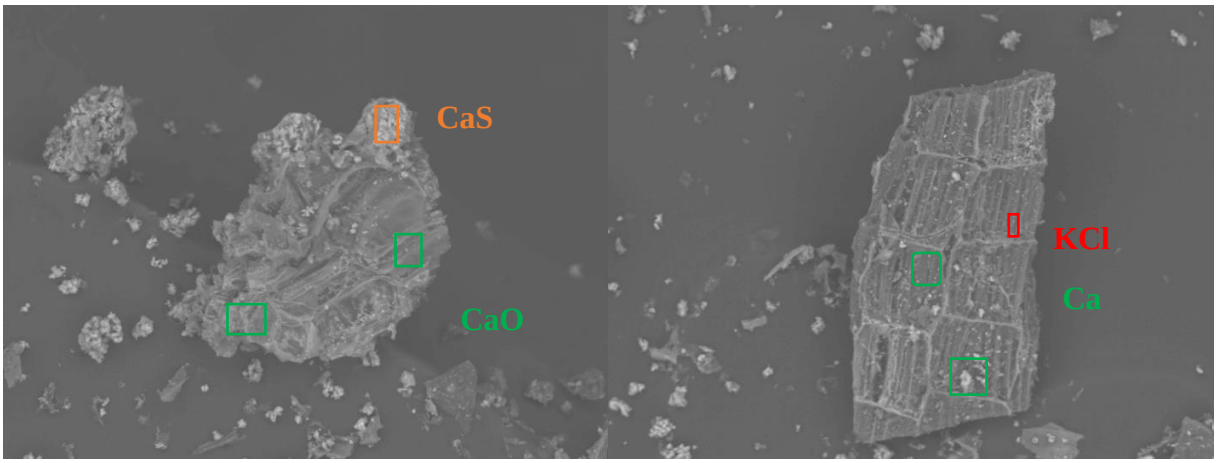

(a)

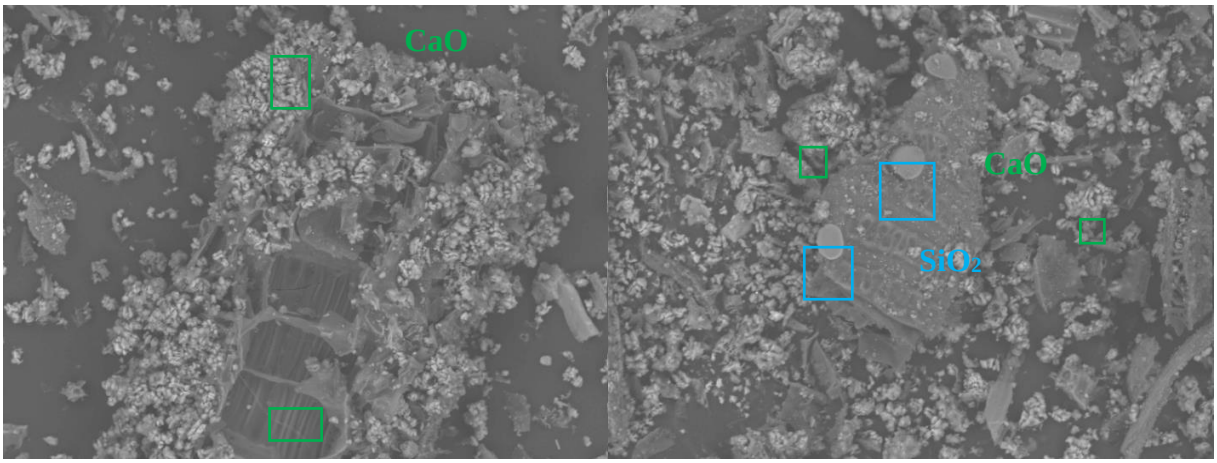

(b)

Figure 36: SEM observations of the chars obtained after pyrolysis at 800°C of the mixtures Colza straw/CaO (a) and Corn–residues/CaO (b)

For the chars obtained from the pyrolysis and gasification of colza straw with CaO **(Figure 35(a))**, the relative weight fractions of CaO logically increase significantly in comparison to the char obtained from colza straw alone, especially for pyrolysis. In addition, we observe peaks corresponding to CaS and C that are also present in the char of colza straw alone.

For the char of corn residues with $CaCO_3$ (**Figure 35(b)**), the main phase observed is CaO with some peaks corresponding to $CaCO_3$ and $Ca(OH)_2$, which shows that $CaCO_3$ decomposes into CaO. For the char obtained from pyrolysis and gasification of corn residues with CaO, in addition to the main component CaO, we observe peaks corresponding to KCl that are already present in the char of corn residues alone. The absence of $MgCl_2$ peaks, that are visible after pyrolysis or gasification without additive, could be due to their potential overlap with CaO peaks due to their similar positions. Moreover, K_2SO_4 is not detected neither in chars with additive.

For the char obtained from the pyrolysis of cardboard with CaO, the main phase observed is CaO with some peaks corresponding to $Ca(OH)_2$ (**Figure 35(c)**). Unlike the char of the pyrolysis of cardboard alone, $CaCO_3$ is not detected.

For wool with $CaCO_3$ (**Figure 35(d)**), peaks corresponding to $CaCO_3$, CaO and CaS are observed. For the cases of wool with CaO or $Ca(OH)_2$, the main phase observed is CaO with peaks corresponding to CaS. In addition, only in the case of the gasification with CaO, we observe peaks corresponding to $CaSO_4$ that is also present in the char of the gasification of wool alone.

In all cases, the addition of CaO induces a high fraction of it among the crystalline phases in the XRD patterns. Indeed, in the different mixtures of resources with additives, the mass of the additive is higher than that of the ash in the initial resource, which can explain the prevalence of the dominant CaO phase observed in the diffraction patterns.

When $CaCO_3$ is used, a part of it can still be detected in the chars, together with CaO, which suggests that part of the $CaCO_3$ is transformed into CaO. When $Ca(OH)_2$ is added, only CaO shows up in the XRD pattern, indicating that $Ca(OH)_2$ likely transforms into CaO.

The SEM observations presented in **Figure 36** as well as those for the other chars that are not presented here show the presence of dispersed CaO particles. Furthermore, in the char of colza straw with CaO, Cl is found in a phase in association with K, which could correspond to KCl, even if KCl is not detected in the XRD analysis. S is found with Ca that could correspond to CaS, which is consistent with the XRD analysis. In the char of corn residues with CaO, we observe grains containing Si and O with quantities that well fit with the composition of SiO_2 while the XRD results do not show the presence of SiO_2 in the char sample. Nevertheless, the detection of SiO_2 by EDX is consistent with its presence in the chars of corn residues without additive. The discrepancies between SEM-EDX and XRD can here again come from difficulties in identifying minor phases by XRD in the chars in which the CaO peaks are predominant and may hide the other phase peaks.

The quantitative analysis of sulfur retention in the chars show some variations of moderate extent rather than significant deviations between the individual feedstocks and the feedstock mixed with the calcium-based additive. The interaction between the calcium-based additive and sulfur may not have been as effective as anticipated. This is supported by the XRD analyses, which do not attest of any strong interaction between the feedstock and additive, with the

absence of new sulfur-containing compounds, or increase in CaS content, in comparison with pyrolysis or gasification without additive.

The mass ratios between the additive and the dried feedstock are 25, 14 and 18 wt. % for $CaCO_3$, CaO and $Ca(OH)_2$ respectively, and the total molar ratios Ca/S in the feedstock-additive mixtures are much higher than 1, which shows that calcium is in excess relatively to sulfur for the formation of CaS. Therefore, the interpretation, suggesting that the concentration of the calcium-based additive used in the mixtures is not sufficient to cause a noticeable improvement in sulfur retention, can be excluded.

In literature, the studies highlighting improved gas desulfurization through the incorporation of calcium-based additives have mostly been conducted in fluidized bed setups (Pinto et al., 2014a; Recari et al., 2016a; Schmid et al., 2018; Schweitzer et al., 2018). In contrast, similarly to our results, a minimal impact of CaO and $Ca(OH)_2$ additives was observed during wheat straw pyrolysis within a batch reactor (Khalil et al., 2008). This shows that fluidized beds might provide better mixing compared to fixed bed setups, which could potentially contribute to the efficiency of these additives. Despite our efforts to ensure uniform distribution of the additive throughout the sample, achieving an optimal contact between the additives and the resources might necessitate additional considerations. This perspective could provide further insight into the limited effectiveness of the additives as observed in our results.

Moreover, upon a closer examination of the sulfur retention values across the various resource-additive mixtures and their comparison with the initial inorganic sulfur content of the resources shown in **Figure 6**, the sulfur retention values often approach the levels of inorganic sulfur content, with only marginal exceptions for cardboard. As highlighted in **Chapter 3**, organic forms of sulfur are released at relatively low temperatures, below 550°C. At these temperature levels, the expected reactions between the calcium-based additives and H_2S may not occur effectively. Although we could not find specific details about the most effective temperature for these reactions in the literature, it is important to highlight that many studies have primarily focused on experiments conducted between 760 and 850°C. By the time the desired operational temperature is attained in the sample, the major part of the organic sulfur has already been released into the gas phase. Consequently, the attainable maximum sulfur retention becomes constrained, aligning closely with the levels of inorganic sulfur content.

For chlorine, the XRD analysis and SEM observations revealed the presence of chlorine-containing compounds in some cases that could explain the increase in the chlorine retention obtained. KCl is detected in the char of the gasification of corn residues with CaO and in the

char of the pyrolysis of colza straw with CaO. Moreover, for the mixture PVC-CaO, the XRD diffractogram reveals the presence of calcium chloride $CaCl_2$.

Our quantitative results show significant improvements in chlorine retention when CaO is added to the agricultural residues and PVC during pyrolysis at 800°C, but to a lesser extent during gasification at 800°C. On the other hand, previous studies have shown the effectiveness of calcium-based additives in reducing HCl emissions during gasification and pyrolysis (Cho et al., 2015; Recari et al., 2016a). These additives were shown to lower HCl emissions by undergoing a gas-to-solid reaction, forming calcium chloride.

This reaction supports the observed improvements in chlorine retention when CaO is added to PVC, for which $CaCl_2$ is detected. However, in the case of agricultural residues, as shown in Chapter 3, the released chlorine is not only in the form of HCl, but also KCl. It is possible that the chlorine is retained in other forms that are not detected by the XRD or SEM techniques used in the study. Additional analytical methods or characterization techniques would be needed to elucidate the exact mechanism of chlorine retention in these mixtures.

4.2. Co-pyrolysis and co-gasification of resources

With the same objective of enhancing interactions between inorganic elements to increase the retention of S and Cl in the solid residue, pyrolysis and gasification experiments were carried out on different mixtures of resources. All these experiments were performed at 800°C with a holding time of 20 min. The experimental conditions are detailed in **section 2.2.4.3**. Cardboard, colza straw and oak bark, because of their high calcium content, were chosen to be mixed with other resources (wool, colza straw, corn residues, PVC). The results are presented in separate sections for each of these feedstocks.

To evaluate the influence of mixing resources on the S and Cl retention in the char, we compare the obtained experimental results with the theoretical ones.

These are calculated with the retention fractions obtained experimentally in pyrolysis or gasification tests for each individual resource R1 and R2 with an assumption of no interaction between the resources:

$$Theoretical\ retention_i = \frac{(retention_{i-R1} \times m_{i-R1}) + (retention_{i-R2} \times m_{i-R2})}{m_{i-(R1+R2)}} \quad [4.1]$$

where $retention_{i\text{-}R1}$ and $retention_{i\text{-}R2}$ represent the retention fractions of *i* (S or Cl) obtained from the experiments for resources R1 and R2, $m_{i\text{-}R1}$ and $m_{i\text{-}R2}$ correspond to the masses of *i* (S or Cl) in each individual resource R1 and R2, and $m_{i\text{-}(R1+R2)}$ represents the total mass of i (S or Cl) in the (R1 - R2) mixture.

Oak bark was not subjected to pyrolysis nor gasification alone. For the determination of the theoretical values with oak bark, we assume that 0 or 100% of the sulfur or chlorine is retained in the char in order to compare the experimental retention results to the lowest or highest theoretically reachable ones.

4.2.1. Mixture of Wool with calcium-rich resources

Figure 37 shows the theoretical and experimental sulfur retention in the chars of the mixtures Colza Straw + Wool, Cardboard + Wool and Oak Bark + Wool as a function of the fraction of wool in the mixtures. The calcium content in the mixture is plotted and shown on the right hand side axis, in order to investigate its possible influence on sulfur retention.

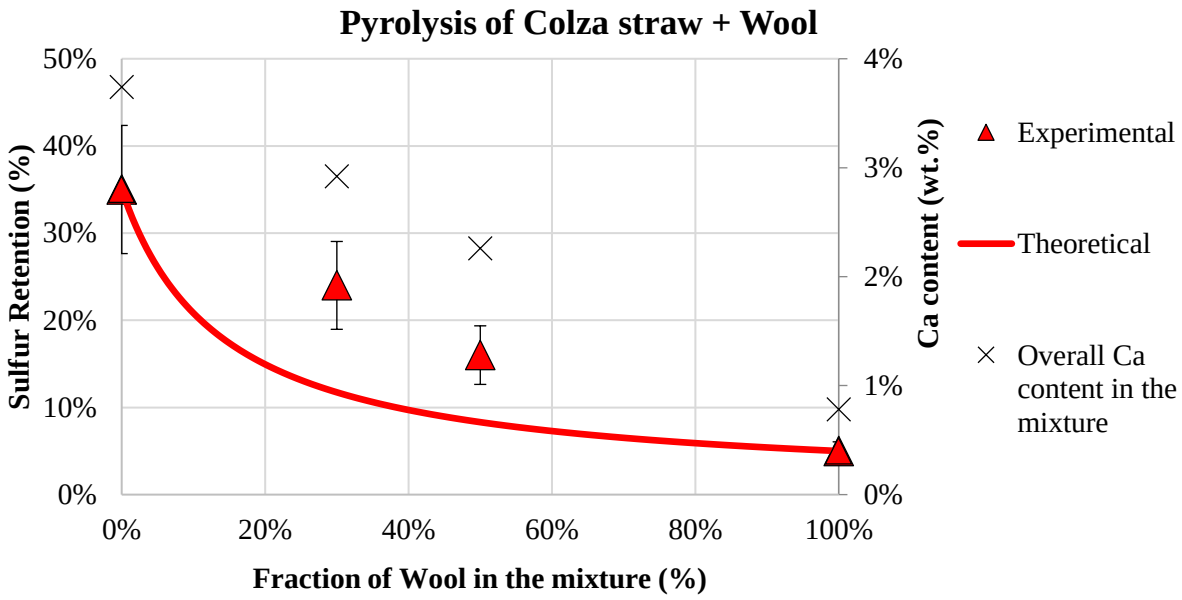

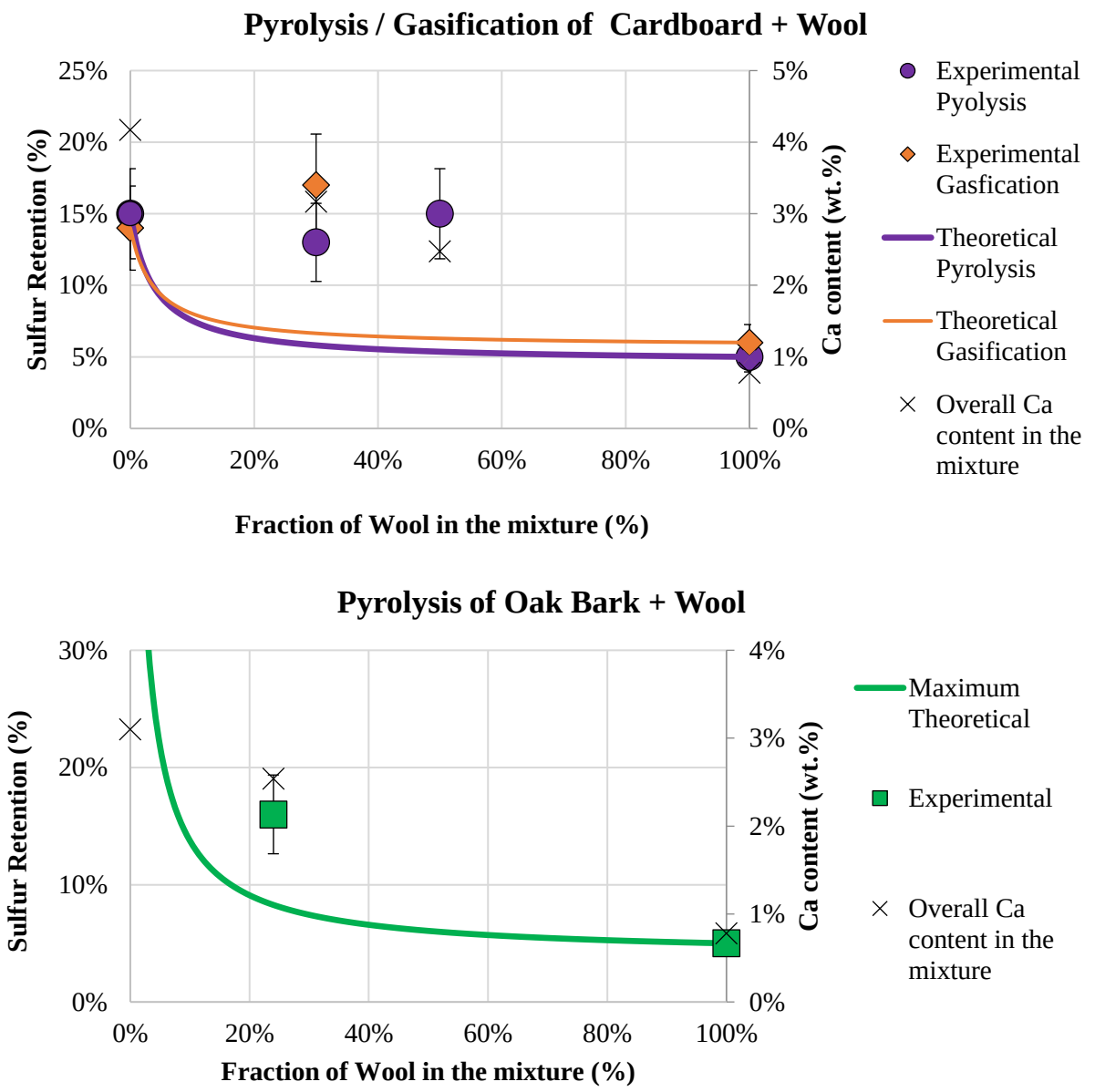

Figure 37: Theoretical and experimental sulfur retention in the chars of the mixtures Colza Straw + Wool, Cardboard + Wool and Oak Bark + Wool, and calcium content in the mixtures, as a function of the fraction of wool

35% and 15% of the initial sulfur content is retained in the char of colza straw and cardboard respectively after pyrolysis experiments. As already presented in **Chapter 3**, when wool is pyrolyzed alone, only 5% of the initial sulfur content is retained in the char. However, when wool is co-pyrolyzed with any of the calcium-rich resources (cardboard, colza straw or oak bark) in a 70/30 wt. % or 50/50 wt. % mixture, the fraction of sulfur retained in the char significantly increases to at least 16%.

The result obtained from the co-gasification experiment of cardboard with wool is comparable to the one obtained in the co-pyrolysis experiment, and this similarity is consistent with the individual pyrolysis and gasification experiments for each resource presented in **Chapter 3**.
The sulfur retention values for all the mixtures are twice as much the theoretical values, that assume no interaction between the resources, which demonstrates a clear interaction between the two resources in the mixture. These results highlight the positive impact of incorporating these calcium-rich resources to wool for its pyrolysis or gasification.
It is normal that as the fraction of wool in the mixtures increases, the overall calcium content decreases, since wool has a lower calcium content compared to the calcium-rich resources. In the case of the mixture of wool with colza straw, there might exist a linear relationship between sulfur retention and calcium content. However, this correlation is not evident in the case of the mixture of wool with cardboard, as the sulfur retention then remains at 13-15%, similarly to cardboard alone.

The XRD and SEM-EDX analyses were conducted to further investigate the characteristics of the chars and explore potential interactions between wool and the calcium-rich components (cardboard, colza straw, and oak bark) used in the mixture. **Figure 38** shows the diffractograms of the chars of the individual resources (cardboard and colza straw,) alongside those of the mixtures obtained from the co-pyrolysis experiments. The char from wool pyrolysis shows no clear mineral phases, therefore its XRD diffractogram is not presented. The XRD diffractogram for oak bark is not included in the figure since it was not pyrolyzed alone. **Figure 39** shows the SEM observations of the char obtained from co-pyrolysis at 800°C of the mixture containing 70 wt. % of cardboard and 30 wt. % of wool.

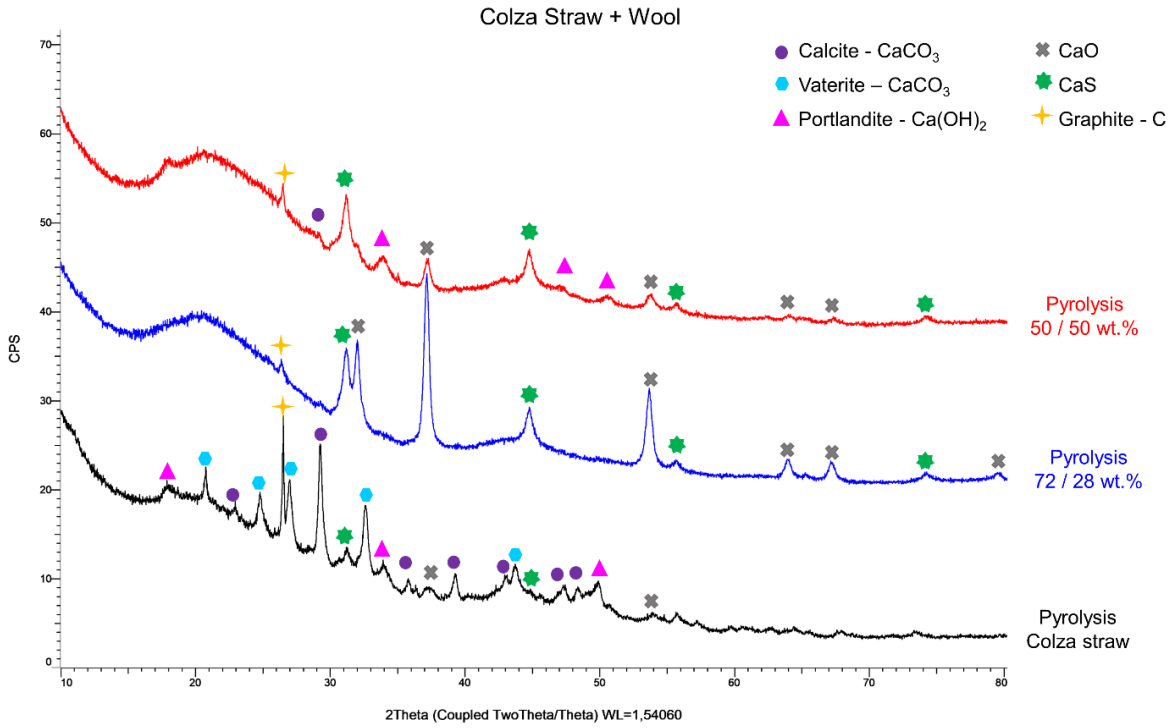
Colza Straw + Wool
Calcite - CaCO3
Vaterite – CaCO3
Portlandite - Ca(OH)2
CaO
CaS
Graphite - C
Pyrolysis 50 / 50 wt.%
Pyrolysis 72 / 28 wt.%
Pyrolysis Colza straw
CPS
2Theta (Coupled TwoTheta/Theta) WL=1,54060

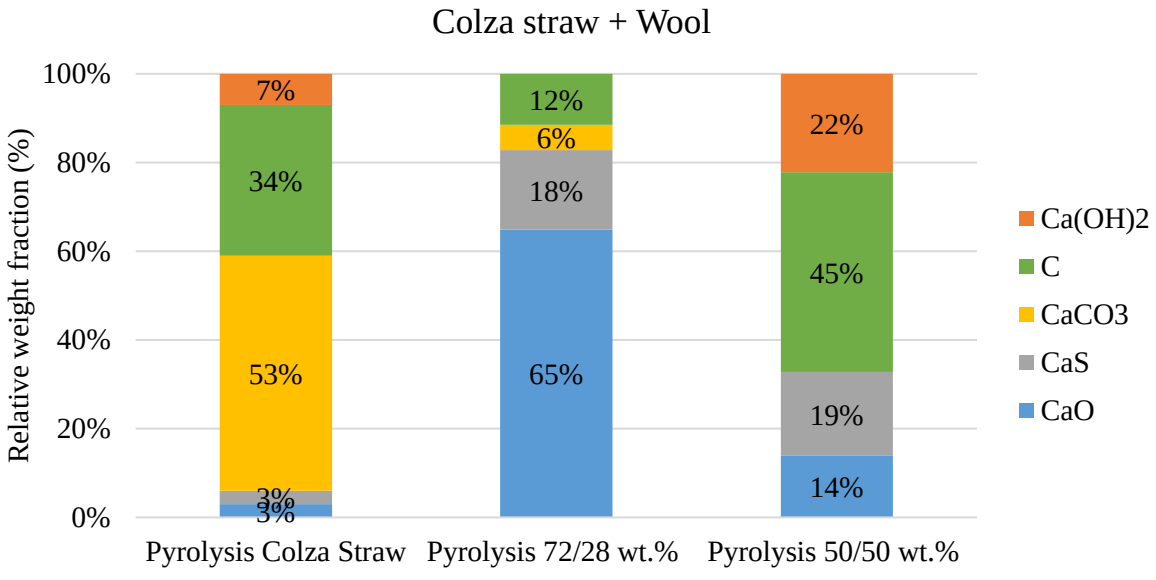
Colza straw + Wool
Relative weight fraction (%)
100%
80%
60%
40%
20%
0%
7%
34%
53%
3%
12%
6%
18%
65%
22%
45%
19%
14%
Pyrolysis Colza Straw
Pyrolysis 72/28 wt.%
Pyrolysis 50/50 wt.%
Ca(OH)2
C
CaCO3
CaS
CaO

(a)

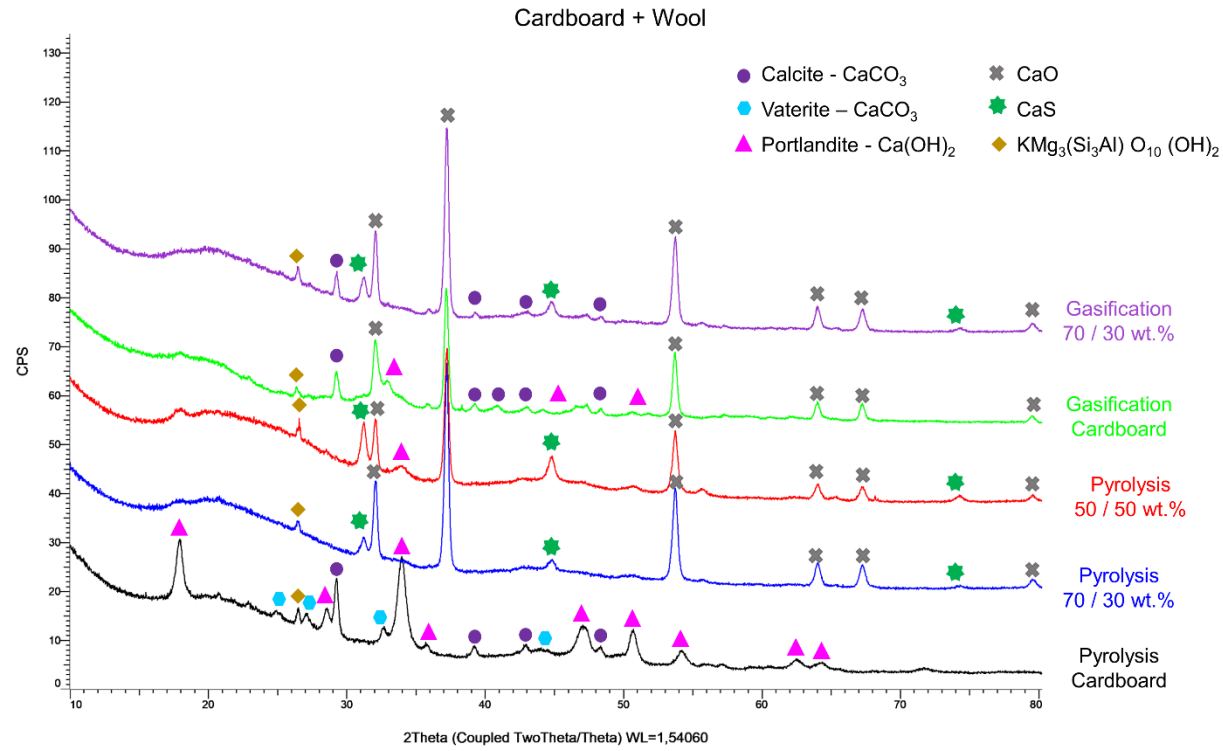
Cardboard + Wool
Calcite - CaCO3
Vaterite – CaCO3
Portlandite - Ca(OH)2
CaO
CaS
KMg3(Si3Al) O10 (OH)2
Gasification 70 / 30 wt.%
Gasification Cardboard
Pyrolysis 50 / 50 wt.%
Pyrolysis 70 / 30 wt.%
Pyrolysis Cardboard
CPS
2Theta (Coupled TwoTheta/Theta) WL=1,54060

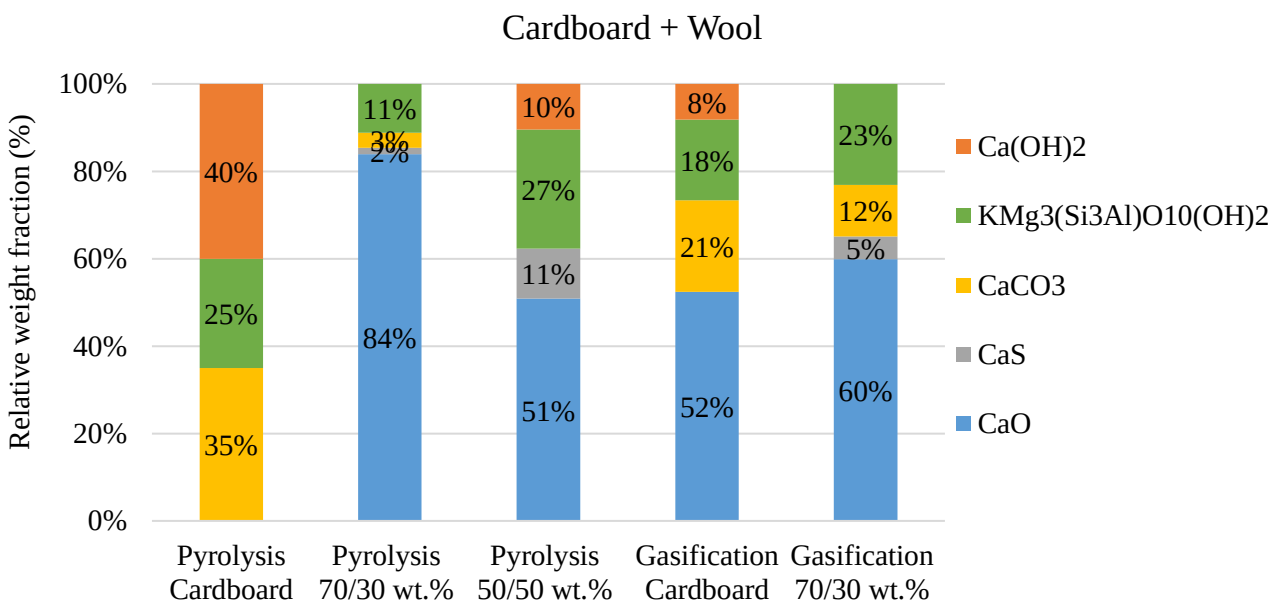
Cardboard + Wool
Relative weight fraction (%)
100%
80%
60%
40%
20%
0%
40%
25%
35%
11%
3%
2%
84%
10%
27%
11%
51%
8%
18%
21%
52%
23%
12%
5%
60%
Pyrolysis Cardboard
Pyrolysis 70/30 wt.%
Pyrolysis 50/50 wt.%
Gasification Cardboard
Gasification 70/30 wt.%
Ca(OH)2
KMg3(Si3Al)O10(OH)2
CaCO3
CaS
CaO

(b)

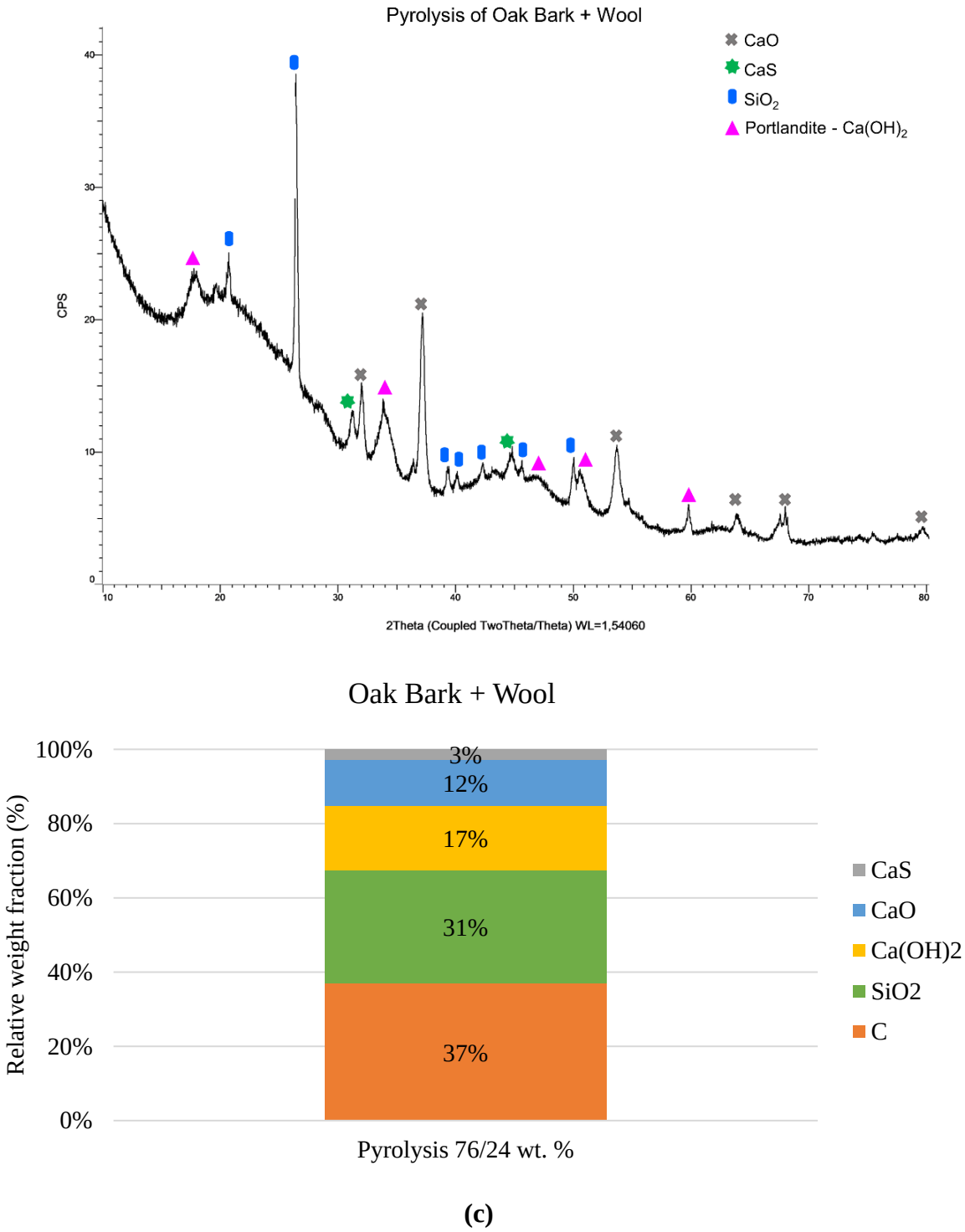

(c)

Figure 38: XRD diffractograms of the chars of the individual resources and the mixtures of wool with colza straw (a), cardboard (b) and oak bark (c) obtained from pyrolysis or gasification at 800°C

Figure 39: SEM observations of the char from co-pyrolysis at 800°C of 70/30 wt. % Cardboard + Wool mixture

For the mixtures of wool with colza straw (**Figure 38 (a)**), the relative weight fractions of CaO and CaS phases significantly increase compared to the char of colza straw alone according to the semi-quantitative analysis. Similar to the diffractogram of colza straw alone, peaks corresponding to C, $CaCO_3$ and $Ca(OH)_2$ are also present.

The XRD analysis of the chars obtained from the mixtures of wool with cardboard (**Figure 38 (b)**) reveals the presence of new peaks, which are not detected in the cardboard char, corresponding to calcium oxide (CaO) and calcium sulfide (CaS). In addition, peaks corresponding to $Ca(OH)_2$, $CaCO_3$ and $KMg_3(Si_3Al)O_{10}(OH)_2$ that originate from cardboard, are identified for mixtures. The SEM observations shows the presence of SiO_2, which is not detected in XRD but can be linked to the relatively high content of Si in cardboard (2.0 wt%, Table 2.1). SEM-EDX observations further confirm the presence of CaO and CaS detected in the XRD analysis in the chars of the mixtures with cardboard (**Figure 39**).

In the mixture of wool with oak bark (**Figure 38(c)**), in addition to the peaks corresponding to CaO and CaS, peaks corresponding to SiO_2 and $Ca(OH)_2$ are also present likely originating from oak bark.

These observations show that sulfur seems to be retained in the char primarily in the form of CaS. The calcium in the mixture mainly originates from the Ca-rich resource, while the sulfur predominantly originates from the wool, which suggests that sulfur in the mixtures undergoes a reaction with calcium, resulting in the formation of calcium sulfide, which could be the cause of enhancement of sulfur retention obtained in the quantitative results.

Moreover, an intriguing finding is the relatively high abundance of CaO in the mixtures, despite their low content in cardboard or colza straw alone. These results could suggest that the co-

pyrolysis or co-gasification of wool with the calcium-rich resources leads to potential interactions between the components, resulting in the appearance of new phases or modifications in phase compositions.

4.2.2. Mixture of colza straw with calcium-rich resources

Figure 40 shows the sulfur retention in the chars of the mixtures of colza straw with cardboard and oak bark. Similarly, to the previous figures, the Ca content of the mixtures is also represented.

Colza straw contains 3.7 wt% of calcium, making it a Ca-rich resource. The focus here shifts from examining the interaction between a calcium-poor and calcium-rich resource, as seen in the preceding section, to exploring potential interactions between different Ca-rich resources. In the case of colza straw and cardboard mixtures, it is important to note that the cardboard, used as an additive, exhibits a lower sulfur retention compared to colza straw. Additionally, both resources, colza straw and cardboard, have high calcium content, and consequently, the overall calcium content in the mixtures is constant at around 4 wt. %. In the case of colza straw and oak bark mixture, the calcium content in colza straw is a bit higher than in oak bark, and the overall calcium content in the mixture is 3 wt. %.

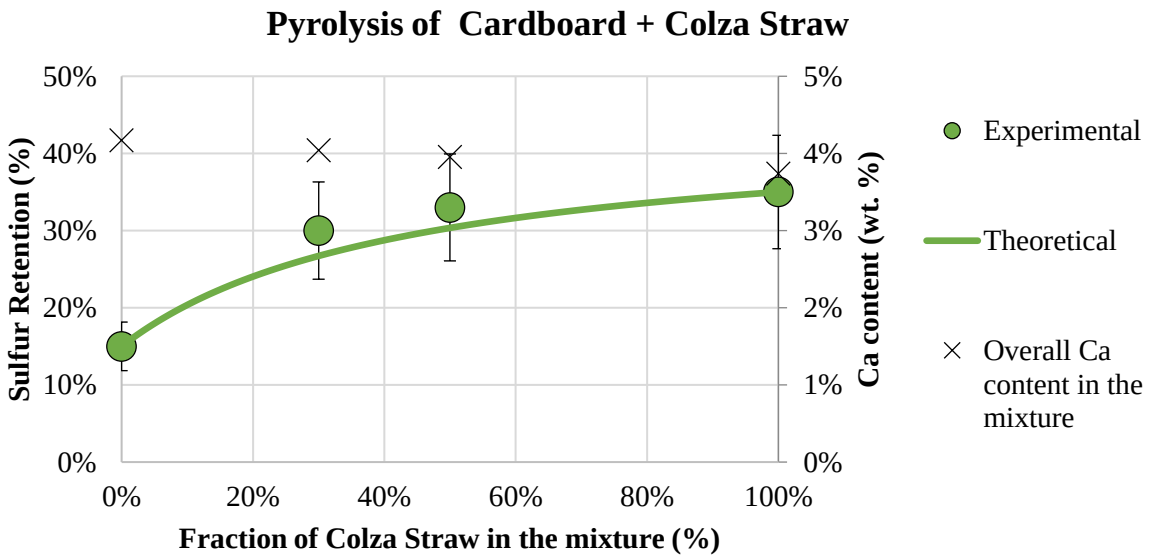

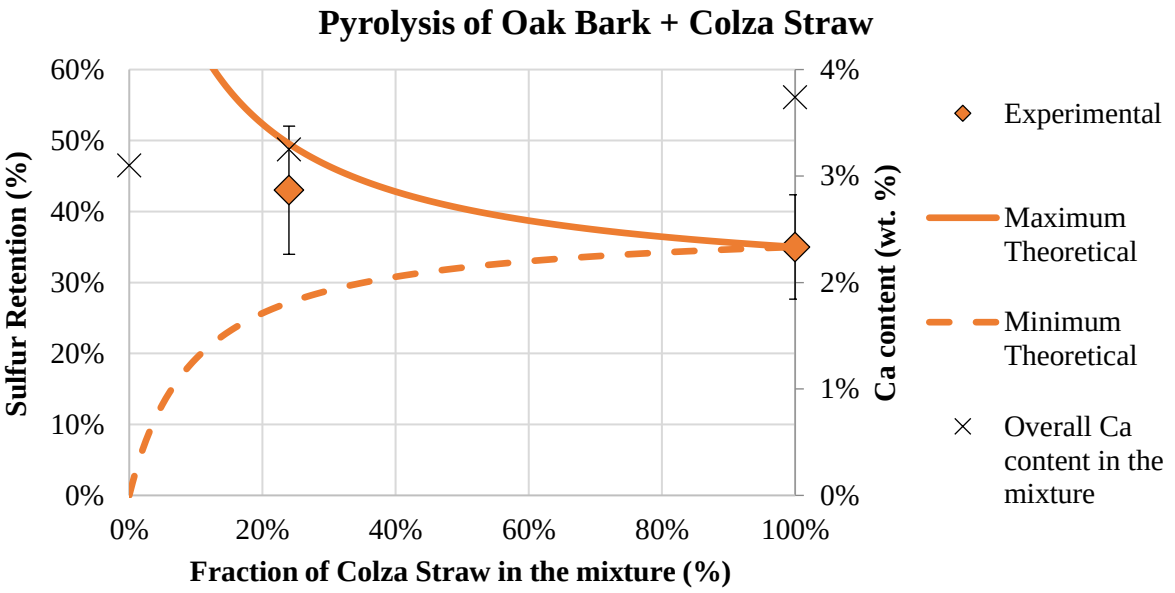

Figure 40: Theoretical and experimental sulfur retention in the chars of the mixtures Cardboard + Colza Straw and Oak Bark + Colza Straw, and calcium content in the mixtures, as a function of the fraction of colza straw

In both mixtures, the experimental sulfur retention values are close to the theoretical values. This indicates that there does not seem to be any interaction between the resources that would lead to a modification of the sulfur retention capacity of the chars.

While in the case of wool we focused only on the sulfur evolution, in these co-pyrolysis tests we also investigate the chlorine retention in the mixtures. **Figure 41** compares the experimental and theoretical chlorine retention in the chars of the mixtures of colza straw with cardboard and oak bark.

The graphs reveal interesting insights into the behavior of chlorine retention. Unlike sulfur, the chlorine retention values in the mixtures of colza straw with cardboard obtained experimentally are twice as much as the theoretical values. This suggests that there is a synergistic interaction between the cardboard and colza straw contributing to the increased chlorine retention observed in the chars. However, for the mixture of colza straw with oak bark, the retention obtained experimentally is comprised between the minimum and maximum theoretical values, assuming 0% and 100% chlorine retention in oak bark respectively, which do not allow providing any conclusion on interaction between aok bark and colza straw. More experimental investigations is needed to determine the Cl retention of oak bark alone and subsequently evaluate its effect when combined with colza straw in terms of chlorine retention. Anyway, even if an interaction

occurs between the two mixed resources, it is not as efficient as in the case of the cardboard-colza straw mixture, which presents a 100% chlorine retention.

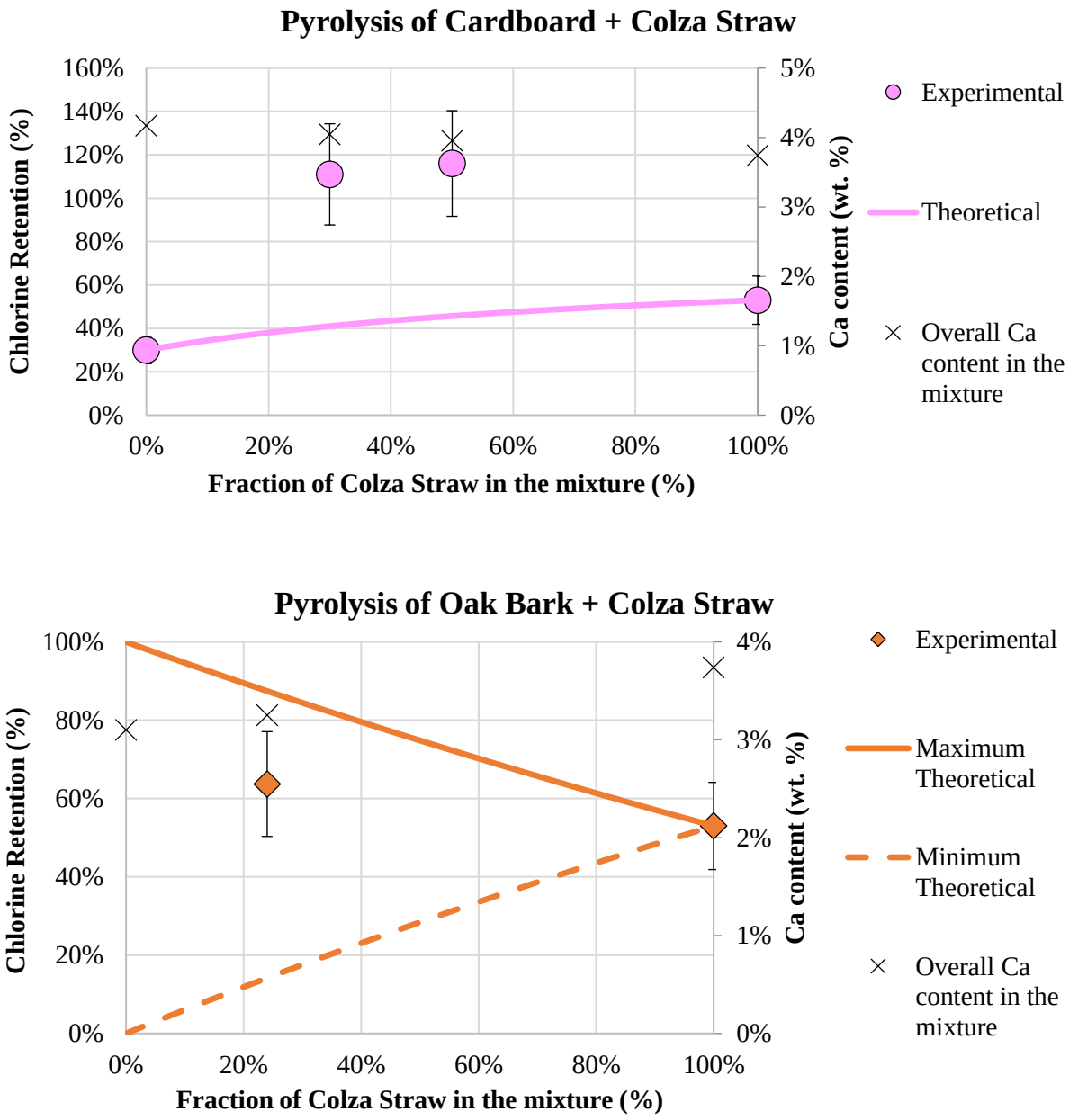

Figure 41: Theoretical and experimental chlorine retention in the chars of the mixtures Cardboard + Colza Straw and Oak Bark + Colza Straw, and calcium content in the mixtures, as a function of the fraction of colza straw

Figure 42 shows the XRD diffractograms of the chars of the individual resources and the mixtures of colza straw with cardboard and oak bark as well as the semi-quantitative results. **Figure 43** presents SEM observations of the chars of 50/50 wt. % Cardboard + Colza straw mixture.

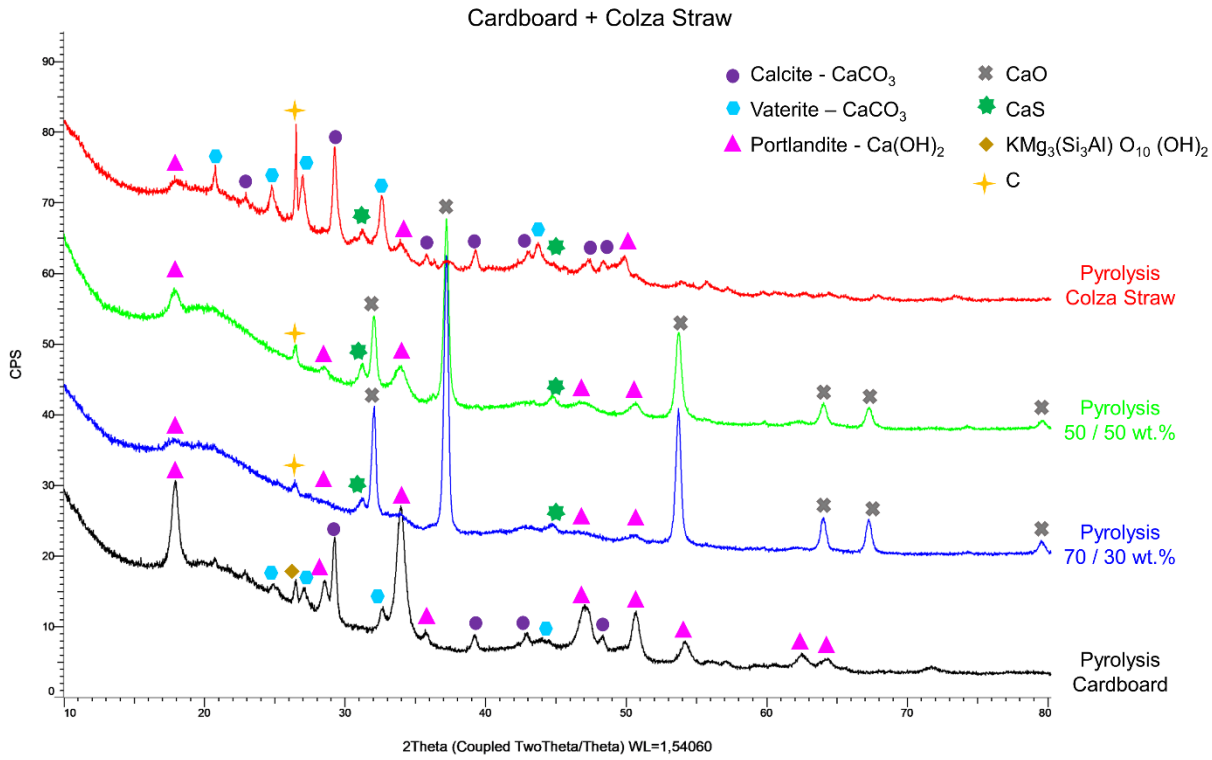
Cardboard + Colza Straw
Calcite - CaCO3
Vaterite – CaCO3
Portlandite - Ca(OH)2
CaO
CaS
KMg3(Si3Al) O10 (OH)2
C
Pyrolysis Colza Straw
Pyrolysis 50 / 50 wt.%
Pyrolysis 70 / 30 wt.%
Pyrolysis Cardboard
CPS
2Theta (Coupled TwoTheta/Theta) WL=1,54060

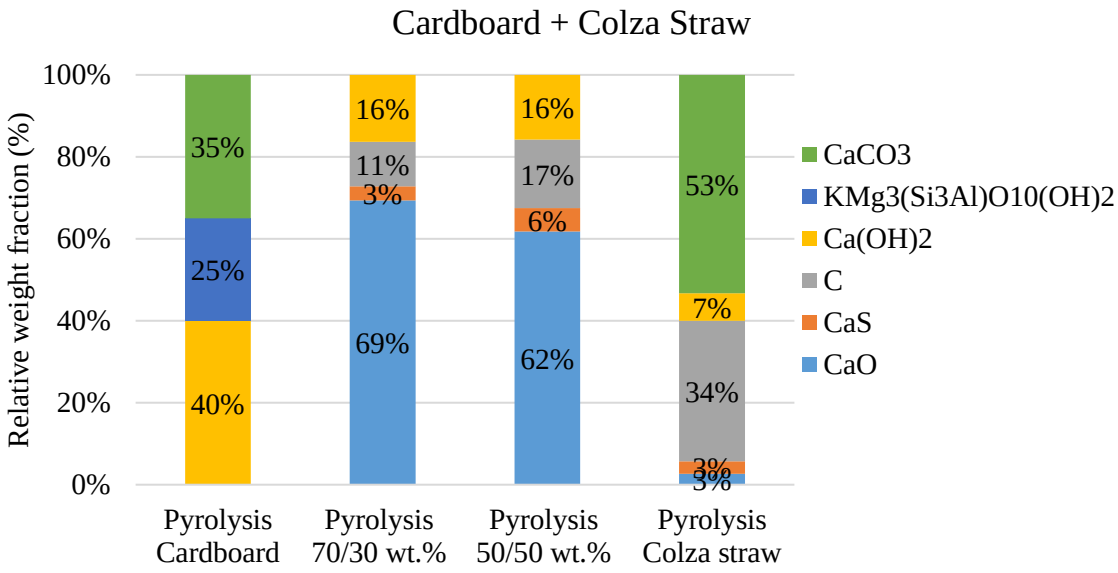
Cardboard + Colza Straw
Relative weight fraction (%)
100%
80%
60%
40%
20%
0%
35%
25%
40%
16%
11%
3%
69%
16%
17%
6%
62%
53%
7%
34%
3%
3%
CaCO3
KMg3(Si3Al)O10(OH)2
Ca(OH)2
C
CaS
CaO
Pyrolysis Cardboard
Pyrolysis 70/30 wt.%
Pyrolysis 50/50 wt.%
Pyrolysis Colza straw

(a)

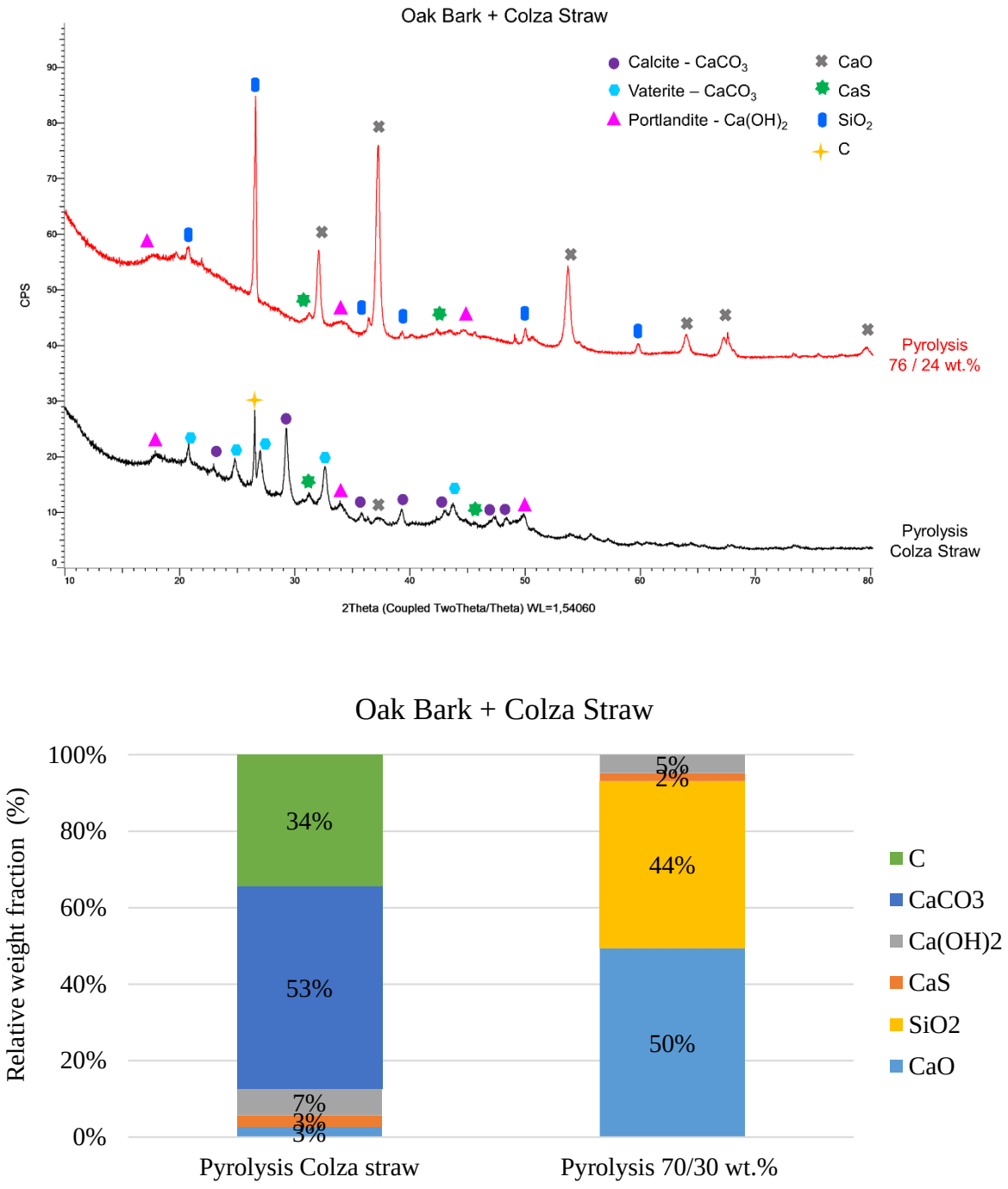

(b)

Figure 42: XRD diffractograms of the chars of the individual resources and the mixtures of colza straw with cardboard (a) and oak bark (b) obtained from pyrolysis at 800°C

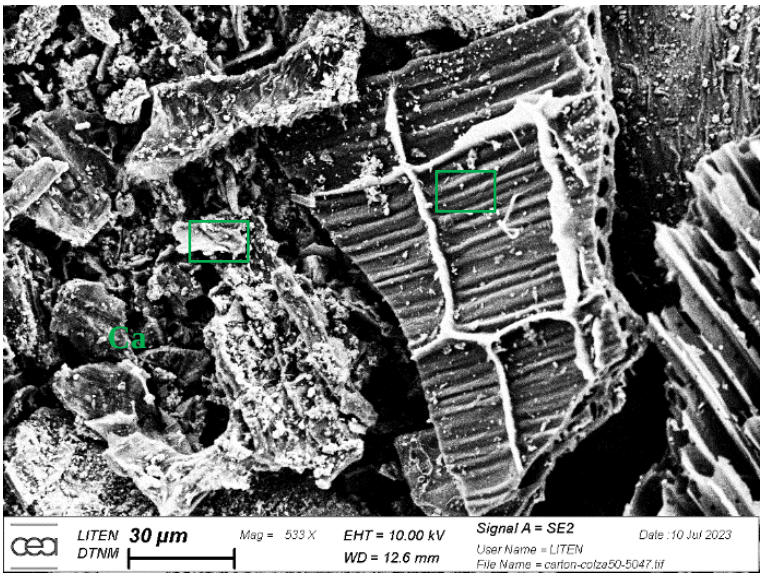

Figure 43: SEM observations of the char from co-pyrolysis at 800°C of 50/50 wt.% Cardboard + Colza straw mixture

Upon analyzing the diffractograms of the mixtures of colza straw with cardboard (**Figure 42(a)**), the main phase observed in the char is identified as CaO. The only sulfur-containing compound detected in the char of this mixture is CaS, which is already present in the individual char of colza straw. In the char of the mixture of colza straw with oak bark (**Figure 42 (b)**), additional peaks of SiO_2 are identified, likely originating from the oak bark component. There is more CaO in the mixtures than what would be expected from just cardboard or colza straw alone.

None of the diffractograms of the mixtures exhibit peaks corresponding to chlorine-containing compounds that could account for the observed increase in chlorine retention as shown in the quantitative results.

The SEM observations (**Figure 43**) show phases corresponding to CaO but do not reveal any distinct phases corresponding to sulfur or chlorine-containing species in the mixtures. On the other hand, they provide insights into the morphology of the chars. They confirm the presence of the fibrous morphology of the agricultural residues consisting of elongated and interconnected fibers and a particle-like or chunky morphology of cardboard.

The absence of specific peaks or regions indicating the presence of sulfur or chlorine compounds suggests that these elements might not form separate, identifiable phases within the char structure that are easily detected by the XRD or SEM-EDX analysis. It is important to consider that these techniques provide valuable information on the mineral phases present in

the chars but may not capture certain chemical species or compounds in lower concentrations or amorphous nature.

Considering the possibility of a synergistic interaction between the components in the mixtures leading to enhanced chlorine retention, it is plausible that the phenomenon is related to the formation of distinct chlorine-containing phases. However, additional techniques capable of providing detailed insights are required to further characterize and confirm these phases.

4.2.3. Mixture of corn residues with cardboard

Cardboard can be considered here as a calcium-rich resource compared to corn residues. **Figure 44** shows the sulfur and chlorine retention in the char of the mixture of corn residues with cardboard, together with the Ca content in each feedstock.

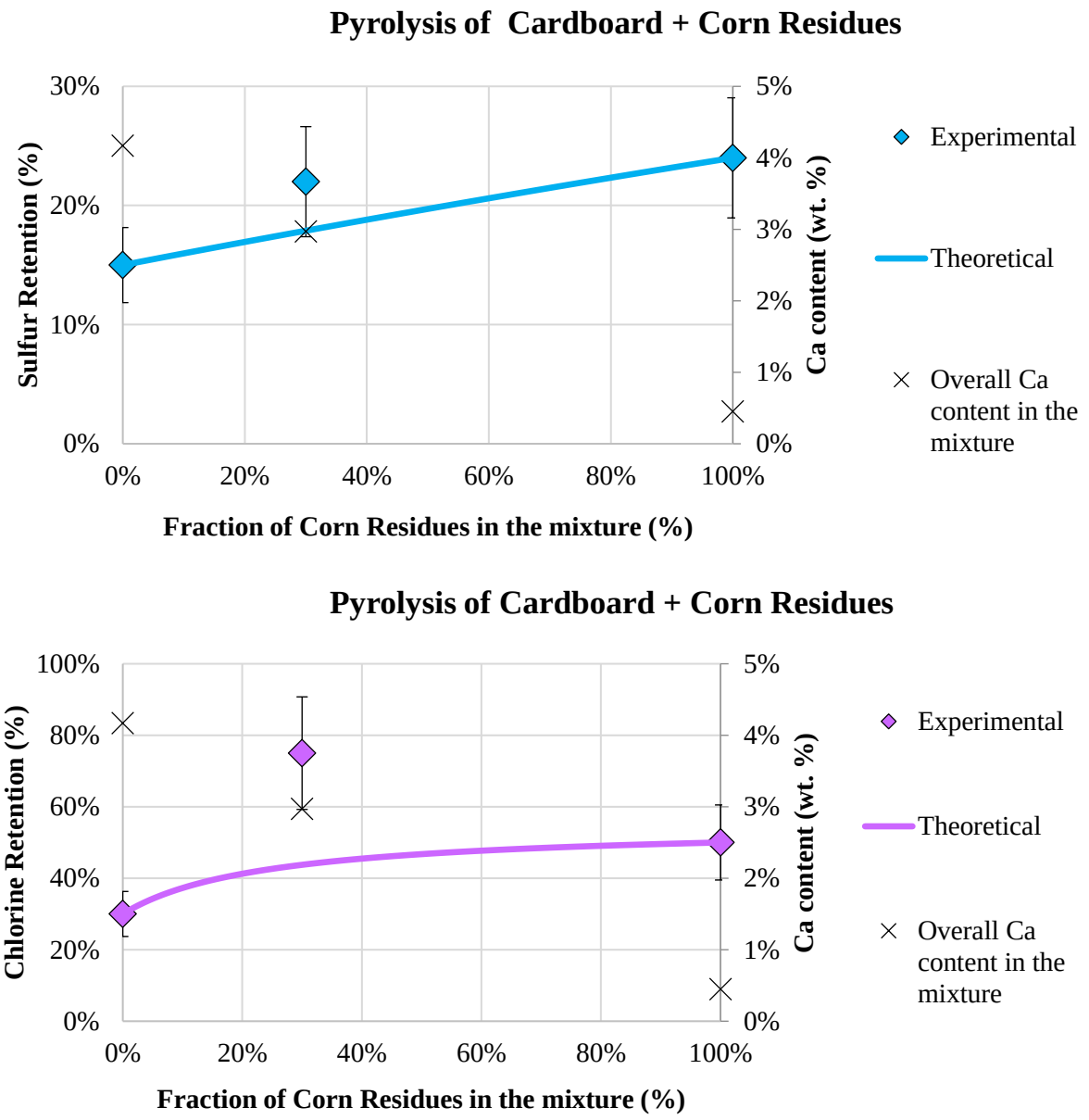

Figure 44: Theoretical and experimental sulfur and chlorine retention in the char of the mixture Cardboard + Corn Residues, and calcium content in the mixture, as a function of the fraction of corn residues

The mixture of corn residues with cardboard yields a higher overall calcium content compared to corn residues alone. Despite this elevated calcium presence, by considering the uncertainty, the sulfur retention for the mixture do not show a significant improvement compared to the theoretical value.

In contrast, the experimental chlorine retention is twice as much as the theoretical value, which suggests a synergistic interaction between corn residues and cardboard contributing to the increased chlorine retention.

The enhancement of chlorine retention obtained in the mixture of corn residues with cardboard is similar to the one obtained in the mixtures of colza straw with cardboard also.

Figure 45 shows the XRD diffractograms of the char of the individual resources and the mixture of corn residues with cardboard as well as the semi-quantitative results. **Figure 46** presents the SEM observations of the char of 70/30 wt. % Cardboard + Corn residues mixture. The XRD analysis shows that the char main phase is CaO and a silicate with the formula $KMg_3(Si_3Al)O_{10}(OH)_2$, which originates from cardboard. The SEM observations (**Figure 46**) show phases containing Ca and O with quantities that well fit with the composition CaO and Si and O with the composition of SiO_2.

The absence of well-defined peaks in the XRD analysis or phases in the SEM-EDX results indicating the presence of specific chlorine compounds, which could potentially explain the increased chlorine retention in the char of the mixture, suggests that chlorine may not exist in identifiable phases within the char structure, that are detectable through XRD or SEM-EDX analysis.

.

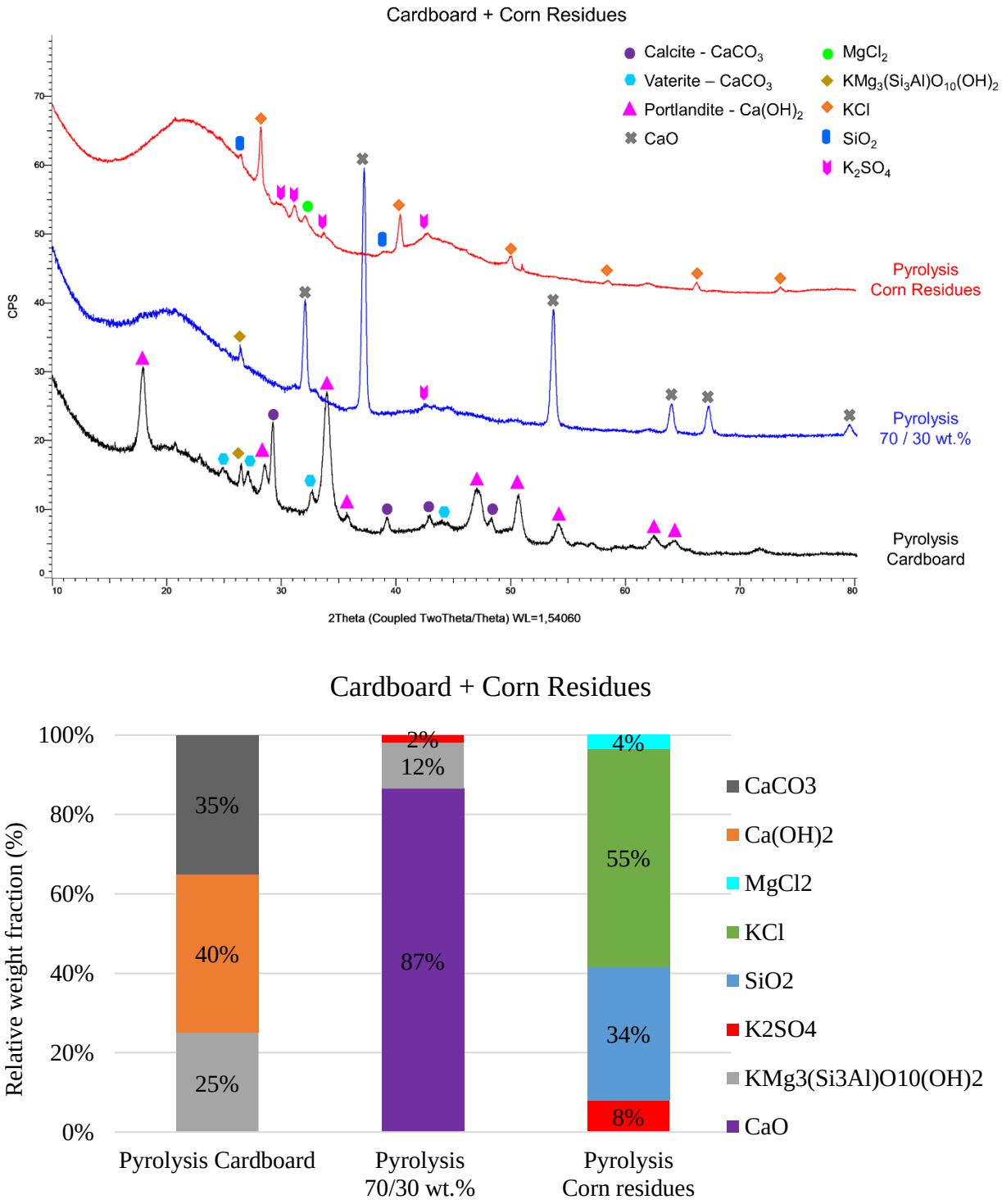

Figure 45: XRD diffractograms of the chars of the individual resources and the mixture of corn residues with cardboard obtained from pyrolysis at 800°C

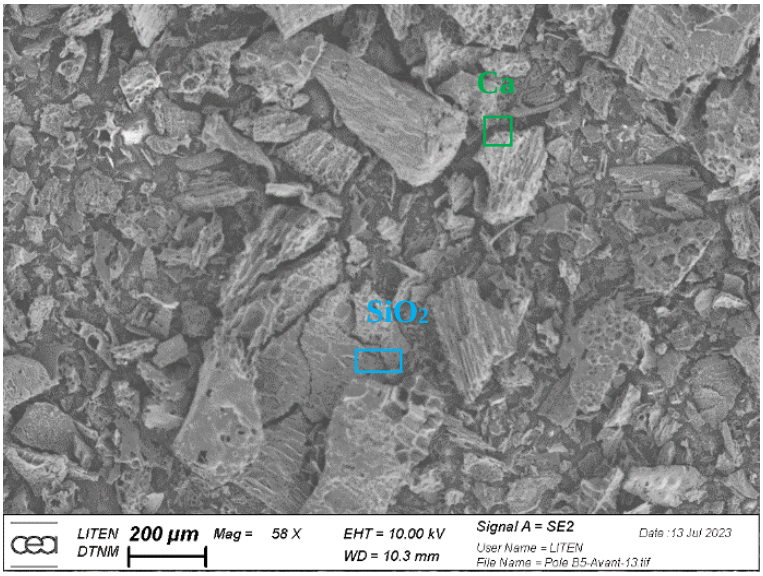

Figure 46: SEM observations of the char from co-pyrolysis at 800°C of 70/30 wt.% Cardboard + Corn residues mixture

4.2.4. Mixture of PVC with cardboard

Figure 47 compares the theoretical and experimental chlorine retention in the char of the mixture of cardboard with PVC as a function of the fraction of PVC in the mixture.

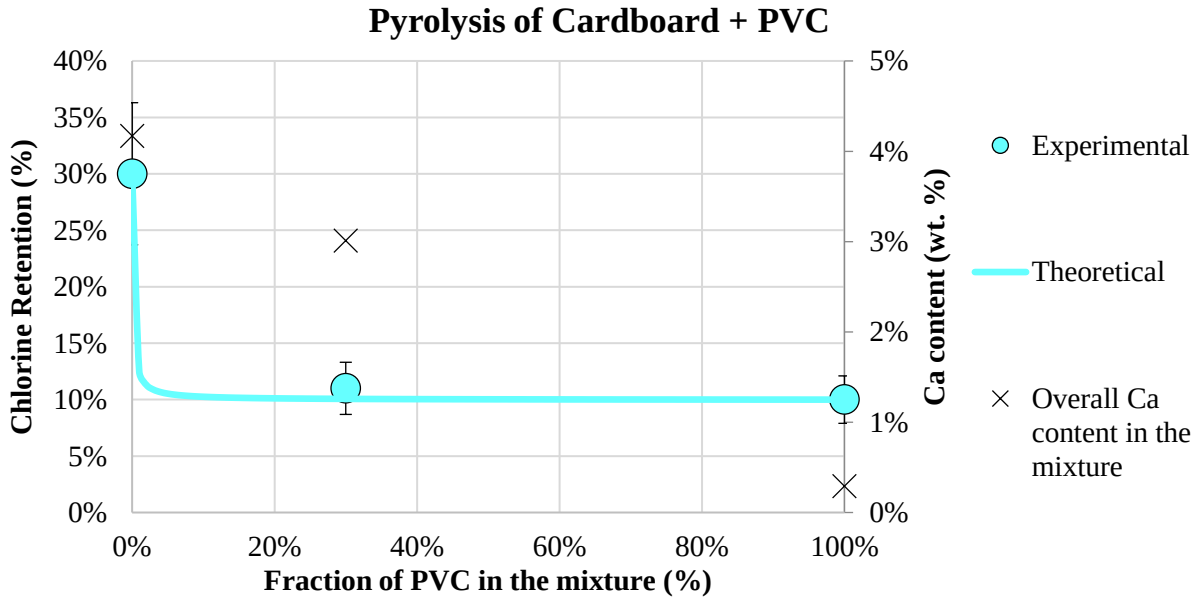

Figure 47: Theoretical and experimental chlorine retention in the char of the mixture of Cardboard with PVC, and calcium content in the mixture, as a function of the fraction of PVC

The chlorine retention value obtained experimentally is very close to the theoretical value, which suggests that there is no significant interaction between cardboard and PVC which would influence chlorine retention. PVC, alone, has a low calcium content; however, although its mixture with cardboard increases significantly the overall calcium content, it does not appear to have any effect on the chlorine retention.

Figure 48 shows the XRD diffractograms of the chars of the individual cardboard and the mixture PVC + Cardboard obtained from pyrolysis at 800°C. There are unidentified peaks in the diffraction pattern that could signify the occurrence of additional mineral phases or chemical compounds. Due to the presence of unidentified peaks, a semi-quantitative analysis of the char composition could not be provided in this case.

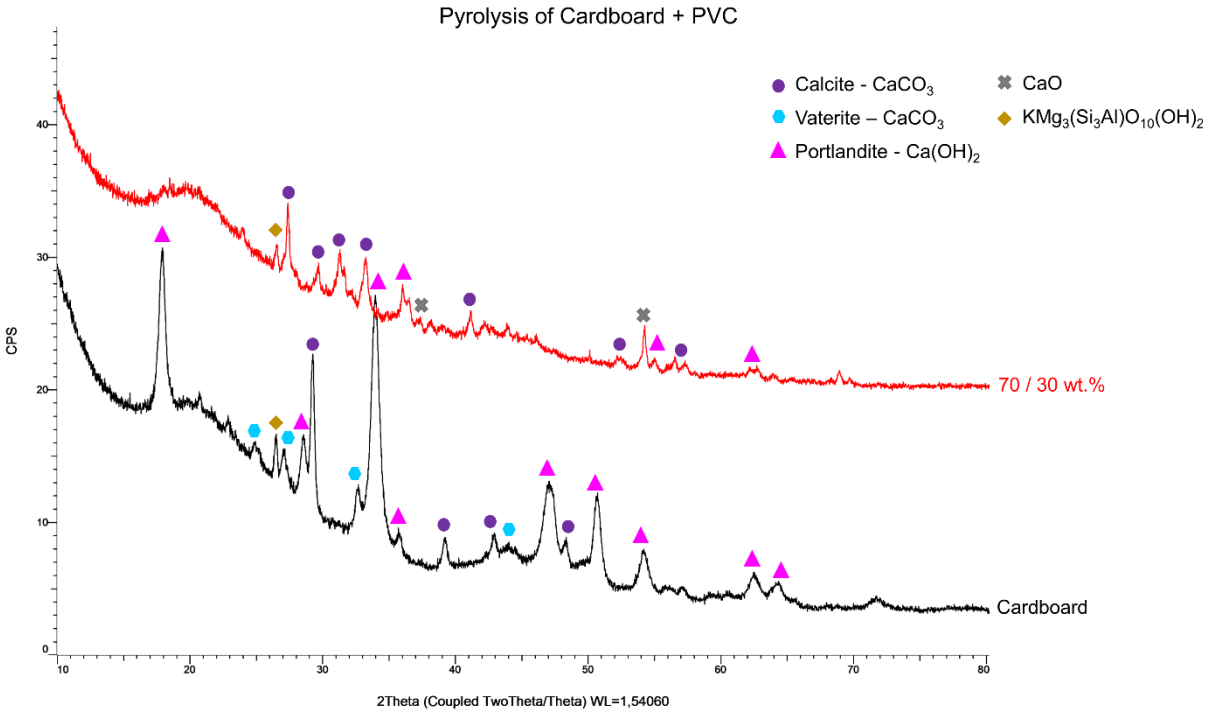

Figure 48: XRD diffractograms of the chars of the individual cardboard and the mixture PVC + Cardboard obtained from pyrolysis at 800°C

The XRD diffractogram of the char for the mixture of PVC + Cardboard shows the presence of peaks corresponding to $CaCO_3$, $Ca(OH)_2$, CaO and $KMg_3(Si_3Al)O_{10}(OH)_2$. These peaks are all present in the char coming from cardboard. Unlike the mixture of PVC with CaO additive, no peaks corresponding to chlorine-containing compounds are present, suggesting that chlorine retention in the PVC + Cardboard mixture might not involve the formation of distinct chlorine phases identifiable through XRD analysis. This could confirm that chlorine is released

independently within both the PVC and the cardboard and no interaction is occurring between the two components.

4.2.5. Discussion on the co-pyrolysis and co-gasification of resources

Table 21 and **Table 22** shows the main results of S and Cl retention obtained in the pyrolysis of mixtures of resources.

Table 21: Main results of S retention obtained in the mixtures of resources

R1 / R2	Cardboard	Colza Straw	Bark Oak
Wool	2x the theoretical values	2x the theoretical values	2x the theoretical values
Corn Residues	no effect	-	-
Colza Straw	no effect	-	no effect

Table 22: Main results of Cl retention obtained in the mixtures of resources

R1 / R2	Cardboard	Bark Oak
Corn Residues	1.7x the theoretical values	-
Colza Straw	2.5x the theoretical values (full Cl retention in the char)	need more experimental investigations before conclusion
PVC	no effect	-

When wool is mixed with calcium-rich resources (cardboard, colza straw, or oak bark), a significant improvement in sulfur retention is obtained, as the experimental values exceed twice the values calculated theoretically by assuming no interaction between the resources. Moreover, calcium sulfide (CaS) is observed in the chars, suggesting a reaction between sulfur and calcium during the co-pyrolysis or co-gasification. However, in the case of agricultural residues mixed with cardboard or oak bark, no substantial enhancement in sulfur retention is observed,

indicating a lack of meaningful interaction between the calcium-rich components and the agricultural residues concerning sulfur retention.

A possible factor that could explain this disparity is the nature of sulfur present in the resources. As demonstrated in **Chapter 3**, the majority of sulfur in wool, classified as organic sulfur, is released in the gas phase in the form of H_2S and COS during pyrolysis or gasification. This released H_2S is expected to react with calcium provided from the calcium-rich resources to produce calcium sulfide (CaS), thereby enhancing the retention of sulfur within the char. However, in our results, although the fraction of retained sulfur increases from 6 – 11% to 13 – 24% there is still a non-negligible amount of S released in the gas. This shows that only a small fraction of H_2S reacts with calcium. The scenario changes when considering agricultural residues, which contain both organic and inorganic sulfur forms. Inorganic sulfur forms are mainly retained in the char, they might partially be emitted into the gas phase, and therefore, they may not participate in the same type of chemical reactions with calcium-rich resources, which leads to a less pronounced enhancement in sulfur retention.

Figure 49 presents the total molar Ca/S ratios for individual resources as well as their corresponding mixtures. The Ca/S ratio provides insights into the availability of calcium for the formation of CaS with sulfur. Wool stands out as the only resource where its initial molar ratio Ca/S is below 1, and for which the mixture with Ca-rich resources induces the increase of this ratio above 1. Moreover, only on the case of wool does the mixture with Ca-rich resources induce a significant enhancement in sulfur retention. On the other hand, for the agricultural residues, the initial Ca/S molar ratios are already above 1, and their mixture with Ca-rich resources do not induce any change in sulfur retention. The increase of the Ca/S ratio above 1 for wool's mixture could be an explanation for the substantial improvements in sulfur retention, with more calcium available for reaction with sulfur.

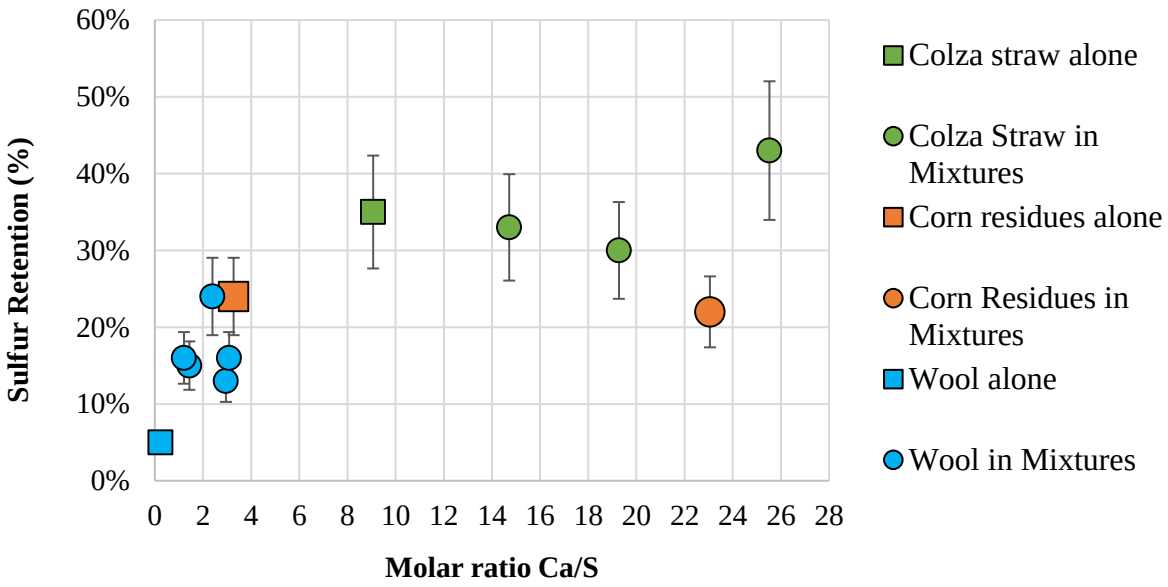

Figure 49: S retention for the chars obtained from the pyrolysis of the resources alone and their mixtures with other resources as a function of the total molar ratio Ca/S

The experiments reveal a significant increase in chlorine retention, as the experimental values exceed 2.5 and 1.7 times the values calculated theoretically, when mixing cardboard with colza straw or corn residues respectively, while for the mixture of cardboard with PVC, no enhancement in chlorine retention is observed, suggesting a lack of significant interaction between the two materials.

A crucial aspect to consider when discussing the lack of enhancement in chlorine retention when mixing cardboard with PVC is their differences in their thermal decomposition behavior during pyrolysis highlighted in **Chapter 3** and the organic nature of chlorine in PVC. PVC, being a polymer with relatively low thermal stability, is known to undergo a first decomposition around 250-300°C (dechlorination). Consequently, the organic chlorine present in PVC could be rapidly released as volatile chlorinated compounds during the early stages of pyrolysis. In contrast, cardboard as a cellulose-based material may require higher temperatures to undergo complete decomposition, and the presence of calcium-rich compounds within the cardboard, such as $CaCO_3$, might also require elevated temperatures to initiate reactive pathways for chlorine capture. The early release of chlorine in PVC could reduce chlorine retention in the char before cardboard's decomposition and the initiation of calcium-chlorine interactions. This temperature mismatch between the two components could lead to differences in the timing and extent of chlorine release and calcium reactivity, potentially limiting their synergistic interaction during pyrolysis.

An additional factor that could contribute to the contrasting behavior in chlorine retention is the amount of Ca and Cl in the resources. As for the mixture of oak bark with colza straw, they both have a similar amount of chlorine content, which suggests a relatively balanced contribution of chlorine from both components, therefore, efficient chlorine capture can be challenging due to potential competition for calcium. Further experimental investigations are needed before reaching a conclusive assessment in the regard of the mixture of colza straw with oak bark. To completely capture Cl into $CaCl_2$, the molar ratio Ca/Cl should be higher than 0.5, providing that all Ca reacts with Cl. **Figure 51** presents the total molar Ca/Cl ratios for individual resources as well as their corresponding mixtures. PVC presents a very high chlorine content, resulting in a Ca/Cl molar ratio lower than 0.5. This low molar ratio means that there is an excess of chlorine relative to calcium, making it difficult for calcium to efficiently retain the chlorine.

4.3. Conclusions

The mass fractions of some mixtures were initially determined to incorporate equivalent amounts of added calcium as in the experiments with additives. However, the S and Cl retention results obtained with resource mixtures are difficult to be directly compared with the results obtained with one resource with a Ca-based additive. Indeed, in the mixtures, the S and Cl come from both resources, and their release are influenced by the behavior of each of them. In order to gather all S and Cl retention results in one unique figure, the Ca/S and Ca/Cl molar ratios were selected as possible influent parameters. **Figure 50** and **Figure 51** represent the sulfur and chlorine retention for the chars obtained from the pyrolysis of the resources alone, when mixed with additives and with other resources as a function of the total molar ratio Ca/S and Ca/Cl, respectively.

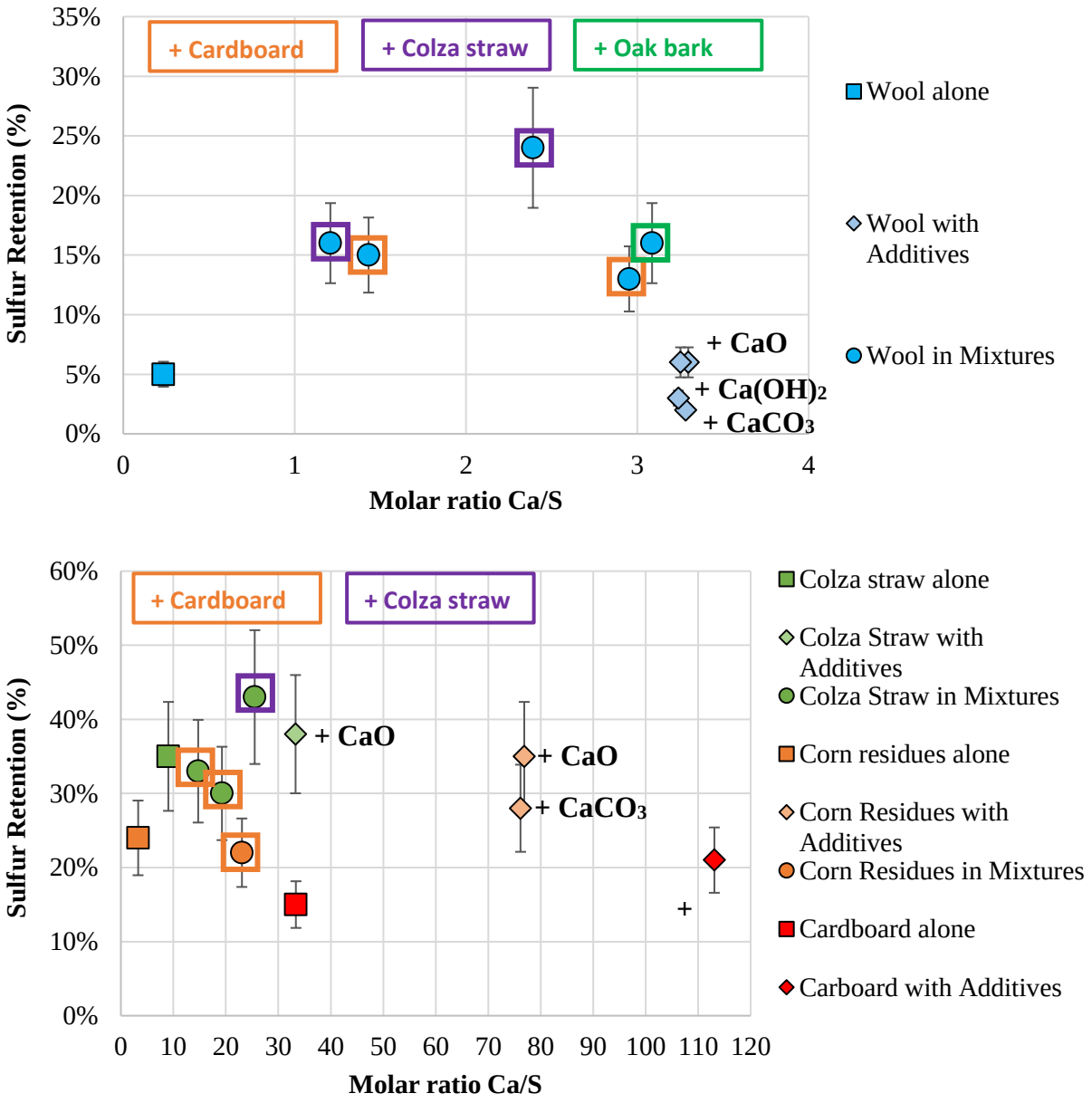

Figure 50: S retention for the chars obtained from the pyrolysis of the resources alone, when mixed with additives and with other resources as a function of the total molar ratio Ca/S

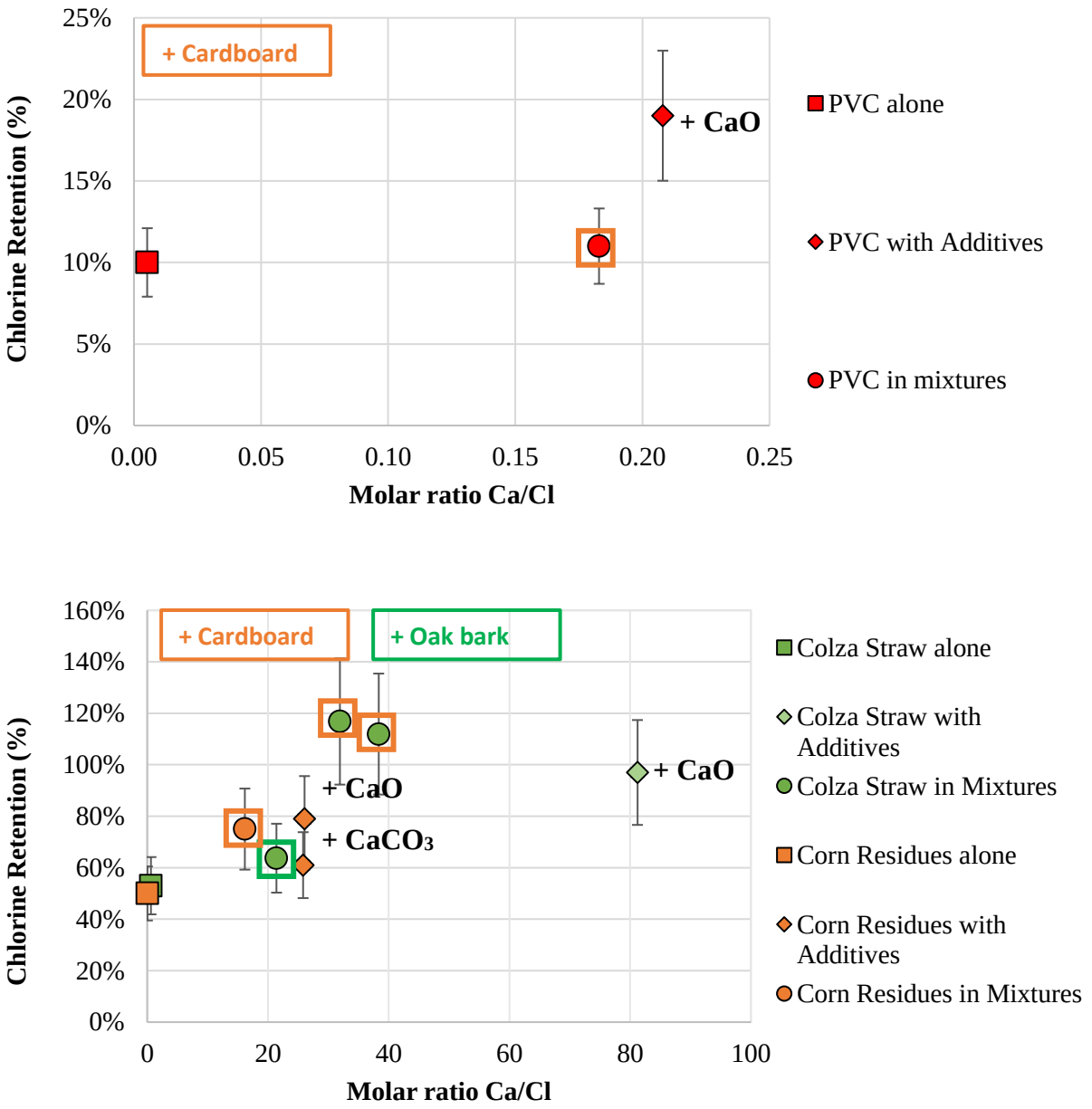

Figure 51: Cl retention for the chars obtained from the pyrolysis of the resources alone, when mixed with additives and with other resources as a function of the total molar ratio Ca/Cl

For wool, the difference is significant, when compared at the same molar ratio Ca/S, the sulfur retention increases for mixtures of wool with other resources, whereas no corresponding increase is observed with additives. The physical contact and distribution between the additives and wool may not be as effective, which reduces the opportunities for sulfur capture by the additives, leading to the observed lack of increase in sulfur retention. However, for cardboard and the agricultural residues, neither the mixtures nor the additives appear to result in any enhancement in sulfur retention, even when assessed across varying Ca/S ratios.

Regarding chlorine, the mixtures of agricultural residues with calcium-based additives and cardboard result in an increase in the chlorine retention. In addition, when mixing PVC with CaO during pyrolysis, the chlorine retention increases with the detection of $CaCl_2$. However, with a very close molar ratio Ca/Cl, no such enhancement is observed in the co-pyrolysis of PVC with cardboard.

The chemistry involved in sulfur and chlorine retention is complex and multifaceted. The S and Cl retention may be influenced by different factors for the two scenarios under investigation: the use of additives and the co-pyrolysis/co-gasification of resources.

In the case of additives, the Ca/S ratio remains significantly higher than 1, which suggests that there is a surplus of calcium available relative to the sulfur content, which should theoretically favor sulfur retention. However, it is crucial to acknowledge that the chemistry involved is not always straightforward. The effectiveness of sulfur retention is likely influenced not only by the quantity of calcium but also by other factors, such as the mixing of these additives with the resources and the kinetics of sulfur-calcium reactions. It is possible that sulfur compounds, particularly organic forms, are being released before reaching the appropriate temperature range necessary to activate the sulfur capture capabilities of the additives.

Moreover, for chlorine, potassium can influence its retention as well. The interactions between calcium, potassium, and chlorine in the pyrolysis or gasification can lead to the formation of various compounds and influence the overall chlorine retention.

On the other hand, the nature of sulfur and chlorine present in the materials (organic or inorganic forms) and the thermal behavior and decomposition temperatures of the materials might influence the timing and extent of sulfur and chlorine release and calcium reactivity, affecting the overall char retention. While actual evidence is lacking in our study, it is possible that the surface area and the physical structure of the components in the mixtures could also be influencing factors.

Conclusion and Perspectives

The first objective of this study was to characterize the behavior of inorganic volatile elements, specifically sulfur and chlorine, during the pyrolysis and gasification of biomass and waste of various types and compositions. We evaluated the influence of the type of feedstock and its initial chemical composition (particularly its inorganic content and composition) as well as the effect of the operating conditions (temperature and atmosphere) on this behavior. The second objective was to propose and test in-situ cleaning methods based on chemical interactions between inorganic elements to enhance the retention of sulfur and chlorine in the char and thus limit their harmful release in the gas.

To achieve these objectives, we adopted a comprehensive approach that encompassed thermodynamic equilibrium calculations performed using the FactSage software, experimental investigations conducted using a lab-scale induction heated reactor and various analytical techniques employed to quantitatively and qualitatively assess the behavior of sulfur and chlorine.

Two agricultural residues (colza straw and corn residues) with different ash content and composition and three waste components (cardboard, wool and PVC) were selected as feedstock. A leaching technique was applied to the selected resources to determine the repartition of initial sulfur and chlorine into organic and inorganic forms. In the two agricultural residues, S was found in its two chemical forms as organically bonded to the carbon matrix and as inorganic soluble sulfates ($CaSO_4$, K_2SO_4). Cl is mainly in the form of inorganic salts (KCl, $KClO_4$). However, in wool and cardboard, sulfur was mainly found in an organic form, while in PVC, Cl is known to be organically bonded in the polymer structure.

Thermodynamic equilibrium calculations revealed that the influence of temperature and equivalence ratio on the distribution of S and Cl in both gaseous and solid products is minimal. Nevertheless, these calculations highlighted the substantial role played by the ash-forming elements (Ca, K, and Si) on the distribution of S and Cl species in gaseous and solid products for each feedstock. The results obtained from experimental investigations were not in full agreement with the equilibrium predictions especially on a quantitative scale, showing the limitations of thermodynamic equilibrium calculations to represent the experimental results.

In the first experimental trials, an attempt was made to quantify the sulfur and chlorine released in the gas phase, to ensure the best possible closure of the elemental balances of S and Cl. However, the mass balances showed low recoveries which could be attributed to factors such as trapping and measurement difficulties and potential interactions with the experimental setup.

Therefore, we decided to focus solely on investigating their retention in the char, this choice allowing to reach the second objective of the thesis, which consisted in exploring methods for improving retention.

Pyrolysis tests performed at variable temperatures between 365 and 850°C showed a resource -dependent retention of S and Cl in the char. For wool and cardboard, approximately 100% and 65% of S was released in the gas respectively, which corresponded to the fraction of S initially present in organic form. For PVC, more than 90% of Cl was released into the gas as HCl. This can be linked to the volatility of the organic forms of S and Cl, which are easily released into the gas phase even at low temperatures without interacting with other inorganic elements, even in high ash content resources. For agricultural residues, in addition to the organic S and Cl, a part of the inorganic S and Cl was also released in the gas. Different crystallized S and Cl containing forms were identified in the chars ($CaSO_4$, CaS and KCl for colza straw, K_2SO_4, KCl, and $MgCl_2$ for corn residues), which depended on the pyrolysis temperature and the ash composition.

The addition of air in the gasification experiment for 20 minutes did not have a significant impact on the sulfur and chlorine retention compared to pyrolysis. The only exception was for colza straw, which unexpectedly retained all of its Cl content after gasification. However, when extending the gasification experiments to 60 minutes, the S and Cl retention for agricultural residues decreased significantly, bringing us closer to the thermodynamic equilibrium.

We explored the use of calcium-based additives ($CaCO_3$, $Ca(OH)_2$ and CaO) and the co-pyrolysis and co-gasification of resources with the objective to enhance the retention of S and Cl in the char through interaction with inorganic elements, particularly focusing on calcium.

Our results revealed varying degrees of effectiveness of the additives. Despite employing enough quantities of additives ensuring an excess of calcium for the formation of CaS, we observed only moderate variations in sulfur retention across different feedstock-additive mixtures. This suggests that the anticipated interaction between these calcium-based additives and sulfur may not have been fully realized, possibly due to limitations in achieving optimal contact or mixing of additives within the resources.

Concerning chlorine, for PVC, the enhancement in chlorine retention appeared to be directly linked to the formation of $CaCl_2$, as confirmed by X-ray diffraction analysis. However, for the agricultural residues, the chlorine retention significantly increased without a clear

understanding of the underlying mechanisms. The inorganic content of these resources, in particular potassium, may then play a role in influencing chlorine retention.

Co-pyrolysis or co-gasification effectively influenced the retention of S or Cl only in some cases. The most notable enhancement in sulfur retention was observed when co-pyrolyzing wool with a calcium-rich resource (cardboard, colza straw, or oak bark) and in chlorine retention when mixing colza straw or corn residues with cardboard. In these cases, the obtained sulfur and chlorine retention exceeded twice the values that were calculated theoretically by assuming no interaction between the resources. Therefore, this clearly suggests that interactions are taking place among the two resources, significantly improving the mechanisms of sulfur and chlorine retention in the char.

The observed enhancement in sulfur and chlorine retention within the char, achieved either through the incorporation of calcium-based additives or during the co-pyrolysis and co-gasification of resources, currently lacks a comprehensive explanation. It is essential to examine deeper into the underlying chemical processes and mechanisms governing these methods to optimize their effectiveness, in order to significantly limit the release of sulfur and chlorine into the gas phase.
While the impacts of these findings on the overall pyrolysis and gasification processes themselves appear to be relatively minor, they have important implications for downstream gas cleaning and synthesis gas conditioning. This opens up possibilities to reduce the need for extensive gas cleaning and to improve and optimize the dimensioning of the cleaning process.

Multiple perspectives for future exploration have been identified:

- Considering the unquantified fraction of sulfur and chlorine released in the gas, it is crucial to refine the experimental setup and analysis techniques to ensure accurate measurements. Specifically, addressing the issues related to unmeasured sulfur-containing tars and potential chlorine condensation can significantly enhance the completeness and reliability of our results. A more comprehensive analysis of the GC-FPD along with the appropriate columns could potentially provide the quantities and detailed compositions of these sulfur-containing tars. In addition, optimizing the reactor output design could minimize the potential for chlorine losses due to condensation.

- The use of more advanced analytical techniques (e.g. X-ray photoelectron spectrometry) could allow improving the charaterization of minerals in the char, including amorphous

compounds, and gaining a detailed understanding of the chemical and physical transformations occurring within the char

- Although the particle shape and size in the form of pellet did not have a substantial impact on the sulfur and chlorine behavior during pyrolysis of colza straw at 800°C, there remains potential for exploration. Future investigations can focus on the effects of particle morphology and dimensions, as well as shaping of the materials into pellets that could enhance contact within the mixtures involving additives or other feedstock materials. .

- The methods used for enhancing S and Cl retention, especially the use of additives, could be tested in a fluidized bed reactor to assess its efficiency in a well-mixed reactor. After evaluating their effectiveness on a smaller scale, the next step involves scaling up of these methods to an industrial level to explore their feasibility in an industrial setting, considering factors beyond mixing efficiency.

- A detailed techno-economic analysis could be performed to determine the cost-effectiveness and viability of incorporating the enhanced retention techniques into existing waste-to-energy facilities. This analysis should consider factors such as additive costs and the expenses associated with preparing (size reduction, drying) and blending resources.

References

Abraham, T.W., Höfer, R., 2012. 10.03 - Lipid-Based Polymer Building Blocks and Polymers, in: Matyjaszewski, K., Möller, M. (Eds.), Polymer Science: A Comprehensive Reference. Elsevier, Amsterdam, pp. 15–58. https://doi.org/10.1016/B978-0-444-53349-4.00253-3

Aljbour, S.H., Kawamoto, K., 2013. Bench-scale gasification of cedar wood – Part II: Effect of Operational conditions on contaminant release. Chemosphere 90, 1501–1507. https://doi.org/10.1016/j.chemosphere.2012.08.030

Andrea Jordan, C., Akay, G., 2012. Speciation and distribution of alkali, alkali earth metals and major ash forming elements during gasification of fuel cane bagasse. Fuel 91, 253–263. https://doi.org/10.1016/j.fuel.2011.05.031

Anniwaer, A., Chaihad, N., Zhang, M., Wang, C., Yu, T., Kasai, Y., Abudula, A., Guan, G., 2021. Hydrogen-rich gas production from steam co-gasification of banana peel with agricultural residues and woody biomass. Waste Manag. 125, 204–214. https://doi.org/10.1016/j.wasman.2021.02.042

Aravind, P.V., de Jong, W., 2012. Evaluation of high temperature gas cleaning options for biomass gasification product gas for Solid Oxide Fuel Cells. Prog. Energy Combust. Sci. 38, 737–764. https://doi.org/10.1016/j.pecs.2012.03.006

Arena, U., 2012. Process and technological aspects of municipal solid waste gasification. A review. Waste Manag., Solid Waste Gasification 32, 625–639. https://doi.org/10.1016/j.wasman.2011.09.025

Bale, C.W., Bélisle, E., Chartrand, P., Decterov, S.A., Eriksson, G., Gheribi, A.E., Hack, K., Jung, I.-H., Kang, Y.-B., Melançon, J., Pelton, A.D., Petersen, S., Robelin, C., Sangster, J., Spencer, P., Van Ende, M.-A., 2016. FactSage thermochemical software and databases, 2010–2016. Calphad 54, 35–53. https://doi.org/10.1016/j.calphad.2016.05.002

Basu, P., 2010. Biomass Gasification and Pyrolysis: Practical Design and Theory. Academic Press.

Baxter, L.L., Miles, T.R., Miles, T.R., Jenkins, B.M., Milne, T., Dayton, D., Bryers, R.W., Oden, L.L., 1998. The behavior of inorganic material in biomass-fired power boilers: field and laboratory experiences. Fuel Process. Technol. 54, 47–78. https://doi.org/10.1016/S0378-3820(97)00060-X

Benson, S.A., Holm, P.L., 1985. Comparison of inorganics in three low-rank coals. Ind. Eng. Chem. Prod. Res. Dev. 24, 145–149. https://doi.org/10.1021/i300017a027

Berrueco, C., Recari, J., Abelló, S., Farriol, X., Montané, D., 2015. Experimental Investigation of Solid Recovered Fuel (SRF) Gasification: Effect of Temperature and Equivalence Ratio on Process Performance and Release of Minor Contaminants. Energy Fuels 29, 7419–7427. https://doi.org/10.1021/acs.energyfuels.5b02032

Bläsing, M., Hasir, N.B.A., Müller, M., 2015a. Release of Inorganic Elements from Gasification and Co-Gasification of Coal with Miscanthus, Straw, and Wood at High Temperature. Energy Fuels 29, 7386–7394. https://doi.org/10.1021/acs.energyfuels.5b01892

Bläsing, M., Oga, I.O., Müller, M., 2017a. Co-Gasification of Turkey Manure and Meat Bone with Hard Coal and Lignite: Release of Condensable and Noncondensable Species. Ind. Eng. Chem. Res. 56, 14396–14400. https://doi.org/10.1021/acs.iecr.7b03892

Bläsing, M., Oga, I.O., Müller, M., 2017b. In Situ Determination of Gaseous Inorganic Species Released during Gasification of Sewage Sludge and Coal. Energy Fuels 31, 14423–14425. https://doi.org/10.1021/acs.energyfuels.7b02797

Bläsing, M., Weigand, M., Fasenacht, J., Müller, M., 2015b. Effect of temperature and oxygen content on the release of organic and inorganic species during high temperature thermochemical conversion of PVC-condensate. Fuel Process. Technol. 134, 85–91. https://doi.org/10.1016/j.fuproc.2015.01.018

Bläsing, M., Zini, M., Müller, M., 2013. Influence of Feedstock on the Release of Potassium, Sodium, Chlorine, Sulfur, and Phosphorus Species during Gasification of Wood and Biomass Shells. Energy Fuels 27, 1439–1445. https://doi.org/10.1021/ef302093r

Borgianni, C., De Filippis, P., Pochetti, F., Paolucci, M., 2002. Gasification process of wastes containing PVC. Fuel 81, 1827–1833. https://doi.org/10.1016/S0016-2361(02)00097-2

Boström, D., Skoglund, N., Grimm, A., Boman, C., Öhman, M., Broström, M., Backman, R., 2012. Ash Transformation Chemistry during Combustion of Biomass. Energy Fuels 26, 85–93. https://doi.org/10.1021/ef201205b

Boufi, S., González, I., Delgado-Aguilar, M., Tarrès, Q., Pèlach, M.À., Mutjé, P., 2016. Nanofibrillated cellulose as an additive in papermaking process: A review. Carbohydr. Polym. 154, 151–166. https://doi.org/10.1016/j.carbpol.2016.07.117

Bryers, R.W., 1996. Fireside slagging, fouling, and high-temperature corrosion of heat-transfer surface due to impurities in steam-raising fuels. Prog. Energy Combust. Sci. 22, 29–120. https://doi.org/10.1016/0360-1285(95)00012-7

Burra, K.G., Gupta, A.K., 2018. Synergistic effects in steam gasification of combined biomass and plastic waste mixtures. Appl. Energy 211, 230–236. https://doi.org/10.1016/j.apenergy.2017.10.130

Cai, J., Zeng, R., Zheng, W., Wang, S., Han, J., Li, K., Luo, M., Tang, X., 2021. Synergistic effects of co-gasification of municipal solid waste and biomass in fixed-bed gasifier. Process Saf. Environ. Prot. 148, 1–12. https://doi.org/10.1016/j.psep.2020.09.063

Campuzano, F., Cardona-Uribe, N., Agudelo, A.F., Sarathy, S.M., Martínez, J.D., 2021. Pyrolysis of Waste Tires in a Twin-Auger Reactor Using CaO: Assessing the Physicochemical Properties of the Derived Products. Energy Fuels 35, 8819–8833. https://doi.org/10.1021/acs.energyfuels.1c00890

Carmo-Calado, L., Hermoso-Orzáez, M.J., Mota-Panizio, R., Guilherme-Garcia, B., Brito, P., 2020. Co-Combustion of Waste Tires and Plastic-Rubber Wastes with Biomass Technical and Environmental Analysis. Sustainability 12, 1036. https://doi.org/10.3390/su12031036

Casari, N., Pinelli, M., Suman, A., Candido, A., Morini, M., 2020. Deposition of syngas tar in fuel supplying duct of a biomass gasifier: A numerical study. Fuel 273, 117579. https://doi.org/10.1016/j.fuel.2020.117579

Casazza, A., Spennati, E., Converti, A., Busca, G., 2019. Study on the Thermal Decomposition of Plastic Residues. Chem. Eng. Trans. 74, 1141–1146. https://doi.org/10.3303/CET1974191

Cheah, S., Malone, S.C., Feik, C.J., 2014. Speciation of Sulfur in Biochar Produced from Pyrolysis and Gasification of Oak and Corn Stover. Environ. Sci. Technol. 48, 8474–8480. https://doi.org/10.1021/es500073r

Chen, R., Zhang, J., Lun, L., Li, Q., Zhang, Y., 2019. Comparative study on synergistic effects in co-pyrolysis of tobacco stalk with polymer wastes: Thermal behavior, gas formation, and kinetics. Bioresour. Technol. 292, 121970. https://doi.org/10.1016/j.biortech.2019.121970

Cheng, S.-Y., Ngoc Lan Thao, N.T., Chiang, K.-Y., 2020. Hydrogen gas yield and trace pollutant emission evaluation in automotive shredder residue (ASR) gasification using prepared oyster shell catalyst. Int. J. Hydrog. Energy, Special Issue on The international conference on Sustainable Energy and Green Technology (SEGT 2018) 45, 22232–22245. https://doi.org/10.1016/j.ijhydene.2020.01.005

Chin, B.L.F., Yusup, S., Al Shoaibi, A., Kannan, P., Srinivasakannan, C., Sulaiman, S.A., 2014. Comparative studies on catalytic and non-catalytic co-gasification of rubber seed shell and high density polyethylene mixtures. J. Clean. Prod. 70, 303–314. https://doi.org/10.1016/j.jclepro.2014.02.039

Cho, M.-H., Choi, Y.-K., Kim, J.-S., 2015. Air gasification of PVC (polyvinyl chloride)-containing plastic waste in a two-stage gasifier using Ca-based additives and Ni-loaded activated carbon for the production of clean and hydrogen-rich producer gas. Energy 87, 586–593. https://doi.org/10.1016/j.energy.2015.05.026

Choi, Y.-K., Cho, M.-H., Kim, J.-S., 2016a. Air gasification of dried sewage sludge in a two-stage gasifier. Part 4: Application of additives including Ni-impregnated activated carbon for the production of a tar-free and H2-rich producer gas with a low NH3 content. Int. J. Hydrog. Energy 41, 1460–1467. https://doi.org/10.1016/j.ijhydene.2015.11.125

Choi, Y.-K., Mun, T.-Y., Cho, M.-H., Kim, J.-S., 2016b. Gasification of dried sewage sludge in a newly developed three-stage gasifier: Effect of each reactor temperature on the producer gas composition and impurity removal. Energy 114, 121–128. https://doi.org/10.1016/j.energy.2016.07.166

Chou, C.-L., 2012. Sulfur in coals: A review of geochemistry and origins. Int. J. Coal Geol. 100, 1–13. https://doi.org/10.1016/j.coal.2012.05.009

Das, D., Das, S., 2022. Chapter 2 - Wool structure and morphology, in: Thomas, S., Jose, S. (Eds.), Wool Fiber Reinforced Polymer Composites, The Textile Institute Book Series. Woodhead Publishing, pp. 13–32. https://doi.org/10.1016/B978-0-12-824056-4.00013-3

Davidsson, K.O., Pettersson, J.B.C., Nilsson, R., 2002. Fertiliser influence on alkali release during straw pyrolysis. Fuel 81, 259–262. https://doi.org/10.1016/S0016-2361(01)00172-7

Dayton, D.C., Jenkins, B.M., Turn, S.Q., Bakker, R.R., Williams, R.B., Belle-Oudry, D., Hill, L.M., 1999. Release of Inorganic Constituents from Leached Biomass during Thermal Conversion. Energy Fuels 13, 860–870. https://doi.org/10.1021/ef980256e

de Almeida, V.F., Gómez-Barea, A., Arroyo-Caire, J., Pardo, I., 2020. On the Measurement of the Main Inorganic Contaminants Derived from Cl, S and N in Simulated Waste-Derived Syngas. Waste Biomass Valorization 11, 6869–6884. https://doi.org/10.1007/s12649-019-00879-4

De Kok, L., Rennenberg, H., Brunold, C., Rauser, W., 1993. Sulfur Nutrition and Assimilation in Higher Plants; Regulatory, Agricultural and Environmental Aspects.

De, S., Agarwal, A.K., Moholkar, V.S., Thallada, B. (Eds.), 2018. Coal and Biomass Gasification: Recent Advances and Future Challenges, Energy, Environment, and Sustainability. Springer Singapore, Singapore. https://doi.org/10.1007/978-981-10-7335-9

de Wild, P., 2011. Biomass pyrolysis for chemicals (PhD Thesis). Rijksuniversiteit Groningen, Groningen.

Defoort, F., Dupont, C., Durruty, J., Guillaudeau, J., Bedel, L., Ravel, S., Campargue, M., Labalette, F., Da Silva Perez, D., 2015. Thermodynamic Study of the Alkali Release Behavior during Steam Gasification of Several Biomasses. Energy Fuels 29, 7242–7253. https://doi.org/10.1021/acs.energyfuels.5b01755

Deng, L., Huang, X., Tie, Y., Jiang, J., Zhang, K., Ma, S., Che, D., 2022. Experimental study on transformation of alkali and alkaline earth metals during biomass gasification. J. Energy Inst. 103, 117–127. https://doi.org/10.1016/j.joei.2022.06.003

Du, S., Wang, X., Shao, J., Yang, H., Xu, G., Chen, H., 2014. Releasing behavior of chlorine and fluorine during agricultural waste pyrolysis. Energy 74, 295–300. https://doi.org/10.1016/j.energy.2014.01.012

Dunnu, G., Panopoulos, K.D., Karellas, S., Maier, J., Touliou, S., Koufodimos, G., Boukis, I., Kakaras, E., 2012. The solid recovered fuel Stabilat®: Characteristics and fluidised bed gasification tests. Fuel 93, 273–283. https://doi.org/10.1016/j.fuel.2011.08.061

Ephraim, A., 2016. Valorization of wood and plastic waste by pyro-gasification and syngas cleaning Simulation of biomass char gasification in a downdraft reactor for syngas production (These de doctorat). Ecole nationale des Mines d'Albi-Carmaux.

Fortuna, M., Andrei, L., Cosovanu, L.-M., Harja, M., 2020. Effects of In-Situ Filler Loading vs. Conventional Filler and the Use of Retention-Related Additives on Properties of Paper. Materials 13, 5066. https://doi.org/10.3390/ma13225066

Froment, K., Defoort, F., Bertrand, C., Seiler, J.M., Berjonneau, J., Poirier, J., 2013. Thermodynamic equilibrium calculations of the volatilization and condensation of inorganics during wood gasification. Fuel 107, 269–281. https://doi.org/10.1016/j.fuel.2012.11.082

Gai, C., Dong, Y., Zhang, T., 2014. Distribution of sulfur species in gaseous and condensed phase during downdraft gasification of corn straw. Energy 64, 248–258. https://doi.org/10.1016/j.energy.2013.11.052

Gerassimidou, S., Velis, C.A., Williams, P.T., Castaldi, M.J., Black, L., Komilis, D., 2021. Chlorine in waste-derived solid recovered fuel (SRF), co-combusted in cement kilns: A systematic review of sources, reactions, fate and implications. Crit. Rev. Environ. Sci. Technol. 51, 140–186. https://doi.org/10.1080/10643389.2020.1717298

Godinho, M., Birriel, E.J., Marcilio, N.R., Masotti, L., Martins, C.B., Wenzel, B.M., 2011. High-temperature corrosion during the thermal treatment of footwear leather wastes. Fuel Process. Technol. 92, 1019–1025. https://doi.org/10.1016/j.fuproc.2010.12.025

Godinho, M., Marcilio, N., Vilela, A., Masotti, L., Martins, C., 2007. Gasification and combustion of the footwear leather wastes. J. Am. Leather Chem. Assoc. 102, 182–190.

Gursel, I.V., Groenestijn, J. van, Elbersen, W., Schelhaas, M.-J., Nabuurs, G.-J., Kranendonk, R., Jong, A. de, Leeuwen, M. van, Smits, M.-J., 2020. Local supply of lignocellulosic biomass to paper industry in Gelderland: Development of circular and value-added chains. Wageningen Food & Biobased Research. https://doi.org/10.18174/522235

Hepola, J., Simell, P., 1997. Sulphur poisoning of nickel-based hot gas cleaning catalysts in synthetic gasification gas: I. Effect of different process parameters. Appl. Catal. B Environ. 14, 287–303. https://doi.org/10.1016/S0926-3373(97)00031-3

Hervy, M., Remy, D., Dufour, A., Mauviel, G., 2021. Gasification of Low-Grade SRF in Air-Blown Fluidized Bed: Permanent and Inorganic Gases Characterization. Waste Biomass Valorization. https://doi.org/10.1007/s12649-021-01434-w

Higman, C., Van der Burgt, M., 2003. GASIFICATION. Gulf Professional Publishing.

Hongrapipat, J., Saw, W.L., Pang, S., 2015. Co-gasification of blended lignite and wood pellets in a dual fluidized bed steam gasifier: The influence of lignite to fuel ratio on NH3 and H2S concentrations in the producer gas. Fuel 139, 494–501. https://doi.org/10.1016/j.fuel.2014.09.030

Hu, H., Fang, Y., Liu, H., Yu, R., Luo, G., Liu, W., Li, A., Yao, H., 2014. The fate of sulfur during rapid pyrolysis of scrap tires. Chemosphere 97, 102–107. https://doi.org/10.1016/j.chemosphere.2013.10.037

Hu, J., Xiao, Z., Zhou, R., Deng, W., Wang, M., Ma, S., 2011. Ecological utilization of leather tannery waste with circular economy model. J. Clean. Prod. 19, 221–228. https://doi.org/10.1016/j.jclepro.2010.09.018

Hubbe, M.A., Gill, R.A., 2016. Fillers for Papermaking: A Review of their Properties, Usage Practices, and their Mechanistic Role. Bioresources 11, 2886–2963. https://doi.org/10.15376/BIORES.11.1.2886-2963

Husmann, M., Hochenauer, C., Meng, X., Jong, W. de, Kienberger, T., 2014. Evaluation of Sorbents for High Temperature In Situ Desulfurization of Biomass-Derived Syngas. Energy Fuels 28, 2523–2534. https://doi.org/10.1021/ef402254x

Husmann, M., Müller, M., Zuber, C., Kienberger, T., Maitz, V., Hochenauer, C., 2016a. Application of BaO-Based Sulfur Sorbent for in Situ Desulfurization of Biomass-Derived Syngas. Energy Fuels 30, 6458–6466. https://doi.org/10.1021/acs.energyfuels.6b00957

Husmann, M., Zuber, C., Maitz, V., Kienberger, T., Hochenauer, C., 2016b. Comparison of dolomite and lime as sorbents for in-situ H2S removal with respect to gasification parameters in biomass gasification. Fuel 181, 131–138. https://doi.org/10.1016/j.fuel.2016.04.124

Ingraham, T.R., Marier, P., 1963. Kinetic studies on the thermal decomposition of calcium carbonate. Can. J. Chem. Eng. 41, 170–173. https://doi.org/10.1002/cjce.5450410408

Järup, L., 2003. Hazards of heavy metal contamination. Br. Med. Bull. 68, 167–182. https://doi.org/10.1093/bmb/ldg032

Johansen, J.M., Jakobsen, J.G., Frandsen, F.J., Glarborg, P., 2011. Release of K, Cl, and S during Pyrolysis and Combustion of High-Chlorine Biomass. Energy Fuels 25, 4961–4971. https://doi.org/10.1021/ef201098n

Jong, W. de, Ommen, J.R. van, 2014. Biomass as a Sustainable Energy Source for the Future: Fundamentals of Conversion Processes. John Wiley & Sons.

Jung, I.-H., Van Ende, M.-A., 2020. Computational Thermodynamic Calculations: FactSage from CALPHAD Thermodynamic Database to Virtual Process Simulation. Metall. Mater. Trans. B 51, 1851–1874. https://doi.org/10.1007/s11663-020-01908-7

Kemona, A., Piotrowska, M., 2020. Polyurethane Recycling and Disposal: Methods and Prospects. Polymers 12, 1752. https://doi.org/10.3390/polym12081752

Keown, D.M., Favas, G., Hayashi, J., Li, C.-Z., 2005. Volatilisation of alkali and alkaline earth metallic species during the pyrolysis of biomass: differences between sugar cane bagasse and cane trash. Bioresour. Technol. 96, 1570–1577. https://doi.org/10.1016/j.biortech.2004.12.014

Khalil, R.A., Seljeskog, M., Hustad, J.E., 2008. Sulfur Abatement in Pyrolysis of Straw Pellets. Energy Fuels 22, 2789–2795. https://doi.org/10.1021/ef8001235

Kluska, J., Ochnio, M., Kardaś, D., Heda, Ł., 2019. The influence of temperature on the physicochemical properties of products of pyrolysis of leather-tannery waste. Waste Manag. 88, 248–256. https://doi.org/10.1016/j.wasman.2019.03.046

Knudsen, J.N., Jensen, P.A., Dam-Johansen, K., 2004a. Transformation and Release to the Gas Phase of Cl, K, and S during Combustion of Annual Biomass. Energy Fuels 18, 1385–1399. https://doi.org/10.1021/ef049944q

Knudsen, J.N., Jensen, P.A., Lin, W., Frandsen, F.J., Dam-Johansen, K., 2004b. Sulfur Transformations during Thermal Conversion of Herbaceous Biomass. Energy Fuels 18, 810–819. https://doi.org/10.1021/ef034085b

Kopriva, S., 2017. Quo Vadis Sulfur Investigation?: 25 Years of Research into Plant Sulfate Reduction, in: De Kok, L.J., Hawkesford, M.J., Haneklaus, S.H., Schnug, E. (Eds.), Sulfur Metabolism in Higher Plants - Fundamental, Environmental and Agricultural Aspects, Proceedings of the International Plant Sulfur Workshop. Springer International Publishing, Cham, pp. 13–30. https://doi.org/10.1007/978-3-319-56526-2_2

Kuramochi, H., Wu, W., Kawamoto, K., 2005. Prediction of the behaviors of H2S and HCl during gasification of selected residual biomass fuels by equilibrium calculation. Fuel 84, 377–387. https://doi.org/10.1016/j.fuel.2004.09.009

Lemmens, B., Elslander, H., Vanderreydt, I., Peys, K., Diels, L., Oosterlinck, M., Joos, M., 2007. Assessment of plasma gasification of high caloric waste streams. Waste Manag. 27, 1562–1569. https://doi.org/10.1016/j.wasman.2006.07.027

Lopez, G., Alvarez, J., Amutio, M., Mkhize, N.M., Danon, B., van der Gryp, P., Görgens, J.F., Bilbao, J., Olazar, M., 2017. Waste truck-tyre processing by flash pyrolysis in a conical spouted bed reactor. Energy Convers. Manag. 142, 523–532. https://doi.org/10.1016/j.enconman.2017.03.051

Lu, P., Huang, Q., (Thanos) Bourtsalas, A.C., Chi, Y., Yan, J., 2018. Synergistic effects on char and oil produced by the co-pyrolysis of pine wood, polyethylene and polyvinyl chloride. Fuel 230, 359–367. https://doi.org/10.1016/j.fuel.2018.05.072

Ma, W., Hoffmann, G., Schirmer, M., Chen, G., Rotter, V.S., 2010. Chlorine characterization and thermal behavior in MSW and RDF. J. Hazard. Mater. 178, 489–498. https://doi.org/10.1016/j.jhazmat.2010.01.108

Marsh, K., Bugusu, B., 2007. Food Packaging—Roles, Materials, and Environmental Issues. J. Food Sci. 72, R39–R55. https://doi.org/10.1111/j.1750-3841.2007.00301.x

Martínez, I., Callén, M.S., Grasa, G., López, J.M., Murillo, R., 2022. Sorption-enhanced gasification (SEG) of agroforestry residues: Influence of feedstock and main operating variables on product gas quality. Fuel Process. Technol. 226, 107074. https://doi.org/10.1016/j.fuproc.2021.107074

Materazzi, M., Lettieri, P., Mazzei, L., Taylor, R., Chapman, C., 2013. Thermodynamic modelling and evaluation of a two-stage thermal process for waste gasification. Fuel 108, 356–369. https://doi.org/10.1016/j.fuel.2013.02.037

McKinsey & Company, 2020. Net-Zero Europe - Decarbonization pathways and socioeconomic implications.

McNeill, I.C., Memetea, L., Cole, W.J., 1995. A study of the products of PVC thermal degradation. Polym. Degrad. Stab. 49, 181–191. https://doi.org/10.1016/0141-3910(95)00064-S

Murena, F., 2000. Kinetics of sulphur compounds in waste tyres pyrolysis. J. Anal. Appl. Pyrolysis 56, 195–205. https://doi.org/10.1016/S0165-2370(00)00091-7

Nagel, F.P., Ghosh, S., Pitta, C., Schildhauer, T.J., Biollaz, S., 2011. Biomass integrated gasification fuel cell systems–Concept development and experimental results. Biomass Bioenergy 35, 354–362. https://doi.org/10.1016/j.biombioe.2010.08.057

Nasrullah, M., 2015. Material and energy balance of solid recovered fuel production. Aalto University.

Nzihou, A. (Ed.), 2020. Handbook on Characterization of Biomass, Biowaste and Related By-products. Springer International Publishing. https://doi.org/10.1007/978-3-030-35020-8

Pandey, D.S., Yazhenskikh, E., Müller, M., Ziegner, M., Trubetskaya, A., Leahy, J.J., Kwapinska, M., 2021. Transformation of inorganic matter in poultry litter during fluidised bed gasification. Fuel Process. Technol. 221, 106918. https://doi.org/10.1016/j.fuproc.2021.106918

Pedersen, A.J., van Lith, S.C., Frandsen, F.J., Steinsen, S.D., Holgersen, L.B., 2010. Release to the gas phase of metals, S and Cl during combustion of dedicated waste fractions. Fuel Process. Technol. 91, 1062–1072. https://doi.org/10.1016/j.fuproc.2010.03.013

Pettersson, A., Zevenhoven, M., Steenari, B.-M., Åmand, L.-E., 2008. Application of chemical fractionation methods for characterisation of biofuels, waste derived fuels and CFB co-combustion fly ashes. Fuel 87, 3183–3193. https://doi.org/10.1016/j.fuel.2008.05.030

Phyllis2 [WWW Document], n.d. . Database Treat. Biomass Algae Feedstock Biogas Prod. Biochar TNO Biomass Circ. Technol. URL https://phyllis.nl/ (accessed 2.9.21).

Piispanen, M.H., Niemelä, M.E., Tiainen, M.S., Laitinen, R.S., 2012. Prediction of Bed Agglomeration Propensity Directly from Solid Biofuels: A Look Behind Fuel Indicators. Energy Fuels 26, 2427–2433. https://doi.org/10.1021/ef300173w

Pina, A.C., Tancredi, N., Ania, C.O., Amaya, A., 2021. Stabilisation of sheep wool fibres under air atmosphere: Study of physicochemical changes. Mater. Sci. Eng. B 268, 115115. https://doi.org/10.1016/j.mseb.2021.115115

Pinto, F., André, R.N., Carolino, C., Miranda, M., Abelha, P., Direito, D., Perdikaris, N., Boukis, I., 2014a. Gasification improvement of a poor quality solid recovered fuel (SRF). Effect of using natural minerals and biomass wastes blends. Fuel 117, 1034–1044. https://doi.org/10.1016/j.fuel.2013.10.015

Pinto, F., André, R.N., Carolino, C., Miranda, M., Abelha, P., Direito, D., Perdikaris, N., Boukis, I., 2014b. Gasification improvement of a poor quality solid recovered fuel (SRF). Effect of using natural minerals and biomass wastes blends. Fuel 117, 1034–1044. https://doi.org/10.1016/j.fuel.2013.10.015

Pinto, F., André, R.N., Franco, C., Lopes, H., Carolino, C., Costa, R., Gulyurtlu, I., 2010. Co-gasification of coal and wastes in a pilot-scale installation. 2: Effect of catalysts in syngas treatment to achieve sulphur and nitrogen compounds abatement. Fuel 89, 3340–3351. https://doi.org/10.1016/j.fuel.2010.03.017

Piotrowska, P., Zevenhoven, M., Davidsson, K., Hupa, M., Åmand, L.-E., Barišić, V., Coda Zabetta, E., 2010. Fate of Alkali Metals and Phosphorus of Rapeseed Cake in Circulating Fluidized Bed Boiler Part 1: Cocombustion with Wood. Energy Fuels 24, 333–345. https://doi.org/10.1021/ef900822u

Porbatzki, D., Stemmler, M., Müller, M., 2011. Release of inorganic trace elements during gasification of wood, straw, and miscanthus. Biomass Bioenergy, CHRISGAS 35, S79–S86. https://doi.org/10.1016/j.biombioe.2011.04.001

Prabir Basu, 2006. Combustion and Gasification in Fluidized Beds, 1st Edition. ed. CRC Press. https://doi.org/10.1201/9781420005158

Priscak, J., Fürsatz, K., Kuba, M., Skoglund, N., Benedikt, F., Hofbauer, H., 2020. Investigation of the Formation of Coherent Ash Residues during Fluidized Bed Gasification of Wheat Straw Lignin. Energies 13, 3935. https://doi.org/10.3390/en13153935

Recari, J., Berrueco, C., Abelló, S., Montané, D., Farriol, X., 2016a. Gasification of two solid recovered fuels (SRFs) in a lab-scale fluidized bed reactor: Influence of experimental

conditions on process performance and release of HCl, H2S, HCN and NH3. Fuel Process. Technol. 142, 107–114. https://doi.org/10.1016/j.fuproc.2015.10.006

Recari, J., Berrueco, C., Abelló, S., Montané, D., Farriol, X., 2016b. Gasification of two solid recovered fuels (SRFs) in a lab-scale fluidized bed reactor: Influence of experimental conditions on process performance and release of HCl, H2S, HCN and NH3. Fuel Process. Technol. 142, 107–114. https://doi.org/10.1016/j.fuproc.2015.10.006

Rhyner, U., 2013. Reactive hot gas filter for biomass gasification (Doctoral Thesis). ETH Zurich. https://doi.org/10.3929/ethz-a-009917147

Richardson, Y., Blin, J., Julbe, A., 2012. A short overview on purification and conditioning of syngas produced by biomass gasification: Catalytic strategies, process intensification and new concepts. Prog. Energy Combust. Sci. 38, 765–781. https://doi.org/10.1016/j.pecs.2011.12.001

Santanu, D., Avinash, K.A., V. S., M., Bhaskar, T. (Eds.), 2018. Coal and Biomass Gasification - Recent Advances and Future Challenges. Springer Nature, Singapore.

Schmid, M., Beirow, M., Schweitzer, D., Waizmann, G., Spörl, R., Scheffknecht, G., 2018. Product gas composition for steam-oxygen fluidized bed gasification of dried sewage sludge, straw pellets and wood pellets and the influence of limestone as bed material. Biomass Bioenergy 117, 71–77. https://doi.org/10.1016/j.biombioe.2018.07.011

Schweitzer, D., Gredinger, A., Schmid, M., Waizmann, G., Beirow, M., Spörl, R., Scheffknecht, G., 2018. Steam gasification of wood pellets, sewage sludge and manure: Gasification performance and concentration of impurities. Biomass Bioenergy 111, 308–319. https://doi.org/10.1016/j.biombioe.2017.02.002

Shamiri, A., Chakrabarti, M.H., Jahan, S., Hussain, M.A., Kaminsky, W., Aravind, P.V., Yehye, W.A., 2014. The Influence of Ziegler-Natta and Metallocene Catalysts on Polyolefin Structure, Properties, and Processing Ability. Materials 7, 5069–5108. https://doi.org/10.3390/ma7075069

Sikarwar, V.S., Zhao, M., Fennell, P.S., Shah, N., Anthony, E.J., 2017. Progress in biofuel production from gasification. Prog. Energy Combust. Sci. 61, 189–248. https://doi.org/10.1016/j.pecs.2017.04.001

Sini Eräjää, 2015. Cascading use of biomass: opportunities and obstacles in EU policies.

Sosa Sabogal, O., 2022. Pyrolysis and gasification of a solid recovered fuel (SRF) and its model materials (These de doctorat). Ecole nationale des Mines d'Albi-Carmaux.

Struis, R.P.W.J., Ludwig, C., Barrelet, T., Krähenbühl, U., Rennenberg, H., 2008. Studying sulfur functional groups in Norway spruce year rings using S L-edge total electron yield spectroscopy. Sci. Total Environ. 403, 196–206. https://doi.org/10.1016/j.scitotenv.2008.05.034

Suárez-García, F., Martínez-Alonso, A., Fernández Llorente, M., Tascón, J.M.D., 2002. Inorganic matter characterization in vegetable biomass feedstocks. Fuel 81, 1161–1169. https://doi.org/10.1016/S0016-2361(02)00026-1

Tchoffor, P.A., Davidsson, K.O., Thunman, H., 2014. Effects of Steam on the Release of Potassium, Chlorine, and Sulfur during Char Conversion, Investigated under Dual-Fluidized-Bed Gasification Conditions. Energy Fuels 28, 6953–6965. https://doi.org/10.1021/ef501591m

Tchoffor, P.A., Davidsson, K.O., Thunman, H., 2013. Transformation and Release of Potassium, Chlorine, and Sulfur from Wheat Straw under Conditions Relevant to Dual Fluidized Bed Gasification. Energy Fuels 27, 7510–7520. https://doi.org/10.1021/ef401703a

Tchoffor, P.A., Moradian, F., Pettersson, A., Davidsson, K.O., Thunman, H., 2016. Influence of Fuel Ash Characteristics on the Release of Potassium, Chlorine, and Sulfur from Biomass Fuels under Steam-Fluidized Bed Gasification Conditions. Energy Fuels 30, 10435–10442. https://doi.org/10.1021/acs.energyfuels.6b01470

Tillman, D.A., Duong, D., Miller, B., 2009. Chlorine in Solid Fuels Fired in Pulverized Fuel Boilers — Sources, Forms, Reactions, and Consequences: a Literature Review. Energy Fuels 23, 3379–3391. https://doi.org/10.1021/ef801024s

Valin, S., Ravel, S., Pons de Vincent, P., Thiery, S., Miller, H., 2019. Fluidized bed air gasification of solid recovered fuel and woody biomass: Influence of experimental conditions on product gas and pollutant release. Fuel 242, 664–672. https://doi.org/10.1016/j.fuel.2019.01.094

van Paasen, S.V.B., Cieplik, M.K., Phokawat, N.P., 2006. Gasification of Non-woody Biomass Economic and Technical Perspectives of Chlorine and Sulphur Removal from Product Gas (Non-confidential version) (No. ECN-C-06-032). Energy research Centre of the Netherlands (ECN), Netherlands.

Vassilev, S.V., Baxter, D., Andersen, L.K., Vassileva, C.G., Morgan, T.J., 2012. An overview of the organic and inorganic phase composition of biomass. Fuel 94, 1–33. https://doi.org/10.1016/j.fuel.2011.09.030

Velis, C., Wagland, S., Longhurst, P., Robson, B., Sinfield, K., Wise, S., Pollard, S., 2012. Solid Recovered Fuel: Influence of Waste Stream Composition and Processing on Chlorine Content and Fuel Quality. Environ. Sci. Technol. 46, 1923–1931. https://doi.org/10.1021/es2035653

Velis, C.A., 2010. Solid recovered fuel production through the mechanical-biological treatment of wastes (Ph.D.). Cranfield University.

Vinas, J., Dufils, P.E., 2012. Poly(Vinylidene Chloride), in: Ullmann’s Encyclopedia of Industrial Chemistry. American Cancer Society. https://doi.org/10.1002/14356007.a22_017.pub2

Vonk, G., Piriou, B., Wolbert, D., Cammarano, C., Vaïtilingom, G., 2019. Analysis of pollutants in the product gas of a pilot scale downdraft gasifier fed with wood, or mixtures of wood and waste materials. Biomass Bioenergy 125, 139–150. https://doi.org/10.1016/j.biombioe.2019.04.018

Walsh, M.E., 2014. Biomass Resource Assessment☆, in: Reference Module in Earth Systems and Environmental Sciences. Elsevier. https://doi.org/10.1016/B978-0-12-409548-9.09046-1

Wang, S.-J., Zhang, H., Shao, L.-M., Liu, S.-M., He, P.-J., 2014. Thermochemical reaction mechanism of lead oxide with poly(vinyl chloride) in waste thermal treatment. Chemosphere 117, 353–359. https://doi.org/10.1016/j.chemosphere.2014.07.076

Wang, Z., Huang, H., Li, H., Wu, C., Chen, Y., Li, B., 2002. HCl Formation from RDF Pyrolysis and Combustion in a Spouting-Moving Bed Reactor. Energy Fuels 16, 608–614. https://doi.org/10.1021/ef0101863

Werkelin, J., Skrifvars, B.-J., Zevenhoven, M., Holmbom, B., Hupa, M., 2010. Chemical forms of ash-forming elements in woody biomass fuels. Fuel 89, 481–493. https://doi.org/10.1016/j.fuel.2009.09.005

Williams, P.T., Besler, S., 1995. Pyrolysis-thermogravimetric analysis of tyres and tyre components. Fuel 74, 1277–1283. https://doi.org/10.1016/0016-2361(95)00083-H

Woolcock, P.J., Brown, R.C., 2013. A review of cleaning technologies for biomass-derived syngas. Biomass Bioenergy 52, 54–84. https://doi.org/10.1016/j.biombioe.2013.02.036

Xu, W., Song, G., Song, Q., Yao, Q., 2022. Study on the mechanism of lead release from ash under the action of high-temperature flue gas. Fuel Process. Technol. 227, 107089. https://doi.org/10.1016/j.fuproc.2021.107089

Yan, M., Feng, H., Zheng, R., Yu, C., Hantoko, D., Zhou, Z., Zhang, Y., Kanchanatip, E., 2021. Sulfur conversion and distribution during supercritical water gasification of sewage sludge. J. Energy Inst. 95, 61–68. https://doi.org/10.1016/j.joei.2021.01.002

Zevenhoven, M., Yrjas, P., Skrifvars, B., Hupa, M., 2012. Characterization of Ash-Forming Matter in Various Solid Fuels by Selective Leaching and Its Implications for Fluidized-Bed Combustion. https://doi.org/10.1021/EF300621J

Zevenhoven, Maria, Yrjas, P., Skrifvars, B.-J., Hupa, M., 2012. Characterization of Ash-Forming Matter in Various Solid Fuels by Selective Leaching and Its Implications for Fluidized-Bed Combustion. Energy Fuels 26, 6366–6386. https://doi.org/10.1021/ef300621j

Zevenhoven-Onderwater, M., 2001. Ash-forming matter in biomass fuels (PhD Thesis). Aabo Akademi, Turku (Finland).

Zevenhoven-Onderwater, M., Backman, R., Skrifvars, B.-J., Hupa, M., 2001. The ash chemistry in fluidised bed gasification of biomass fuels. Part I: predicting the chemistry of melting ashes and ash–bed material interaction. Fuel 80, 1489–1502. https://doi.org/10.1016/S0016-2361(01)00026-6

Zhang, C., Lu, Q., Li, Y., 2023. A review on sulfur transformation during anaerobic digestion of organic solid waste: Mechanisms, influencing factors and resource recovery. Sci. Total Environ. 865, 161193. https://doi.org/10.1016/j.scitotenv.2022.161193

Zhang, J., Zhu, M., Jones, I., Okoye, C.O., Zhang, Z., Zhang, D., 2020. The transformation and fate of sulphur during CO2 gasification of a spent tyre pyrolysis char. Proc. Combust. Inst. https://doi.org/10.1016/j.proci.2020.06.037

Zhou, C., Yang, W., Blasiak, W., 2013. Characteristics of waste printing paper and cardboard in a reactor pyrolyzed by preheated agents. Fuel Process. Technol. 116, 63–71. https://doi.org/10.1016/j.fuproc.2013.04.023

Zoller, U. (Ed.), 2008. Handbook of Detergents, Part E : Applications, 1ère. ed. CRC Press, Boca Raton. https://doi.org/10.1201/9781420018165

Appendices

Appendix A. Calculation of released inorganic pollutants concentrations in function of the initial S and Cl contents

The initial inorganic content will be linked to the potential quantity of gaseous inorganic pollutants (H_2S, COS, HCl, Alkali) released in the syngas. The released quantities of gaseous inorganic pollutants must exceed the tolerance levels of syngas end-use systems (to have a need for syngas cleaning), and they should be high enough for their accurate measurement in the analytical experimental device.

Calculations of the released amount of inorganic pollutants in function of the initial sulfur and chlorine content were made with Factsage. A typical biomass composition of C (45wt. %), H (5 wt. %), O (calculated by difference), N (0.7 wt. %), was used as an input with a varying S or Cl content between 0 and 0.1 wt.% at 800°C. The figures below show the concentrations of gaseous sulfur species (H_2S, COS) and chlorine species (HCl) released in the gas phase (ppmv) as a function of the initial S and Cl content, respectively.

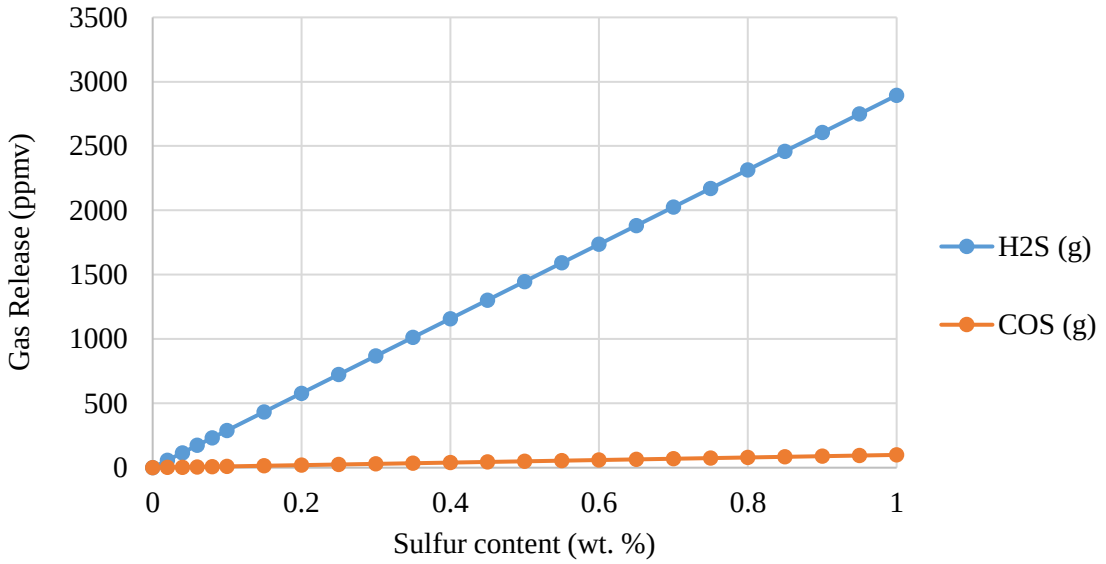

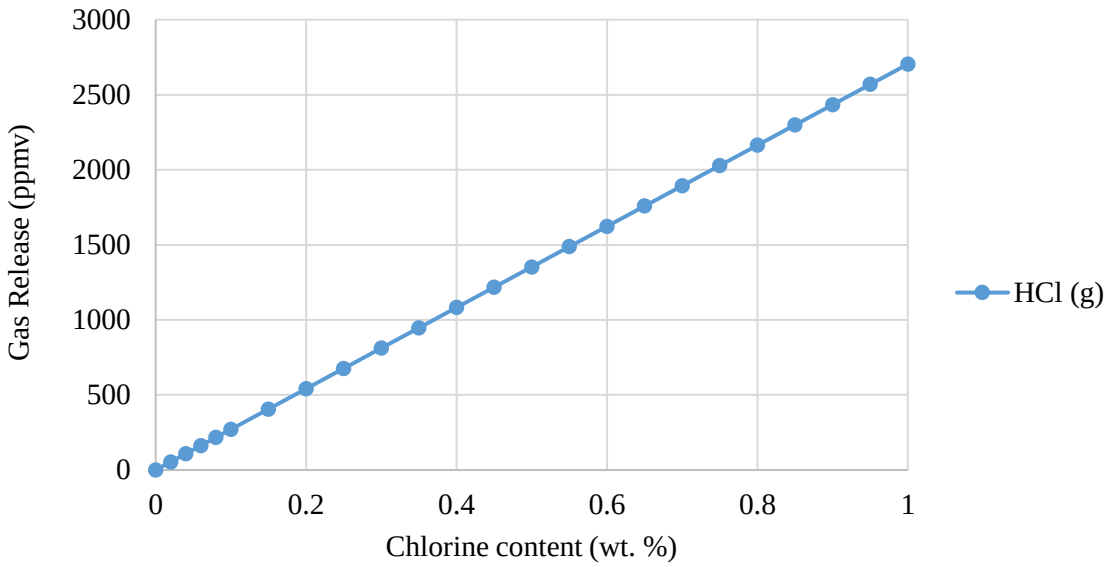

In these calculations, the possible interactions of S and Cl with other inorganic elements that might retain them in the solid phase are not considered. However, even at very low sulfur and chlorine contents (0.01 wt. %), the concentrations of pollutants released (>25 ppmv) exceed the concentrations of syngas purity requirements showed in the literature review in chapter 1.

Appendix B. Error calculation

Propagation of uncertainties is a technique used in mathematical and statistical calculations to estimate the uncertainty or error in the result of a calculation based on the uncertainties or errors in the input quantities.

Suppose we have two quantities, A and B, with uncertainties denoted as δA and δB, respectively.

To calculate the result of their division, C = A / B, and estimate the uncertainty in C using error propagation. The formula for estimating the uncertainty in the division C is given by:

$$\delta C = |C| \times \sqrt{\left(\frac{\delta A}{A}\right)^2 + \left(\frac{\delta B}{B}\right)^2}$$

where δC is the uncertainty in C, δA is the uncertainty in A, δB is the uncertainty in B, and |C| denotes the absolute value of C.

To calculate the result of their sum, D = A + B, and estimate the uncertainty in D using error propagation. The formula for estimating the uncertainty in the sum D is given by:

$$\delta D = \sqrt{(\delta A)^2 + (\delta \mathrm{B})^2}$$

where δD is the uncertainty in D, δA is the uncertainty in A, and δB is the uncertainty in B.

A.1. Retention of inorganic elements (S, Cl, K, Si, Ca) in the char after pyrolysis

The relative uncertainty of a retention of an inorganic element in the char is detailed below:

	Calculation	Uncertainty
R: retention of an inorganic element in the char	$R = \frac{m_{i-c}}{m_{i-f}}$	$\delta R = \lvert R \rvert \times \sqrt{(\frac{\delta m_{i-c}}{m_{i-c}})^2 + (\frac{\delta m_{i-f}}{m_{i-f}})^2}$

where

	Calculation	Uncertainty
m_{i-c} : mass of the inorganic element in the char	$m_{i-c} = \frac{xi_c}{100} \times m_c$	$\delta m_{i-c} = m_{i-c} \times \sqrt{(\frac{\delta[\,xi_c]}{[\,\%i_c]})^2 + (\frac{\delta m_{c,}}{m_c})^2}$
m_{i-f} : mass of the inorganic element in the feedstock sample	$m_{i-f} = \frac{xi_f}{100} \times m_f$	$\delta m_{i-f} = m_{i-f} \times \sqrt{(\frac{\delta[\,xi_f]}{[\,xi_f]})^2 + (\frac{\delta m_{f,}}{m_f})^2}$

Where $\delta xi_f/xi_f$ and $\delta xi_c/xi_c$ are the relative uncertainties of the mass fractions of the inorganic elements in the char (c) and the feedstock (f) with a coverage factor of k=2. They are equal to 15% for S and Cl and 10% for K, Si and Ca.

δm_f and δm_c are the absolute uncertainties of the mass of the samples of feedstock and char determined from the incertitude of the balance used to measure these samples. They are equal to 0.001mg.

A.2. Chemical fractionation analysis: fraction of inorganic elements (S, Cl, K, Si, Ca) in the leachates and solid residue

In the chemical fractionation results, the relative uncertainty of the total fraction of the inorganic element recovered in the leachates and in the solid residue is detailed below:

	Calculation	Uncertainty
F_{total}: total fraction of the inorganic element i	$F_{total} = F_{i-H2O} + F_{i-NH4Ac} + F_{i-solid}$	$\delta F_{i-total} = \sqrt{(\delta F_{i-H2O})^2 + (\delta F_{i-NH4Ac})^2 + (\delta F_{i-solid})^2}$

where

	Calculation	Uncertainty
$F_{i-leachate}$: fraction of the inorganic element i recovered in the leachate (leachate=H2O or NH4Ac)	$F_{i-leachate} = \frac{m_{i-leachate}}{m_{i-f}}$	$\delta F_{i-leachate} = \lvert F_{i-leachate} \rvert \times \sqrt{(\frac{\delta[\, m_{i-leachate}]}{[m_{i-leachate}]})^2 + (\frac{\delta m_{i-f}}{m_{i-f}})^2}$
$F_{i-solid}$: fraction of the inorganic element i recovered in the solid residue	$F_{i-solid} = \frac{m_{i-solid}}{m_{i-f}}$	Same calculation as R

$m_{i-leachate}$ is the mass of the element i recovered in the leachate calculated as the concentration measured multiplied by the collected volume of the leachate:

$$m_{i-leachate}\,(mg) = Concentration\,(mg/L) \times Volume\ of\ Leachate\,(L)$$

And thus $\delta\, m_{i-leachate} = \lvert m_{i-leachate} \rvert \times \sqrt{(\frac{\delta[C]}{[C]})^2 + (\frac{\delta V}{V})^2}$

$\delta C/C$ is the relative uncertainty of the concentration of the inorganic element measured in the leachate given by the ICP-OES for S and Si. It is equal in average to 2% with a confidence interval of 95%. The determination of the uncertainties of the concentration of the anions Cl^- and PO_4^{3-} and cations K^+, Na^+, Ca^{2+}, and Mg^{2+} by the ion chromatography was not possible.
δV is the uncertainty of the mass of the leachates determined from the

Appendix C. Thermal Characterization of the reactor at the setpoint of 860°C

The evolution of temperature on the outer surface of the susceptor and inside the quartz tube as a function of time at a setpoint of 860°C are presented in the two figures below, respectively.

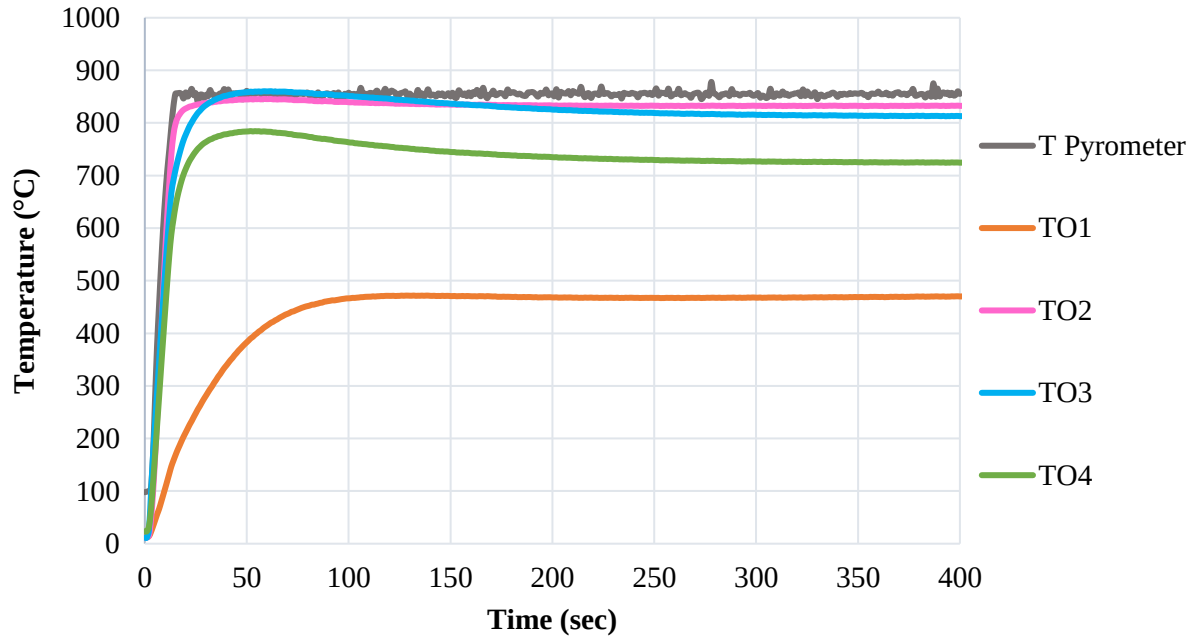

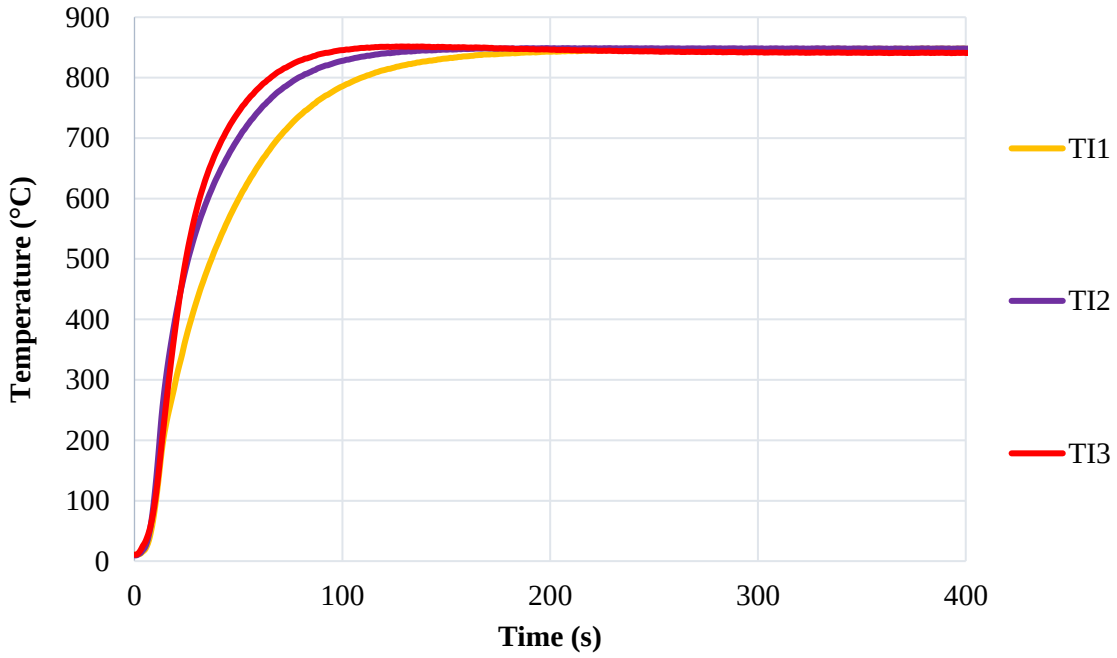

Appendix D. Examples of sample temperature measurement during the pyrolysis experiments with interrupted heating

In the pyrolysis experiments that were carried out with interruption of the heating at different times, each sample reached a different temperature. The temperature considered for each sample is the maximum average temperature reached inside the sample, since after the interruption of heating the temperature shortly continues to increase before it starts to decrease. The graph below shows an example of the determination of the maximum temperature for each feedstock.

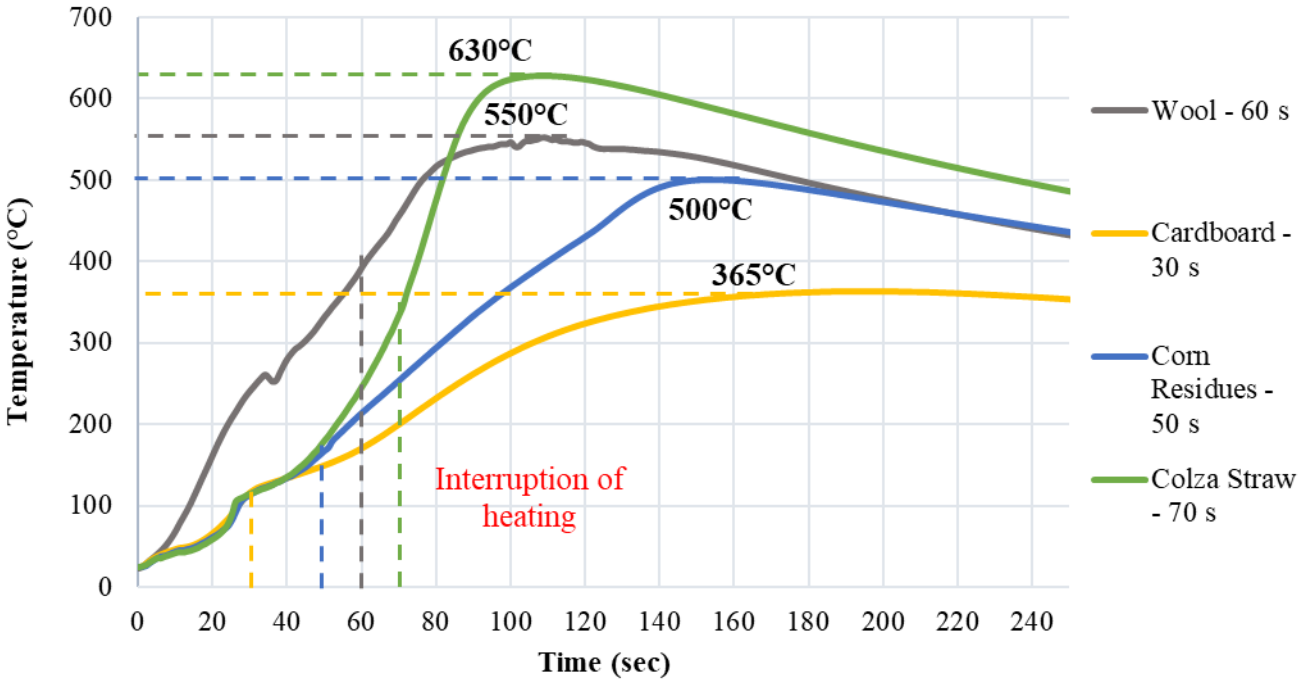

Appendix E. Elemental composition of the chars obtained from pyrolysis and gasification

The sum of the percentages for each element in the tables does not add up to 100%. This discrepancy can be attributed to the omission of specific elements, notably the oxygen content and other inorganic trace elements present in smaller amounts. These elements were not included in the analysis, contributing to the observed deviation from the expected total.

Colza Straw	**Pyrolysis**						**Gasification**		
	410°C	**630°C**	**710°C**	**800°C**		**850°C**	**800°C 20 min**		**800°C 60 min**
C (wt. %)	57.91	58.22	58.84	57.9	54.6	54.57	49.47	61	5.99
H (wt. %)	4.10	2.02	1.69	1.20	1.38	1.39	1.39	1.14	0.58
N (wt. %)	1.07	0.95	0.91	0.97	1.09	1.09	1.04	1.32	0.01
S (wt. %)	0.31	0.37	0.38	0.47	0.45	0.45	0.61	0.6	1.11
Cl (wt. %)	0.19	0.34	0.34	0.33	0.33	0.33	0.94	0.72	0.08
Ca (wt. %)	7.19	10.1	9.56	10.51	n.a	12.24	n.a	n.a	n.a
Al (wt. %)	0.09	0.12	0.82	0.16	n.a	0.18	n.a	n.a	n.a
K (wt. %)	2.31	2.96	3.06	3.05	n.a	2.79	n.a	n.a	n.a
Na (wt. %)	0.04	0.04	0.04	0.07	n.a	0.04	n.a	n.a	n.a
Mg (wt.%)	0.28	0.37	0.37	0.39	n.a	0.43	n.a	n.a	n.a
Fe (wt. %)	0.14	0.27	0.24	0.33	n.a	0.28	n.a	n.a	n.a
P (wt. %)	0.31	0.42	0.42	0.47	n.a	0.64	n.a	n.a	n.a
Si (wt. %)	1.3	1.6	1.8	2	n.a	2.1	n.a	n.a	n.a

Corn Residues	Pyrolysis			Gasification	
	500°C	**800°C**	**850°C**	**800°C 20 min**	**800°C 60 min**
C (wt. %)	70.46	68.55	77.08	73.48	45.27
H (wt. %)	3.43	1.23	1.60	1.06	1.24
N (wt. %)	1.93	1.53	1.71	2.46	1.33
S (wt. %)	0.12	0.12	0.14	0.18	0.13
Cl (wt. %)	0.70	0.74	0.85	1.14	0.56
Ca (wt. %)	1.41	1.48	1.57	n.a	n.a
Al (wt. %)	<0.03	0.06	0.04	n.a	n.a
K (wt. %)	2.83	2.77	3.01	n.a	n.a
Na (wt. %)	<0.04	0.28	<0.04	n.a	n.a
Mg (wt. %)	0.68	0.71	0.74	n.a	n.a
Fe (wt. %)	0.06	0.17	0.08	n.a	n.a
P (wt. %)	0.52	0.68	0.69	n.a	n.a
Si (wt. %)	1.1	5.6	1.2	n.a	n.a

Cardboard	Pyrolysis			Gasification
	365°C	**800°C**	**850°C**	**800°C**
C (wt. %)	47.17	54.79	55.04	15.83
H (wt. %)	4.53	1.69	1.32	0.67
N (wt. %)	0.43	0.56	0.59	0.23
S (wt. %)	0.02	0.06	0.06	0.12
Cl (wt. %)	0.08	0.09	0.09	-
Ca (wt. %)	7.92	13.43	13.22	n.a
Al (wt. %)	1.42	2.41	2.32	n.a
K (wt. %)	0.15	0.19	0.18	n.a
Na (wt. %)	0.29	0.48	0.55	n.a
Mg (wt. %)	0.29	0.51	0.51	n.a
Fe (wt. %)	0.34	0.47	0.5	n.a
P (wt. %)	0.07	0.12	0.23	n.a
Si (wt. %)	2.1	3.7	4	n.a

Wool	**Pyrolysis**			**Gasification**
	550°C	**800°C**	**850°C**	**800°C**
C (wt. %)	67.25	74.62	78.41	63.81
H (wt. %)	3.36	2.01	1.20	1.4
N (wt. %)	13.72	11.6	11.13	1
S (wt. %)	0.86	0.83	0.99	1.5
Cl (wt. %)	0.05	-	-	-
Ca (wt. %)	1.58	1.82	n.a	n.a
Al (wt. %)	0.04	0.06	n.a	n.a
K (wt. %)	0.06	<0.04	n.a	n.a
Na (wt. %)	0.08	0.08	n.a	n.a
Mg (wt. %)	0.13	0.15	n.a	n.a
Fe (wt. %)	0.03	0.04	n.a	n.a
P (wt. %)	0.09	0.09	n.a	n.a
Si (wt. %)	0.2	0.4	n.a	n.a

n.a: not analyzed

Appendix F. S and Cl contents of the chars obtained from the mixtures of resources with additives and with calcium-rich resources

Resource	Additive	S (wt. %)	Cl (wt. %)
Colza Straw	Pyrolysis with CaO	0.32	0.37
	Gasification with CaO	0.38	0.47
	Gasification with CaO	0.34	0.74
Corn Residues	Pyrolysis with CaO	0.11	0.78
	Pyrolysis with $CaCO_3$	0.09	0.63
	Gasification with CaO	0.08	0.85
Cardboard	Pyrolysis with CaO	0.07	0.12
Wool	Pyrolysis with CaO	0.51	0.2
	Pyrolysis with $CaCO_3$	0.14	0.05
	Pyrolysis with $Ca(OH)_2$	0.46	0.16
	Gasification with CaO	0.24	0.09
PVC	Pyrolysis with CaO	0.02	23.3

Resource	Ca-rich resource	S (wt. %)	Cl (wt. %)
Colza Straw	Pyrolysis with Cardboard (50 wt. %)	0.3	0.54
	Pyrolysis with Cardboard (70 wt. %)	0.21	0.44
	Pyrolysis with Oak bark (76 wt. %)	0.15	0.29
Corn Residues	Pyrolysis with Cardboard (70 wt. %)	0.11	0.56
Wool	Pyrolysis with Cardboard (70 wt. %)	0.5	0.2
	Pyrolysis with Cardboard (50 wt. %)	1.02	0.15
	Gasification with Cardboard (70 wt. %)	0.7	0.13
	Pyrolysis with Oak Bark (76 wt.%)	0.38	0.04
	Pyrolysis with Colza Straw (72 wt. %)	0.98	0.5
	Pyrolysis with Colza Straw (50 wt. %)	1.1	0.41
PVC	Pyrolysis with Cardboard (70 wt. %)	0.02	6.61

Appendix G. Yield of the chars obtained from the mixtures of resources with additives and with calcium-rich resources

Resource	Additive	Char yield (g/g dry resource)
Colza Straw	Pyrolysis with CaO	0.34
	Gasification with CaO	0.33
	Gasification with CaO	0.28
Corn Residues	Pyrolysis with CaO	0.32
	Pyrolysis with $CaCO_3$	0.28
	Gasification with CaO	0.29
Cardboard	Pyrolysis with CaO	0.31
Wool	Pyrolysis with CaO	0.27
	Pyrolysis with $CaCO_3$	0.25
	Pyrolysis with $Ca(OH)_2$	0.27
	Gasification with CaO	0.29
PVC	Pyrolysis with CaO	0.36

Resource	Ca-rich resource	Char yield (g/g dry resource)
Colza Straw	Pyrolysis with Cardboard (50 wt. %)	0.24
	Pyrolysis with Cardboard (70 wt. %)	0.24
	Pyrolysis with Oak bark (76 wt. %)	0.30
Corn Residues	Pyrolysis with Cardboard (70 wt. %)	0.22
Wool	Pyrolysis with Cardboard (70 wt. %)	0.22
	Pyrolysis with Cardboard (50 wt. %)	0.20
	Gasification with Cardboard (70 wt. %)	0.20
	Pyrolysis with Oak Bark (76 wt. %)	0.22
	Pyrolysis with Colza Straw (72 wt. %)	0.24
	Pyrolysis with Colza Straw (50 wt. %)	0.22
PVC	Pyrolysis with Cardboard (70 wt. %)	0.25